DEVELOPMENT OF AN INTEGRATED DECISION SUPPORT SYSTEM FOR SUPPORTING OFFSHORE OIL SPILL RESPONSE IN HARSH ENVIRONMENTS

by

A thesis submitted to the School of Graduate Studies
in partial fulfillment of the requirements for the
Degree of Doctor of Philosophy

Faculty of Engineering and Applied Science
Memorial University of Newfoundland
May, 2014

St. John's   Newfoundland and Labrador   Canada

ABSTRACT

Offshore oil spills can lead to significantly negative impacts on socio-economy and constitute a direct hazard to the marine environment and human health. The response to an oil spill usually consists of a series of dynamic, time-sensitive, multifaceted and complex processes subject to various constraints and challenges. In the past decades, many models have been developed mainly focusing on individual processes including oil weathering simulation, impact assessment, and clean-up optimization. However, to date, research on integration of offshore oil spill vulnerability analysis, process simulation and operation optimization is still lacking. Such deficiency could be more influential in harsh environments. It becomes noticeably critical and urgent to develop new methodologies and improve technical capacities of offshore oil spill responses. Therefore, this proposed research aims at developing an integrated decision support system for supporting offshore oil spill responses especially in harsh environments (DSS-OSRH). Such a DSS consists of offshore oil spill vulnerability analysis, response technologies screening, and simulation-optimization coupling. The uncertainties and/or dynamics have been quantitatively reflected throughout the modeling processes.

First, a Monte Carlo simulation based two-stage adaptive resonance theory mapping (MC-TSAM) approach has been developed. A real-world case study was applied for offshore oil spill vulnerability index (OSVI) classification in the south coast of Newfoundland to demonstrate this approach. Furthermore, a Monte Carlo simulation based integrated rule-based fuzzy adaptive resonance theory mapping (MC-IRFAM) approach has been developed for screening and ranking for spill response and clean-up

I

technologies. The feasibility of the MC-IRFAM was tested with a case of screening and ranking response technologies in an offshore oil spill event. A novel Monte Carlo simulation based dynamic mixed integer nonlinear programming (MC-DMINP) approach has also been developed for the simulation-optimization coupling in offshore oil spill responses. To demonstrate this approach, a case study was conducted in device allocation and oil recovery in an offshore oil spill event. Finally, the DSS-OSRH has been developed based on the integration of MC-TSAM, MC-IRFAM, and MC-DSINP. To demonstrate its feasibility, a case study was conducted in the decision support during offshore oil spill response in the south coast of Newfoundland.

The developed approaches and DSS are the first of their kinds to date targeting offshore oil spill responses. The novelty can be reflected from the following aspects: 1) an innovative MC-TSAM approach for offshore OSVI classification under complexity and uncertainty; 2) a new MC-IRFAM approach for oil spill response technologies classification and ranking with uncertain information; 3) a novel MC-DMINP simulation-optimization coupling approach for offshore oil spill response operation and resource allocation under uncetainty; and 4) an innovational DSS-OSRH which consists of the MC-TSAM, MC-IRFAM, and MC-DMINP, supporting decision making throughout the offshore oil spill response processes. These methods are particularly suitable for offshore oil spill responses in harsh environments such as the offshore areas of Newfoundland and Labrador (NL). The research will also promote the understanding of the processes of oil transport and fate and the impacts to the affected offshore and shoreline area. The methodologies will be capable of providing modeling tools for other related areas that require timely and effective decisions under complexity and uncertainty.

ACKNOWLEDGEMENT

TABLE OF CONTENTS

LIST OF TABLES

LIST OF FIGURES

XI

LIST OF SYMBOLS AND ABBREVIATIONS

[C]	centroid matrix of each cluster
$[CR_k]$	group k of the classification result
[CT]	matrix of centroid values
$[G_r]$	the rth group from the unsupervised classification
[I]	Input matrix for classification
$[I_a]$	fuzzified input for classification
$[I_b]$	matrix of fuzzified criteria combination
$[I_{b0}]$	matrix of criteria combination
$[I_N]$	normalized matrix for classification
[O]	final classification result
$[O_c]$	matrix containing the certain ranked groups
$[O_u]$	unsupervised classification result
$[UCR_l]$	ranked group I in the classification result
[Y]	fuzzified matrix for a feature
A	area of the oil slick, m^2
AI	artificial intelligence
A_{ij}	constraint coefficients
AMSA	Australian Maritime Safety Authority
ANN	artificial neural networks
ART	adaptive resonance theory
ARTMap	adaptive resonance theory mapping
B_i	constraint right hand sides

BOEMRE	Bureau of Ocean Energy Management, Regulation, and Enforcement
c	equation parameters of evaporation for specific oil
C	matrix of objective function coefficient
C_0	oil dispersion parameter related to oil viscosity
C_{0e}	oil concentration after absorption balance
C_3	final fraction water content
C_A	non-dimensional constant for evaporation
C_B	non-dimensional constant for evaporation
C_C	constant for specific oil
CCG	Canadian Coast Guard
$C_h(t)$	amount of a hydrocarbon component at time t
C_j	coefficients of objective function
C-NLOPB	Canada-Newfoundland and Labrador Offshore Petroleum Board
COZOIL	Coastal Zone Oil Spill Model
CREAM	Chemical Risk Effects Assessment Models
d	equation parameters of evaporation for specific oil
d_0	oil droplet diameter, mm
DE	dispersion rate, $m^3/s/m^3$ of oil
DECC	Department of Energy and Climate Change
DFO	Fisheries and Oceans Canada
DMINP	dynamic mixed integer nonlinear programming
DP	dynamic programming

d_s	sediment particle diameter, mm
D_s	depth of sediments on beach, m
DSS	decision support system
DV	evaporated amount of oil, m^3
E	mathematical expectation
EPA	Environmental Protection Agency
EPPR	Emergency Prevention, Preparedness and Response Working Group
EU	European Union
f	objective function
F_2^a	feature representation field
F_2^b	category representation field
F^{ab}	map field
FAM	fuzzy adaptive resonance theory mapping
FE	evaporation rate, m^3/hour/m^3 of oil
FNN	fuzzy-neural networks
f_{opt}	optimized objective value
FP	fuzzy programming
FSILP	fuzzy-stochastic-interval linear programming
fv	value of the feature in each pattern
FV	evaporated amount of oil, m^3
FW	fractional water content
F_{wc}	fraction of the sea surface hit by breaking waves
G	group

g	matrix of objective function coefficient
GEAEs	generic ecological assessment endpoints
GEV	generalized extreme value
GIS	geographical information system
GNOME	General NOAA Operational Modeling Environment
H	significant wave height, m
HHRAP	Human Health Risk Assessment Protocol
HSE	Health, safety and environmental departments
IC	incident controller
ILP	interval linear programming
IMMS	Interior Minerals Management Service
IMO	International Maritime Organization
IP	interval programming
IRFAM	integrated rule-based fuzzy adaptive resonance theory mapping
j	index
J	chosen category
K_1	constant with default value of 150 s^{-1}
K_A	curve fitting constant relating to wind speed
k_a	sum of the values for all wavelengths of sunlight absorbed by the PAH
K_a	cure fitting constant
K_{ab}	absorption parameter for sedimentation, /day
K_b	mousse viscosity constant

K_c	oil-dependent constant
K_d	dissolution mass transfer coefficient, m^3/hour
k_e	coefficient evaluated from experiments
K_E	mass transfer coefficient, m/s
k_{max}	maximum fist-order hydrocarbon biodegradation rate, mg/kg/day
K_n	half-saturation concentration for a specific nutrient, mg/L
k_{obs}	observed fist-order hydrocarbon biodegradation rate, mg/kg/day
K_p	absorption parameter for sedimentation, /day
I	index of trial
L(t)	ratio of the average residual nitrogen concentration to oil loading at time t
LHS	left-hand-side
L_{ow}	vertical length-scale parameter
LP	linear programming
L_s	length of sediments on beach, m
M	molecular weight, g/mol
MC	Monte Carlo
MC-DMINP	Monte Carlo simulation based dynamic mixed integer nonlinear programming
MCFP	Monte Carlo simulation based fuzzy programming
MC-IRFAM	Monte Carlo simulation based integrated rule-based fuzzy adaptive resonance theory mapping
MC-TSAM	Monte Carlo simulation based two-stage adaptive resonance theory

	mapping
MEPA	Meteorology and Environmental Protection Administration
MIDO	mixed-integer dynamic optimization
MLP	multilayer perceptron
MMO	Marine Management Organisation
MPC	marine pollution controller
n	number of input patterns or number of data points in the cluster.
N	preset number of trials
NASA	National Aeronautics and Space Administration
NCA	Norwegian Coastal Administration
NCS	National Contingency System
NDVI	normalized difference vegetation index.
NF	neuro-fuzzy
NFS	neural-fuzzy systems
NN	neural network
NOAA	National Oceanic and Atmospheric Administration
NOSCP	National Oil Spill Contingency Plan
NOWPAP	Northwest Pacific Action Plan
NRT	National Response Team
NT	Northern Territory
OILMAP	Oil Spill Model and Response System
OPEP	Oil Pollution Emergency Plan
ORE	oil recovery efficiency, m^3/hour

ORR	oil recovery rate, m^3/hour
ORR_n	net oil recovery oil, m^3/hour
OSIS	Oil Spill Information System
OSPAR	Oil Spill Preparedness and Response in Asia
OSRA	Oil Spill Risk Analysis
OSRCAP	Marine Oil Spill Response and Contingency Action Plan
P	vapor pressure, Pa
p	desired number of final groups
p(t)	polar fraction of oil at time t
P_0	initial vapor pressure, Pa
PAH_d	concentration of dissolved PAH, mg/L
PBPK	physiologically-based pharmacokinetic
PD	pharmacodynamics
PEMSEA	Partnerships in Environmental Management for the Seas of East Asia
P^{sat}	vapour pressure of the spill, Pa
q	desired/final number of classified groups
Q	entrainment rate of oil droplets, kg/m^2/s
Q_{max}	maximum capacity of a beach for oil, m^3
Q_s	total absorption capacity by sediment, m^3
R	gas constant, 8.314 $m^3 \cdot$Pa/mol/K
R^2	correlation coefficient
RHS	right-hand-side

RV	remaining volume of spilled oil, m^3
S	matrix of slack variables
s	index of stage
S_0	solubility for fresh oil, g/L
S_{cov}	sea coverage factor of oil
S_d	total dissolution rate of the oil slick, g/hour
SK	number of skimmer, set
SOT	slick thickness, mm
SP	stochastic programming
s_t	oil-water interfacial tension, dyne/m
st	index of stage
S_t	interface tension of oil and water, dyne/m
SVM	support vector machine
T	temperature, K
t	time, hour
T_0	initial boiling point, K
T_G	gradient of the boiling point, K
TGV	typical group value
T_j	choice function
TM	thematic mapper
t_s	controllable time interval, hour
TSAM	two-stage adaptive resonance theory mapping
TSAM	two-stage adaptive resonance theory mapping

U	wind speed, m/s
V	cumulatively recovered oil, m^3
V_0	initial volume of spilled oil, m^3
$\vec{V}'$	turbulent fluctuation of the drift velocity, m/s
$\vec{V}$	advection or drift velocity, m/s
V_b	volume of oil on the shoreline, m^3
V_h	collected oil in stage h, m^3
V_m	collected oil in stage m, m^3
V_t	collected oil at time t, m^3
$\vec{V}_c$	depth-averaged current velocity, m/s
$\vec{V}_w$	wind velocity, m/s
w	adaptive weights
w_j	weight vector
WOSM	World Oil Spill Model
W_s	width of sediments on beach, m
x	data set in the input matrix
X	decision variable in optimization
x^{ab}	output vector
x_i	centroid value for each feature
X_{opt}	optimized decision variable
Y	fraction of water in oil
y	value of the feature in each data point

y^b	input pattern to ART_b.
y_{ij}	inputs which membership function equal to 1
Y_w^F	stable water content of the emulsion
Z	amount of oil fraction
α	choice parameter
α_b	fitting parameters determined from the multiple regression analysis
α_c	current drift factor
α_d	decay constant, /day
α_h	coefficient for the mixing depth
α_w	wind drift factor
β	learning rate
γ	dimensionless damping coefficient
γ_b	fitting parameters determined from the multiple regression analysis
δ	spread of membership function
δ_b	fitting parameters determined from the multiple regression analysis
ΔV_b	volume of beached oil reenter to the sea, m^3
ε	assumed multiplicative error term
η_{eff}	effective porosity of the sediments
θ	evaporation open factor
λ	control decision variables corresponding to the membership grade
λ_h	half-life, hour
μ	membership function
μ^o	dynamic viscosity of oil, cP

ρ	vigilance parameter
ρ_{ab}	map field vigilance parameter
ρ^o	density of oil, kg/m^3
$\bar{\rho}_a$	baseline vigilance
ρ_w	density of water, kg/m^3
ϕ	molar yield coefficient
Ψ	function of dynamic relation
ω	wave frequency, Hz
ω_b	fitting parameters determined from the multiple regression analysis

CHAPTER 1

INTRODUCTION

1.1 Offshore Oil Spills

Pollution caused by accidentally release (spillage or leakage) of pollutants such as offshore oil spills cannot only cause significantly negative impacts on the environment and socio-economy but constitutes a direct hazard to marine life and human health. It is reported that in the last decade over one billion gallons of oil spilled worldwide and about six million tonnes/year entered the oceans (OPEC, 2013). Over 20 years passed after the Exxon Valdez oil spill, significant efforts have been made to study oil spills and improve response capacities and practices (Etkin and Welch, 1997). However, it is obviously not enough to match the steps of oil and gas development. The recent Deepwater Horizon catastrophe is shaping up to be one of the largest offshore oil spills in American history and an ecological nightmare of epic proportions (Bly, 2011; BOEMRE/USCG, 2011; MMC, 2011). It resulted in a set of government penalties of US $4.5 billion and an estimated total liability up to US $100 billion. When the effects to the economy and environment are taken into account, the final cost is estimated to be twice that at $240 million (Griggs, 2011).

In Canada, Newfoundland and Labrador (NL) produces about 100 million barrels of crude oil every year, representing ten percent of national crude oil production (C-NLOPB, 2011). Oil spills in NL offshore happen more often than environmental assessments predicted (Terry, 2008). Since 1997, it is estimated that roughly 2,703 barrels of drilling fluids and other hydrocarbons have been spilled into the ocean through the about 340

spills reported from NL's offshore (Terry, 2008). In 2004, about 1,040 barrels of crude oil were spilled at Terra Nova, followed by a penalty of $290,000 (C-NLOPB, 2007). In 2004, approximately 96.6 m^3 of synthetic based mud was spilled at the surface at White Rose. Husky Energy pleaded guilty to two of three counts in connection with this spill, with a penalty of $50,000 comprised of a fine of $10,000 for each count, and $30,000 to the Environmental Damages Fund (C-NLOPB, 2008). Oil spills are arising more and more concerns in harsh environments because of significant negative impacts on the marine environment and eventually human health, as well as difficulties in the physical recovery (Chen et al., 2012b).

The response to an oil spill is a dynamic, time-sensitive, multifaceted and complex process subject to various constraints and challenges. The response is dependent on a variety of factors including quantity and properties of the spilled product, location, environmental conditions, and availability and utilization of response resources at various degrees of oil weathering (Nordvik, 1999; Ornitz and Champ, 2003). The success and effectiveness of a response much rely on how efficiently the information and response recourses (vessels, devices, manpower, money, etc.) can be utilized and how optimally the decision and actions can be made (Li et al., 2012a, 2012b, 2013d). While technologies are 21st century, emergency and post emergency response to accidental pollution have remained an awkward situation with an infrastructure that is now proving to be woefully inadequate to the response in accidental pollution events such as the

Deepwater Horizon oil spill (You and Leyffer, 2011).

Meanwhile, environmental conditions always play a critical role in responses and any extreme or unfriendly conditions can further challenge the effectiveness (Jing et al., 2012a, 2013b, 2013). This is especially true in the offshore areas of Arctic and Northern Atlantic oceans, where harsh conditions such as cold water, low temperature, limited visibility, rough sea, sea ice, and strong wind, are prevailing (Owens et al., 1998; Brandvik et al., 2006). Accidental oil spills are more problematical in harsh environments due to the fragile ecosystems and the logistic challenges of cleaning up spills in regions that less accessible for sea transport (Huntington, 2008; Turner, 2010). Besides, most offshore oil recoveries require support from aircrafts, vessels and trained personnel which can be highly hindered by harsh conditions (Fingas, 2011). Due to the fast growth of offshore oil and gas development and shipping operations in northern regions of Canada, it is noticeably urgent and critical to develop new methods and improve knowledge and technical capacity for ensuring more effective responses to accidental spills in harsh environments.

1.2 Challenges in Offshore Oil Spill Response Decision Making

A necessary and important component for supporting offshore oil spill response decision making is the spill risk mapping and classification, which can support the practice of oil spill response, impacts and options evaluation, operation cost reduction,

and efficiency improvement (Richard et al., 2001; Fernando et al., 2005). The risk to an area caused by any potential offshore oil spills can be described by the offshore oil spill vulnerability index (OSVI), introduced by Gundlach and Hayes (1978), instead of Environmental Sensitivity Index (ESI) to better describe vulnerability of a shoreline area that would potentially expose to oil spills. Classification approaches are able to categorize offshore areas into zones with different levels of OSVI based on the associated impacts and probability and identify the zones which can represent significantly different characteristics from each other (Ertekin and Rudin, 2011). In current ocean and coastal management practice, the existing offshore OSVI classification focuses mainly on ecological impacts and protection of fishery or seabirds, and offshore oil spill risks have not been well considered and reflected (Chen and Li, 2012). One of the key reasons is the lack of scientific support and insufficient knowledge about oil spill risks and the uncertainties due to the inherent dynamic and complex features with meteorological, oceanic and ecological conditions (Chen et al., 2012b).

Furthermore, there is still a lack of risk assessment model in handling the variance of such vulnerabilities of different zones (i.e., local areas) (Queensland Transport, 2000). Once spilled into the marine environment, the fate and subsequent impact of oil on the environment in general and the shoreline in particular are dependent on many complex and interactive factors that may be nearly impossible to do any meaningful analysis of the subsequent outcomes (IMO, 2010). Hence a classification approach which can delineate a

region into different risk zones with similar vulnerability to an oil spill is significantly helpful to the risk assessment in an offshore oil spill event.

A few decision support systems (DSSs) have been developed for oil spill response and countermeasures (Fingas, 2001; Ornitz and Champ, 2003). For example, Pourvakhshouri et al. (2006) developed a Geographical Information System (GIS) based DSS for management plans to enable the decision maker to choose the most effective combating method for prevention, control, and/ or cleanup way against the oil spills pollution in the Strait of Malacca. Meanwhile, some models were also developed to diagnose and alert the oil spill based on the geomatic analysis (Assilzadeh et al., 2001; Brimicombe, 2003). There are also developed models out of geomatic analysis, such as Oil Spill Information System (OSIS) (Leech et al., 1993), Oil Spill Risk Analysis (OSRA) model, and General National Oceanic and Atmospheric Administration (NOAA) Operational Modeling Environment (GNOME) (Price et al., 2003; Beegle-Krause and O'Connor, 2005). However, these models usually determine response technologies based on only experience and suggest operations without support of optimization, and few of them involve approaches to handle uncertainties which widely appear in and highly affect oil spill response decisions and actions (Wilhelm and Srinivasa, 1997; Reed et al., 1999; Brebbia, 2001). Challenges also remain in resources and settings optimization for decision support in offshore oil spill due to lack of simulation of spill transport and fate. Furthermore, limited attempts have been reported in coupling of response optimization

and offshore oil spill simulation which can effectively increase the efficiency and reduce the time of response (You and Leyffer, 2011).

1.3 Research Objectives

The goal of this research is to develop a DSS to support offshore oil spill response and countermeasures in harsh environments based on the integration of offshore OSVI classification, technology screening, and a simulation-based optimization under uncertainties. The major research tasks include: 1) to develop a set of approaches of multi-features classification and ranking for offshore OSVI classification and technologies screening/ranking under uncertainties and complexities; 2) to develop a simulation-based optimization approach under dynamics and uncertainties based on the integration of simulations of oil weathering and recovery processes, dynamic programming, and uncertainty analysis; 3) to develop a DSS framework by integrating offshore OSVI classification, technologies screening and ranking, and the simulation-based optimization approaches for supporting offshore oil spill response.

1.4 Structure of the Thesis

Chapter 2 mainly focuses on the comprehensive reviews of modeling and decision support approaches and their applications in offshore oil spills, classification, simulation,

simulation-optimization coupling, as well as discussion of the key challenges in cold and harsh environments. Specific reviews efforts are given to 1) offshore oil spills and their impacts as well as corresponding preparedness and contingency planning; 2) classification under complexity and uncertainty as well as their coexistence; and 3) optimization under uncertainty and its coupling with simulation to support offshore oil spill response.

Chapter 3 describes the development of a Monte Carlo simulation based two-stage adaptive resonance theory mapping (MC-TSAM) approach for offshore OSVI classification and its application to a case study in the south coast of Newfoundland. This chapter also provides the details about the development of a Monte Carlo simulation based integrated rule-based fuzzy adaptive resonance theory mapping (MC-IRFAM) approach for response technologies screening along with a case study to test its feasibility.

Chapter 4 provides the development of 1) a fuzzy-stochastic-interval linear programming (FSILP) approach and a Monte Carlo simulation based fuzzy programming (MCFP) approach for optimization under uncertainty; 2) a dynamic mixed integer nonlinear programming (DMINP) approach for simulation-optimization coupling; and 3) a Monte Carlo simulation based dynamic mixed integer nonlinear programming (MC-DMINP) for simulation-optimization coupling under uncertainty, based on DMINP, Monte Carlo simulation, and oil weathering and recovery process modeling. A case study

8

of decision support to oil recovery and devices allocation during an offshore oil spill response process is also discussed.

Chapter 5 presents the development of an integrated DSS by integrating offshore OSVI classification, technology screening and ranking, and simulation-based optimization approaches. A case study in the south coast of Newfoundland is also provided to demonstrate the DSS.

Chapter 6 concludes this study with summarized contribution and recommendations for future research.

CHAPTER 2

LITERATURE REVIEWS

_____

The partial contents of the chapter were modified based on the following paper under preparation for journal publication:

1. Li P., Cai Q.H., Lin W. Y., Chen B., and Zhang B.Y. (2013). From Challenges to Opportunities: Towards Future Strategies and a Decision Support Framework for Oil Spill Preparedness and Response in harsh environment. Environmental Science & Technology. (Submitted).

   Role: Pu Li has been working as the leader of the student team and the leading author of the manuscript. Particularly, the contents in this chapter were solely written by Pu Li. Qinhong Cai and Weiyun Lin are members of the student team. Dr. Bing Chen is the supervisor of Pu Li and Qinhong Cai. Dr. Baiyu Zhang is the supervisor of Weiyun Lin and co-supervisor of Qinhong Cai.

2.1 Oil Spills

2.1.1 Background of offshore oil spills

A spill is usually described as accidental, occasional, or intentional release of oil. Some major spills include: the Exxon Valdez incident, the Hebei Spirit spill, the Prestige spill, the Deepwater Horizon oil spill, etc. The large-scale spills (>30 tonnes) account for merely 0.1% of incidence but make up almost 60% of the total amount of spillage (Fingas, 2011). Spills usually happen worldwide in various types of environments such as land, ocean, and watershed. The composition and behaviour of spills is dependent on types of oil. Despite the various sources, oil contains large number of same compounds and molecular structures. The chemical and physical properties of a spill usually rely on the existence and quantity of substantive compounds in oil, leading to difficulties in the evaluation of toxicity (McCoy et al., 2010).

The sources of offshore oil spills are usually varied from exploration, transportation, and other offshore activities, due to anthropogenic (e.g., equipment malfunctions, human errors) and natural (e.g., earthquakes, weather-related accidents) events. The OCEAN National Research Council (NRC) of Canada categorized all oceanic petroleum input into four categories: natural seeps, petroleum extraction, petroleum transportation, and petroleum consumption (NRC, 2003). Some studies estimated that $0.2 \sim 2.0 \times 10^6$ tonnes of oil have naturally leaked to the global marine environment in each year, with a best estimation of 600,000 tonnes (Kvenvolden and Cooper, 2003; NRC, 2003; GESAMP,

2007).

The world history witnessed a large number of oil spills and some of them had led to devastating impacts. In 1942, an alarming 484,200 tonnes of oil was reported releasing from torpedoed tankers in the eastern U.S. coastal area, equivalent to a weekly release of 20,000 tonnes of oil over 6 months (Campbell et al., 1977). In-situ burning was conducted as one of the few offshore oil spill countermeasure practices at that era. In January 1969, the Union Alpha Well blowout in Santa Barbara, southern California resulted in a release of 14,300 tonnes crude oil into the environment. Being the largest oil spill in the U.S. waters at that time, the Santa Barbara oil spill raised public outrage and caused catholic concern in the environmental protection, prompting the founding of U.S. Environmental Protection Agency (EPA) (Easton, 1999). Large-scale oil spills continued to occur in the 1970s, such as the Arrow (1970 in Canada), the tanker Metula (Chile in 1974), the tanker Urquiola (1977 in Spain), the Ekofisk blowout (1977 in Norway), the tanker Amoco Cadiz (France in 1978), the tanker Atlantic Empress (1979 in Trinidad and Tobago/Barbados), and the Ixtoc I well blowout (1979 in Gulf of Mexico) (Hayes, 1999). Despite the occurrence of large spills, the frequency of global offshore oil spills had significantly decreased since 1970s, mainly due to the enhancements of operation and prevention techniques. For example, a 46% decrease was estimated from 1988 to 1999. Such a decreasing trend was of significance because the offshore oil-related activities have remarkably increased (Etkin, 2001). Asia is the largest source of oil release with

12

over 3.4 million tonnes of spilled oil in a 50-year-period, partly due to the 1991 Gulf War (Etkin, 2002; Fingas 2010; Tunnell, 2011).

In the United States, the daily usage of petroleum products is about 3 million tons (Fingas, 2011). The north western Gulf of U.S. contains about 3,500 platforms, over 25,000 miles of pipeline, and about 50,000 drilling wells (Tunnell, 2011). A U.S. 1998-2007 statistics in oil spills indicated a moderate annual spillage from tank ships (500 tons), compared to major spillage from inland pipelines and inland tanker trucks (11,000 tons and 1,300 tons, respectively). However, tank ships were and still remain a high risk source of large spills (Fingas, 2011). On March 24, 1989, the tank vessel Exxon Valdez struck the Bligh Reef of Prince William Sound, Alaska, and released approximately 11 million gallons of crude oil to the southwestern Prince William Sound and the western coast of the Gulf of Alaska (Exxon Valdez Oil Spill Trustee Council, 1994). This incident was the largest tanker oil spill in the U.S. history at that time, and challenged the nation of its vulnerability when confronting large spills especially in cold and harsh environments (Etkin and Tebeau, 2003). More recently, the Deepwater Horizon spill (also known as the BP oil spill, and the Gulf of Mexico oil spill) has been identified as the largest marine oil spill in history (Bly, 2011; BOEMRE/U.S. Coast Guard, 2011; MMC, 2011). The spill was caused by an explosion of the Deepwater Horizon oil rig on April 20, 2010, and the subsequent sinking of the platform on April 22 in the Gulf of Mexico. Over 600,000 tons of crude oil were estimated to spill into the Gulf of Mexico,

lasted for almost three months until the Macondo well was capped on July 20 (Tunnell, 2011). The incident had brought multitudinously catastrophic impacts to human and environment, marine and wildlife habitats, economy, including: 11 deaths and 17 injuries, over 600,000 tons (or 4.9 million barrels of oil) of oil spillage, over 400 threatened species the spilled area, and severer lost for fishing industry and Gulf Coast tourism (Robinson Jr, 2010; Vilcáez et al., 2013).

In Canada, spills occures on land, at petroleum production facilities and wells. Most of offshore oil spills are from marine or refinery terminals. The Multi-State Aquatic Resources Information System (MARIS) database estimated that 1,048 accidents happened from 1980 to 2005 in the the South Coast of Newfoundland, Canada (Transport Canada, 2007b). In 2004, two large oil spills occurred in offshroe Sable Island of Nova Scotia; one spill released 4,000 litres of diesel and the other released 354,000 litres of drilling mud at an exploratory well (Amec, 2013).

2.1.2 Impacts caused by offshore oil spills

Offshore oil spills are of tremendous concern due to the enormous economic loss and the harm to ecological systems, public health, society and community they may cause. During the long run of oil and gas exploitation, the adverse impacts of oil spills have been documented in various aspects including economy, ecology and environment, public health and society/community. The total economic impact of oil spill could be broken

down into socioeconomic losses, cleanup costs, environmental damages, research costs and other costs (Liu and Wirtz, 2006). These costs could either be assigned with monetary values in a real economic world, or estimated through modeling which has been the primary tool to estimate environmental damages (Liu and Wirtz, 2006).

Based on historical data on oil spill cleaning cost, important factors driving the costs included oil type, proximity to the shoreline, location, cleanup methodology, and spill size (Etkin, 2000). After normalization to the 1999 U.S. dollar, it was estimated that the cleanup cost per unit of spilled oil followed a sequence of No.2 diesel fuel < light crude < crude < heavy crude < No. 6 fuel < No.5 fuel < No. 4 fuel. Spills of more persistent products require expensive spill response operations, and generally, fuel requires more expensive treatment than crude (Etkin, 2000). Studies also concluded that the shoreline length oiled (Etkin, 2000) and spill size (Etkin, 1999) were positively correlated with the cleaning cost, while the distance (Etkin, 1998b) from the shoreline was negatively related to costs. On the other hand, the cleanup methods were estimated with a sequence of natural attenuation ($1,286.00/ton) < in-situ burning ($3,127.87/ton) < dispersants ($5,633.78/ton) < mechanical ($9,611.97/ton) < manual (23,403.45/ton) (Etkin, 1998a).

During the Deepwater Horizon oil spill, approximately 430 miles of marsh shorelines were oiled, among which 41% (176 miles) were either heavily or moderately oiled (Zengel and Michel, 2011). Although few quantitative data were yet available on the extent of vegetation impacts, recent findings for the salt marshes in the Bay Jimmy area

of northern Barataria Bay, Louisiana documented variable impacts depending on oiling intensity (Lin and Mendelssohn, 2012). Since the spill, some recovery has been noted for oiled marshes (Mendelssohn et al., 2011). However, as of the fall of 2011, many of the most heavily oiled shorelines had minimal to no recovery (Mendelssohn et al., 2012), and only time will tell whether these shorelines will revegetate naturally before shoreline erosion occurs.

As regards to the transference of toxicity to the food chain, studies have demonstrated that oil-contaminated food can cause genotoxic damage to consumers (Lemiere et al., 2005; Chaty et al., 2008). Chaty et al. (2008) showed evidence for the bioaccumulation of oil compounds and their transference to the food chain in oil-contaminated marine food, which was agreed with Bro-Rasmussen (1996) that persistent chemicals might create a human hazard after bioconcentration when climbing the food chain. The study also demonstrated the induction of DNA damage by the metabolic transferred products which might be more toxic than their parent compounds (Chaty et al., 2008). After the Prestige oil, researchers found significantly higher DNA damage, but not cytogenetic damage (Laffon et al., 2006; Pérez-Cadahía et al., 2006, 2007) or alterations in the endocrine status in relation to the exposure (Pérez-Cadahía et al., 2008a). They also found general increases in micronucleus frequency and decreases in the proliferation index in the individuals with longer time of exposure (Pérez-Cadahía et al., 2008c). Finally, they investigated the relationship between blood levels of heavy

metals and genotoxic or endocrine parameters in the individuals (Pérez-Cadahía et al., 2008b). The authors suggested plasma levels of cortisol as a potentially relevant biomarker to assess the effects of exposure to heavy metals.

2.1.3 Preparedness and contingency planning for offshore oil spills

Most oil spills are accidental, so no one can know when, where, or how they will occur. Spills can happen on land or in water, at any time of day or night, and in any weather condition. Preventing oil spills is the best strategy for avoiding potential damage to human health and the environment. However, once a spill occurs, the best approach for containing and controlling the spill is to respond quickly and in a well-organized manner. A response will be quick and organized if response measures have been planned ahead of time. A management strategy/contingency plan is a set of instructions outlining the steps that should be taken before, during, and after an emergency.

In June 2010, Transport Canada released a plan and a policy for preparedness and response, aiming to Canada's Marine Oil Spill Preparedness and Response Regime. This plan indicates the roles and responsibilities of all sectors in an offshore oil spill, including the Transport Canada, the Canadian Coast Guard (CCG), the Environment Canada, certified response organizations, vessels, response facilities etc. (Vaughan, 2010). In addition, the Transport Canada also operates the National Aerial Surveillance Program and the Environment Canada's Canadian Ice Service to detecting oil spills at sea. The

Canadian Coast Guard (CCG) plays an important role in the response to shop-source oil spills. In 2011, the CCG updated and released the National Environmental Response Strategy for responding to major offshore oil spill happening in national or international level. The strategy is to be followed by the development of a national response policy and plan for directing its efforts, including those related to a major incident (Fisheries and Oceans Canada, 2010). Furthermore, the Environment Canada's main responsibility is to provide advice on potential risks and ecologically sensitive areas as well as key physical, biological, and cultural resources that received from Regional Environmental Emergencies Team (Ministry of the Environment Canada, 2012). In the case of any spill, the offshore operator is in charge and must activate its response plan. Operators have a tiered response program, with each tier providing equipment and resources appropriate to the size of the spill. Tier One, small spills can be dealt with immediately by the operator itself onsite, while others would require further outside assistance, in addition to the operator's on-site resources and assets. Tier Two response will in-corporate on-site equipment and resources from a Tier One response. A Tier Three response will bring additional resources on top of the assets and personnel mobilized during Tier Two (Angus and Mitchell, 2010).

In United States, before any exploration, development, or production activities, the offshore petroleum facility owners or operators must submit an oil spill contingency plan for approval according to the Bureau of Ocean Energy Management, Regulation,

and Enforcement (BOEMRE) (BOEMRE, 2010; Peterson and Fensling, 2011). The Marine Oil Spill Response and Contingency Action Plan (OSRCAP) is the most integrated method in offshore security, spill detection and tracking, spill management and mitigation, and the deployment of rapid and effective spill clean-up (Long, 2012).

When an offshore oil spill occurs in Australia, with the activation of the National Plan, the incident controller (IC) or the marine pollution controller (MPC) are required to submit a request to the Australian Maritime Safety Authority (AMSA) from the National Response Team (NRT) for personnel from the other states or the Northern Territory (NT) to assist the response (Maritime Safety Queensland, 2011; Flinders Ports, 2012). The corresponding agency is required to provide details on the management of the health and safety of individuals where an extension of deployment is undertaken (Government of Australia, 2005; Brown, 2005).

In United Kingdom, Petroleum operators are required to have Oil Pollution Emergency Plans (OPEPs) as required by the Offshore Installations (Emergency Pollution Control) Regulations 2002 (Government of United Kingdom, 2002), and the Merchant Shipping (Oil Pollution and Preparedness, response Co-operation Convention) Regulations 1998 (Government of United Kingdom, 1998; DECC, 2010). All operators must have OPEP test in offshore every year according to the International Convention on Oil Pollution Preparedness, Response and Co-operation Convention 1990 (Maritime and Coastguard Agency of United Kingdom, 2009; Britain, 2010; MMO, 2012).

In Norway, the Pollution Control Act released in 1981 describes the responsibilities and obligations of different corresponding sectors regard to the offshore oil spill in the National Contingency System (NCS) (Government of Norway, 1981). The municipalities also have the responsibility to assist the national government once a major offshore oil spill happens (Sydnes and Sydnes, 2011). The Norwegian Coastal Administration (NCA) is responsible for coordinating the private, municipal, and governmental contingency plans into a national emergency response system (Vik, 2005; EPPR, 2012).

As a member of Northwest Pacific Action Plan (NOWPAP) regional contingency plan, China has established joint training programs with Oil Spill Response and East Asia Response Limited (OSRL/EARL) (Qiao et al., 2002; PEMSEA, 2008; Song, 2008). The Japanese Ministry of Transport, through the Oil Spill Preparedness and Response in Asia (OSPAR) scheme, has provided spill response equipment including boom, skimmers, portable storage as well as dispersant spraying equipment (Assilzadeh and Mansor, 2003). The Saudi Arabian Meteorology and Environmental Protection Administration (MEPA) acts as the national response coordinator for coordinating the offshore oil spill response in the marine environment and the coastline of Saudi Arabia based on available regional and international resources (Zaindin, 1995;). The Malaysian National Oil Spill Contingency Plan (NOSCP) was formulated to control oil spill occurring within Malaysian water, and deal with adjacent oil spill in the Straits of Malacca and bordering

Asean countries (Wing, 2005).

The oil spill management strategy/contingency plan helps to minimize potential danger to human health and the environment by ensuring a timely and coordinated response. Well-designed local, state, regional, and national contingency plans can assist response personnel in their efforts to contain and clean up oil spills by providing information that the response teams will need before, during, and after spills occur. Developing and exercising the plan provide opportunities for the response community to work together as a team and develop the interpersonal relationships that can mean so much to the smooth functioning of a response. An effectively decision support system for generating such the contingency planning will significantly help improve the efficiency of offshore oil spill response.

2.2 Classification and its Application in Offshore Oil Spill Management

2.2.1 Conventional classification methods

Classification methods are used, in practice, to group simulation units into clusters, and each cluster should represent a certain type of unit characteristics (Richard et al., 2001). Ranking is a process that orders objects based on a proposed set of criteria. Sometimes, ranking can be considered to be a special process from supervised classification (Ertekin and Rudin, 2011). Classification and ranking are of necessity and

importance to support the decision making and in practice of oil spill monitoring, spill alert and response, helping reduce the set up and running cost and improves efficiency (Fernando et al., 2004). For example, it is usually time-consuming and costly to set up monitoring stations or trips in an offshore area potentially affected by oil spills (i.e., an area near offshore platform). Regions classification is able to categorize the stations or locations of monitoring trips and identify the ones which can sufficiently represent significantly different characteristics from each. However, a marine system is usually characterized by a large variety of meteorological, hydrological, and ecological features, which provides the basis for the classification and also makes it more challenging under the inherent complexity and uncertainty.

Various classification methods have been developed in the past decades (Gopal et al., 1999; Tso and Mather, 2001; Varshney and Arora, 2004; Hashemi et al., 2007; Oyana, 2009). The traditional methods can be grouped into supervised classification such as K-Nearest Neighbor (Franco-Lopez et al., 2001), Decision Tree (Yuan and Shaw, 1995), and Naive Bayes (Rish, 2001) and unsupervised classification such as Maximum Likelihood (Santosh and Yousif, 2004) and Clustering (Ng and Han, 1994). Geographical information system (GIS) and expert knowledge combined with the traditional supervised and unsupervised methods have gained recognition in classification for some environmental aspects (Hashemi et al., 2007). Running et al. (1995) developed a simple logic for classifying global vegetation based on observable and unambiguous

characteristics of vegetation structure that were important to ecosystem biogeochemistry and could be monitored on-site for model validation purposes.

Clustering (Bock, 1993; Jain et al., 1999) is one of the most commonly used traditional classification approaches. It is an exploratory data analysis method that aims to group a set of items into clusters such that items within a given cluster have a high degree of similarity, while items belonging to different clusters have a high degree of dissimilarity. A number of cluster analysis techniques have been developed such as hierarchical, partitioning, and dynamic methods (Spaeth, 1980; Gordon, 1999; Everitt et al., 2009).

Hierarchical methods yield complete hierarchy, i.e., a nested sequence of partitions of the input data. Hierarchical methods can be either agglomerative or divisive. Agglomerative methods start with trivial clustering, where each item is in a unique cluster, and end with the trivial clustering, where all items are in the same cluster. A divisive method starts with all items in the same cluster and performs divisions until a stopping criterion is met (Kraskov, 2003).

Partitioning methods try to obtain a single division of the input data into a fixed number of clusters. Often, these methods look for a partition that optimizes (usually locally) a criterion function. To improve the cluster quality, the algorithm is run multiple times with different starting points, and the best configuration obtained from all the runs is used as the output clustering. The partitioning methods mainly include k-means

clustering (Ding and He, 2004) and Fuzzy c-means clustering (Erminio and Guerrisi, 2002).

Dynamic cluster algorithms (Diday and Simon, 1976; Abrantes and Marques, 1998) are iterative two-step relocation algorithms including the construction of the clusters and the identification of the suitable representative of exemplar (means, exes, probability laws, groups of elements, etc.) of each cluster by locally optimizing an adequacy criterion between the clusters and their corresponding, representatives. The k-means algorithm, with class representatives updated after all objects have been considered for relocation, is a particular case of dynamical clustering with the adequacy criterion being a variance criterion such that the class exemplar equals the center of gravity for the cluster.

The adaptive dynamic clusters algorithms also optimize a criterion based on a measure of fit between the clusters and their representation, but at each loop of iteration there is a different distance for the comparison of each cluster with its representative (Diday and Govaert, 1977; Wang et al., 2006). The idea is to associate each cluster with a distance which is defined according to the intra-class structure of the cluster. These distances are not determined once and for all, and they are different from one class to another. The advantage of these adaptive distances is that the clustering algorithm is able to recognize clusters of different shapes and sizes.

Besides clustering approaches, statistical approaches are also most used methods in classification. Many times the training patterns of various classes overlap for example

when they are originated by some statistical distributions. In this case a statistical approach is appropriate, particularly when the various distribution functions of the classes are known. A statistical classifier must also evaluate the risk associated with every classification which measures the probability of misclassification. For example, the Bayes classifier based on Bayes formula from probability theory minimizes the total expected risk. This method is a fundamental statistical approach to the problem of pattern classification, which is based on quantifying the tradeoffs between various classification decisions using probability and the costs that accompany such decisions. It makes the assumption that the decision problem is posed in probabilistic terms, and that all of the relative probability values are known. To use Bayes classifier one must know the pattern distribution function for each class. If these distributions are not known they must be approximated using the training patterns. Sometimes the functional form of these distributions is known and one must only estimate its parameters. However, in some applications even the distribution's from is unknown and must be found (Friedman and Kandel, 1999).

The syntactic pattern classifications which are also traditional classification approaches, utilizes the structure of the patterns. Typical patterns which are subject to syntactic pattern classification are characters, fingerprints, chromosomes, etc. In general, given a specific class, a grammar whose language consists of patterns in this class is designed. For an unknown new pattern a syntax classifier analyzes the pattern (a string)

in a process called parsing and determines whether or not that string belongs to the language (class) (Friedman and Kandel, 1999).

Although various classification approaches have been developed, many environmental problems usually feature complex topographical, hydrological, and ecological characteristics and dynamic interactions of the system components and will be further complicated by incomplete knowledge and uncertain information. Such sources include but are not limited to incomplete information, sampling errors, subjective judgment, random variations of and dynamic interactions among operating factors, approximations and assumptions in measurement, and changes in environmental conditions. These challenge effective classification in environmental engineering (Bai, 2009). Conventional automated classification approaches tend to be less effective in the classification under complexity and uncertainty (Yang et. al., 2013).

2.2.2 Classification under complexity

Complexity is a property of a system which makes it difficult to characterize its overall behavior in a given language, even when given reasonably complete information about its atomic components and their interrelations (Edmonds, 1995). Complexities arise when the dimension of pattern features in classification increases and interactions among these features become more complicated. These complexities can compromise efficiency and reliability and increase the computation time of classification (Varshney and Arora,

2004; Richards and Jia, 2006).

When the number of classes is known and when the training patterns are such that there is geometrical separation between the classes a set of decision functions can be often used to classify an unknown pattern (Friedman and Kandel, 1999). The main obstacles to the achievement of high-quality classification are small sample sizes and complex distributions. On the one hand, a too strict limitation on the class of decision functions poses the question of whether this class is adequately consistent with the true distribution; the greater the inconsistency, the poorer is the classification. On the other hand, the more complex the class of functions used for a small sample size, the greater is the classification error. Consequently, the complexity of the chosen class of functions must match the existing sample size. The relation between the complexity of the class of decision functions, the sample size, and the complexity of the distributions comprises the sum and substance of the statistical robustness problem for classification decision functions (Richard et al., 2001).

The characters of environmental problems are complex due to a variety of features. Complexities develop when the number of input features in the system expands and the interactions in these features become intricate, as well as the influence by factors outside the system. The complexities can reduce the efficiency and increase the required time for classification process. Furthermore, complexities may also lead to low accuracy in classification results. How to better handle uncertainty and complexity has become more

prominent in watershed classification (Richards and Jia, 2006). Therefore, a classification method that can efficiently handle the complexity is critical and desired to support efficient environmental modeling and management practices.

In order to handle complexities, artificial neural networks (ANN), which is a series of mathematical or computational models that are inspired by the structure and/or functional aspects of biological neural networks, was also introduced as an alternative to statistical classifiers (Carpenter and Grossberg, 2003; Jeffrey et al., 2004; Xu et al., 2009). For example, an unsupervised classification approach, adaptive resonance theory (ART), and its supervised extension, adaptive resonance theory mapping (ARTMap), are among the most widely recognized ANN approaches for classification/ranking (Carpenter and Grossberg, 2003; Tang and Yan, 2007).

The neural network approach assumes that a set of training patterns and their correct classifications are given. The architecture of the net including input layer, output layer and hidden layers may be very complex. It is characterized by a set of weights and activation function which determine how any information (input signals) is being transmitted to the output layer. The neural network is trained by training patterns and adjusts the weights until the correct classifications are obtained. It is then used to classify arbitrary unknown patterns (Abe, 1997; Friedman and Kandel, 1999).

Neural networks have much in common with the structures needed for pattern classification. Pattern classification and neural networks go back to the same roots in the

historic evolution of artificial intelligence (AI) techniques. The idea of neural networks is taken from biological systems performing pattern classification functions. It is no wonder that neural networks are considered to be predestined pattern classifiers. In this role they agree with the concepts developed in conventional pattern classification (Mandic and Chambers, 2001; Dunne, 2007).

The neural network research, from the viewpoint of information processing, started from the neuron model proposed by McCulloch and Pitts (1943). The output of the model takes the values of 1 and 0 as discussed afterwards, and when the input exceeds some predetermined threshold, the output changes stepwise from 0 and 1. From the end of the 1950's to the 1960's, Rosenblatt et al. (1962) developed preceptrons which connect the above neurons in layers and used them to study pattern classification. The perceptron is the origin of the now widely used multilayered network. Minsky and Papert (1969) showed the limitation of perceptrons, i.e., that they are only applicable when data belonging to different classes are linearly separable, interest in neural network rapidly shrank.

Neural networks have been shown (Cybenko, 1989; Funahashi, 1989; Hornik et al., 1989) to be able to approximate any continuous function arbitrarily well when sufficiently many hidden nodes are used. In the Bayesian context, the posterior is consistent (Lee, 2000). These properties make neural networks a good method for nonparametric regression. Thus, they do not have to choose a particular parametric form

for the model.

In supervised classification tasks, a classification model is usually constructed according to a given training set. Once the model has been built, it can map a test data to a certain class in the given class set. Many classification techniques including decision tree (Qinlan, 1986; Freund, 1995), neural network (NN) (Lu et al., 1996), support vector machine (SVM) (Boser et al., 1992; Vapnik, 1995), rule based classifiers systems etc. have been proposed. Among these techniques, decision tree is simple and easy to be comprehended by human beings. SVM is a new machine learning method developed on the Statistical Learning Theory. SVM is gaining popularity due to many attractive features, and promising empirical performance. SVM is based on the hypothesis that the training samples obey a certain distribution which restricts its application scope. Neural network classification, which is supervised, has been proved to be a practical approach with lots of success stories in several classification tasks. However, its training efficiency is usually a problem, training on only the new silhouette could result in the network learning that pattern quite well, but forgetting previously learned patterns. Although retraining may not take as long as the initial training, it still could require a significant investment. Adaptive resonance theory (ART) was developed to solve this problem by using the short-term memory to storage the contrast-enhanced pattern, and the long-term memory to implement an arousal mechanism, whereas the STM is used to cause gradual changes in the long-term memory (Grossberg, 1976).

2.2.3 Classification under uncertainty

Many features and their interrelationships are hardly measured or quantified accurately, leading to uncertainties. Uncertainty is a state of having limited knowledge where it is impossible to exactly describe existing state or future outcome. It can arise at any stage of a pattern classification process, resulting from incomplete or imprecise information, ambiguity or vagueness in inputs, ill-defined and/or overlapping boundaries among classes or regions, and indefiniteness in defining/extracting features and relations. It is therefore necessary in classification to make sufficient provision for representing uncertainties at every stage of classification so that results are associated with the least possible uncertainty (Richard et al., 2001; Lloyd, 2006).

In order to deal with uncertainties, fuzzy set theory, which uses sets whose elements have degrees of membership, is integrated with traditional classification methods (Patino, 2005; Bai, 2009). For example, Sauder et al. (2003) used fuzzy classification, which is a process of grouping elements into a fuzzy set whose membership function is defined by the truth value of a fuzzy propositional function, to characterize watershed heterogeneity with more accurate predictions than those in supervised classification. The supervised classification analyzes the training data and produces an inferred function to predict or classify the inputs into certain preset groups. Lucas et al. (2008) developed a fuzzy classifier as an extension of the approach in which uncertainty was represented by an

additional dimension in land cover classification.

Quite often classification is performed with some degree of uncertainty. Modern control theory owes much in its development to mathematical models. However, when it is applied to real problems, difficulties are often encountered in approximating real controlled objects by models because of the vagueness or fuzziness of the controlled objects. In addition, since most control theory is based on linear systems, it is difficult to develop control systems with good performance when real controlled objects have strong nonlinearity (Friedman and Kandel, 1999). Since the fuzzy set theory is a generalization of the classical set theory, it has greater flexibility to capture various aspects of incompleteness or imperfection about real life situations (Zadeh, 1965). The significance of fuzzy set theory in the realm of pattern classification is effectively justified in various areas such as representing input patterns as an array of membership values denoting the degree of possession of certain properties, representing linguistically defined input features, representing multiclass membership of ambiguous patterns, generating rules and inferences in linguistic form, extracting ill-defined image regions, and describing relations among them (Pedrycz, 1990; Pal et al., 2000).

To apply fuzzy set theory to a system, experts' knowledge on the system needs to be expressed explicitly in if-then fuzzy rules. When the input to the fuzzy rules is given, the output is determined by inference using the fuzzy rules. This process of determining the output from input is one method of function approximation which is one of the major

uses of multilayered networks. Function approximation is readily extended to pattern classification (Abe, 1997). Either the classification outcome itself may be in doubt, or the classified pattern may belong in some degree to more than one class. It is thus introduced fuzzy classification where a pattern is a member of every class with some grade of membership between 0 and 1 (Friedman and Kandel, 1999).

2.2.4 Classification under coexistence of uncertainty and complexity

Given that uncertainty and complexity coexist in real-world systems, many attempts have been made in the last decade to design hybrid approaches, which focus on the integration and complementation of different approaches to handle complex situations, to pattern classification by combining the merits of individual techniques (Gamba and Dellacqua, 2003; Qiu and Jensen, 2004). Fuzzy set theory and neural network can be integrated together to handle the system where complexity and uncertainty coexist. For example, Giles (1995) used ANN as an alternative to the statistical classifiers and integrated fuzzy output from a remote sensing data set that was preprocessed with ancillary data available in a GIS to increase the accuracy with which land cover was mapped. Lee et al. (1999) developed a neural-fuzzy classifier derived from the generic model of a 3-layer fuzzy perceptron for land cover classification and compared it with the maximum-likelihood classifiers. The result showed that the neural-fuzzy classifier was considerably more accurate in general but less accurate in some particular areas. They

33

concluded that the neural-fuzzy model could be used to classify the mixed composition area. Han et al. (2002) conducted a comparative evaluation of Neural-Fuzzy, Neural Network, and Maximum Likelihood Classifiers for land cover classification. Their results indicated that the neural-fuzzy classifier was the most accurate method for land cover classification and suitable under the condition of uncertainty and complexity. Gopal et al. (1999) used the adaptive resonance theory mapping (ARTMap) networks to conduct the classification of global land cover based on normalized difference vegetation index (NDVI) providing a viable technique for global land cover classification.

Different pattern classifiers trained for the same application can be viewed as approximations from different directions to the same goal, just as different starting point are possible to reach the same peak in a mountainous territory. Therefore, different pattern classifiers, derived from different concepts, using different sets of measurements, or designed with different constellations of their basic design parameters tend to behave differently in the individual case, even if they may exhibit the same long-term error rates. Under these circumstances combining different pattern classifiers developed for the same task bears the promise of improving the overall performance, just as in everyday life more than one expert is consulted if a difficult case is to be settled. Since different pattern classifiers have different strengths and weaknesses, classifier combination must be led by the goal of making the respective strengths effective and repelling the deficiencies (Schurmann, 1996). Many attempts have been made in the last decades to design hybrid

systems for pattern classification by combining the merits of individual techniques. An integration of neural networks (NNs) and fuzzy set theory is one such hybrid technique and known as neuro-fuzzy (NF) computing (Pal and Ghosh, 1996; Pal and Mitra, 1999; Abe, 2001).

Both NNs and fuzzy approaches are adaptive in the estimation of the input-output function without any precise mathematical model. NNs handle numeric and quantitative information while fuzzy approaches can handle symbolic and qualitative data. Apart from this, in a fuzzy classifier patterns are assigned with a degree of belonging to different classes. Thus the partitions in fuzzy classifiers are soft and gradual rather than hard and crisp. Therefore, an integration of neural network and fuzzy approaches should have the merits of both and enable one to build more intelligent decision making systems. Fuzzy set theory is found to be more suitable and appropriate to handle these situations reasonably (Pedrycz, 1990; Kuncheva, 2000).

In the NF paradigm, much research effort has been made (Keller and Hunt, 1985; Ghosh and Pal, 1993; Pal and Ghosh, 1996; Pal and Mitra, 1999; Abe, 2001; Baraldi et al., 2001; Boskovitz and Guterman, 2002; Han et al., 2002; Gamba and Dellacqua, 2003; Qiu and Jensen, 2004). NF hybridization is done broadly in two ways: NNs that are capable of handling fuzzy information (named as fuzzy-neural networks, FNN), and fuzzy systems augmented by NNs to enhance some of their characteristics such as flexibility, speed and adaptability (named as neural-fuzzy systems, NFS) (Pal and Ghosh,

1996; Pal and Mitra, 1999).

The NN and fuzzy approaches discussed so far can be applied to pattern classification and function approximation. Buckley et al. (1992) reported that fuzzy systems and multilayered networks were mathematically equivalent in that they are convertible. But since the two approaches differ, they have their own advantages and disadvantages.

With multilayered networks, knowledge acquisition is done by network training. Namely, by gathering input-output data for pattern classification of function approximation and training the network using these data by the back propagation algorithm, the desired function is realized. On the other hand, fuzzy rules need to be acquired by interviewing experts. But for complicated system expert knowledge that is obtained intuition and experience is difficult to express in a rule format. Thus rule acquisition requires much time. As methods to extract fuzzy rules from numerical data, Wang and Mendel's method (1992) extracts fuzzy rules directly from data and Lin and Lee's method (1991) uses neural networks to train the neural network in which fuzzy rules were imbedded, extract fuzzy rules from the trained network, and tune the membership functions of extracted fuzzy rules using the same neural network.

The major shortcoming of neural networks is represented by their low degree of human comprehensibility. Many attempts have been made to solve this shortcoming of neural networks, by compiling the knowledge captured in the topology and weight matrix

of a neural network, into a symbolic form; most of them into sets of ordinary if-then rules (Towell and Shavlik, 1993; Yoo, 1993; Craven and Shavlik, 1993), or into sets of fuzzy rules (Lin and Lee, 1991). The fuzzy neural networks are often used as an auto-tuning method for the determination and the adjustment of fuzzy rules. However, major challenges to existing neuro-fuzzy approaches remain: 1) complicated process in input data preparation and selection for fuzzy combinations and model calibration (Moghaddamnia et al., 2009); 2) decreasing efficiency in treating dispersive data; and 3) difficulties in generating fuzzy membership from insufficient information (Li et al., 2009a, 2011; Chen et al., 2012a).

2.2.5 Offshore oil spill vulnerability index (OSVI) classification in offshore oil spill

Classification are necessary and important to support decision making and practice in monitoring and early warning of offshore oil spill, as well as the risk/vulnerability zone classification and characterization, helping to reduce the set up and running cost and improving efficiency (Richard et al., 2001; Fernando et al., 2004). For example, regions classification is able to categorize the stations or locations of monitoring trips and identify the ones which can represent significantly different characteristics from each (Ertekin and Rudin, 2011). However, a marine system is usually characterized by a large variety of meteorological, hydrological, and ecological features, which provides the basis for the classification and also makes it more challenging

because of the inherent complexity and uncertainty. Ranking extends conventional multiclass classification in the sense that it does not only predict candidates to groups but instead gives an ordering of all candidates. Besides, it is well-known that a number of other learning tasks can be formalized within the setting of ranking (Furnkranz et al., 2008).

Recently, classification techniques employed in offshore oil spill are mainly focusing on determination of the occurrence of a spill, and the type of spilled oil. Fingas (2001) describes the guidelines for estimating oil thickness using visual surveillance by the appearance of oil varying from silvery-sheen to dark brown. Usually, this visual detection for oil spill is not reliable because oil can be confused with many natural and atmospheric phenomena (e.g., sea weeds and fish sperm) which can produce dark areas in images similar to oil spills. The presence of these dark areas (usually referred to as look-alikes) is significantly challenging to the detection of oil spills (Migliaccio and Trangaglia, 2004; Brekke and Solberg, 2005). Therefore, classification techniques are usually employed to process the remote sensing information to determining an offshore oil spill (Ivanov and Zatyagalova, 2008; Topouzelis, 2008; Topouzelis et al., 2009).

The application of risk assessment techniques to oil spills at sea is primarily used as a way by which to determine the level of the threat of an oil spill from shipping activities or offshore oil and gas production activities in a defined area of the coast. Methods of determining levels of risk/vulnerability are generally categorized as

Qualitative, Semi-Quantitative and Quantitative. The application of risk/vulnerability in a comparative way allows identification of activities which result in higher levels of risk, without the need to determine the absolute value of the risk. This alone dramatically reduces the cost of the assessment and can provide the key information needed to establish safety priority and thus inform the initiation of an offshore oil spill management system. The depth of the analysis depends on the magnitude of the risk and the details in classification and characterization of risk/vulnerability zones (IMO, 2010).

Risk assessment underpins all preparation and planning for marine oil spill response includes the assessment of both the likelihood of a spill occurring and the consequences or effects of spill (Maritime New Zealand, 1992, 2006).Tremendous works have been made to evaluate risks due to marine oil spills in many maritime countries including Norway, United Kingdom, United States, Canada, and Austria (Turner, 2010). Many existing risk analysis tools are available to help understand the risks. One of the most widely used toos is the Exposure Related Dose Estimating Model (ERDEM) which is a physiologically-based pharmacokinetic (PBPK) and pharmacodynamic (PD) modeling system, developed by EPA scientists to predict how chemicals move through and concentrate in human tissues and body fluids. The PBPK/PD model structure in ERDEM consists of a series of differential mass balance equations in the physiological compartments of humans and laboratory animals. The system enables users to study the exposure and tissue dosimetry relationships and the toxicological risk metrics of interest

(U.S. EPA, 2004; Blancato et al., 2006; Zhang et al., 2007). The U.S. EPA has also provided a tool of generic ecological assessment endpoints (GEAEs) to help identify and specifically define assessment endpoints for particular assessments. This tool has been widely applied to various assessment scenarios, providing a foundation for the development of endpoints for specific assessments during problem formulation. It has also been used by risk assessors and risk managers for generic ecological assessment endpoints, supporting policies and precedents establishment, and improving the scientific basis for ecological risk management decisions (U.S. EPA, 2004; Landis and Kaminski, 2007). In order to conduct comprehensive risk assessment for multi-pathway ecological by simultaneously calculating risk values for multiple chemicals, from multiple sources, at multiple exposure locations, an integrated system of EcoRisk View has been developed to fully implement the U.S. EPA guidance for evaluating ecological risk (U.S. EPA, 1999). By integrating with the U.S. EPA Human Health Risk Assessment Protocol (HHRAP) module (U.S. EPA, 1998), a BREEZE Risk Analyst modeling system was developed for human health and ecological risk assessment. This system was designed to conduct multi-pathway human health risk assessments and food-web based ecological risk assessment modeling with geographic information system (GIS) functions. Recently, a series of mechanistic risk assessment models have developed for the European Union (EU) such as the mechanistic effect models for ecological risk assessment of chemicals (MEMoRisk) (Preuss et al., 2009) and the Chemical Risk Effects Assessment Models

(CREAM) (Grimm et al., 2009).

Risk assessment appears to be a natural tool for oil spill risk management. However, the concept of risk in the context of oil spill prevention, preparedness and response is complicated by the range of possible spill scenarios and of the different outcomes that can occur as a result of a single scenario. Although risk assessment is widely used, the application of risk assessment methodology to oil spills has not been standardized. In the absence of such a standardized methodology, it is often difficult to know how best to evaluate the risks associated with oil spills. Only few preliminary studies were conducted in the risk assessment for offshore oil spills (IMO, 2010). Such assessment efforts have never been linked with oil spill modeling and response decision making in a real-time and interactive manner (Bogdanovsky, 2005; James et al., 2006; Rotkin-Ellman et al., 2012; Deng et al., 2013). Therefore, there is a lack of scientific understanding and effective control of the influence caused by response decisions and actions on the risk levels in the concerned areas, and consequently it is hard to make real-time adjustments to mitigate any negative effects (James et al., 2006; Moharramnejad et al., 2010; Depellegrin and Blazauskas, 2013). The other difficulty with determining the relative vulnerability/risk of each region is the assessment units are based on regions rather than local areas. This means that each regional unit may contain areas of high vulnerability/risk to oil spills. There is still lack of risk assessment model in handling the variance of such vulnerabilities of different zones (i.e., local areas)

(Queensland Transport, 2000). Once spilled into the marine environment, the fate and subsequent impact of oil on the environment in general and the shoreline in particular are dependent on so many factors that it may be nearly impossible to do any meaningful analysis of the subsequent outcomes (IMO, 2010). Hence a classification approach which can delineate a region into different risk zones with similar vulnerability to an oil spill is significantly helpful to the risk assessment in an offshore oil spill event. The other challenge in the existing risk assessment models for offshore oil spill still remains in the dynamical linkage with the response operations (Queensland Transport, 2000).

Spill risk maps are based on classification of the concerned offshore areas which are necessary and important to support decision making and practice of oil spill response, facilitating impacts and options evaluation, set-up and running cost reduction, and efficiency improvement (Richard et al., 2001; Fernando et al., 2005). Classification approaches are able to categorize offshore areas into zones (or risk profiles) with different levels of risk to oil spills based on the associated impacts and probability and identify the zones which can represent significantly different characteristics from each other (Ertekin and Rudin, 2011). The existing classification or delineation of risk zones are mainly focus on ecological impacts and protection of fishery or seabirds. Offshore oil spills have not been well considered and reflected in ocean and coastal management practice (Chen and Li, 2012). One of the key reasons is the lack of scientific support and insufficient knowledge about oil spill risks and the uncertainties due to the inherent dynamic and

complex features with meteorological, oceanic and ecological conditions (Chen et al., 2012b).

Another challenge is how to screen response technologies once an oil spill happens. Recent practices in screening technologies for offshore oil spill responses are mainly based on experiences which may cause high uncertainties to operation. There are only a few preliminary attempts that have been made regarding these perspectives (Li et al., 2013a). Therefore, classification techniques with additional consideration of multi-features in eco-environment and social-economy of the region are necessary to further support screening technologies.

2.3 Optimization and Simulation-Optimization Coupling

2.3.1 Optimization in environmental engineering

Environmental engineering is involved with the monitoring, prevention, control, and remediation of contaminants, as well as the efficient, economic utilization and management of natural resources like water, including the preservation of its quality (Koutseris et al., 2010). Areas of environmental engineering which really pioneered the use of optimization techniques include water resource management, wastewater treatment, and municipal solid waste management design, operation and management (Li and Chen, 2011; Chen et al., 2012a). Optimization tools are utilized to facilitate optimal decision

making in the planning, design and operation in environmental management. The use of optimization tools as the most important component of decision support systems are not confined only to the quantity aspect of resource, but also the mitigation of pollutants in a regional scale, operation of treatment plants and scheduling, designing of optimal strategies for treatment process, minimizing system cost or maximizing profit etc. (Mayer and Muñoz-Hernandez, 2009).

The application of optimization techniques is most challenging in offshore oil spill response, due to the large number of decision variables involved, uncertain information of the inputs, and multiple objectives, as well as the real-time operation of a system.

2.3.2 Optimization under uncertainties

Uncertainty is one of the major hindrances in improving the efficiency of optimization for environmental management, which may arise from a variety of possible sources. Such sources include but not limited to incomplete information, errors in sampling, subjective judgment, random variations of and dynamic interactions among operating factors, approximations and assumptions in measurement, and changes of environmental conditions (Huang et al., 1993). The uncertainties lead to difficulties in developing optimization models for supporting decision making in environmental management and impair the confidence of decisions. Consequently traditional deterministic programming methods may face dilemma in supporting optimization for

environmental management because of their weakness in reflecting uncertain information. Uncertainties in environmental management can be classified into two categories - probabilistic and possibilistic, which are commonly represented by stochastic analysis and fuzzy set theory, respectively (Ramik and Vlach, 2004, Lin et al., 2009, Liu et al., 2009).

In previous studies, the commonly used methods for handling the above uncertainties include fuzzy programming (FP) (Huang et al., 1993; Chang and Lu, 1997; Ramik and Vlach, 2004), stochastic programming (SP) (Pereira and Pinto, 1985; Schultz, 1996; Lin et al., 2009), and interval programming (IP) (Huang et al., 1992; Liu et al., 2009; Lv et al., 2009). The FP method, which considers such uncertainty as fuzzy sets, is effective in reflecting ambiguity and vagueness in resource availabilities; the SP method has the ability to handle random input information; while the IP method uses upper and lower bounds to approximate uncertainties when the data are insufficient (Huang et al., 1992). However, each of these methods only focuses on one type of uncertainty, leading to difficulties in handling coexistence of uncertainties which is commonly observed in a environmental management system. For example, for a waste generation rate, it may have different levels with corresponding probabilities, and the definition for each level may also be uncertain due to subjective judgments or ambiguities (Huang et al., 2001). Consequently, FP, SP, and IP were combined together to treat the coexistence of various types of uncertainties in environmental management (Li et al., 2007).

For example, Huang et al. (2001) developed an integrated fuzzy-stochastic linear programming model and applied the model to environmental management, which could effectively communicate uncertainties into the optimization process and generate reliable solutions under different significance levels. As another example, Maqsood and Huang (2003) and Li et al. (2008) developed the mixed integer two-stage interval stochastic linear programming by integrating two-stage stochastic programming and chance constrained programming, and interval mathematical programming within an integer programming framework. The developed approach could reflect the dynamic, interactive, and uncertain characteristics of the solid waste management system, and address issues concerning waste diversion and landfill prolongation as deemed critical by the local authority. Li et al. (2006) developed an interval fuzzy two-stage stochastic mixed-integer linear programming method to facilitate capacity-expansion planning for waste-management facilities within a multi-period context, and for examining various policy scenarios that are associated with different levels of economic penalties when the promised targets are violated.

Stochastic techniques can handle the probabilistic type of uncertainties in which the probability distributions are used to represent random variability of parameters (Blair et al., 2001; Seuntjens, 2002; Baudrit et al., 2007). Fuzzy techniques can be used to express the possibilistic type of uncertainties where vagueness of parameters is characterized by membership functions (Qin and Huang, 2008; Xu et al., 2009; Yang et al., 2010).

46

However, the definition of probability distributions is usually suffered from lack of sufficient data; and membership functions may lead to loss of information when some parameters are represented by stochastic variables and/or when inappropriate subjective judgment is involved (Li et al., 2007; Qin and Huang, 2008; Yang et al., 2010). Furthermore, the two types of uncertainties frequently coexist, so called dual uncertainties, in environmental systems. Consequently integration of both methods has been considered in the literature (Cheng et al., 2009). However, the previous studies usually face the difficulties ineffective linkage of these two different algorithms and appropriate interpretation of the relevant results. Therefore, many of these studies treat dual uncertainties separately instead integratively (Liu et al., 2004; Li et al., 2006; Qin and Huang, 2008; Yang et al., 2010).

Although many studies on environmental management were conducted under uncertain conditions of fuzzy, stochastic, and interval coexistence (Guo et al., 2010), the solution to the programming problems of integrating fuzzy method with the other two was inefficient (Nguyen, 2007a, 2007b, 2007c). The commonly used approaches of integrating FP with SP and IP were featured by defuzzifying and derandomizing fuzzy random variables in a sequential (Luhandjula, 1996, 2004; Iskander, 2005) or in a simultaneous manner (Liu, 2001; Liu and Liu, 2002, 2005). Either defuzzification or derandomization could only be applied before or after the SP or IP approach, which limited their abilities in dynamic integration. In the sequential approaches, the

defuzzifying process was applied followed by the derandomizing, which led to a major disadvantage in generating a large number of additional constraints and variables. In the simultaneous approaches, both defuzzifying and derandomizing processes were simultaneously employed by calculating the expected value of fuzzy random variables. The obtained deterministic linear program was relatively simple, but the process for determining the expected value was complicated and time consuming (Nguyen, 2007a).

In order to surmount these drawbacks, Nguyen (2007a, 2007b, 2007c) developed a new method to convert the fuzzy and fuzzy stochastic linear programming (LP) problems into the conventional LP models by measuring the attainment values of fuzzy numbers and/or fuzzy random variables as well as superiority and inferiority between triangular fuzzy numbers (or triangular fuzzy stochastic variables). An attainment value is a degree of attainment of the fuzzy goal that is considered to be a concept similar to a degree of satisfaction of the fuzzy decision when the fuzzy constraint is replaced by the fuzzy expected payoff. It can also be interpreted as a possibility of attainment of the fuzzy goal.

Nguyen's method finally resulted in a simple deterministic LP model, which contained a few additional constraints and variables and could be solved easily. However, this method only considered the situation when the source (right-hand-side, RHS) is a strict constraint demand (left-hand-side, LHS), otherwise, significant errors may occur. Furthermore, the uncertainty represented by interval parameter was not taken into account.

There are some attempts to deal with stochastic and fuzzy uncertainties simultaneously. For instance, Huang et al. (2001) proposed an integrated fuzzy-stochastic linear programming model which could effectively deal with different types of uncertainties in optimization process and could obtain reasonable and reliable solution under different significant levels. Guo and Huang (2009) proposed an approach to consider the dual uncertainties in water resource management by describing the parameters as probability distribution and fuzzy sets. They also proposed a concept of distribution with fuzzy probability to reflect the dual-uncertainty characteristics of parameters. Li et al. (2009b) proposed an inexact fuzzy-stochastic constraint-softened programming method to deal with possibilistic and probabilistic uncertainties, and applied to long term planning of an environmental management system. Based on a multistage fuzzy-stochastic integer programming model, a fuzzy-stochastic-based violation analysis approach was developed to help water resources management (Li et al., 2009b). These studies propose some possible solutions to handle dual uncertainties of possibility and probability. However, they are significantly restrained on how to simultaneously deal with continuous stochastic variables and subjective information (presented by probability density function and fuzzy sets) (Yang et al., 2010).

To address the limitation in treating continuous stochastic variables, Monte Carlo simulation can be used to generate enough required input parameters to solve the insufficient data problems if the probability density function can be accurately estimated

or subjectively selected (Freeze et al., 1991; Vose, 1996; Garthwaite et al., 2005). In real-world situations, the continuous stochastic variables usually include subjective and objective information, leading to the dual uncertainties of possibility and continuous probability. To handle such dual uncertainties is beyond the ability of Monte Carlo simulation itself (Guyonnet et al., 2003; Yang et al., 2010). The integration of fuzzy programming with Monte Carlo simulation can be a promising solution (Sadeghi et al., 2010). However, due to the difficulties in integrating fuzzy programming with Monte Carlo simulation, only a few studies are reported and they are all used to assess health risk issues (Guyonnet et al., 2003; Chen et al., 2003; Liu et al., 2004; Sadeghi et al., 2010; Ping, 2010). In addition, because of the complex iteration in optimization algorithm, the integration of fuzzy programming and Monte Carlo simulation becomes challenging, and no such study is applied in optimization especially offshore oil spill response and countermeasures.

2.3.3 Coupling of optimization and simulation

Computer simulations are used extensively as models of real systems to evaluate output responses. Applications of simulation are widely found in many areas including supply chain management, finance, manufacturing, engineering design and medical treatment (Fu and Hu, 1995; Kim and Ding, 2005; Semini and Fauske, 2006). The choice of optimal simulation parameters can improve the efficiency of operation, but configuring

them well remains a challenging problem. Historically, the parameters are chosen by selecting the best from a set of candidate parameter settings (Kappa et al., 2012). Simulation based optimization is an emerging field which integrates optimization techniques into simulation analysis (Fu, 1994, 2002; Andradottir, 1998; Rubinstein and Melamed, 1998; Law and Kelton, 2000; Gosavi, 2003). The corresponding objective function is an associated measurement of an experimental or numerical simulation. However, due to the complexity of the simulation, the objective function may be difficult and expensive to evaluate. Moreover, the inaccuracy of the objective function often complicates the optimization process, and deterministic optimization tools may lead to inaccurate solutions.

Dynamic Programming (DP) problems are a special type of simulation-based optimization problems with internal time stages and state transitions (Bertsekas, 2005). The objective function of these problems is not a single black-box output, but typically is a combination of intermediate costs during state transitions plus a cost measurement of the final state. Appropriate controls are determined at each time stage, typically in a sequential favor (Djennas et al., 2012).

2.3.4 Offshore oil spill simulation

After offshore oil spill, various transformation processes will occur and many of these processes are relating to the behavior of the oil. A series of processes regarding the

physical and chemical properties of the oil occur right after the oil spill, which are the weathering processes with the most important processes of evaporation and emulsification. The other important group processes are relating to the oil movement in offshore (Fingas, 2010). Usually the weathering and movement processes can strongly interact with each other in the offshore environment. These processes mainly include evaporation, dissolution, emulsification, dispersion, biodegradation, spreading, photolysis, advection, diffusion, sedimentation, and the interaction of oil slick with the shoreline (Gundlach and Hayes, 1978; Torgrimson, 1980; Korotenko et al., 2001). Generally, the oil properties, hydrodynamics, meteorological and environmental conditions play important roles in the physical, chemical and biological processes for the spilled oil transport and fate (Reed et al., 1999; Brebbia, 2001). Some of the widely used weathering and movement processes of offshore spilled oil are listed in Table 2.1.

In the past three decades, many integrated models have been developed for the spilled oil transport and fate based on trajectory method, many of which focus on the surface movement of spilled oil (Mackay et al., 1980; Huang, 1983; Shen et al., 1986; Shen and Yapa, 1988; Yapa et al., 1994; Spaulding, 1995; Lonin, 1999; Chao et al., 2001). These sytems have been applied in river-lake system (Shen et al., 1986; Shen and Yapa, 1988; Yapa et al., 1994); and seas (Lonin, 1999; Chao et al., 2001; Wang et al., 2005, 2008). Some commercial oil spill models, such as, the Coastal Zone Oil Spill Model (COZOIL) (Reed et al., 1989), GNOME (Galt et al., 1991), Oil Spill Model and

Response System (OILMAP) (Howlett et al., 1993), World Oil Spill Model (WOSM) (Kolluru et al. 1994), have been used to determine the oil movement and distribution in the ocean. However, there only few researches focus on the transport of spilled oil associating with the simultaneous tidal currents, and no study is conducted in the field of strong tide and tidal currents (Wang et al., 2005, 2008). Furthermore, there are limited studies in the vertical distribution of oil droplets and the advection forces (Wang et al., 2008; Wang and Shen, 2010). The studies in the coupling of these simulations with the optimization for offshore oil spill response and countermeasures are significantly rare (You and Leyffer, 2011; Li et al., 2012b, 2013c).

Table 2.1 Weathering and movement processes of offshore spilled oil

Process	Description of process	Frequently used equations	Relative reference
Evaporation	• volatile components escape from the spilled oil surface to the atmosphere • the most important weathering process • the primary reason of oil volume reduction in the initial stage of spill (about 20~50% of crude oil and over 75% of refined products) • components with boiling points that are lower than 200 °C will evaporate within 24 hours after spill • relies on the physicochemical properties of oil, temperature, wind, and wave • can increase the viscosity and density of oil	$FE = 1 - \exp\left(-\left(\left(\dfrac{1.5 \times 10^{-5} TU_w^{0.5}}{M^2}\right)\left(\dfrac{P}{\rho}\dfrac{M}{RT}\right)\right)/h_s\,t\right)$ $FE = \dfrac{BT_G}{T}\ln\left(1 + C_B\dfrac{T_G}{T}\exp\left(C_A - C_B\dfrac{T_0}{T}\right)\right)$ $FE = \dfrac{c + d \times (T - 273.15) \times Ln(t)}{100}$ $FE = (\ln P_0 + \ln(C_C K_E t + 1/P_0))/C_C$ $FE = \dfrac{K_E AZP}{RT}\,t\,\dfrac{M}{\rho}$	Mackay et al., 1980; Stiver and Mackay, 1984; Fingas, 1995; Brebbia, 2001; Wang et al., 2005; Nazir et al., 2008; Inan and Balas, 2010; Galeev and Ponikorov, 2011; Fingas, 2011; Zhong and You, 2011; Berry et al., 2012.
Dissolution	• soluble components (light aromatic hydrocarbons compounds) dissolve in to the water column • immediately occurs after the oil spill • relies on the physicochemical properties of the spilled oil • more less than the evaporative amount (about 1/100 to 1/10) • dissolved components can be quickly diluted • environmental consequences are of significance due to toxic effect on marine organisms	$S_d = K_d AS_0 \exp\left(-\alpha_d t\right)$ $S_d = K_d AZS_0 t\dfrac{M}{\rho}$	Cohen et al., 1980; Huang and Monastero, 1982; Chao et al., 2001, 2003; Wang et al., 2005; Riazi and Roomi, 2008; Goncharov, 2009.

Emulsification	• water droplets enters the oil slick • unstable (30-40% of water), semi-stable (40-60% of water), and stable (60-80% of water) forms in the oil slick • can lead to emulsion with up to 70% of water • significantly changes the physicochemical properties of oil (i.e., density and viscosity) • light oil is usually not emulsified, while the crude oil is easily emulsified	$\dfrac{dY}{dt} = 2 \times 10^{-6}(U_w + 1)^2\left(1 - \dfrac{Y}{C_3}\right)$ $Y = \left(1 - \exp\left(-\dfrac{K_a}{Y_w^F}(1 + U_w)^2 t\right)\right)$	Mackay et al., 1980; Rasmussen, 1985; Mackay and McAuliffe, 1988; Sebastiao and Sores, 1995; Wang et al., 2005; Nazir et al., 2008; Xie et al., 2007; Zhong and You, 2011; Berry et al., 2012.
Dispersion	• spilled oil is broke into small droplets and enters the water column due to wave or turbulence • relies on the oil properties and the energy from the surrounding environment • reduces the volume of spilled oil on the sea surface • will not change the physicochemical properties of the spilled oil • the droplets will not reenter to the surface if their sizes are small • is a major part of oil removal from the sea surface in practice	$DE = \left(0.11(U + 1)^2\right) \times \left(1 + 50\mu^{0.5}s_t SOT\right)^{-1}$ $\left.\dfrac{\partial Q}{\partial d}\right|_{d_0} = C_0 D_{ba}^{0.57} S_{cov} F_{wc} d_0^{0.7}$ $DE = \dfrac{K_e \varpi \gamma H}{16\alpha_h L_{ow}}$	Delvigne and Sweeney, 1988; Tkalich and Chan, 2002; Perianez, 2007; Nazir et al., 2008; Guo and Wang, 2009; Wang and Shen, 2010; Zhong and You, 2011; Berry et al., 2012.
Spreading	• pour point should be lower than the sea surface temperature. • occurs quickly after the oil spill until the slick thickness achieves 0.1mm or less • relies on the interaction of gravity, wind, current, inertia, viscosity, and surface tension of oil • stops when the slick thickness of crude oil reaches 0.01mm or the slick thickness of light oil (i.e., gasoline) reaches 0.001mm. • significantly affect the evaporation, dispersion, and emulsification	$\dfrac{dA}{dt} = K_1 A^{1/3}\left(\dfrac{V}{A}\right)^{4/3}$ $A = 10^5 V^{3/4}$ $A = 2270\left(\dfrac{\rho_w - \rho}{\rho}V\right)^{2/3} + 40\left(\dfrac{\rho_w - \rho}{\rho}VU_w\right)^{1/3} t$	Fay, 1971; Lehr et al., 1984; Reed, 1989; Korotenko et al., 2001; French-McCay, 2004; Wang et al., 2005; Chen et al., 2007; Nazir et al., 2008; Inan and Balas, 2010; Zhong and You, 2011.

Biodegradation	- some compounds can be digested by micro-organisms or microbes - transforms the compounds into water soluble compounds and eventually carbon dioxide and water - highly depends on the level of nutrients, the temperature, and the oxygen - can only occur at the oil-water interface and can be strengthen by the dispersion and spreading - degradation rate is very low and difficult to be described by any general mathematical model in the marine environment	$C_h(t) = \alpha(1-p(t))^{\gamma_b} e^{\delta_b L(t)+\varpi_b t} \varepsilon_b$ $k_{obs} = k_{max}\left(\dfrac{N}{K_n+N}\right)$	Bragg et al., 1994; Prince et al., 1994; Atlas, 1995; Venosa et al., 1996; Essaid et al., 1995; Zhu et al., 2001; Wenger and Isaksen, 2002; French-McCay, 2004; Camilli et al., 2010.
Photolysis	- some compounds can react with oxygen by the promoting of sunlight - relies on the type of oil and the form in which it is exposed to sunlight - transforms the compounds into soluble products or persistent ones - occurs in a very low rate even with a strong sunlight - affects less than 1% (or 0.1% per day) of spilled oil	$\dfrac{dPAH_d}{dt} = \phi k_a (PAH_d)$	Zepp and Cline, 1977; Payne and Phillips, 1985; Essaid et al., 1995; Richard, 2003.
Sedimentation	- heavy compounds with densities greater than the density of sea water sink to the bottom of the sea - usually happens due to the adhesion of particles or organic matter from the sea water to the oil slick - insignificant in the initial stage because most of the oils have not enough density - the percentage can be increase with the emulsification and in-situ burning - oil washed off from the shoreline can also sink after reach back to the sea	$Q_s = \dfrac{bK_{ab}C_{0e}}{1+K_{ab}C_{0e}} + K_p d_s^m$	Chao et al., 2001; 2003; Payne et al., 2003; French-McCay, 2004; Fingas, 2010.

Advection	• the movement of oil slick is due to the influence of overlying winds and/or underlying currents • the advection velocity of the spilled oil on the sea surface is considered to be a vector sum of a wind-induced drift and a water-current drift	$\vec{V} = \vec{V}_c + \vec{V}'$ $\vec{V} = \alpha_w \vec{V}_w + \alpha_c \vec{V}_c$	Shen and Yapa, 1987; Al-Rabeh et al., 1989, 1992; Chao et al., 2001, 2003; Korotenko et al., 2001; Nazir et al., 2008; Wang et al., 2008; Guo and Wang, 2009; Wang and Shen, 2010; Wu, 2010; Berry et al., 2012.
Oil-shoreline interactions	• the spilled oil can deposit or reenter to the sea after reaching the shoreline • mainly relies on the oil properties, types of shoreline, wind, and tidal • stranded oil often mixes with the sand • will sink if washed back into near-shore waters by tidal rise or precipitation • interaction with very small particles (< 4μm) can lead to the formation of oil–shoreline interactions	$\dfrac{\Delta V_b}{V_b} = 1 - 0.5^{\Delta t/\lambda_h}$ $Q_{max} = L_s W_s D_s \eta_{eff}$	Shen and Yapa, 1988; Humphrey, 1993; French-McCay, 2004; Wang et al., 2005; Guo and Wang, 2009; Inan and Balas, 2010; Xiong et al., 2010.

Note: FE is the evaporation rate, m^3/hour/m^3; T is the temperature, K; U is the wind speed, m/s; P is the vapor pressure, Pa; M is the molecular weight, g/mol; ρ is the density of oil, kg/m^3; R is the gas constant, 8.314 m^3·Pa/mol/K, SOT is the slick thickness, mm; t is time; c and d are equation parameters for specific oil; T_0 is the initial boiling point, K; T_G is the gradient of the boiling point, K; θ is evaporation open factor; C_A and C_B are non-dimensional constant; K_E is the mass transfer coefficient, m^3/hour; P_0 is the initial vapor pressure, Pa; C_C is the constant for specific oil; A is the area of the oil slick, m^2; Z is the amount of oil fraction; S_d is the total dissolution rate of the oil slick, g/hour; K_d is the dissolution mass transfer coefficient, m^3/hour; S_0 is the solubility for fresh oil, g/L; α_d is the decay constant; Y is the fraction of water in oil; C_3 is the final fraction water content; K_A is the curve fitting constant relating to wind speed; Y_w^F is the stable water content of the emulsion; DE is the dispersion rate, m^3/s/m^3 of oil; μ is the oil viscosity, cSt; s_t is the oil–water interfacial tension, dyne/m; Q is the entrainment rate of oil droplets, kg/m^2/s; S_{cov} is the sea coverage factor of oil; d_0 is the oil droplet diameter, mm; C_0 is the oil dispersion parameter related to oil viscosity; F_{wc} is the fraction of the sea surface hit by breaking waves; k_e is the coefficient evaluated from experiments; ω is the wave frequency, Hz; γ is the dimensionless damping coefficient; H is the significant wave height, m; α_h is the coefficient for the mixing depth; L_{ow} is the vertical length-scale parameter; K_1 is the constant with default value of 150 s^{-1}; ρ_w is the density of water, kg/m^3; $C_h(t)$ is the amount of a hydrocarbon component at time t; p(t) is the polar fraction of oil; L(t) is the ratio of the average residual nitrogen concentration to oil loading; α_b, δ_b, γ_b, and ω_b fitting parameters determined from the multiple regression analysis; ε is the assumed multiplicative error term; k_{obs} and k_{max} are the observed and maximum fist-order hydrocarbon biodegradation rate, mg/kg/day; K_n is the half-saturation concentration for a specific nutrient, mg/L; N is the interstitial pore water residual nutrient concentration; ϕ is the molar yield coefficient; k_a is the sum of the values for all wavelengths of

sunlight absorbed by the PAH; PAH_d is the concentration of dissolved PAH, mg/L; Q_s is the total absorption capacity by sediment, m^3; C_{0e} is the oil concentration after absorption balance; d_s is the sediment particle diameter, mm; K_p, and K_{ab} are absorption parameters; $\vec{v}$ is the advection or drift velocity, m/s; α_w is the wind drift factor; $\vec{V}_w$ is the wind velocity, m/s; α_c is the current drift factor; $\vec{V}_c$ is the depth-averaged current velocity, m/s; $\vec{v}'$ is the turbulent fluctuation of the drift velocity/s; ΔV_b is the volume of beached oil reenter to the sea, m^3; V_b is the volume of oil on the shoreline, m^3; λ_h is the half-life, hour; Q_{max} is the maximum capacity of a beach for oil, m^3; L_s, W_s, and D_s are the length, width, and depth of sediments on the beach, m; and η_{eff} is the effective porosity of the sediments.

2.2.5 Optimization applications in offshore oil spill response

As spilled oil can cause significant impacts to the marine environment and economy, an emergency clean-up response is inevitable to be undertaken immediately for removing the oil and protecting sensitive areas nearby. The clean-up response to an oil spill can be described as a complex combination of numerous dynamic processes. It usually consists of the use of dispersant chemicals, the containment and recovery of oil using boom and skimmers, and some other alternative techniques such as in-situ burning (Price et al., 2003). Undoubtedly, the cross-disciplinary nature and knowledge requirement of these processes make it challenging to implement them at the best practice levels (Fingas, 2011). Their effectiveness largely depends on oil properties and ambient environmental conditions, such as oil slick thickness, oil viscosity, air/water temperature, wave height and wind speed (Jing et al., 2012a, 2012b; Li et al., 2012b, 2013a, 2013c). Therefore, how to understand, simulate and optimize these processes under varying circumstances becomes vital to evaluate the possible outcomes of a clean-up response and to aid the decision makers in preparing an effective operation plan.

The simulation-based optimization for emergency response has been well documented in the literature, ranging from public-health infrastructure (e.g., ambulance operations) to urban hazard and disasters (e.g., evacuation from buildings) (Peleg amd Pliskin, 2004; Massaguer et al., 2006; Dimakis et al., 2010). When speaking of offshore oil spill clean-up, spill responders usually require both fast and accurate estimates of the spill situation to make critical decisions about deploying skimmers, spreading dispersants and other response activities before, during and after events. However, the complexity of the fate and transport of spilled oil and the dynamics of climatic and oceanic conditions

can cause significant challenges in providing such information by using traditional physics-based models. Although a few studies have explored the possibility of simulating oil recovery based on empirical oil weathering models and artificial equipment performance settings (Buist et al., 2011; El-Zahaby et al., 2011; You and Leyffer, 2011; Zhong and You, 2011), there are still technical and knowledge gaps in how to obtain accurate and timely forecasting results under varying environmental conditions. This is especially true in the harsh environments where extreme weathers prevail and the response time window is reasonably short.

Limited studies have been conducted to deal with the decision-making problems in oil spill response., but most of these studies focus on the simulation of oil transport and weathering process (Brebbia, 2001; Reed et al., 1999), and a few have addressed the decision problems in oil response planning and on-site actions (Zhong and You, 2011). A review of the planning models for oil spill response is given by Iakovou et al. (1994). Psaraftis and Ziogas (1985) developed an integer programming model for optimal dispatching of oil spill cleanup equipment with the objective to minimize the total response costs. Wilhelm and Srinivasa (1997) developed an integer programming model for the response of oil spill cleanup operations with the objective of minimizing the total response time of equipment. Limited literature exists that addresses the integration of oil properties, the weathering model, and the planning model (Ornitz and Champ, 2003). Gkonis et al. (2007) presented a mixed-integer linear programming model that considers the oil weathering process, an important factor for decision making in response

operations.

However, most of these systems provided response operations without any supporting of numerical optimization, and only few of them involved necessary approaches to handle the dynamics which widely appear in and highly affect to the response and countermeasures (Wilhelm and Srinivasa, 1997; Reed et al., 1999; Brebbia, 2001). Only a few attempts were provided in the past decade (Costa et al., 2005; Broje, 2006; You and Leyffer, 2011). Costa et al. (2005) provided a model to locate the protection systems that must be deployed to the priority areas associated with spill scenarios immediately after a spill occurs. Broje (2006) optimized the number of materials and surface patterns in a mechanical oil spill recovery for various environmental conditions. You and Leyffer (2011) developed a mixed-integer dynamic optimization (MIDO) approach for oil spill response planning based on a dynamic oil weathering model for the complex interactions between the spreading, evaporation, dispersion, and emulsification processes. However, only limited attempts were reported on the simulation of oil weathering processes and the optimization of spill recovery processes (e.g., device location and transportation) to support the countermeasures of offshore oil spills (Li et al., 2012b).

2.4 Integrated Decision Support System for Supporting Offshore Oil Spill Response

Management of emergencies resulting from natural or man-made disasters requires enough information as well as experienced responders in both technical and co-ordination matters. It generally means making the best decision at the right moment, which requires a great amount of information (Hernandez and Serrano, 2001). In offshore oil spills, different affected sites have different characteristics depending on various features such as pollutants' properties, hydrological conditions, and a variety of physical, chemical, biological processes, etc. Thus, the response methods selected for different sites vary significantly, and the decision for a suitable method at a given site often requires expertise on both remediation technologies and site conditions (Geng et al., 2001).

Decision support systems (DSSs), which are series of computer-based systems for solving semi-structured problems, allow decision makers to simulate many steps of the process of decision making, to investigate the alternative decision scenarios, and to improve the decision making effectiveness. Although there is no unique definition or standard components of a decision support system, the purpose of a DSS is to increase both the efficiency and effectiveness (Power, 2002). The decision making is a complex process, influenced by many factors, both human and non-human. Recently, many DSSs have been developed aiming for emergency responses to flood (Sanders and Tabuchi, 2000; Castellet et al., 2006; Mirfenderesk, 2009), forest fire (Jaber et al., 2001; Asunción

et al., 2005; Bonazountas et al., 2007), tsunami (Kumar et al., 2010; Steinmetz et al., 2010), etc. However, the effectiveness of these DSS is still challenged by the complexity and uncertainty which widely exist during these emergency responses.

Compared with the DSSs for emergency responses to flood, hurricane, and tsunami, the DSSs for offshore oil spill responses is still immature. In recent years GIS have been increasingly used in conjunction with oil spill modeling tools as a mean of integrating and pre-processing spatial data inputs to the numerical modeling and for post-processing and visualization of the modeling outputs. The integration of GIS and environmental modeling is now widely accepted as desirable, if not essential. Of considerable discussion and research have been levels of coupling achievable or desirable between GIS and environmental models (Li, 2001). However, although classification of response technologies, simulation of oil spill weathering, and optimization of response operation can provide effective help to the decision making, there is still lack of DSS that employs these processes in offshore oil spill response and countermeasures.

2.5 Challenges in Cold and Harsh Environments

There are many environments which could be reasonably classified as harsh environments. The definition of harsh environments in this thesis is limited to offshore environments and specifically to the offshore area of Newfoundland, Canada. Cold and harsh environments are usually characterized by wide range of wind speed and direction,

visibility, and temperature, as well as rough seas, ice coverage, appearance of icebergs, etc., posing unique challenges for oil spill response. For example, in offshore Newfoundland, the waves are too strong to allow containment of oil slicks with booms from October to March. The occurrence of visibility restricted to less than 1 km could be as high as 30% from May to July. The daylight hours in winter are less than 9 hours in various areas (Rainville and Woodgate, 2009). The water surface can experience considerable amounts of ice during the winter months (Cleveland, 2010). Oil spill is more problematical in such harsh conditions because of the simple and highly seasonal ecosystems and the logistic challenges of cleaning up spills in remote regions. Low temperature will also make hydrocarbons persist, making ice-edge communities particularly vulnerable (U.S. Arctic Research Commission, 2004; Turner, 2010).

With respect to oil spill detection, numerous difficulties are encountered. For example, ice is never a homogeneous material but rather incorporates air, sediment, salt, and water, many of which may present false oil-in-ice signals to the detection mechanisms. Snow on top of the ice or even incorporated into the ice adds complications. During freeze-up and thaw in the spring, there may not be distinct layers of water and ice. There are many different types of ice and different ice crystalline orientations, making oil spill monitoring in harsh environment more challenging (Huntington, 2008; Fingas, 2011). Crude oils and oil products behave quite differently if spilled in the cold weather/water and harsh conditions, due to the variations of their physical and chemical

properties. These properties influence the selection of techniques and equipment applicable for monitoring and sampling (Hänninen and Sassi, 2010).

Oil spill forecasting and modeling in cold and harsh environment also face challenges due to the harsh environment (U.S. IMMS, 2008). Oil spill models are very sensitive to errors in the initial input data, such as the details of the release and the wind and current forecasts. Furthermore, the mathematical equations used to simulate oil movement are likely based on empirical approximations and assumptions and are subject to time step and grid limitations (Li et al., 2013c). Trajectory model uncertainty refers to changes in the forecast as a result of these errors. Unfortunately, quantitative assessment of the errors in trajectory modeling is difficult and limited. In addition, oil spills are notorious for usually occurring in areas where the environmental data are temporally and spatially incomplete. This leads to a forecast process that often relies on the forecaster's subjective judgement and approximated input. Therefore, it becomes significantly challenging in oil spill early warning and modeling in cold and harsh environment, especially in winter (Chen et al., 2012b). In harsh environments, it is also extremely important to respond to offshore oil spills in a timely manner, and this response requires more reliable and effective decision making schemes considering limited access time/sites, equipment and man power. Unfortunately there is still no integrated DSS to incorporate modeling processes and support offshore oil spill response in cold and harsh environment (Li et al., 2013b).

The cold and harsh environments also significantly hinder the application of oil spill countermeasures and reduce their effectiveness (Keller and Clark, 2008). Presence of ice is a key factor affecting the ability to respond to a spill (DeCola et al., 2006). The fate and behavior of oil in ice-covered waters is governed by a number of important weathering processes have a direct bearing on oil recovery operations. The physical distribution and condition of spilled oil under, within or on top of the ice plays a major role in determining the most effective response strategies at different stages in the ice growth and decay cycle. Before oil spill response plans are developed or approved, it is necessary and imporant to understand the chemistry and physical behavior of the oil and how its characteristics change over time in harsh environments. Spill response operations in ice and open water are fundamentally different (Owens et al., 1998; Brandvik et al., 2006). These variances must be recognized when determining the most appropriate strategy for dealing with oil in specific ice conditions and seasons, including freeze-up, winter, and break-up. Because of the vastly different ice environments and oil-in-ice situations, over-reliance on a single type of response will likely result in inefficient, ineffective clean-up after an actual spill (Angus and Mitchell, 2010). Also, each season presents different advantages and drawbacks for spill response (Cleveland, 2010). During freeze-up and break-up, drifting ice and limited site access restrict the possible response options and considerably reduce recovery effectiveness (Swail et al., 2006; LGL et al., 2010). Mid-winter, although associated with long periods of darkness and cold

temperatures, provides a stable ice cover that not only naturally contains the oil within a relatively small area but also provides a safe working platform for oil recovery and transport (U.S. IMMS, 2008).

In fact, the presence of ice is not the only environmental factor affecting spill response. Temperature affects the consistency of oil and the speed at which it degrades. Winds and the resulting wave action are other factors (Cleveland, 2010). High energy from wind and waves can help oil to disperse naturally, but it also breaks up a thick slick into multiple thinner slicks, which are more difficult to address. In addition, waves are less effective at naturally dispersing oil in broken ice (Rainville and Woodgate, 2009). Besides, most of the established countermeasures require the support of aircraft, vessels, and trained personnel to properly deploy and operate them. Remote locations and lack of infrastructure can impede these systems considerably. The cumulative impact of such limiting factors can make marine spill response operations almost impossible for long periods of time in cold and harsh environment.

2.6 Summary

The management of an offshore oil spill may appear complicated because it provides many details about the numerous steps required to prepare for and respond to spills. It also covers many different spill scenarios and addresses many different situations that may arise during or after a spill. Despite its complexity, a well-designed contingency plan

should be easy to follow. Although they are different in many respects, contingency plans usually include hazard identification, vulnerability analysis, risk assessment, and response actions.

When an offshore area is affected by an oil spill, contingency plans have been devised to guide actions and cleanup operations. For the majority of coasts, however, no contingency plan exists, and available response options must be reviewed and decisions made in very short time frames, if interventions are to have any chance of being successful. Despite the existence of a large body of experience, challenges still remain in identifying at what point should response actions for offshore oil spills begin and conclude.

Considering significant impacts caused by offshore oil spills, it becomes urgent to provide strategies of offshore oil spill response and countermeasures. A few models have been developed for oil spill response and countermeasures based on decision support system (DSS). However, these systems usually screen response technologies based on experience and suggest operations without the support of numerical optimization, and few of them involve approaches to handle uncertainties which widely appear and highly affect oil spill response. Furthermore, although approaches based on the coupling of optimization and simulation can effectively increase the efficiency and reduce the time of response, limited studies have been involved in the existing offshore oil spill DSS.

Recently, classification techniques employed in offshore oil spill are focusing only

on the determination of the occurrence of a spill, and the type of spilled oil. Challenges are still remaining in how to screen response technologies once an oil spill happens. Recent practices in screening technologies for offshore oil spill responses are mainly based on experiences which may cause high uncertainties in operation. Furthermore, the risk/vulnerability zone classification and characterization based on classification of the concerned offshore areas is necessary and important to support decision making and practice of oil spill response, facilitating impacts and options evaluation, set up and running cost reduction, and efficiency improvement. However, few attempts have been made in this area and none has been found with the involvement of uncertainty and complexity.

Compared with the DSSs for emergency responses to flood, hurricane, and tsunami, the DSSs for offshore oil spill responses is still immature. Although a few models have been developed for oil spill response and countermeasures, they usually separately consider response operations and the oil weathering process where interactions significantly exist. Meanwhile, oil spill cleanup activities change the volume and area of the oil slick and in turn affect the oil transport and weathering process, which also dynamically affects the oil spill response and countermeasures. Furthermore, crude oils and oil products behave quite differently if spilled in a cold and harsh environment such as offshore NL, due to the physical and chemical properties of the oil spilled. These properties influence the selection of response equipment and methods applicable for spill

cleanup. Such challenges become more significant when these influent factors are complex and uncertain.

Therefore, it is critical to integrate the response planning model (i.e., optimization model) with the oil transport and weathering model, although this integration has not been addressed in the existing literature. Although classification of response technologies, simulation of oil spill weathering, and optimization of response operation can provide effective help to the decision making, there is still lack of DSS that employs these processes in offshore oil spill response and countermeasures.

In order to better support offshore oil spill response and countermeasures, new decision making approaches and systems are desired for providing more effective support to stakeholders or decision makers at different levels. Risk/vulnerability zone classification and characterization, technology screening/ranking, and simulation-based optimization models that can determine the risk/vulnerability levels in the spill area, the best combination of technologies and allocation of resources at different response stages should be developed in order to achieve a most time-efficient and cost-effective response to an oil spill. This would be especially valuable for the areas where unpredictable weather conditions and harsh environments prevail.

CHAPTER 3

CLASSIFICATION FOR SUPPORTING OFFSHORE OIL SPILL MONITORING AND RESPONSE

_____
The contents in the chapter are based on or will result in the following publications or potential publications:

1. Li P., Chen B., and Husain T. (2011). IRFAM: An integrated rule-based fuzzy adaptive resonance theory mapping system for watershed modeling. Journal of Hydrologic Engineering-ASCE, 16(1): 21-32.
2. Chen B., Li P., and Husain T. (2012). Development of an integrated adaptive resonance theory mapping classification system for supporting watershed hydrological modelling. Journal of Hydrologic Engineering-ASCE, 17(6): 679-693.
3. Li P., Chen B., and Husain T. (2009). Development of two-stage ART-ARTMap classification system for supporting watershed management. In: Proceedings of CSCE 2009 Annual General Conference, GC-094, May 27-30, 2009, St John's, Canada.
   Role: I developed the model, conducted case studies and drafted manuscript. The other two authors are my M. Eng. Supervisors.

   The models presented in these papers were mainly based on my M. Eng. thesis and have been advanced in this thesis.

4. Li P., Chen B., and Zhang B.Y. (2013). An integrated rule-based adaptive resonance theory mapping approach for technologies screening in offshore oil spill response. In: Proceedings of CSCE 2013 Annual General Conference, GEN-236, May 29 to June 1, 2013, Montréal, Canada.
   Role: I developed the model, conducted case studies and drafted manuscript. Dr. Bing Chen is my PhD supervisor. Dr. Baiyu Zhang provided advice in manuscript drafting.

5. Li P., Chen B., Li Z.L., Zheng X., and Wu H.J. (2013). A Monte Carlo simulation based two-stage adaptive resonance theory mapping approach for site classification in offshore oil spill monitoring. Marine Pollution Bulletin, MPB-D-14-00171. (Under review).
   Role: I developed the model, conducted case studies, drafted main sections of the manuscript and led the student team. Zelin Li collected data for case study and drafted the introduction of the manuscript. Xiao Zheng collected data for case study. Hongjing Wu conducted statistical analysis for results and drafted part of discussion of the manuscript. Dr. Bing Chen is the supervisor of the students.

3.1 Adaptive Resonance Theory (ART) Neural Networks

The adaptive resonance theory (ART), developed and extended to a series of real-time neural network models for unsupervised classification, is capable of learning stable recognition categories in response to arbitrary input (Grossberg, 1976, 1980). Usually, an ART system has two layers connected by long term memory. The input pattern enters one layer, classification occurs in the other. A characterization process begins by extracting features leading to activation in the feature representation field. Expectations stored in long term memory connections will then be used to translate input patterns to categories in the category representation field. The classification is compared to the network's expectation, which resides in long term memory weights from the classification layer to the data entry layer. If there is a match, the expectations are strengthened; otherwise, the classification is rejected (Carpenter and Grossberg, 2003). The ART Mapping (ARTMap) approach consists of two ART modules (ART_a and ART_b) for processing patterns and criteria, and a map field module (F_{ab}) for comparing patterns and criteria. Those patterns that need to be classified are fed to ART_a, criteria are fed to ART_b, and then a comparison between patterns and criteria occurs in F_{ab} (Carpenter and Grossberg, 2003).

There are two major ART paradigms distinguished by their forms of input data and processing. ART-1 is designed to accept only binary input vectors (Carpenter and Grossberg, 1987) whereas ART-2 (Carpenter and Grossberg, 1987) and Fuzzy ART

(Carpenter et al., 1991, 1992) can also classify analog inputs. Both models can stably learn to categorize input patterns presented in an arbitrary order. There are many variations of ART models developed in different application domains, such as geomatic analysis, land cover classification, and Image analysis (Carpenter et al., 1991, 1997; Gopal et al., 1999).

ART models have been proposed under supervised learning conditions (Carpenter et al., 1991). ARTMap, a hierarchical network architecture, is able to rapidly self- organize stable categorical mapping between a given set of binary input vectors and binary output vectors while minimizing predictive error in an online setting. The Fuzzy ARTMap (FAM) model is an extension of ARTMAP that can learn stable recognition categories given both analog and binary input patterns. The ART modules of ARTMAP are replaced by Fuzzy ART modules in FAM. A brief description of ART that forms the basic modules in FAM architecture is given below. In Fuzzy ART the fuzzy logic AND connective, nun, is used to extend the method to real values in ART-1 (Carpenter et al., 1991).

The ART unsupervised approach can provide an accurate classification result, but the number of final output groups is uncontrollable. The group number can be controlled by ARTMap supervised approach; however, it requires specific criteria for supervised learning and is incapable if the input data becomes uncertain. ART and fuzzy set theory can be integrated to handle the watershed classification where complexities and uncertainties coexist. ART can efficiently handle the system complexity and obtain a fast

learning speed but it is weak in handling uncertain inputs. Fuzzy set theory has high ability to handle uncertainties, but it will become inefficient if the system becomes complex. Therefore, the main objective of this study is to develop a neural fuzzy classification system by integrating fuzzy interface operation modules and ART Mapping networks in order to efficiently classify watersheds under complex and uncertain conditions.

3.1.1 ART for unsupervised classification

The ART, developed and extended to a series of real-time neural network models for unsupervised classification (Grossberg 1976, 1980), is capable of learning stable recognition categories in response to arbitrary input. Usually, an ART system has two layers connected by long term memory. The input pattern enters in one layer, classification occurs in the other. A characterization process begins by extracting features leading to activation in the feature representation field. Expectations stored in long term memory connections will then be used to translate input patterns to categories in the category representation field. The classification is compared to the network's expectation, which resides in long term memory weights from the classification layer to the data entry layer. If there is a match, the expectations are strengthened; otherwise, the classification is rejected (Grossberg 1976, 1980; Carpenter and Grossberg 2003).

The computations of fuzzy ART are the same as those of the ART neural network

which are functioning for the special case of binary input vectors and fast learning. Assume each input [I] is an m-dimensional vector ($[I_1]$, $[I_2]$, ..., $[I_m]$). Let each category j correspond to a weight vector $[w_j]$ = $[w_{j1}]$, $[w_{j2}]$, ..., $[w_{jm}]$. The number of potential categories n ($j = 1, 2, ..., n$) is arbitrary. The fuzzy ART weight vector $[w_j]$ subsumes both the bottom-up weight vectors and the top-down weight vectors of ART. The fuzzy ART algorithm, which was first introduced by Grossberg (Carpenter and Grossberg, 2003). Then the value of the choice function T_J is reset to -1 for the duration of the input presentations to prevent its persistent selection during the search. A new index J is chosen. The search process continues until the chosen J satisfies.

There are two options for the fuzzy ART algorithm: the fast-commit-slow-recode option and the input fuzzification option. The former is used to combine fast initial learning with a slow rate of forgetting for efficient coding of noisy input sets in applications. With this option, β =1 is set when J is an uncommitted node; and $\beta < 1$ is set after the category is committed. The latter is to prevent a problem of category proliferation that could otherwise occur in some analog ART systems, when a large number of inputs erode the norm of weight vectors (Carpenter et al., 1991).

3.1.2 ARTMap for supervised classification

The ARTMap consists of two ART modules (ART_a and ART_b) for processing patterns and criteria, and a map field module (F_{ab}) for comparing patterns and criteria. Those

patterns that need to be classified are fed to ART_a, criteria are fed to ART_b, and then a comparison between patterns and criteria occurs in F_{ab} (Carpenter and Grossberg 2003). Both approaches have three control parameters in the interval [0, 1]: vigilance ρ is used to control the definition of classification results; choice parameter α is used to ensure that one category is active at a time; learning rate β determines to what extent the newly acquired information will override the old information (when β = 1 is called fast learning with consideration only on the most recent information) (Bahri and Meybodi 1999). Although slow learning (β < 1) may provide relatively accurate results for a noisy environment, an autonomous learning agent is needed to cope with unexpected events in an uncontrolled environment. In most applications, fast learning is used in an unfamiliar environment (Carpenter et al. 1992).

At the start of each input presentation the ART_a vigilance parameter ρ_a equals the baseline vigilance $\overline{\rho}_a$ which is the minimum matching criterion. Usually the baseline vigilance is set as $\overline{\rho}_a = 0$ to allow the formation of broader categories (Carpenter and Grossberg, 2003). The map field vigilance parameter is ρ_{ab}.

By the operation of the criteria combinations subsystem, the final criteria combinations for the classification are determined. If the final criteria combinations are not fully satisfied in some special case, based on expert knowledge and real-world conditions, human judgments and modifications can be applied at this stage to modify the membership functions for generating criteria combination generation. Then the centroid

determination and the criteria combination steps can be repeated until the final criteria are satisfied.

3.2 A Monte Carlo Simulation based Two-Stage Adaptive Resonance Theory Mapping (MC-TSAM) Approach

3.2.1 A two-stage adaptive resonance theory mapping (TSAM) approach

ART unsupervised classification generates relatively large numbers of unpredictable results; ARTMap can generate predictable results, but it needs criteria for supervised learning. However, because of insufficient reference information the criteria for classification are not easily obtained. In order to address these challenges, a two-stage adaptive resonance theory mapping (TSAM) approach has been developed to feed ARTMap classification with criteria generated from ART unsupervised classification (Li et al. 2009a; Chen et al., 2012a).
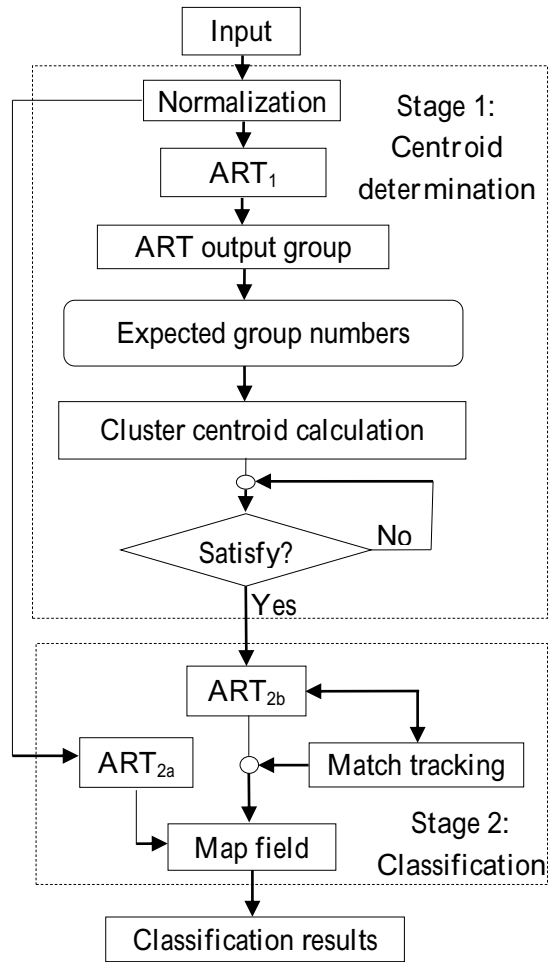
Figure 3.1 Flow chart of the TSAM approach

The TSAM approach consists of an unsupervised ART module, a supervised ARTMap module, and centroid determination modules (Figure 3.1). It includes two stages: The first stage is the centroid determination subsystem which can locate the centroids for the expected target groups by unsupervised ART module, and use the determined centroid as the criteria in the second stage; and the second stage is the classification subsystem which can classify the normalized original input. There are three ART modules integrated in the TSAM which are as follows: ART_1 is used for processing unsupervised classification for the normalized original input and generating the unsupervised classified groups; ART_{2a} and ART_{2b} are used in an ART Mapping module for comparing the combinations determined in the first stage and the normalized original inputs, and classifying them.

The detailed steps of the approach are as follows:

Step 1: Initialization

Choice parameter, learning rate, and vigilance are set. Furthermore, two input variables are required: input data that aim to be classified (Equation 3.1) and the desired number of final groups (Equation 3.2).

$$[I] = \left(x_{ij}\right)_{i=1,\cdots m,\ j=1,\cdots,n} \tag{3.1}$$

where [I] is an m by n matrix; m is the number of input patterns; and n is the number of features for each input pattern.

$$[O] = (CR_k)_{k=1,...,p} \tag{3.2}$$

where p is the desired number of final groups; $[CR_k]$ is the group k in the classification result; and [O] is the final classification result which will contain p classified groups.

Step 2: Normalization

Because the ART system can only handle data between 0 and 1, before the data is fed to the system it is needed to normalize the original data. The equation for normalization is as follows:

$$[I_N] = (v_{ij}) = \left(\frac{x_{ij} - x_{j\,min}}{x_{j\,max} - x_{j\,min}} \right)_{,i=1,\cdots n;\ j=1,\cdots m} \tag{3.3}$$

where $[I_N]$ is the normalized matrix, and v is the normalized value for features.

Step 3: ART classification and centroid calculation

[I_N] is fed to ART module (ART$_1$) for unsupervised classification. The results will be given as follows:

$$[O_u] = (UCR_l)_{l=1,\dots,q} ,$$
(3.4)

where q is the number of classified groups, which is unsupervised and uncontrollable from ART; [UCR_l] is the ranked group l in the classification result, where [UCR_1] contains the most data points, and [UCR_q] contains the least points. [O_u] is the unsupervised classification result which will contain q (q > p) classified groups.

Subsequently, according to Equation 3.2, the first p groups in [O_u] are selected:

$$[O_C] = (UCR_k)_{k=1,\dots,p}$$
(3.5)

where [O_c] is the matrix containing the first p ranked groups. For each selected group [UCR_k], the centroid is calculated as:

$$[CT_k] = (ct_j)_{j=1,\dots,n}$$
(3.6)

where $[CT_k]$ is a 1 by n matrix, and the centroid value for the feature j, ct_j, is given by:

$$ct_j = \begin{cases} vj_t & \text{if } t = 1 \\ \sum_{t=2}^{h} (\frac{t-1}{t} \sum_{1}^{t-1} vj_{(t-1)} + \frac{1}{t} vj_t) & \text{if } t > 1 \end{cases} \qquad (3.7)$$

where h is the number of patterns in the group $[UCR_k]$, and vj is the normalized value for the feature j in the pattern. In this step, human interference can be further applied to adjust the generated criteria, making the classification more suitable in special cases.

Step 4: ARTMap classification

The centroids $[(CT_k)_{k=1,...,p}]$ are fed to the ART_{2b} module as criteria for supervised classification. Meanwhile, the normalized input data $[I_N]$ is also fed to ARTMap and compared with the criteria to generate the final classification [O] (Equation 3.2).

Based on the automatic generation of criteria for classification, the developed TSAM can easily overcome difficulties in criteria generation due to insufficient information or complications in criteria selection in traditional classification approaches.

3.2.2 The MC-TSAM approach

Considering the serious damage that could be caused by an offshore oil spill, it is of great significance to build a reliable spill monitoring system supported by different level of offshore vulnerability levels, which can promptly provide decision makers with accurate information. The impacts to an area caused by any potential offshore oil spills can be described by the offshore Oil Spill Vulnerability Index (OSVI). The OSVI was firstly introduced by Gundlach and Hayes (1978) instead of Environmental Sensitivity Index (ESI) to better describe vulnerability of a shoreline area that would be potentially exposed to oil spills. OSVI maps based on classifying the designated area into multiple different subareas are essential in oil spill responses in terms of impact evaluation, budgeting, and decision support. The classification first defines the local geographic conditions by generating grids of mesh with a certain size (Ng et al., 2008). Offshore environmental conditions, historical meteorological data as well as a hypothetical spill case would be further involved to determine the probability of any related risks (Richard et al., 2001; Price et al., 2003). Site classification with mapping technologies has been widely applied in oil spill monitoring during the recent decades (Romero et al., 2013; Furlan et al., 2011; Jensen et al., 1998). As a complex entity of study, a wide range of parameters within the site needs to be considered during the classification processes, such as meteorological conditions (e.g., temperature, wind, wave and current, etc.), offshore oil production and marine traffic, and adjacent ecosystems.

Therefore, a single indicator is far from sufficient to represent the characteristics of the spilled site (Webler and Lord, 2010). Meanwhile, to make the decision support systems more robust for practical applications, it is worth to note that uncertainty associated with each parameter should not be underestimated (Wirtz et al., 2007). The TSAM approaches can provide efficient and reasonable OSVI classification for a potential spill site with complex information. However, its capability of uncertainty handling still needs to be strengthened for the high uncertainties existing in offshore oil spill events. In order to further tackle the uncertainty, Monte Carlo simulation is integrated with the TSAM, forming the MC-TSAM.

The framework of the Monte Carlo simulation based fuzzy programming (MC-MCFP) is shown in Figure 3.2, where N is the preset number of trials, and I is the index of the current trial. The inputs for the classification may include deterministic and uncertain information. Firstly, historical data and references are collected for uncertain features (e.g., wave height and wind speed in offshore area). Secondly, the collected data is approximated into certain distributions with the best fitness based on statistical analysis. According to the parameters of any fitted distribution, a series of randomized inputs are generated based on the Monte Carlo simulation. In each trial (e.g., trial I), the randomized inputs for the uncertain information are combined with the deterministic inputs and interpolated to the whole target area as inputs ([I] in Equation 3.1) for the TSAM classification.
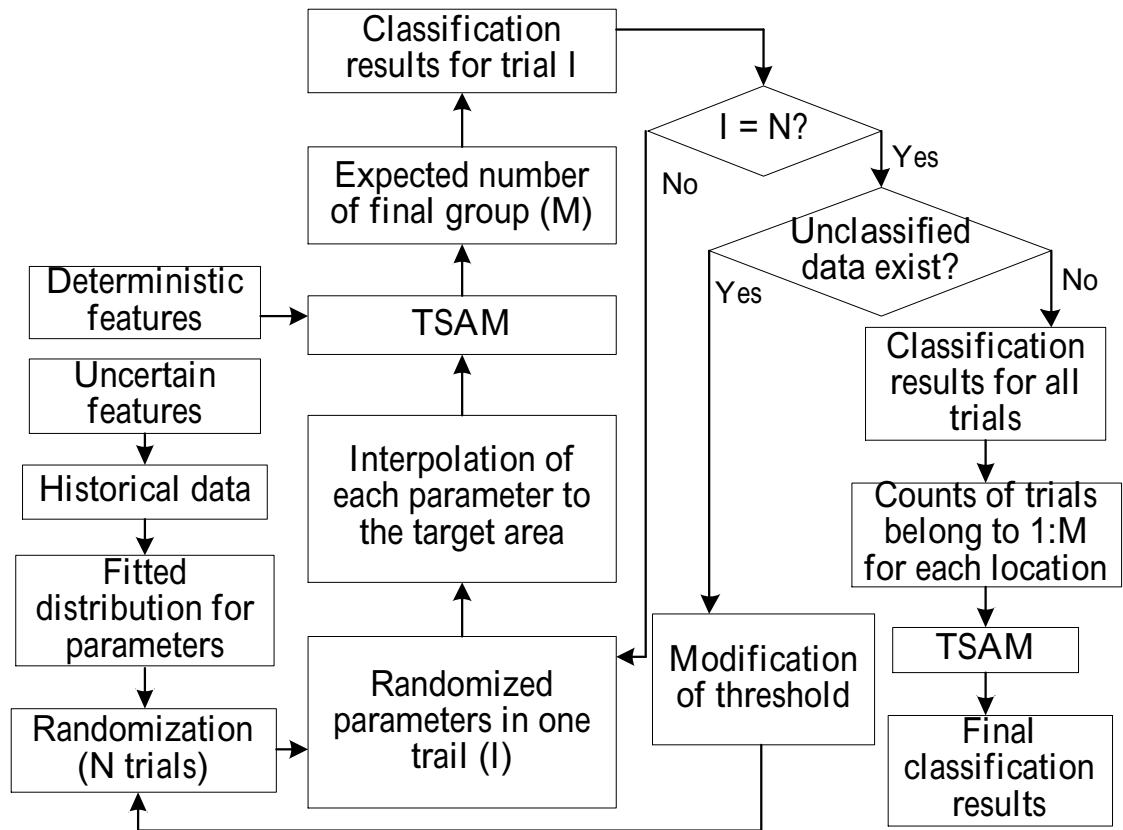
Figure 3.2 Framework of the MC-TSAM approach

As shown in Table 3.1, the indicators for the proposed five inputs are expressively different in different trials, but the grouping situations are similar. Although the label of the category is different, some of the inputs are grouped into the same category in most of the trails. For example, Input 1 is classified to Groups 2, 4 5, and 3 in a 4-trials Monte Carlo simulation, and Input 2 is classified to Groups 3, 4 5, and 3 in the same Monte Carlo simulation. Although the group labels for these two inputs are different in most of the trials (e.g., Group 2 in the first trial and Group 4 in the second trial from Input 1), in most of the time these two inputs are classified into the same group in same trial (e.g., both belong to Group 4 in the second trial). In this case, Inputs 1 and 2 are classified to the same group at 75% of the time in the Monte Carlo simulation. If the trials sufficient are large enough (e.g., 1000), and these two inputs are classified into the same group over 50% of the time, they can be determined to be the same group.

Inputs 1 and 2 actually belong to the same group due to four trials Monte Carlo simulation; Inputs 4 and 5 can be considered to be the same group; and Input 3 is significantly different from the others. Such diversities will lead to conspicuous challenge in determining the final classification result with large number of inputs and trials. In order to address this problem, the TSAM is further applied to assess the similarity of the grouping situation in all the trials during the Monte Carlo simulation and generate the final classification result.

Table 3.1 An example of classification indication for different trials

Input / Trial	1	2	3	4	5
1	2	3	1	3	3
2	4	4	2	5	4
3	5	5	3	2	2
4	3	3	1	4	4

3.2.3 Offshore OSVI classification for the south coast of Newfoundland

In order to test the feasibility and efficiency of the developed MC-TSAM, a case study of offshore OSVI classification and characterization was applied for the south coast of Newfoundland. As shown in Figure 3.3, the target area ranged from 53^0 W to 60^0 W, 45.5^0 N to 47.5^0 N, which was pre-gridded based on 0.1^0 by 0.1^0 cells. The features that might affect the risk and vulnerability of the area in any potential offshore oil spill events were considered in the offshore OSVI classification. These features included: meteorological features (wind speed, m/s; wind direction, degree; sea surface temperature, ^{0}C; and pressure, mb), oceanic features (wave height, m; current speed, m/s; and current direction, degree), ecological features (spawning fish number, /520 m^2; and location of ecological reserves), and oil relative activities features (tanker movement frequency, /year; other vessel movement frequency, /year; and historical oil spill frequency, /year).
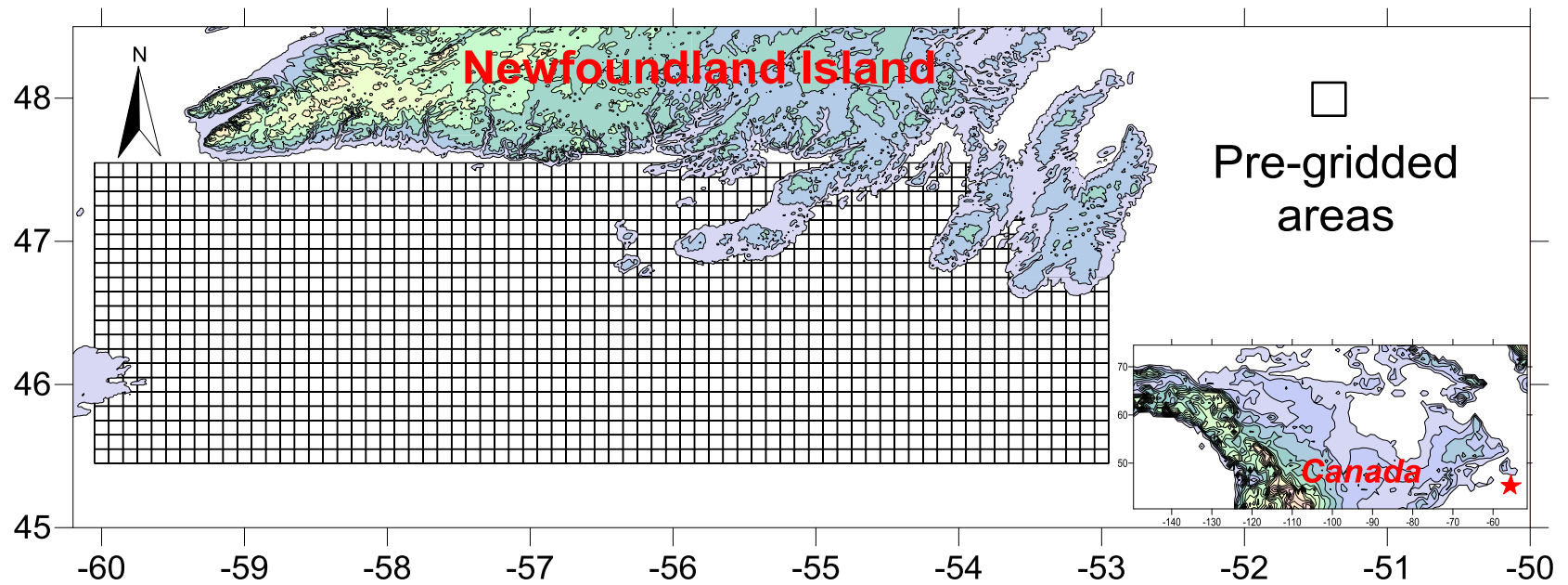
Figure 3.3 The pre-gridded study area

The meteorological as well as the wave data were collected from the Fisheries and Oceans Canada (DFO) in nine monitoring stations/spots, containing corresponding hourly data from 1990 to 2012. The information for the current direction and current speed was collected from the National Aeronautics and Space Administration's (NASA's) Ocean Motion website where provided 5-day average data from 1992 to 2012 in eight locations within the target area. The information regarding the location of the ecological reserves was obtained from the Department of Environment and Conservation, Government of Newfoundland and Labrador, Canada. The information regarding the spawning fish distribution and the oil relative activities features was extracted from the references (Ollerhead et al., 2004; Transport Canada, 2007). Because these data were obtained from different sources via different monitoring stations, the locations for different type of data were different. Therefore, it would be necessary to interpolate these data to eventually distributed gridded cells of the target area. From the analysis, it could be determined that the meteorological, oceanic, and oil relative activities features were uncertain, and the ecological features were deterministic.

Based on the collected data for the uncertain features, the distribution of the each feature in each location was approximated by the distribution with the best fitness. Two examples were given in Figure 3.4. Based on the distribution fittings for the wave height and the pressure from two different locations, the best distribution for the wave height was the Generalized Extreme Value (GEV) distribution (Figure 3.4a) and the one for the

pressure was the Weibull distribution (Figure 3.4b). Similarly, the best fitted distributions were applied for the other uncertain features in all the locations. The parameters for all the uncertain features in all the locations were shown in Tables 3.2 to 3.4. As one of the two deterministic features, the data of spawning fish number was obtained from 39 locations based on reference (Ollerhead et al., 2004). Ten locations of the ecological reserves were also determined according to the Department of Environment and Conservation, Government of Newfoundland and Labrador, Canada. The ecological reserve affected areas were determined as the areas which were close to the ecological reserves (within a distance of 0.1 degree to the boundary of the reserves). The spawning fish distribution after interpretation and the area that might affect the ecological reserves were shown in Figure 3.5c.
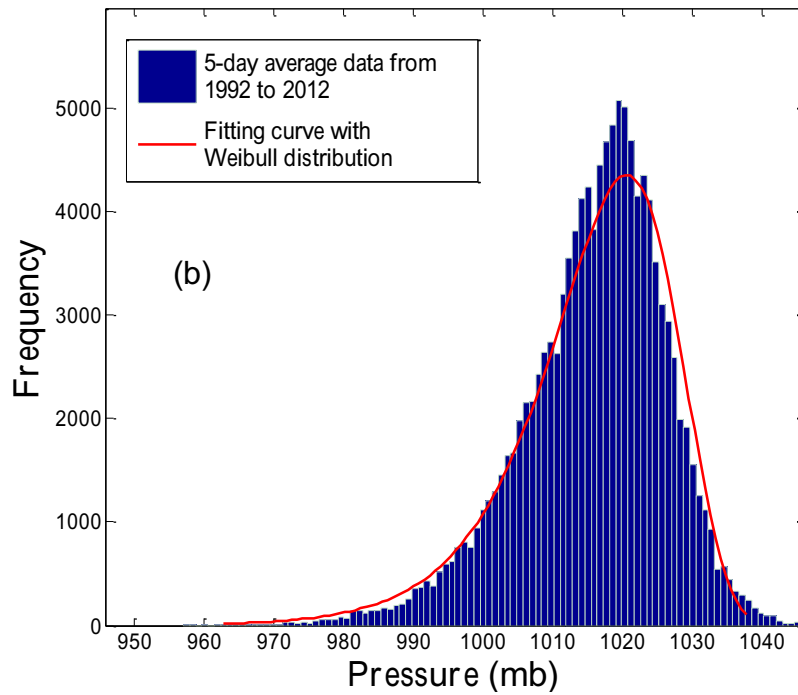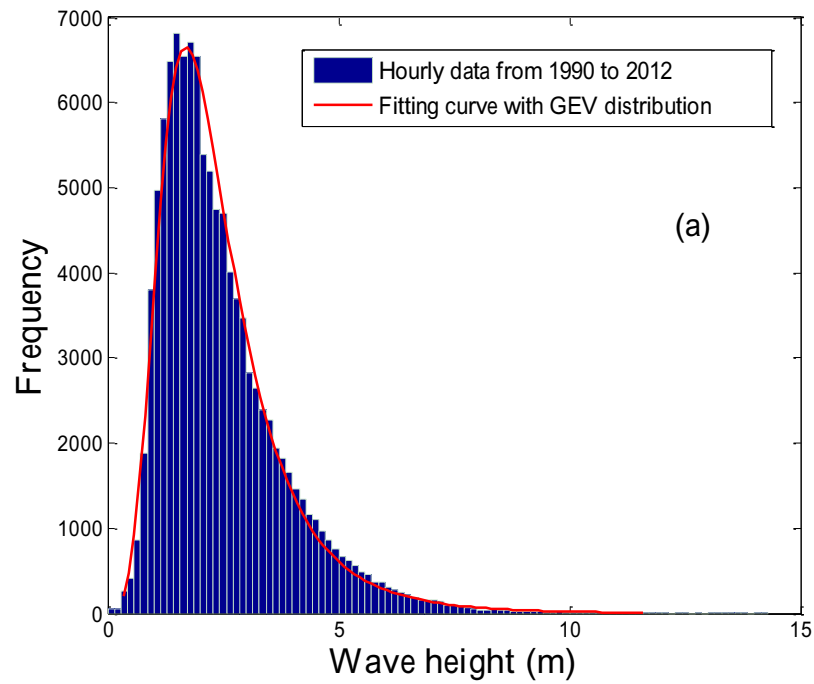
Figure 3.4 Distribution fitting for (a) wave height and (b) pressure in two different locations

Table 3.2 Parameters of the fitted distributions for meteorological features and wave height

Latitude (deg)	Longitude (deg)	Wave height (GEV)			Wind direction (GEV)			Wind speed (GEV)			Pressure (Weibull)		Sea surface temperature (GEV)		
		k	sigma	mu	k	sigma	mu	k	sigma	mu	mu	sigma	k	sigma	mu
45.90	-51.00	1.21	0.22	0.16	-0.62	104.00	196.29	-0.07	2.81	4.64	1020.05	112.43	-0.52	6.83	8.65
44.25	-53.62	0.15	0.88	1.81	-0.57	122.62	152.11	-0.14	3.63	5.09	1019.73	112.38	Normal	5.35	10.41
44.32	-57.35	0.11	0.89	1.62	-0.63	122.51	169.36	-0.10	3.30	5.38	1019.26	112.88	-0.20	5.46	6.79
42.73	-50.61	0.12	0.89	1.90	-0.50	100.03	175.41	-0.08	3.15	5.39	1020.62	113.08	Normal	6.65	10.18
42.12	-56.13	0.20	0.89	1.79	-0.66	114.49	189.30	-0.12	3.49	4.92	1020.03	115.08	Normal	6.51	14.61
45.89	-49.98	-0.13	1.02	2.90	-0.71	118.34	192.90	-0.13	3.53	5.61	1018.69	94.13	Normal	1.80	3.05
46.88	-62.00	0.13	0.38	0.48	-0.30	88.57	149.63	-0.14	2.37	4.30	1019.21	127.43	-0.44	6.34	11.05
46.44	-53.39	0.14	0.72	1.48	-0.55	99.32	183.21	-0.12	3.46	5.43	1018.43	106.40	-0.06	4.56	3.80
47.28	-57.35	0.25	0.62	1.09	-0.57	103.75	182.03	-0.07	3.29	5.15	1017.34	109.49	-0.06	5.89	4.31

93

Table 3.3 Parameters of the fitted distributions for current speed and direction

Latitude (deg)	Longitude (deg)	Current speed (GEV)			Current direction (GEV)		
		k	sigma	mu	k	sigma	mu
45.2	-53.2	0.009	0.016	0.048	Normal	2.966	8.263
47.2	-53.2	0.030	0.017	0.057	-0.508	2.926	9.203
45.2	-55.2	-0.010	0.021	0.060	Weibull	4.952	10.939
47.2	-55.2	-0.010	0.018	0.060	-0.180	3.068	4.619
45.2	-57.2	-0.074	0.019	0.065	Weibull	3.446	10.757
47.2	-57.2	-0.053	0.017	0.066	0.385	1.674	2.151
45.2	-59.2	-0.152	0.018	0.065	0.046	2.213	4.505
47.2	-59.2	-0.055	0.023	0.066	Normal	2.388	6.972

Table 3.4 Parameters of the fitted distributions for oil relative activities features

Latitude	Longitude	Annual movements of tankers (Normal)		Annual movements of other vessels (Normal)		Spill Frequency (Normal)	
		mu	sigma	mu	sigma	mu	sigma
47.7	-54.1	1276	120	7010	700	2.34	0.2
47.2	-55.1	1276	120	7010	700	1.29	0.1
46.8	-56	933	90	5063	500	1.43	0.1
45.8	-59.3	590	60	3117	300	2.69	0.2
47.8	-51.4	190	21	7070	700	1.47	0.1

In each loop/ trial of the Monte Carlo simulation, a series of random numbers was generated for the uncertain features based on the approximated distribution of the corresponding feature in each location. These random numbers (e.g., wave height and wind speed) along with the deterministic numbers (i.e., the number of spawning fish and the ecological reserve affected areas) were fed to the MC-TSAM. Each input feature (uncertain or deterministic) in all their available locations were then interpolated in to the 0.1^0 by 0.1^0 grids based on the MATLAB$^{®}$ griddata method.

Interpolation is a method of constructing new data points within the range of a discrete set of known data points. Data interpolation is usually based on underlying geometric algorithms. Data may be uniform (sampling occurs over uniform intervals) or scattered (sampling occurs over irregular intervals). When the sample data is scattered (e.g., different location of stations for different features in this case), the interpolation is usually based on triangulation-based approach. MATLAB$^{®}$ griddata method uses the Delaunay triangulation for interpolation. The Delaunay triangulation method can generate interpolated surfaces from many different data sources such as point data, lines, breaklines, and polygons (erase, replace, or clip). It can provide more accurate interpolation results then the other methods because the original data points are located exactly on the surface. Because of this flexibility and the speed of interpolation, triangulation has become a popular interpolation method (Hu, 1995). The method defines the type of surface fit to the data, producing smooth surfaces that always pass through the

data points and forming a uniform grid (Hajovsky et al., 2012).

As examples, Figures 3.5a and 3.5b showed the current direction and the historical oil spill frequency in the target area after the interpolation based on the mean values of their fitted distributions. Furthermore, Figure 3.5c indicated the distribution of the spawning fish and the locations of the areas affected by the ecological reserves. The figures regarding the other parameters were shown in Figures A3.1 to A3.8 in Appendix A. The interpolated values of all the features in gridded cells formed the [I] (Equation 3.1) for MC-TSAM classification (Figure 3.1). The number of trials was set to N = 500. After completing the classifications in all the trials preset for the Monte Carlo simulation, a TSAM module was further applied to handle the grouping of the classification results from these trials and generated the final classification results for the study area (Figure 3.2).

Newfoundland Island

Current direction

Canada

(a)
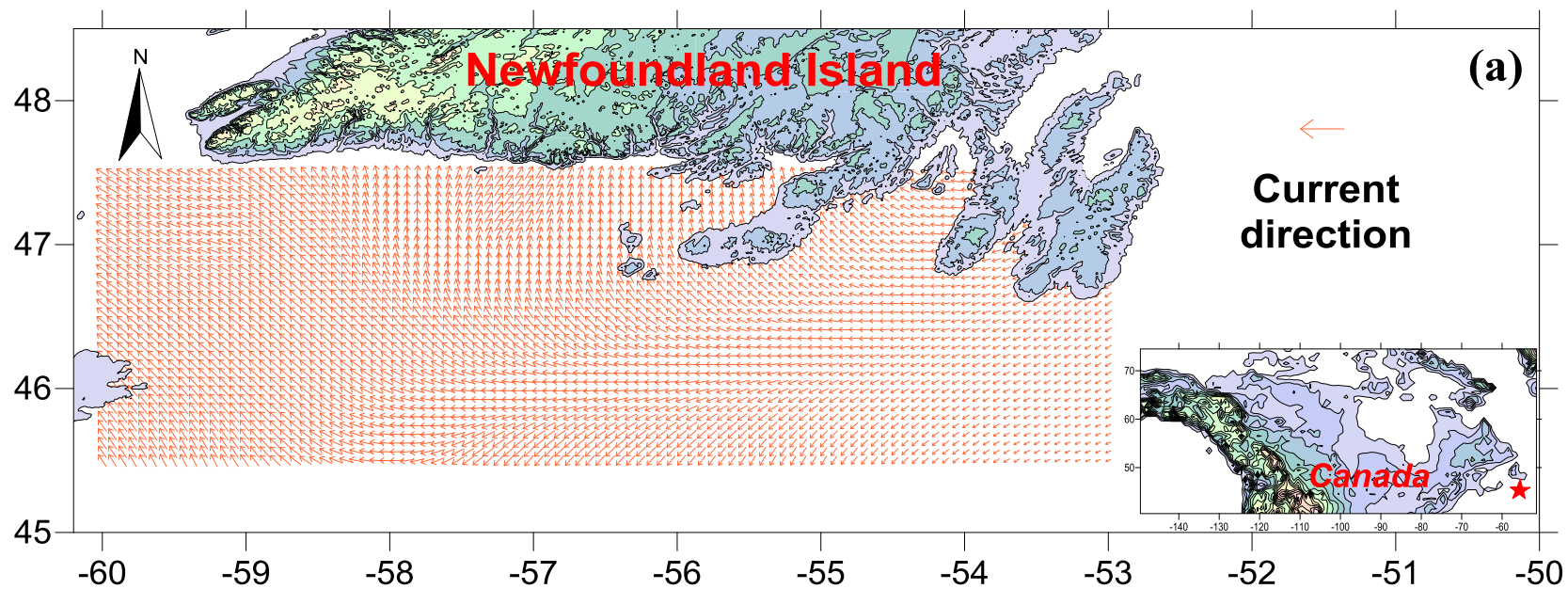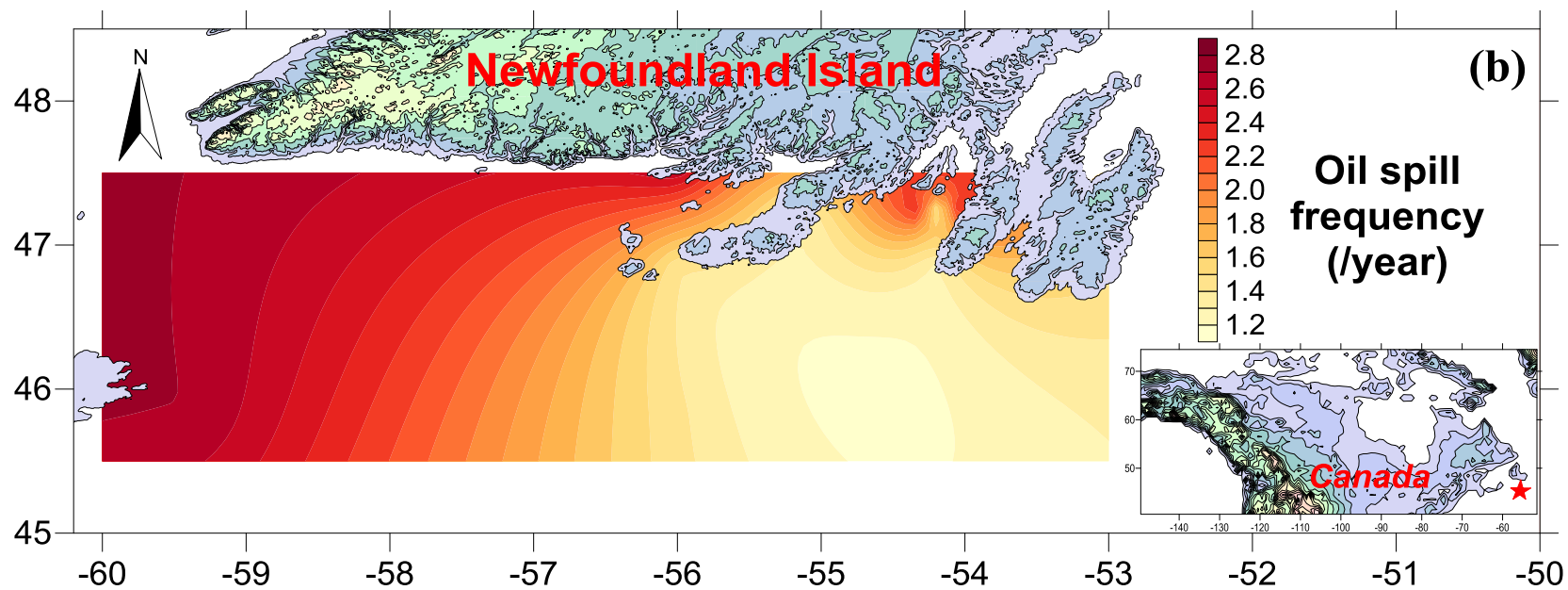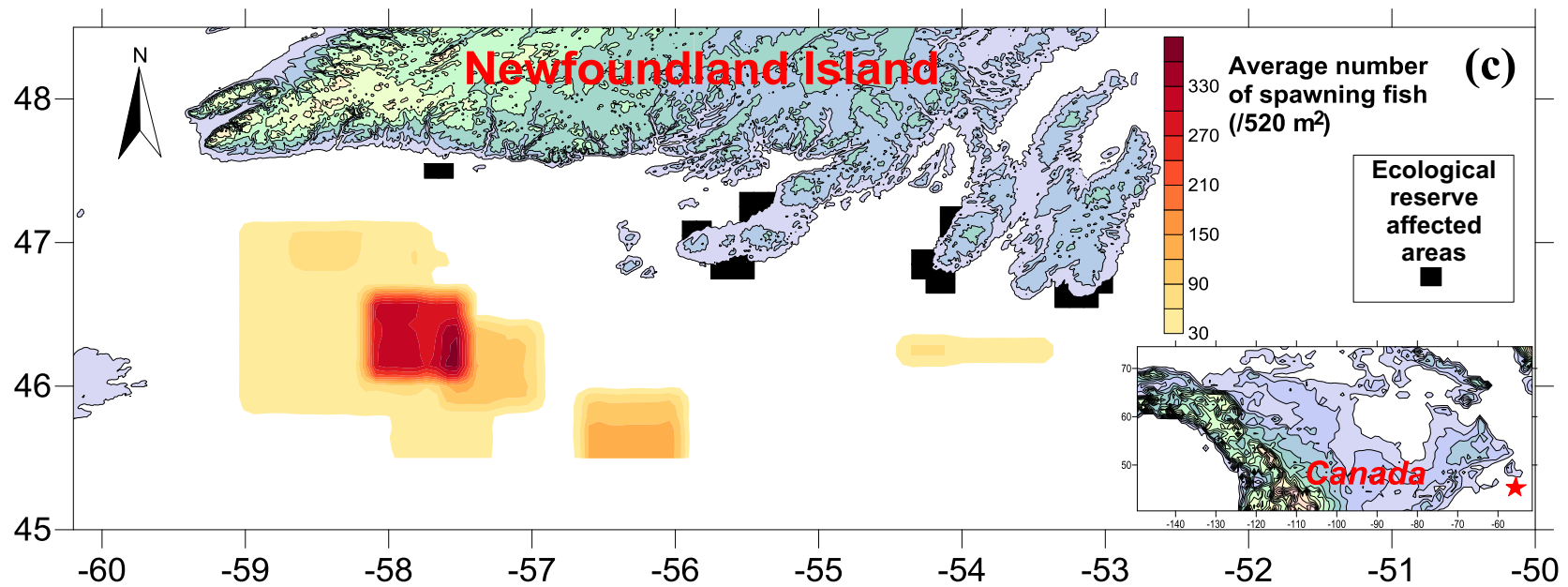
Figure 3.5 Interpolated (a) prevailing current direction, (b) mean historical spill frequency and (c) number of spawning fish and ecological reserve affected areas

By assessing the similarities within a zone and the differences in different zones based on MC-TSAM, the study area was finally classified into five different zones as shown in Figure 3.6. Generally, Zone 1 covered the area far from the land; Zone 2 covered the area that close to the islands located in the south of Newfoundland; Zones 3 and 4 covered the area that may affected by the outlet of the St Lawrence River; Zone 5 covered the shoreline area of the island.

The comparison of the classification result (Figure 3.6) and the distribution of the main current direction (Figure 3.5a) indicated that the current direction in Zone 1 was mainly from east to west and turning to the south, flowing away from island. The current speed was relatively low (the length of arrows in Figure 3.5a represented the current speed from 0.050 to 0.066 m/s, and the distribution of the prevailing current speed was also shown in Figure A3.6 in the Appendix A). In contrast, the current direction in Zone 5 was mainly from the east to the west and turning north to the island, and the current speed was higher than that in Zone 1. The current directions in Zones 2, 3 and 4 were mainly from southeast to northwest with the highest current speed in the study area. Figures 3.5c and 3.6 also indicated that all the areas that were vulnerable to oil spills were involved in Zone 5 and none was involved in the other zones. Furthermore, all the spawning fishes located in the eastern part of the offshore area were covered by Zone 1 but the amount remained in a low level (< 150 spawning fish/ 520 m^2); the area with the highest level of the spawning fishes (> 330 spawning fish/520 m^2) was located in Zones 4

and 5; the area covered by Zone 3 was with low level of spawning fishes (<60 spawning fish/520m^2); and the area covered by Zone 2 almost had no spawning fish. Furthermore, the tanker and vessel movement frequency in Zone 5 was significantly higher than the others, leading to the highest potential of offshore oil spill in all zones. The pressure and temperature in Zone 5 were significantly lower than the others which caused high impact to the oil weathering (e.g., evaporation and emulsification), leading to difficulties in offshore oil spill response and countermeasures. The highest wave height appeared in Zone 1 and then the Zone 5, which might cause effects to the oil weathering and difficulty to the offshore oil spill response and countermeasures. The wind speed in Zones 1 and 5 were considerably higher than which in the other zones and the prevailing wind directions in the whole study area were from south to north, which meant that if any oil spill would happen in this area, the shoreline of the island might be endangered, especially which would happen in Zone 1.

The area in Zone 5 appeared to have the highest OSVI level if any oil spill occurs in this area, while Zone 1 had the lowest OSVI level with the occurrence of oil spills. Oil spills occurring in Zones 2, 3 and 4 might not cause significant impacts to Newfoundland. However, as shown in Figure 5b, the historical oil spill frequency in these areas was significantly high than which in Zone 1 and 5 (probably because these areas were located in the exit of the St Laurence River from the mainland of Canada), which might also require high diligence in offshore oil spill monitoring and controlling. Furthermore,

because the spawning fish in Zone 4 was higher than which in Zone 3, and there was almost none in Zone 2. In addition, the location of Zone 4 was closer to Newfoundland than Zone 3, and Zone 2 was the farthest in all the Zones. Therefore, the Zone 5 was the most vulnerable area while Zone 1 was the least vulnerable one. The scales of zones (1 - 5) indicated the OSVI levels (Figure 3.6).
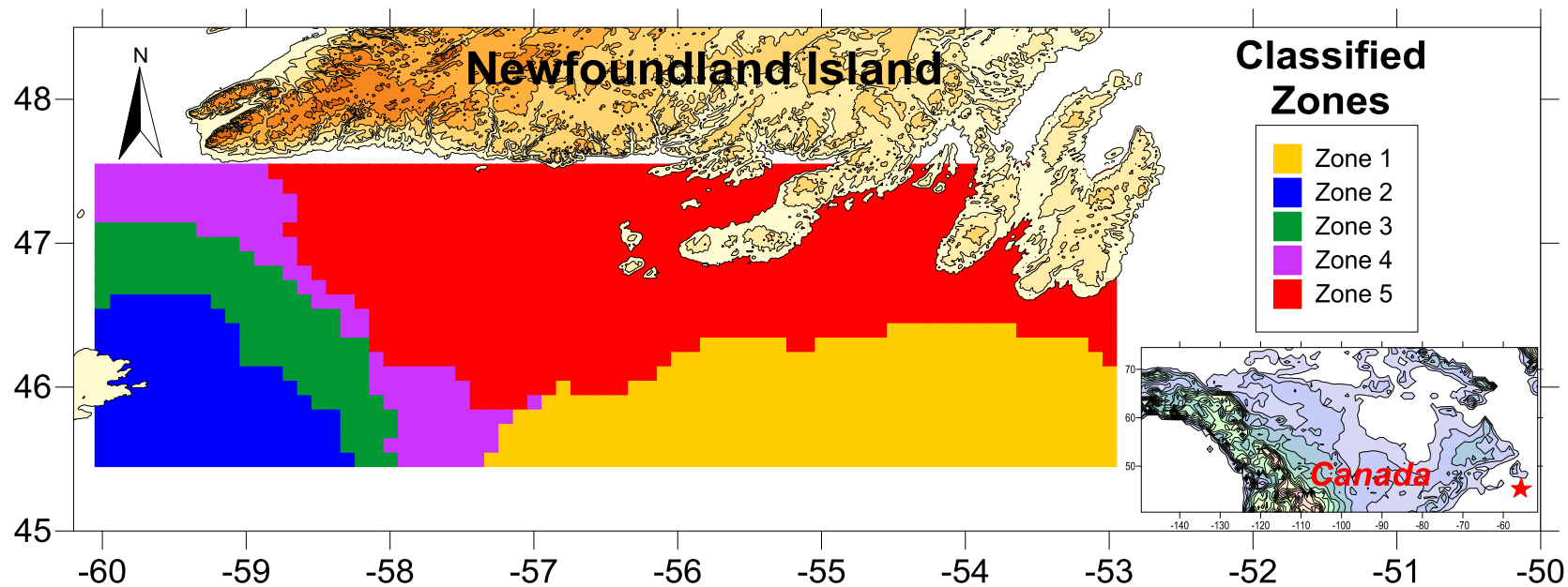
Figure 3.6 Final classification result for the south coast of Newfoundland

To demonstrate the power of the proposed classification method, statistical analysis was conducted. The desired results were the data from five zones are significantly different from each other in this case. Eleven features were considered in the statistical analysis, including wave height, wind direction, wind speed, pressure, surface temperature, current direction, current speed, tanker movement, other vessel movement, spill frequency, and spawning fish. Because the locations of the ecological reserves were categorical numbers and all located in Zone 5, they were not considered in the analysis.

In order to make all the zones comparable, the data of different features among the five zones was standardized, respectively. The data of the 11 features within one zone was added together to generate a new data set for the comparison, called typical group values (TGVs). Correspondingly, the TGV data for five zones could be applied to statistical analysis. The normality test results showed that there was no clear evidence that the TGV data for five zones follows certain distributions.

The Mann-Whitney test (Mann and Whitney, 1947) was also applied in this study. The Mann-Whitney test is a nonparametric method and used for testing whether two independent sample data come from a same population. This method does not require the equal sample size between different zones, making it suitable for this study. If the P-value was smaller than the pre-set significance level (0.05 for this case), the two sample data were considered as significantly different from each other. Table 3.5 shows the results of the Mann-Whitney test for TGV data.

Table 3.5 Statistical analysis results by using the Mann-Whitney Test

	Null Hypothesis	Sig.	Decision
1	The Zone 1 and Zone 2 have same population median	<0.000	Reject the null hypothesis.
2	The Zone 1 and Zone 3 have same population median	<0.000	Reject the null hypothesis.
3	The Zone 1 and Zone 4 have same population median	0.0015	Reject the null hypothesis.
4	The Zone 1 and Zone 5 have same population median.	<0.000	Reject the null hypothesis.
5	The Zone 2 and Zone 3 have same population median	0.0024	Reject the null hypothesis.
6	The Zone 2 and Zone 4 have same population median	0.0010	Reject the null hypothesis.
7	The Zone 2 and Zone 5 have same population median	<0.000	Reject the null hypothesis.
8	The Zone 3 and Zone 4 have same population median	<0.000	Reject the null hypothesis.
9	The Zone 3 and Zone 5 have same population median.	<0.000	Reject the null hypothesis.
10	The Zone 4 and Zone 5 have same population median	<0.000	Reject the null hypothesis.

Table 3.5 clearly indicated that all the null hypotheses were rejected because all the P-value were smaller than 0.05. The data from any two zones were not from a same population, indicating that the data from five zones were significantly different from each other. Therefore, it could be concluded that the statistical analysis results agreed with the classification results, demonstrating the feasibility and reliability of the MC-TSAM.

Another two nonparametric tests for independent samples (more than 2 zones) also were conducted to test the original data of the 11 features among 5 zones, including the Kruskal-Wallis test and the Jonckheere-Terpstra test. Both tests were used for nonparametric test with a similar null hypothesis that several independent samples were coming from the same population (Terpstra, 1952; Jonckheere, 1954; Helsel and Hirsch, 2002). The pre-set significance levels were also 0.05 for these two tests. The rejection of the null hypothesis of the Kruskal-Wallis test indicated that at least one zone were different from other zones. The test results were shown in Table 3.6. The Jonckheere-Terpstra test was more powerful to detect the data with a priori between zones (Vock and Balakrishnan, 2011). Although there was no evidence for the order of the five different classes in this study, this method could still be used for the comparison test. Fail to reject the null hypothesis of the Jonckheere-Terpstra test indicated that data from each zone were not significantly different. The test results were shown in Table 3.7.

Table 3.6 Statistical analysis results by using the Kruskal-Wallis Test

	Null Hypothesis	Sig.	Decision
1	The distribution of Wind Height is the same across categories of Zone.	.000	Reject the null hypothesis.
2	The distribution of Wind Direction is the same across categories of Zone.	.000	Reject the null hypothesis.
3	The distribution of Wind Speed is the same across categories of Zone.	.000	Reject the null hypothesis.
4	The distribution of Pressure is the same across categories of Zone.	.000	Reject the null hypothesis.
5	The distribution of Surface Temp is the same across categories of Zone.	.000	Reject the null hypothesis.
6	The distribution of Current Direction is the same across categories of Zone.	.000	Reject the null hypothesis.
7	The distribution of Current Speed is the same across categories of Zone.	.000	Reject the null hypothesis.
8	The distribution of Tanker movement is the same across categories of Zone.	.000	Reject the null hypothesis.
9	The distribution of Other Vessel Movement is the same across categories of Zone.	.000	Reject the null hypothesis.
10	The distribution of Spill Frequency is the same across categories of Zone.	.000	Reject the null hypothesis.
11	The distribution of spawning fish is the same across categories of Zone.	.000	Reject the null hypothesis.

Table 3.7 Statistical analysis results by using the Jonckheere-Terpstra Test

	Null Hypothesis	Sig.	Decision
1	The distribution of Wind Height is the same across categories of Zone.	.000	Reject the null hypothesis.
2	The distribution of Wind Direction is the same across categories of Zone.	.691	Retain the null hypothesis.
3	The distribution of Wind speed is the same across categories of Zone.	.000	Reject the null hypothesis.
4	The distribution of Pressure is the same across categories of Zone.	.000	Reject the null hypothesis.
5	The distribution of Surface Temp is the same across categories of Zone.	.000	Reject the null hypothesis.
6	The distribution of Current Direction is the same across categories of Zone.	.000	Reject the null hypothesis.
7	The distribution of Current Speed is the same across categories of Zone.	.006	Reject the null hypothesis.
8	The distribution of Tanker movement is the same across categories of Zone.	.308	Retain the null hypothesis.
9	The distribution of Other Vessel Movement is the same across categories of Zone.	.187	Retain the null hypothesis.
10	The distribution of Spill Frequency is the same across categories of Zone.	.000	Reject the null hypothesis.
11	The distribution of Spawning fish is the same across categories of Zone.	.000	Reject the null hypothesis.

Table 3.6 shows that all the null hypotheses were rejected through the Kruskal-Wallis test, indicating that all the 11 features among five zones were significantly different from each other However, Table 3.7 indicated that the null hypotheses had not been rejected for wind direction, tanker movement, and other vessel movement through the Jonckheere-Terpstra test, indicating that there might be some similarity among these features in different zones. It indicated that if only single or limited features were considered for classification, it could lead to unreliable results. However, when all the effects were combined into TGV data, the difference between zones could be emphasized. This demonstrated that the proposed MC-TSAM could capture the combined effects from uncertain and complex features, showing its advantages over traditional methods.

3.3 A Monte Carlo Simulation Based Integrated Rule-based Fuzzy ARTMap (MC-IRFAM) Approach

3.3.1 An integrated rule-based fuzzy ARTMap (IRFAM) approach

Since the ART/ARTMap system itself does not have the ability to handle uncertainties in supervised classification, fuzzy interface modules were integrated with ART and ART Mapping modules to be used as an alternative in the logic operation, leading to an integrated rule-based fuzzy ARTMap (IRFAM) approach. As shown in Figure 3.7, the IRFAM approach includes three subsystems: 1) centroid determination to

locate the centroids of the expected target groups by unsupervised ART; 2) criteria combination to generate the combined fuzzy criteria; and 3) classification to classify the fuzzified inputs based on rules. There are five ART modules integrated in the IRFAM system as follows: ART_1 is used to process unsupervised classification for the fuzzified inputs; ART_{2a} and ART_{2b} are used to screen the criteria combinations into the preset target groups; ART_{3a} and ART_{3b} are used to conduct the supervised classification based on a comparison of the combined criteria with the inputs.
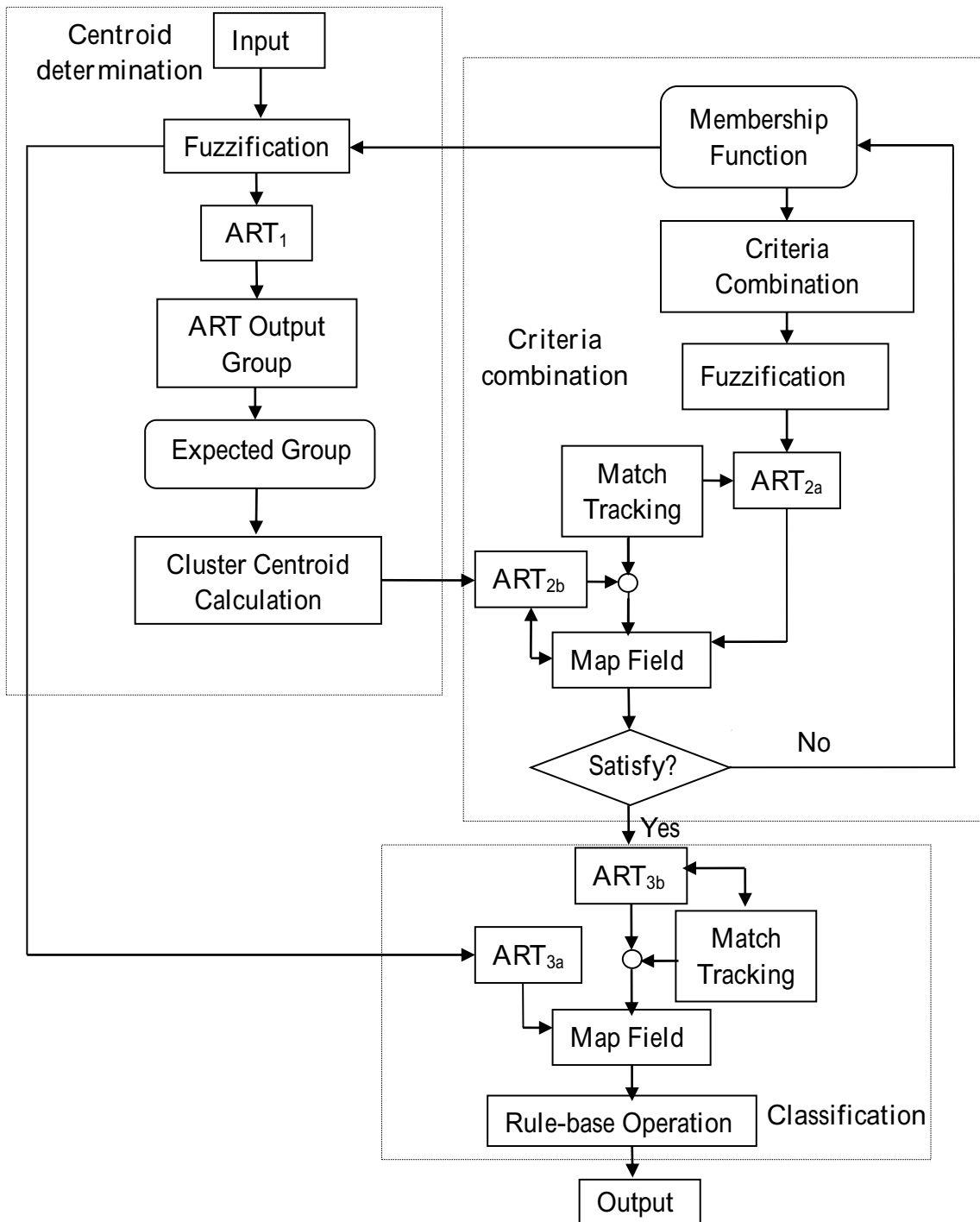
Figure 3.7 Flowchart of the IRFAM approach

Criteria combination

A fuzzy set is a class of objects with continuous grades of membership which represents the degree of truth as an extension of valuation (Zadeh, 1965). Fuzzy sets generalize classical sets. The indicator functions of these sets are special cases of the membership functions of fuzzy sets for the latter only take values 0 or 1.

Let [X] be a set of data points, with series of data points of x, therefore, [X] = {x}. A fuzzy set [Y] in [X] is characterized by a membership function $\mu(x)$. It can be used to describe the means in measuring the degree of compatibility of a data value to a fuzzy set, or to describe the probability that this data value belongs to a fuzzy set [Y] in the interval [0, 1]. The $\mu(x)$ value at x indicates the grade of membership of x in [Y]. Therefore, the closer the value of $\mu(x)$ to 1, the higher the grade of membership of x in [Y] appears (Zadeh 1968). The commonly used membership functions are triangular, trapezoidal, and bell shaped. A fuzzy set operation is an operation on fuzzy sets, which are a generalization of crisp set operations. The most widely used operations are called standard fuzzy set operations, which include unions, complements, and intersections (Dubois and Prade, 1988).

For the triangle membership function, $\mu_i(x)$ can be described as follows:

$$\mu_i(x) = \begin{cases} \dfrac{x-d}{c-d} & \text{if } d \leq x \leq c \\ \dfrac{e-x}{e-c} & \text{if } c \leq x \leq e \\ 0 & \text{otherwise} \end{cases} \tag{3.8}$$

where d is the lower bound of the i level membership function, e is the upper bound of the i level membership function, and c is the point where $\mu_i(x) = 1$.

The original input is formed as follows:

$$\left[I_{a_p}\right] = \left(x_{kj}\right)_{k=1,\cdots,p;\ j=1,\cdots,n} \tag{3.9}$$

where p is the number of samples, and n is the number of features in each sample.

Based on the membership function, the fuzzy set [Y] is given as follows:

$$\left[Y\right] = \left(\mu_i(x)\right)_{i=1,\cdots,m} \tag{3.10}$$

where m is the number of the membership levels, $\mu_m(x)$ is the highest level membership function and $\mu_1(x)$ is the lowest level membership function.

Operated by the fuzzification module, the original input [I_{ap}] is converted to:

$$\left[I_a\right] = \left(\mu_i(x_{kj})\right)_{i=1,\cdots,m;\ k=1,\cdots,o;\ j=1,\cdots,n} \tag{3.11}$$

After the input patterns are classified by ART, the centroids are going to be located based on the expected target groups by the operation of the centroids locating module.

114

For m expected target groups, the first m clusters which have the most patterns in the clusters are selected. The centroid of each cluster is given by:

$$[C] = (x_i)_{i=1,\cdots,n} \tag{3.12}$$

where n is the number of features of input data after fuzzification, and x_i is given by:

$$x_i = \begin{cases} fv_i & \text{if } i = 1 \\ \sum\limits_{2}^{q} (\dfrac{i-1}{i} \sum\limits_{1}^{i-1} fv_{i-1} + \dfrac{1}{i} fv_i) & \text{if } i > 1 \end{cases} \tag{3.13}$$

where q is the number of data points in the cluster and fv is the value of the feature in each pattern. The outputs of centroids are going to be used as the classification criteria in the criteria combination subsystem.

Fuzzy criteria combination

The criteria combination is the combination of y_{ij} which has the membership function $\mu(y_{ij}) = 1$, where i is the level of membership function and j is the number of the feature. If there are m features with p levels of membership function, the number of criteria combinations will be in the number of p^m, and the criteria combination $[I_{b_0}]$ is given by:

$$[I_{b_0}] = (y_j(y_i)_{i=1,\,2,\ldots,p})_{j=1,2,\ldots,m} \tag{3.14}$$

115

After being operated by the fuzzification module, the criteria combination I_{b_0} is converted to:

$$[I_b] = \left(\mu(y_j)(\mu(y_i))_{i=1,\dots,p} \right)_{j=1,\dots,m} \tag{3.15}$$

For example, for a series of input patterns with two features in each pattern (e.g., catchment area and elevation), and 3 levels for each parameter (e.g., low, medium, and high), the criteria combination $[I_b]$ will be:

$$[I_b] = \begin{bmatrix} 1 & 0 & 0 & 1 & 0 & 0 \\ 1 & 0 & 0 & 0 & 1 & 0 \\ 1 & 0 & 0 & 0 & 0 & 1 \\ 0 & 1 & 0 & 1 & 0 & 0 \\ 0 & 1 & 0 & 0 & 1 & 0 \\ 0 & 1 & 0 & 0 & 0 & 1 \\ 0 & 0 & 1 & 1 & 0 & 0 \\ 0 & 0 & 1 & 0 & 1 & 0 \\ 0 & 0 & 1 & 0 & 0 & 1 \end{bmatrix} \tag{3.16}$$

where $[I_b]$ lists all the possible combinations based on 2 features with 3 membership levels. The number of these combinations is $3^2 = 9$, which determines the number of rows in $[I_b]$. In contrast, the number of columns in $[I_b]$ is $3 \times 2 = 6$. Each row is in the sequence from the lowest level to the highest one for the first feature and then the second one.

116

[I_b] in Equation 3.15 and C in Equation 3.12 are used as inputs for the ART_{2a} and the ART_{2b} modules. Each input criteria combination in $\left\lfloor I_{b_0} \right\rfloor$ is compared with each centroid pattern by the operation of the ART Mapping system. Finally, the criteria combinations are classified into the target groups. ART_{2a} and ART_{2b} are linked together via an inter-ART module [F^{ab}] called the map field.

Classification

The classification subsystem consists of two modules: the mapping module including ART_{3a}, ART_{3b}, and map field, and rule-based operation module. The mapping module is almost the same as the one used in the centroid determination subsystem. The only difference is that the vigilance for classification is higher than the one for centroid determination.

[I_a] and [I_b] are used as inputs for the ART_{3a} and the ART_{3b} modules. The comparison of each input pattern with criterion is handled by the ARTMap learning to determine their similarity. When the ARTMap learning finishes, the final pair of input pattern and criterion is supposed to have the highest similarity which indicates the best match. Consequently, the input patterns in [I_a] are captured by certain criteria combinations in [I_b] after the ARTMap supervised leaning. Then by the operation of the rule-based operation module, the input patterns are finally classified into the target groups in the criteria combination subsystem.

A set of fuzzy if-then rules are used in the form of: if a set of conditions can be

satisfied, then a relative set of consequences can be determined. The if-then rule is applied after the matching of input patterns with criteria combinations:

$$\text{Rule } R_r : \text{if } \left[I_{as} \right] \in \left[y_t \right], \text{ and } \left[y_t \right] \in \left[G_r \right], \text{ then } \left[I_{as} \right] \in \left[G_r \right] \tag{3.17}$$

where $[I_{as}]$ is the sth input pattern; $[y_t]$ is the tth criteria combination; and $[G_r]$ is the rth group. By using the rule-based operation, the input patterns in $[I_a]$ are properly classified into the group set which is preset by rule R_r.

3.3.2 The MC-IRFAM approach

It is still practically difficult to directly apply a conventional IRFAM to classification with coexistence of complexity and uncertainty in offshore oil spill response and countermeasures. First, values for the features are not deterministic. For example, meteorological data in an oil spill area are obtained through various monitoring devices with time series, which lead to uncertainties resulting from sensor resolution, instrument errors, and dynamics. Secondly, there may be difficulty in determining the criteria for classification because of uncertainty and complexity of the spill site condition. The determination of specific criteria (i.e., what values for temperature, wave height, wind speed and direction, and slick thickness can be used to represent a type of common features in an offshore oil spill) is usually based on insufficient references and historical

118

records in the target area, which also leads to uncertainties. Furthermore, these difficulties will be worsened when multiple features are considered. The introduction of likelihoods/memberships based on fuzzy set theory becomes necessary to reflect such uncertainties and to resolve difficulties with the ARTMap method.

In offshore oil spills, different affected sites have different characteristics depending on various features such as pollutants' properties, hydrological conditions, and a variety of physical, chemical, and biological processes. Thus, the response technologies selected for different sites significantly vary. The classification/ranking for a suitable method at a given site often requires expertise on both response technologies and site conditions. Recently there are number of technologies developed for offshore oil spill response and countermeasures, however, each type of technology have its advantages or disadvantages in treating different types of oils. Furthermore, the site conditions (e.g., temperature, wave, wind, oil viscosity, and slick thickness) are usually uncertain, and the feasibility/efficiency of a response technology is also varied with these uncertain conditions. Thus, it becomes a challenge to classify/rank numerous existing technologies for an offshore oil spill.

In order to address this challenge, a Monte Carlo simulation is introduced to generate random numbers of parameters within their feasibility range based on uniform distribution, leading to a Monte Carlo simulation based IRFAM (MC-IRFAM) approach. According to the operations shown in Figure 3.8, the available technologies are ranked

with highest to lowest feasibilities based on the spilled site condition. After processed by

the MC-IRFAM approach with certain trails (e.g., N = 10,000), the information about

overall scores for the technologies can be obtained.

3.3.3 Technology screening for offshore oil spill response

Assume a set of criteria for temperature, wave, wind, oil viscosity, and slick

thickness as follows in Figure 3.9. Furthermore, consider an offshore oil spill with site

conditions of temperature: about 10 ^oC, wave height: about 0.4 m, wind speed: about 10

m/s, viscosity of spill oil: about 100 cSt, slick thickness: about 0.5 mm. There are four

technologies (denoted as A, B, C, D) available and their feasibilities in the corresponding

parameters are shown in Table 3.8. According to the membership functions (Figure 3.9),

the parameters for the site conditions and the feasibility of the technologies can be

fuzzified as in Table 3.9.
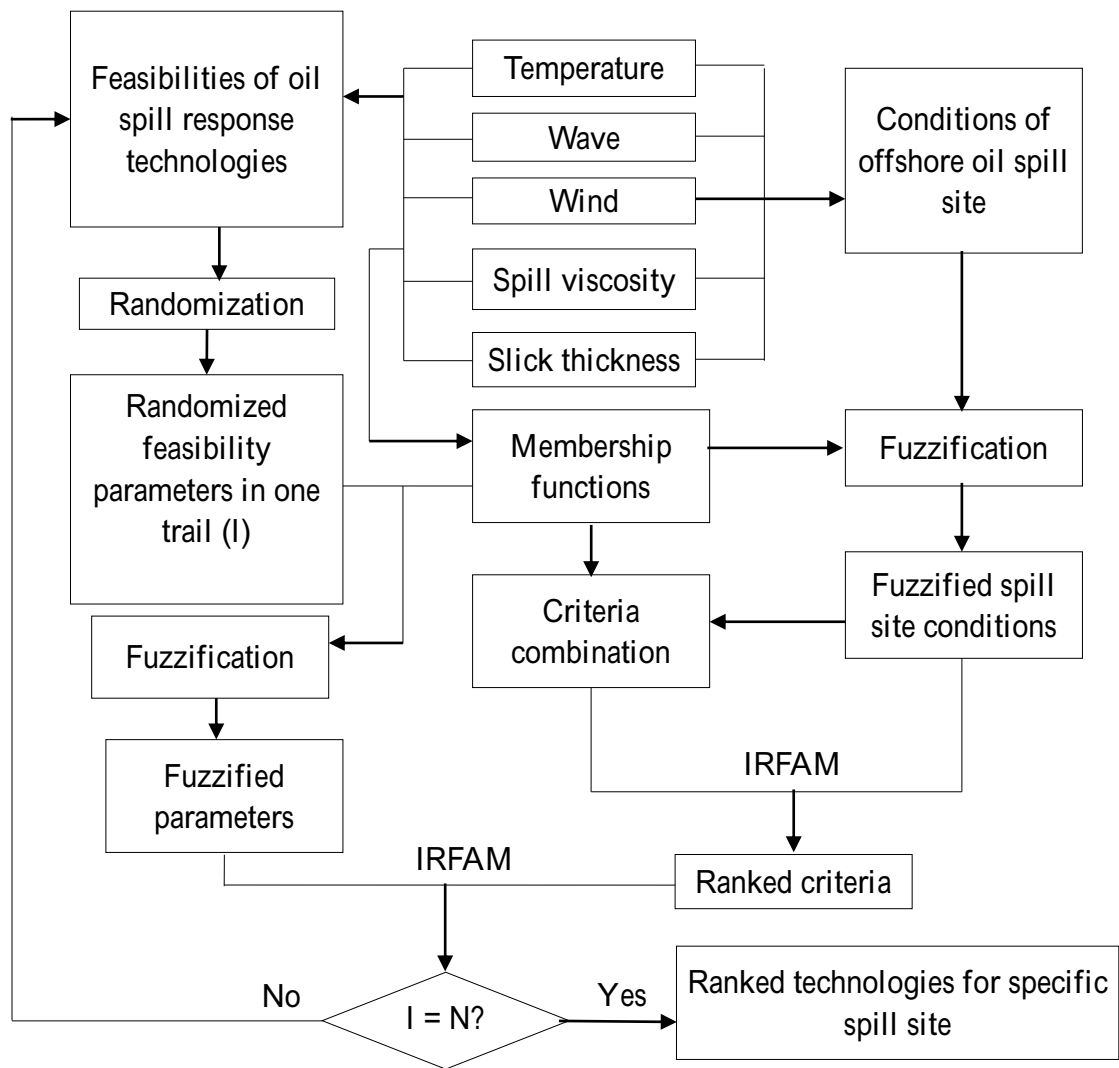
Figure 3.8 The MC-IRFAM approach for technology screening and ranking in an offshore spill
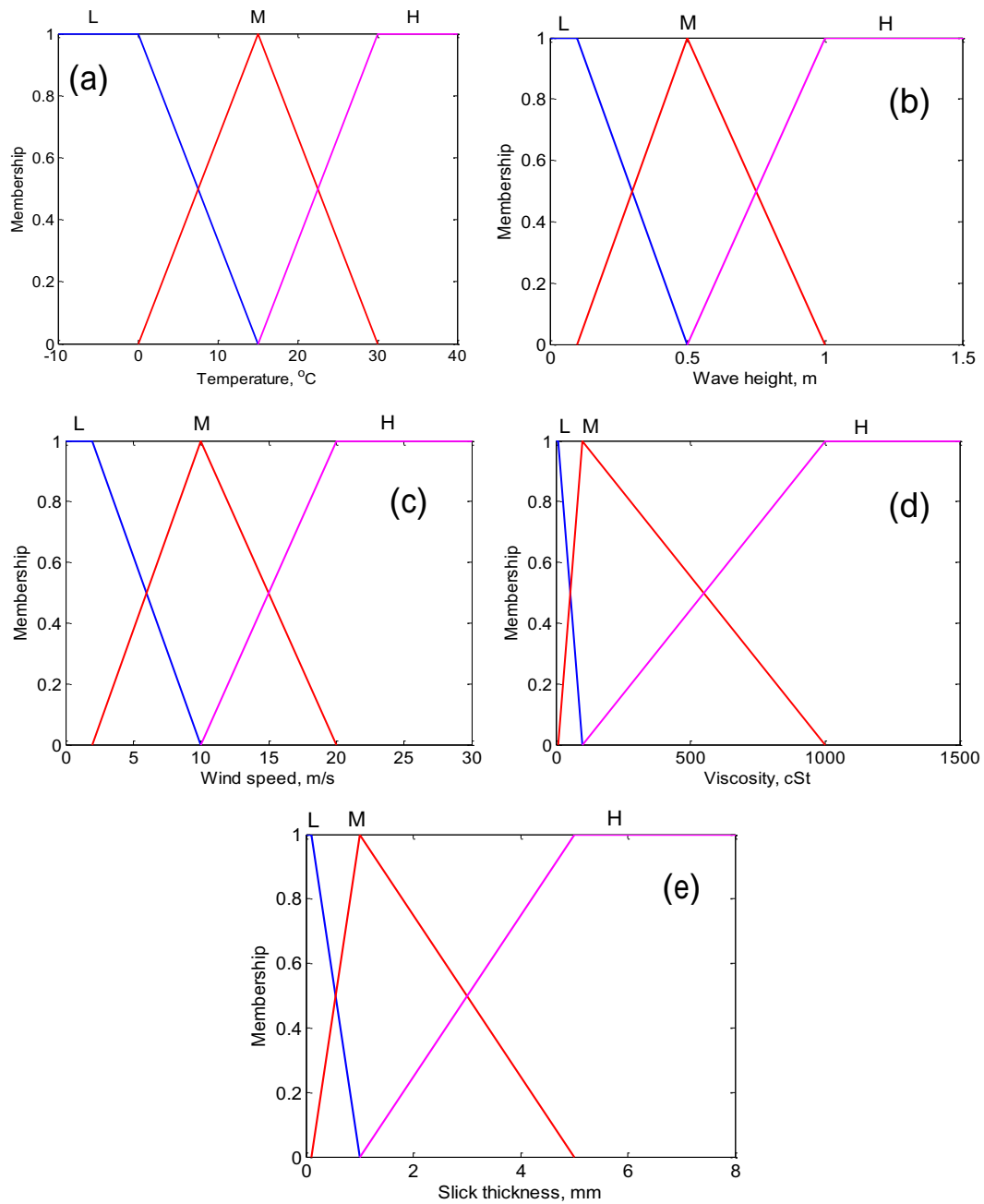
Figure 3.9 The membership function of (a) temperature, (b) wave height, (c) wind speed, (d) oil viscosity, and (e) slick thickness

As shown in Tables 3.8 and 3.9, the parameters presenting the feasibilities of the technologies are in ranges, which may lead to difficulty in matching the parameters in technologies with site conditions. For example, the feasibility of the Technology A in temperature is 5-20 ^{o}C and the site temperature is around 15 ^{o}C, which means the Technology A is 100% feasible in the spilled site according to temperature. However, the fuzzy set of the temperature in spilled site is (0.33, 0.66, 0) and for the feasibility of Technology A is (0.66, 1, 0.33). An overall score from the IRFAM approach which indicating the match of two samples (e.g., temperature of site conditions and the feasibility of Technology A in this case) in a range of [0, 1] (0 represents totally unmatched and 1 represents perfect matched) is used for the technologies ranking. The overall score of the site conditions and Technology A in temperature is only 0.6667 by direct comparison with the IRFAM, which is much lower than the one from physical comparison. Therefore, it may be inaccurate to classify/rank the technologies with direct fuzzification of the parameters.

Table 3.8 Parameters for the feasibilities of technologies

	Temperature (^{o}C)	Wave height (m)	Wind speed (m/s)	Spill viscosity (cSt)	Slick thickness (mm)
Technology A	5-20	0-0.5	>20	100-200	0.01 - 1
Technology B	20-30	0.5-2	0-5	500-1000	1-5
Technology C	>30	0-0.2	>10	>1000	>4
Technology D	10-15	0-0.3	0-10	>50	0.1-0.5

Table 3.9 Fuzzified parameters of the site conditions and the feasibility of the technologies

	Temperature (°C)	Wave height (m)	Wind speed (m/s)	Spill viscosity (cSt)	Slick thickness (mm)
Site conditions	(0.33, 0.66, 0)	(0.25, 0.75, 0)	(0, 1, 0)	(0, 1, 0)	(0.44, 0.56, 0)
Technology A	(0.66, 1, 0.33)	(1, 1, 0)	(0, 0, 1)	(0, 1, 0.11)	(1, 1, 0)
Technology B	(0, 0.66, 1)	(0, 1, 1)	(1, 0.63, 0)	(0, 0.56, 1)	(0, 1, 1)
Technology C	(0, 0, 1)	(1, 0.5, 0)	(0 1 1)	(0, 0, 1)	(1, 1, 0.75)
Technology D	(0.33, 1, 0)	(1, 0.5, 0)	(1, 1, 0)	(0.44, 1, 1)	(1, 0.56, 0)

In order to address this challenge, a Monte Carlo simulation is introduced to generate random numbers of parameters within their feasibility range based on uniform distribution, leading to a Monte Carlo simulation based IRFAM (MC-IRFAM) approach. According to the operations shown in Figure 3.8, the available technologies are ranked with highest to lowest feasibilities based on the spilled site condition. After processed by the MC-IRFAM approach with 10,000 trials (N = 10,000), the information about overall scores for the technologies are obtained as in Figure 3.10.

The ranking results indicate that the Technology D is highly feasible for responding to the offshore oil spill. The overall score of the Technology A is a little lower than the Technology D but still indicates a high feasibility of Technology A. Although the max and mean scores of the Technology B are close to the Technology A, the distribution of overall scores of Technology B tends to the lower level (Figure 3.10b). It may lead to a high possibility of low efficiency when this technology is applied in the spill site. In general, Technology C is infeasible for this spill site.
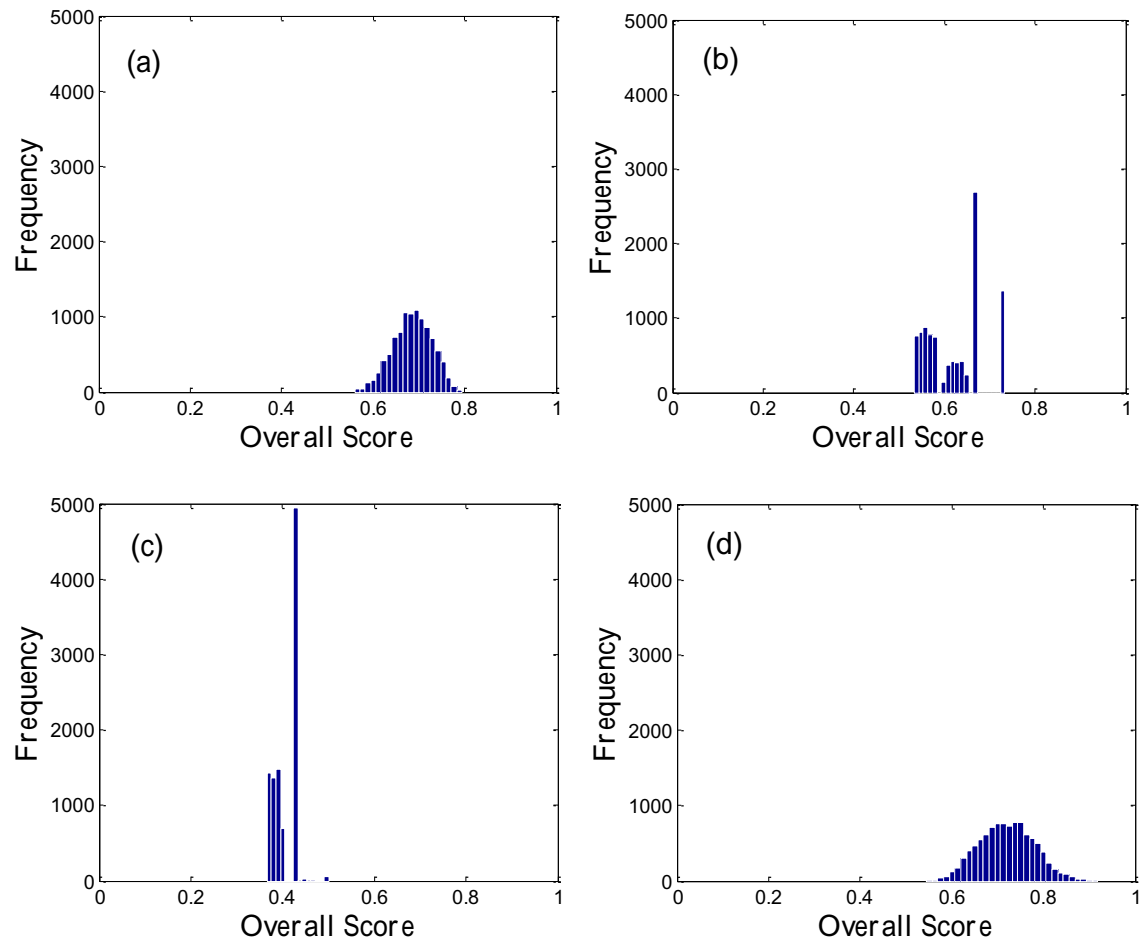
Figure 3.10 Overall scores for the (a) Technology A, (b) Technology B, (c) Technology C, and (d) Technology D

3.4 Summary

This chapter firstly describes a Monte Carlo simulation-based two-stage adaptive resonance theory mapping (MC-TSAM) approach for unsupervised learning under uncertain and complex conditions. The approach can classify a site that is potentially affected by offshore oil spill into certain distinctive groups, representing the risk/vulnerability of the whole site. It is an advancement of the two-stage adaptive resonance theory mapping (TSAM) approach that was previously developed by the author. The TSAM approach is able to feed an adaptive resonance theory mapping (ARTMap) classification with criteria generated from adaptive resonance theory (ART) unsupervised classification. The TSAM can automatically process the classification according to the inputs. The classification results only depend on the inputs and are not affected by the definition of the criteria which usually require subjective judgements and may lead to uncertainty. In addition, by incorporating Monte Carlo simulation, the MC-TSAM can handle the uncertainties that widely exist in the parameters in the offshore environment (e.g., wind speed, wave height, temperature, etc.).

In order to demonstrate the feasibility, the MC-TSAM was applied to classify the south coast of Newfoundland into five zones with different offshore OSVI under uncertainty and complexity. Ten uncertain features were employed as the inputs for the MC-TSAM, including oceanic conditions (wave height, current speed, and current

direction), meteorological conditions (wind speed, wind direction, pressure, and temperature), and offshore oil spill relative information (tanker movement frequency, other vessel movement frequency, and historical oil spill frequency) and two deterministic features (ecological reserves and spawning fish). The classification result indicated that Zone 5 might be most vulnerable if any oil spill occurs in this area, while Zone 1 might be least vulnerable. Oil spills occurring in Zones 2, 3 and 4 might not cause significant impact to the target area; however, the historical oil spill frequency in these areas was significant higher than those in Zones 1 and 5, requiring high diligence in offshore oil spill monitoring and response. The scales of the zones could represent the OSVI levels to offshore oil spills.

Three types of statistical methods (Mann-Whitney Test, Kruskal-Wallis Test, and Jonckheere-Terpstra Test) were applied to analyze the differences of the classified zones based on the single and combine effects from features. The analyses indicated that if only a single feature was considered for classification, unreliable results could be generated. However, when all features were considered, the differences in the classified zones were significant. This demonstrated that the proposed MC-TSAM approach could capture the combined effects from uncertain and complex features, showing considerable advantages over other methods.

The classification results from the MC-TSAM provided different reasonable scenarios in offshore OSVI classification and spill risk mapping. According to different

scenarios of categories, decision makers could apply limited monitoring efforts (e.g., stations) to wisely monitor the areas with different levels of offshore OSVI. The classification result could provide the least or desired number of zones which can sufficiently represent the environmental vulnerability as well as the situation of a spill/leak in the concerned area, saving time and budget in offshore oil spill monitoring and response.

Furthermore, an integrated rule-based adaptive resonance theory mapping (IRFAM) approach was advanced by integrating with the Monte Carlo simulation approach for screening offshore oil spill response technologies. The IRFAM approach was previously developed by incorporating conventional adaptive resonance theory mapping approach with fuzzy set theory. The Monte Carlo simulation based IRFAM (MC-IRFAM) approach can handle the inputs not only with imprecise information but also ranges of uncertainties. It is highly helpful in classifying/ranking the distributive inputs based on some uncertain criteria, such as the case of response technologies screening in an offshore oil spill event. This approach can indicate ranks with distributions, which can help decision makers comprehensively analyze the feasibilities of the technologies and make sound decisions. Therefore, this approach can efficiently process classification under the coexistence of complexity and uncertainty.

The feasibility of the MC-IRFAM approach was tested with a hypothetical case of technologies screening in an offshore oil spill event. The case study demonstrated that the

approach was able to classify and rank technologies containing uncertain information based on uncertain criteria. The approach could generate full fuzzy criteria combinations to match the site conditions as rules to rank the technologies.

In the following chapters, the MC-TSAM and the MC-IRFAM approaches will be further integrated with simulation and optimization approaches in the proposed decision support system framework for supporting offshore oil spill responses in harsh environments.

CHAPTER 4

SIMULATION-OPTIMIZATION COUPLING FOR

OFFSHORE OIL SPILL RESPONSE

_____

The contents in the chapter have led the following publications or potential publications:

1. Li P. and Chen B. (2011). FSILP: Fuzzy-stochastic-interval linear programming for supporting municipal solid waste management. Journal of Environmental Management, 92(4): 1198-1209.
   Roles: I developed the model, conducted case studies and drafted manuscript. Dr. Bing Chen is my PhD supervisor.

2. Li P., Wu H.J., and Chen B. (2013). RSW-MCFP: A resource-oriented solid waste management system for a mixed rural-urban area through Monte Carlo simulation-based fuzzy programming. Mathematical Problems in Engineering, 2013 (2013), 15pp.

3. Chen B., Li P., and Wu H.J. (2013). MCFP: A Monte Carlo simulation based fuzzy programming approach for municipal solid waste management under dual uncertainties of possibility and continuous probability. Journal of Environmental Informatics. (Under review)
   Role: I developed the model, conducted case studies and drafted manuscript. Dr. Bing Chen is the supervisor of the other student authors. Hongjing Wu conducted statistical analysis for results and drafted part of introduction of the manuscript.

4. Li P., Chen B., Zhang B.Y., Jing L., and Zheng J.S. (2014). Monte Carlo Simulation-based Dynamic Mixed Integer Nonlinear Programming for Supporting Oil Recovery and Devices Allocation during Offshore Oil Spill Responses. Ocean & Coastal Management, 89C (2014), 58-70.

5. Li P., Chen B., Zhang B.Y., Jing L., and Zheng J.S. (2012). A multiple-stage simulation-based mixed integer nonlinear programming approach for supporting offshore oil spill recovery with weathering process. Journal of Ocean Technology, 7(4): 87-105.

6. Li P., Chen B., Zhang B. Y., Jing L., and Zheng J. S. (2012). Development of a multiple-stage simulation based mixed integer nonlinear programming approach for supporting offshore oil spill recovery. In: Proceeding of the 35th AMOP Technical Seminar on Environmental Contamination and Response, June 5-7, 2012, Vancouver, Canada, 434-447.
   Role: I developed the model, conducted case studies and drafted manuscript. Dr. Bing Chen is the supervisor of the other student authors. Dr. Baiyu Zhang provided advice in manuscript drafting. Liang Jing polished the manuscript. Jisi Zheng collected data for oil recovery simulation.

4.1 Optimization under Uncertainty

4.1.1 Fuzzy-Stochastic-Interval Linear Programming (FSILP)

Nguyen (2007a, 2007b, 2007c) developed a new method to convert the fuzzy and fuzzy stochastic linear programming (LP) problems into the conventional LP models by measuring the attainment values of fuzzy numbers and/or fuzzy random variables as well as superiority and inferiority between triangular fuzzy numbers (or triangular fuzzy stochastic variables). An attainment value is a degree of attainment of the fuzzy goal that is considered to be a concept similar to a degree of satisfaction of the fuzzy decision when the fuzzy constraint is replaced by the fuzzy expected payoff. It can also be interpreted as a possibility of attainment of the fuzzy goal. Nguyen's method finally resulted in a simple deterministic LP model, which contained a few additional constraints and variables and could be solved easily. However, this method only considered the situation when the source (right-hand-side, RHS) is a strict constraint demand (left-hand-side, LHS), otherwise, significant errors may occur. Furthermore, the uncertainty represented by interval parameter was not taken into account.

In this section, a new fuzzy-stochastic-interval linear programming (FSILP) method has been developed for supporting environmental management. Nguyen's method has been adapted and integrated with an interval linear programming (ILP) (Liu et al., 2009). The developed method can be highly capable of handling the coexistence of fuzzy, stochastic, and interval uncertainties, as well as economic penalties. Meanwhile,

significant reduction of computation time will be achieved in comparison with the conventional methods.

Consider a fuzzy stochastic linear program as follows:

$$\text{Min} \quad f = CX \tag{4.1a}$$

s.t.

$$\sum_{j=1}^{n}(\tilde{A}_{ij}^{1})_{w}X_{j} \leq (\tilde{B}_{i}^{1})_{w}, \quad i = 1, m \tag{4.1b}$$

$$\sum_{j=1}^{n}(\tilde{A}_{kj}^{2})_{w}X_{j} \geq (\tilde{B}_{k}^{2})_{w}, \quad k = 1, o \tag{4.1c}$$

$$X_{j} \geq 0, w \in \Omega \tag{4.1d}$$

where $C \in \{R\}^{1 \times n}$, and $A^{1} \in \{R\}^{m \times n}$, $A^{2} \in \{R\}^{o \times n}$, $B^{1} \in \{R\}^{m \times 1}$, and $B^{2} \in \{R\}^{o \times 1}$ are matrixes of fuzzy random variable constraint coefficients defined on a probability space (Ω, F, P). Assuming all fuzzy numbers are in the form of $\tilde{t} = (t, \delta, \delta)$, according to Nguyen (2007), Equation 4.1 can be converted to:

$$\text{Min} \quad f = CX + E\left[\sum_{i=1}^{m}\lambda_{i}^{1}(w)\right] - E\left[\sum_{i=1}^{m}\lambda_{k}^{2}(w)\right] \tag{4.2a}$$

134

s.t.

$$\frac{1}{2}\left(\sum_{j=1}^{n}\left((\tilde{A}_{ij}^1)_w X_j + \delta X_j + \delta\right) - (\tilde{B}_i^1)_w\right) = \lambda_i^1, \quad i = 1, m \tag{4.2b}$$

$$\frac{1}{2}\left(\sum_{j=1}^{n}\left((\tilde{A}_{kj}^2)_w X_j - \delta X_j - \delta\right) - (\tilde{B}_k^2)_w\right) = \lambda_k^2, \quad k = 1, o \tag{4.2c}$$

$$X_j, \lambda_i^1, \lambda_k^2 \geq 0, w \in \Omega \tag{4.2d}$$

where $\lambda^1 \in \{R\}^{m \times 1}$ and $\lambda^2 \in \{R\}^{o \times 1}$ are matrixes of control decision variables corresponding to the degree (membership grade) to which X solution fulfills the fuzzy constraints; and E denotes the mathematical expectation.

The Equation 4.2 is then converted by using stochastic programming techniques. The corresponding deterministic model for this problem is:

$$\text{Min} \quad f = CX + \sum_{i=1}^{m} p_i^1 \lambda_i^1 - \sum_{i=1}^{m} p_k^2 \lambda_k^2 \tag{4.3a}$$

s.t.

$$\frac{1}{2}\left(\sum_{j=1}^{n}\left((\tilde{A}_{ij}^1)_w X_j + \delta X_j + \delta\right) - (\tilde{B}_i^1)_w\right) = \lambda_i^1, \quad i = 1, m \tag{4.3b}$$

$$\frac{1}{2}\left(\sum_{j=1}^{n}\left((\tilde{A}_{kj}^2)_w X_j - \delta X_j - \delta\right) - (\tilde{B}_k^2)_w\right) = \lambda_k^2, \quad k = 1, o \tag{4.3c}$$

$$X_j, \lambda_i^1, \lambda_k^2 \geq 0, w \in \Omega \tag{4.3d}$$

where $p^1 \in \{R\}^{m \times 1}$ and $p^2 \in \{R\}^{o \times 1}$ are matrixes of probabilities for random variables.

Because the Nguyen's method only considered the situation when the demands (left-hand-sides, LHSs) and sources (right-hand-sides, RHSs) were close, with LHSs ≤ RHSs in minimization problems or LHSs ≥ RHSs in maximization problems. In the situation that sources/RHSs are too abundant to be met by the demands/LHSs, the conversions from less-than signs to equal signs would lead to significant errors by Nguyen's method. A simple example regarding to this problem is shown as follows:

Min $f = X$ (4.4a)

s.t.

$$\begin{pmatrix} 2 \\ 3 \end{pmatrix} X \leq \begin{pmatrix} 10 \\ 12 \end{pmatrix}$$ (4.4b)

$X \geq 0$ (4.4c)

Fuzzy number for X is in the form of $\tilde{t} = (t, 0.5, 0.5)$, and the probability for the random number is set to 0.5, which is:

$$\begin{pmatrix} p & A & B \\ 0.5 & 2 & 10 \\ 0.5 & 3 & 12 \end{pmatrix} \qquad (4.5)$$

According to Equations 4.2 and 4.3, the solution for the problem is f = 4.25, x = 3.8. When the values for B increase to 1,000 and 1,200, the solution for the problem becomes f = 450 and x = 400, respectively. However, $AX \le B$ is only a loose constraint in this problem, and the increasing of B is not supposed to significantly affect the optimal solution.

In order to fix this problem, slack variable is added in the loosing constraint as follows:

$$\text{Min} \quad f = CX + \sum_{i=1}^{m} p_i^1 \lambda_i^1 - \sum_{i=1}^{m} p_k^2 \lambda_k^2 \qquad (4.6a)$$

s.t.

$$\frac{1}{2}\left(\sum_{j=1}^{n} \left((\tilde{A}_{ij}^1)_w X_j + \delta X_j + \delta \right) + S_i - (\tilde{B}_i^1)_w \right) = \lambda_i^1, \quad i = 1, m \qquad (4.6b)$$

$$\frac{1}{2}\left(\sum_{j=1}^{n} \left((\tilde{A}_{kj}^2)_w X_j - \delta X_j - \delta \right) - (\tilde{B}_k^2)_w \right) = \lambda_k^2, \quad k = 1, o \qquad (4.6c)$$

$$X_j, \lambda_i^1, \lambda_k^2 \ge 0, w \in \Omega \qquad (4.6d)$$

137

where $S_i \in \{R\}^{m \times 1}$ is the matrix of slack variables.

According to Equation 4.3 the solution for the previous problem is f = 0, x = 0. When the values for B increase to 1000 and 1200, the solution for the problem becomes f = 0 and x = 0, respectively. This is much more reasonable solution for a minimization problem compared with the solution from Nguyen's method.

Then, according to Huang et al. (1992, 1993), interval parameters are introduced as follows:

$$\text{Min} \quad f^{\pm} = C^{\pm} X^{\pm} + \sum_{i=1}^{m} p_i^1 \lambda_i^{1\pm} - \sum_{i=1}^{m} p_k^2 \lambda_k^{2\pm} \tag{4.7a}$$

s.t.

$$\frac{1}{2} \left(\sum_{j=1}^{n} \left((A_{ij}^{\widetilde{1\pm}})_w X_j^{\pm} + \delta X_j^{\pm} + \delta \right) + S_i^{\pm} - (B_i^{\widetilde{1\pm}})_w \right) = \lambda_i^{1\pm}, \quad i = 1, m \tag{4.7b}$$

$$\frac{1}{2} \left(\sum_{j=1}^{n} \left((A_{kj}^{\widetilde{2\pm}})_w X_j^{\pm} - \delta X_j^{\pm} - \delta \right) - (B_k^{\widetilde{2\pm}})_w \right) = \lambda_k^{2\pm}, \quad k = 1, o \tag{4.7c}$$

$$X_j, \lambda_i^1, \lambda_k^2 \geq 0, w \in \Omega \tag{4.7d}$$

The final model includes three types of uncertainties in the input variables and parameters. The fuzzy uncertainty exists in the decision variable X, while the stochastic uncertainty exists in the resource parameter B, and the interval uncertainty exists in all

the variables, parameters and coefficients. The result provides optimized interval solutions for the decision variables, $X^{\pm}_{j\,opt}$, and objective function values, $f^{\pm}_{opt}$, as follows:

$$X^{\pm}_{j\,opt} = \left[X^{-}_{j\,opt}, X^{+}_{j\,opt}\right] \quad X^{-}_{j\,opt} \leq X^{+}_{j\,opt} \quad \forall j \tag{4.8}$$

$$f^{\pm}_{opt} = \left[f^{-}_{opt}, f^{+}_{opt}\right] \quad f^{-}_{opt} \leq f^{+}_{opt} \tag{4.9}$$

In the solution process, the interval linear programming model is first transformed into two deterministic submodels, which correspond to the upper and lower bounds for the desired objective function value (Huang et al., 1992). The steps for solving a FSILP problem are shown as follows:

Step 1. Formulating the original Model I (Equation 4.1).

Step 2. Reformulating the Model I by introducing the fuzzy and stochastic uncertainties to formulate to Model II (Equation 4.6).

Step 3. Reformulating the Model II by introducing the interval uncertainties to formulate Model III (Equation 4.7).

Step 4. Transforming Model III into two submodels: lower bound submodel (f^{-}) and upper bound submodel (f^{+}).

Step 5. Solving the f^- or f^+ submodel and obtaining corresponding $X_{j_{opt}}^{-/+}$,and

$f_{opt}^{-/+}$.

Step 6. Solving the submodel of the other interval bound according to results from

Step 5 and obtaining corresponding $X_{j_{opt}}^{+/-}$ and $f_{opt}^{+/-}$.

Step 7. Obtaining the values for the optimum solution:

$$X_{j\,opt}^{\pm} = \left[X_{j\,opt}^-, X_{j\,opt}^+\right] \quad X_{j\,opt}^- \le X_{j\,opt}^+ \quad , \text{and}$$

$$f_{opt}^{\pm} = \left[f_{opt}^-, f_{opt}^+\right] \quad f_{opt}^- \le f_{opt}^+ \quad .$$

Step 8. Stop.

4.1.2 Monte Carlo simulation based fuzzy programming (MCFP)

Some approaches have been developed to simultaneously deal with possibility and

probability in the past decade (Li et al., 2009a; Li et al., 2011; Wang et al., 2011).

However, these approaches treat probabilistic uncertainties based on limited, discrete

probability distributions and are unable to simultaneously handle continuous probability

and subjective information (Yang et al., 2010; Chen et al., 2013). In practice, system

variables usually include both subjective and objective information, leading to the

coexistence of possibility and continuous probability (or dual uncertainties), therefore the

incorporation of fuzzy set theory and Monte Carlo simulation becomes necessary and

valuable (Guyonnet et al., 2003; Sadeghi et al., 2010; Yang et al., 2010). Monte Carlo

simulation can address continuous probabilistic uncertainties by using probability density

functions (PDFs) (Freeze et al., 1991; Vose, 1996; Garthwaite et al., 2005). Therefore, the integration of fuzzy programming approaches with Monte Carlo simulation can be promising in addressing the limitations of treating possibilistic and continuous probabilistic uncertainties. However, challenges still remain in finding optimal solutions to the new coupled problem of the fuzzy programming and Monte Carlo simulation. This section attempts to integrate the Monte Carlo simulation with the fuzzy programming module in the developed FSILP approach, forming the Monte Carlo simulation-based fuzzy programming (MCFP) approach.

In the MCFP approach, a Monte Carlo simulation approach is introduced to handle the probabilistic uncertainties (continuous and discrete) (Chen et al., 2013; Li et al., 2013d). By assigning random values to the uncertain parameters, the original problem with dual uncertainties (coexistence of possibilistic and continuously probabilistic uncertainties) can be transformed into a fuzzy problem. Subsequently, the FSILP approach (Li and Chen, 2011) as described in the previous section is introduced to handle the possibilistic uncertainties, converting the fuzzy problem into a conventional linear problem.

The FSILP approach can easily convert a fuzzy problem into a deterministic problem without conventional fuzzification and defuzzification processes, which makes it significantly feasible in coupling with the Monte Carlo simulation. The random values of the parameters are firstly assigned in each Monte Carlo simulation trial according to the

probability distributions of parameters, leading to a fuzzy problem in each trial. Such fuzzy problem is then solved by the fuzzy programming from the FSILP approach. Finally, a group of solutions can be collected to present the most frequently occurrences of results under the different kinds of uncertainties in parameters.

Although the FSILP is capable of handling the coexistence of dual uncertainties, its efficiency will decrease when the number of discrete probabilities increases. Furthermore, when the uncertainty is described as continuous probability, integration is required when numerically processing the optimization, leading to difficulties. Furthermore, some of the distributions may be non-integrable, making the optimization unachievable.

Monte Carlo methods are a class of computation intensive algorithms based on the randomization. These methods can provide equivalent results to deterministic algorithms, which makes it a complement to the theoretical derivations (Anderson, 1986). Monte Carlo methods are especially suitable for the problems with multiple probability distributions, and the handling of such distributions becomes complicated by using numerical methods. These methods are frequently used to treat uncertainties in inputs, especially for evaluating risks (Baeurle, 2009).

The results of an objective function can be regarded as a stochastic one due to randomness of the input parameters. The occurrence of this can be predicted through Monte Carlo simulation based on the help of the probability concept. However, not all the input parameters can be characterized by using probability distributions due to

incomplete or insufficient information from literature and historical data as well as the subjective judgement when choosing values for the parameters. In many cases, the obtained probability distribution may be still uncertain where each data point contains a degree of belief, leading to dual uncertainties of possibility and continuous probability.

As shown in Figure 4.1, a parameter X is uncertain with corresponding probability:

$$X \in \Re \mapsto X = f^{-1}(P) \tag{4.10}$$

However, sometimes the confidence of such a distribution can be impaired by insufficient information. Such a consequence is of a fuzzy nature which can be quantified by degrees of belief (e.g., membership functions) (Li et al., 2007). Each data point (X_i) may contain a membership function as follows:

$$X_i = \{\tilde{t}; \tilde{t} = (t, a, b), a, b \geq 0\} \tag{4.11}$$

and

$$\mu_{\tilde{t}}(X_i) = \begin{cases} \max\left(0, 1 - \dfrac{t-y}{a}\right), & \text{if } y \leq t \\ 1, & \text{if } a = 0, b = 0, t = y \\ \max\left(0, 1 - \dfrac{y-t}{b}\right), & \text{if } y \leq t \\ 0, & \text{otherwise} \end{cases} \tag{4.12}$$

where the scalars $a, b \geq 0 \, (a, b \in \Re)$ are called the left and right spreads of the membership, respectively.

Therefore, in order to effectively tackle such coexistence of dual uncertainties, Monte Carlo simulation and fuzzy programming need to be integrated. The FSILP method can easily convert a fuzzy problem into a deterministic problem without traditional fuzzification and defuzzification processes which significantly obstructs the integration with Monte Carlo simulation. The framework of the MCFP approach is shown in Figure 4.2, where N is the preset number of trials, and I is the index of the current trial.
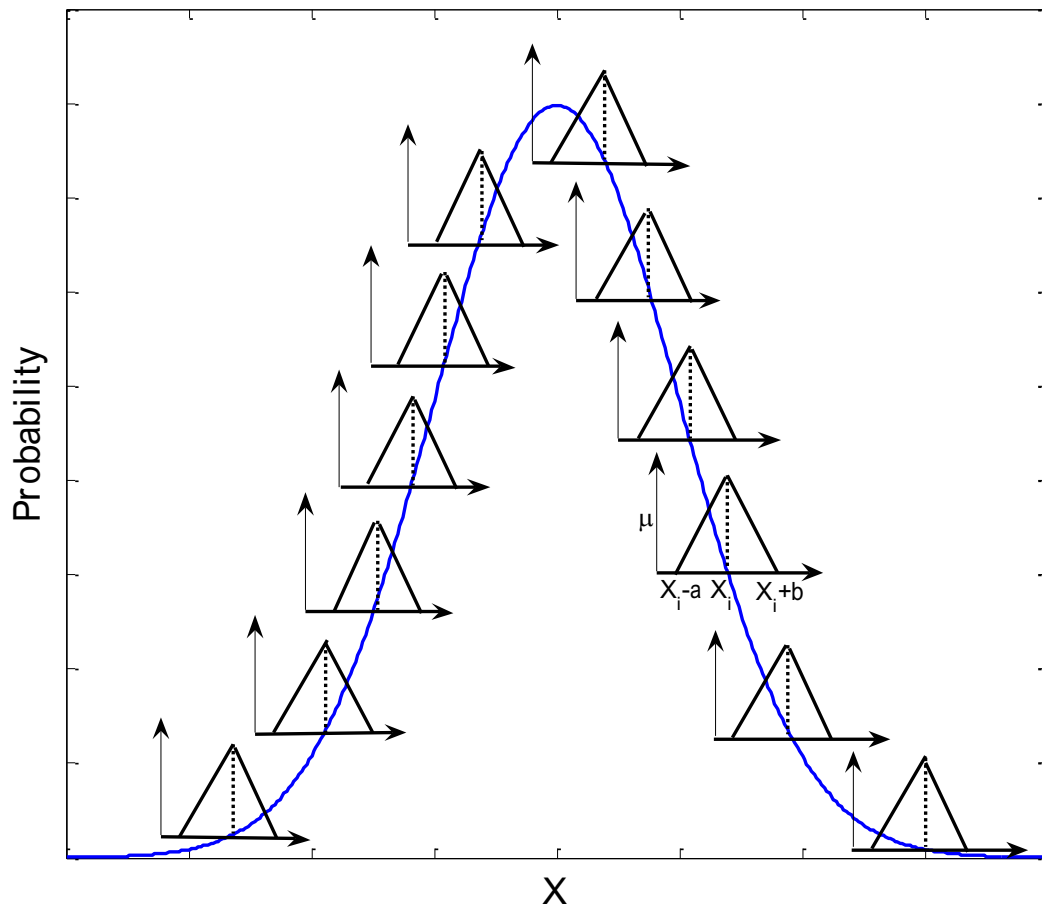
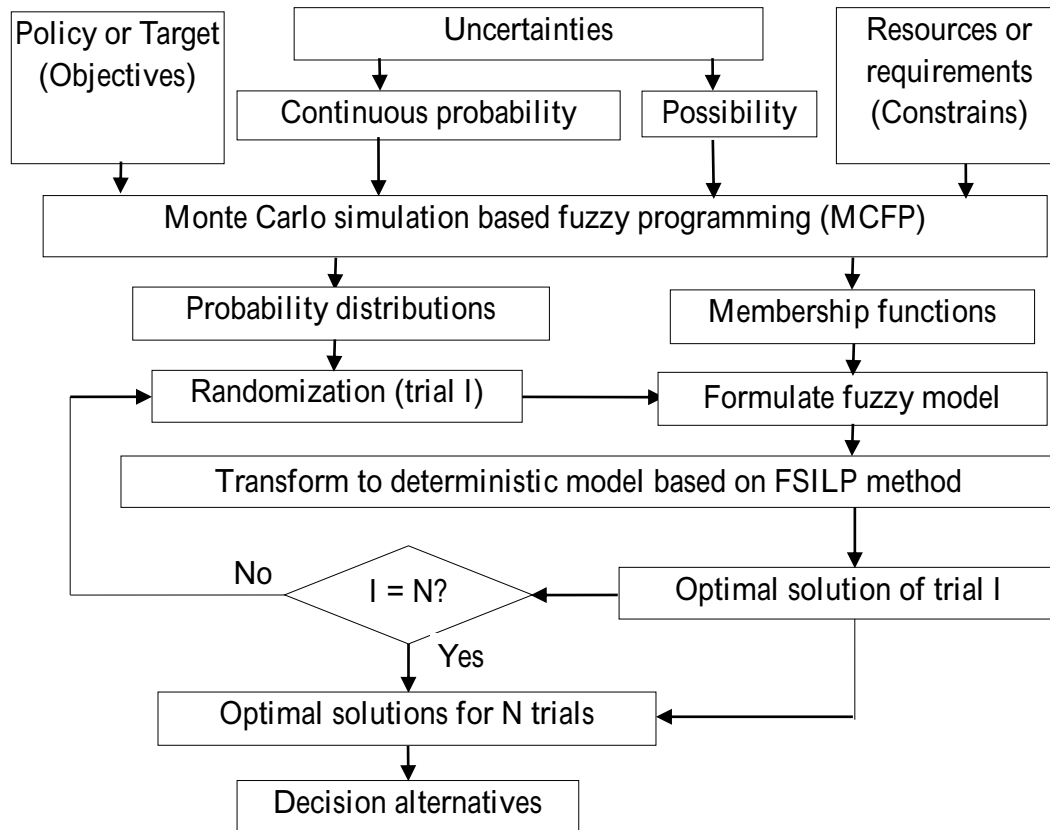Figure 4.1 Dual uncertainties of possibility and contiuous probability

Figure 4.2 Framework of the MCFP approach

Consider a problem which is the same as the one in Equation 4.1. The random values of the parameters are firstly assigned in each Monte Carlo simulation trial according to their probability distributions, leading only to a fuzzy problem in each trial. According to the FSILP approach, in each trial the problem can be converted as follows (Li and Chen, 2011):

$$\text{Min } f = CX + \sum_{i=1}^{m} \lambda_i^1 - \sum_{i=1}^{m} \lambda_k^2 \tag{4.13a}$$

s.t.

$$\frac{1}{2}\left(\sum_{j=1}^{n}\left((\tilde{A}_{ij}^1)_w X_j + \delta_{x_j}^+ X_j\right) + \delta_{B_i^1}^- + S_i - (\tilde{B}_i^1)_w\right) = \lambda_i^1, \quad i = 1, \cdots, u \tag{4.13b}$$

$$\frac{1}{2}\left(\sum_{j=1}^{n}\left((\tilde{A}_{kj}^2)_w X_j - \delta_{x_j}^- X_j\right) - \delta_{B_k^2}^+ - (\tilde{B}_k^2)_w\right) = \lambda_k^2, \quad k = 1, \cdots, v \tag{4.13c}$$

$$\lambda_i^1 \leq \frac{1}{2}\left(\sum_{j=1}^{n}\delta_{x_j}^+ X_j + \delta_{B_i^1}^-\right) \tag{4.13d}$$

$$\lambda_k^2 \leq \frac{1}{2}\left(\sum_{j=1}^{n}\delta_{x_j}^- X_j + \delta_{B_k^2}^+\right) \tag{4.13e}$$

$$X_j, \delta_{x_j}^-, \delta_{x_j}^+, \delta_{B_i^1}^-, \delta_{B_k^1}^+, \lambda_i^1, \lambda_k^2, S_i \geq 0, w \in \Omega \tag{4.13f}$$

After N trials are finished, the sets of the results can be obtained as follows:

$$f_{l,opt} = \{ f(X_{jl,opt}); X_{jl,opt} \geq 0\}, \quad l = 1, \cdots, M; \ j = 1, \cdots, Z \tag{4.14}$$

where M is the number of the feasible solutions after N trials of the Monte Carlo simulation, and Z is the number of decision variables.

Assuming that there is no uncertainty existing in the coefficients of the objective function (C), the definition for the final solution can be stated as follows:

Definition 1:

$$E(f_{opt}) = \{ f(E(x_{jl,opt})); E(x_{jl,opt}) \geq 0\}, \quad l = 1, \cdots, M \tag{4.15}$$

Proof. the corresponding objective function and decision variables are

$$f_{l,opt} = \{ f(x_{jl,opt}); x_{jl,opt} \geq 0\} = \sum_{j=1}^{Z} C_j X_{jl,opt}, \quad l = 1, \cdots, M \tag{4.16}$$

$$\Leftrightarrow E(f_{l,opt}) = \sum_{j=1}^{Z} E(C_j X_{jl,opt}) \tag{4.17}$$

Since C_j are deterministic and independent, we have the relation between the expected values of the optimal function and the decision variables:

$$E(f_{l,opt}) = \sum_{j=1}^{Z} C_j E(X_{jl,opt}) = f(E(X_{jl,opt})) \qquad (4.18)$$

The key steps of the solution algorithm are as follows:

Step 1.   Formulate the fuzzy model (Equation 4.1).

Step 2.   Initialize the model parameters, including probability distributions and membership functions.

Step 3.   Generate a set of random variables according to the probability distributions.

Step 4.   Transform the Equation 4.1 to Equation 4.13 according to the generated random variables in Step 3.

Step 5.   Solve Equation 4.13 and obtain the corresponding $X_{jl,opt}$, and $f_{l,opt}$ of the current trial.

Step 6.   Go to Step 7 if the trial reaches the preset number of trials (I = N); otherwise (I < N) go to Step 3.

Step 7.   Obtain a set of feasible solutions by Equation 4.15 or declare the feasible

solutions are unachievable.

Step 8. Obtain the optimal solutions by Equation 4.18: $X_{j,opt} = E(X_{jl,opt})$, and

$$f_{opt} = E(f_{l,opt}).$$

Step 9. End.

4.2 Simulation-Optimization Coupling

Based on the integration of Monte Carlo simulation with the optimization programming in Section 4.1.2, another innovative development is made in the integration of Monte Carlo simulation with the dynamic programming.

4.2.1 Dynamic Mixed Integer Nonlinear Programming (DMINP)

Consider a linear program as follows:

$$\text{Min}\ \ f = C_j X_j \tag{4.19a}$$

s.t.

$$\sum_{j=1}^{n} A_{ij} X_j \le B_i\ , \quad i = 1, \cdots, m \tag{4.19b}$$

$$X_j \ge 0 \tag{4.19c}$$

where $C \in \{R\}^{1 \times n}$ is the matrix of coefficients of the objective function; and $A_{ij} \in \{R\}^{m \times n}$ as well as $B_i \in \{R\}^{m \times 1}$ are matrices of variable constraint coefficients.

When C_j are not just constants but also functions linking with some other parameters:

$$C_j = g_j(y) \tag{4.20}$$

where $g_j(y)$ are the functions showing the relations between the coefficients C and parameters y, leading to a simulation-based optimization model as follows:

$$\text{Min} \quad f = g_j(y)X_j \tag{4.21a}$$

s.t.

$$\sum_{j=1}^{n} A_{ij} X_j \leq B_i, \quad i = 1, \cdots, m \tag{4.21b}$$

$$X_j \geq 0 \tag{4.21c}$$

The Equation 4.21 will be a simple linear model and can be solved by linear programming if $g_j(y)$ is independent from the decision variables (X_j). However, when

$g_j(y)$ are dependent on the decision variables, the model becomes non-linear. Especially when $g_j(y)$ are dynamically relating with the decision variables (usually with time series), the model becomes dynamic and non-linear, and cannot be easily solved:

$$\text{Min} \quad f_t = \psi\Big(f_{t-1}\big(g_j(y_{t-1})X_j\big), g_j(y_t)X_j\Big) \tag{4.22a}$$

s.t.

$$\sum_{j=1}^{n} A_{ij} X_j \leq B_i, \quad i = 1, \cdots, m \tag{4.22b}$$

$$X_j \geq 0 \tag{4.22c}$$

where t and t-1 are time indicators in a time series, and the $f_t = \psi\Big(f_{t-1}\big(g_j(y_{t-1})X_j\big), g_j(y_t)X_j\Big)$ represents relations between the status from the previous and the current stages. For a single stage or globally continuous problem, the Equation 4.22 can be converted as follows:

$$\text{Min} \quad f = \int_0^T \psi\Big(f_{t-1}\big(g_j(y_{t-1})X_j\big), g_j(y_t)X_j\Big)dt \tag{4.23a}$$

s.t.

$$\sum_{j=1}^{n} A_{ij} X_j \leq B_i, \quad i = 1, \cdots, m \tag{4.23b}$$

$$X_j \geq 0 \tag{4.23c}$$

It will be more convenient to break the time series into certain stages based on a controllable time interval, leading to a multiple-stage simulation based nonlinear programming as follows:

$$\text{Min} \quad f = \sum_{s=1}^{N} \left[\int_0^{t_s} \psi \left(f_{s-1} \left(g_j (y_{t-1}) X_j \right), g_j (y_t) X_j, t \right) dt \right] \tag{4.24a}$$

s.t.

$$\sum_{j=1}^{n} A_{ij} X_j \leq B_i, \quad i = 1, \cdots, m \tag{4.24b}$$

$$X_j \geq 0 \tag{4.24c}$$

where t_s is the time interval in the stage s. In some cases, $g_j(y)$ in the same stage can be assumed to be unchanged and the Equation 4.24 can be correspondingly converted to:

$$\text{Min} \quad f = \sum_{s=1}^{N} \psi \left(f_{s-1} \left(g_j (y_{t-1}) X_j t_{s-1} \right), g_j (y_t) X_j t_s \right) \tag{4.25a}$$

s.t.

$$\sum_{j=1}^{n} A_{ij} X_j \leq B_i, \quad i = 1, \cdots, m \tag{4.25b}$$

$$X_j \geq 0 \tag{4.25c}$$

4.2.2 Monte Carlo simulation-based DMINP

Based on DMINP approach, a Monte Carlo simulation approach is introduced to address the probabilistic uncertainties. Monte Carlo simulation has been a series of computation intensive methods based on randomization, which has been introduced in many modeling fields to handle uncertainty (Chen et al., 2013; Jing et al., 2012c; Li et al., 2013c, 2013d). These methods can provide approximately equivalent results when compared with the analytical algorithms, leading to a complement of the theoretical derivations. Monte Carlo simulation is especially capable of handling multiple probability distributions, which is much challenging by using numerical methods. As shown in Figure 4.3, by assigning random values to the uncertain parameters, the probabilistically uncertain information becomes deterministic in a single trial (i.e., trial I) of Monte Carlo simulation. Consequently, the original problem becomes a deterministic problem in each loop. After finishing all the trials (i.e., N trials), the feasible solutions can be obtained for further trade-off analysis.
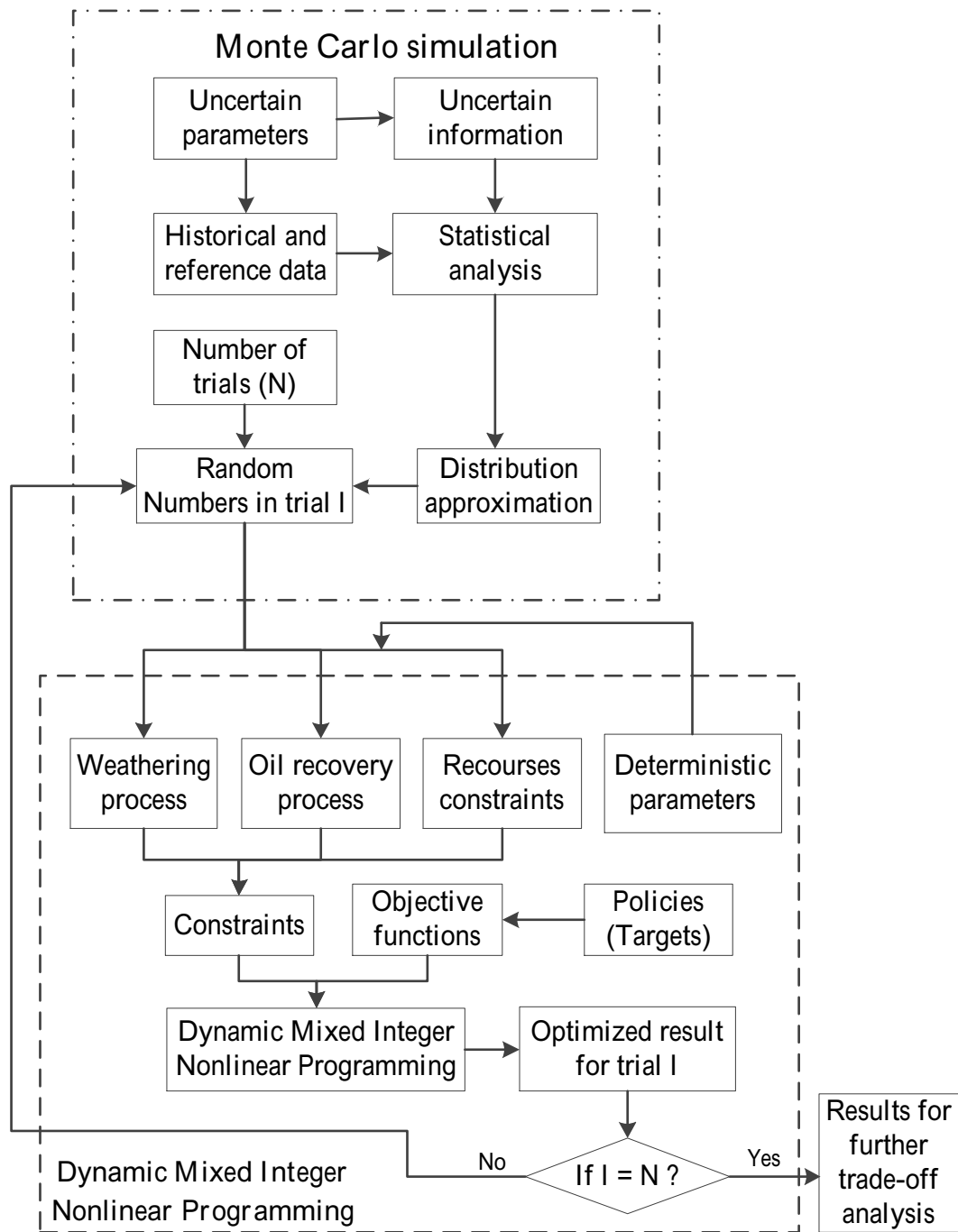
Figure 4.3 Framework of the MC-DMINP approach

4.2.3 Simulation-optimization coupling for supporting offshore oil spill response

In offshore oil spill recovery, the net oil recovery rate (ORR_n, defined as the amount of recovered oil per hour) of skimmer is usually determined by slick thickness (SOT). The function between ORR_n and SOT are as follows:

$$ORR_n = a \times SOT^2 + b \times SOT \tag{4.26}$$

where a and b are empirical coefficients obtained from experimental tests. Correspondingly, the objective function of the offshore oil spill recovery problem by skimmer can be expressed as follows:

$$Max \ V = \int_0^t SK_i \times ORR_{ni} dt \tag{4.27}$$

where V is the volume of recovered oil, t is the operational time, SK_i are the numbers of skimmer type i, and ORR_{ni} are the recovery rates of the corresponding skimmer.

As ORR_{ni} are dynamically related with the objective value (V), the problem becomes dynamic and non-linear, and cannot be easily solved. It will be more convenient to break

the time series into multiple stages based on a controllable time interval defined as the minimal time required for shifting one operational condition to another. The duration of a stage is usually determined by the time for device deployment and allocation, resource arrangement, etc. This leads to a multiple-stage simulation based nonlinear programming as follows:

$$\text{Max } V = \sum_{s=1}^{N} SK_i \times ORR_{nis} \qquad (4.28)$$

where N is the length of an operational period, s is the number of operational stages, ORR_{nis} are net oil recovery rates for SK_i at stage s, which is calculated by the slick thickness or the collected oil from the stage s-1:

$$ORR_{nis} = f_{ORR_{ni}}\left(SOT_{s-1}\right) = f_{ORR_{ni}}\left(\frac{V_0 - \sum_{h=1}^{s-1} V_h}{A}\right) \qquad (4.29)$$

where V_0 is the initial volume of spilled oil, A is the area of the spilled oil, and h is the stage index.

In real-world practices, oil recovery is significantly affected by the weathering processes such as spreading and drift, evaporation, natural dispersion, emulsification, biodegradation, etc. (Fingas, 2010). In a case that spilled oil is boomed and the recovery is required to be done within a short period, evaporation, dispersion, and emulsification may play important roles in oil weathering. Therefore, these processes will also be taken into account in the MC-DMINP approach. According to Fingas (2011), the empirical equation of evaporation for oil is as follows:

$$FE = \frac{c + d \times (T - 273.15) \times Ln(t)}{100} \qquad (4.30)$$

where c and d are equation parameters for specific oil, FE is the evaporation rate (m^3/hour·m^3 of oil), T is temperature (K), and t is time (min).

Furthermore, the equation for the dispersion process is as follows (Mackay et al., 1980):

$$DE = \frac{0.11 \times (U + 1)^2}{1 + 50 \times \mu_o^{0.5} \times SOT \times s_t} \qquad (4.31)$$

where DE is the dispersion rate ($m^3/ (s \cdot m^3$ of oil)), μ_o is the dynamic viscosity of the oil (cP), and S_t is the interface tension between oil and water (dyne/m).

Emulsification is one of the key processes that could change the properties and characteristics of spilled oil. It can affect other weathering processes and consequently the oil recovery operation. Mackay et al. (1980) provided a simulation of emulsification by using the incorporation rate of water into an oil slick:

$$FW = K_b \left(1 - \exp\left(\frac{-K_a}{K_b}(U+1)^2 \times t\right)\right) \tag{4.32}$$

where FW is the fractional water content, K_a is the cure fitting constant that varies with wind speed (2×10^{-6}), K_b is mousse viscosity constant (0.7 for crude oils and heavy fuel oil) (Zadeh and Hejazi, 2012), and t is time (s).

The evaporation process, along with the emulsification process can lead to a significant change of oil density and viscosity as follows (Guo and Wang, 2009):

$$\rho^o = FW\rho_w + (1 - FW)(\rho_{m-1}^o + K_b FE) \tag{4.33}$$

$$\mu^o = \mu_{m-1}^o \exp(K_c FE) \exp\left(\frac{2.5FW}{1 - K_b FW}\right) \tag{4.34}$$

where ρ_w is the density of water, ρ_{m-1}^o is the parent oil density, μ_{m-1}^o is the parent oil viscosity, and K_c is the oil-dependent constant between 1 and 10 (1 is for gasoline or light diesel, and 10 for crude oils).

When considering the simulation of the oil recovery efficiency, along with the weathering processes, the optimization model for oil skimming can be formulated as follows:

$$\text{Max } V = \sum_{s=1}^{N} \sum_{j=1}^{M} SK_j \times ORR_{nsj} \tag{4.35a}$$

$$ORR_{nis} = f_{ORR_{ni}} \left(\frac{V_0 - \sum_{h=1}^{s-1}(V_h + FV_h + DV_h)}{A} \right) \tag{4.35b}$$

$$DE_s = f_{FD}\left(SOT_{s-1}, \mu_s^o\right) = f_{DE} \left(\frac{V_0 - \sum_{h=1}^{s-1}(V_h + FV_h + DV_h)}{A}, \mu_{s-1}^o \right) \tag{4.35c}$$

$$\mu_s^o = f_\mu\left(\mu_{s-1}^o, FE_{s-1}, FW_{s-1}\right) \tag{4.35d}$$

$$FV_s = FE_{s-1} \times \left(V_0 - \sum_{h=1}^{s-1}(V_h + FV_h + DV_h) \right) \tag{4.35e}$$

$$DV_s = DE_{s-1} \times \left(V_0 - \sum_{h=1}^{s-1}(V_h + FV_h + DV_h) \right) \tag{4.35f}$$

$$\sum_{j=1}^{n} SK_j \leq B \tag{4.35g}$$

$SK_j \geq 0$ (4.35h)

4.3 Decision Support for Oil Recovery and Devices Allocation during an Offshore Oil Spill Response

4.3.1 Background and model settings

Consider an offshore spill of Statfjord oil with a total amount of 5,000 m^3. After booms were applied, the spill area is confined to 100,000 m^2. Three types of drum skimmers (SK$_1$, SK$_2$, and SK$_3$) were applied in this area to collect the spilled oil. Each type of skimmer was located in a different warehouse and required a specific period of time for allocation and deployment (Table 4.1). In order to determine their efficiencies, ORRs and OREs of these skimmers were collected from the previous tests conducted by Environmental Canada and OHMSETT (Schulze, 1998). The ORRs is the oil recovery rate (m^3/hour) of the skimmers, but it usually represent the hourly collection of the skimmer not just oil but also water. The OREs is the oil recovery efficiency (m^3 of oil/m^3 of collection) of the skimmers which indicates proportion of pure oil in the collected oil-water mixture. According to the collected information, a series of ORR$_{n1}$, ORR$_{n2}$ and ORR$_{n3}$ were generated based on calculating ORRs * OREs using different oil thickness with a viscosity of 1,000 cSt (Schulze, 1998). Fittings were then applied based on quadratic functions to generate the regression models of ORR$_n$ with the change of spilled oil thickness, representing the recovery efficiencies of the three types of skimmers

(Figure 4.4). Such change of slick thickness is usually caused by the processes of spreading, shifting, weathering (e.g., evaporation, dispersion, dissolution, emulsification, etc.), as well as oil recovery. The details about the ORR_n of the skimmers as well as the regression models of the efficiencies are shown in Table 4.1.

There were 10 sets of each type of skimmer in the warehouse and the capacity of vessels used for operation was 20 sets of skimmers. Due to the challenge of transportation, no more skimmers and vessels can be supplied within 48 hours. Therefore, the objective of the current stage was to determine the combination of the three types of skimmers in each stage to maximize the collected volume of spilled oil in this 48-hour period.

Table 4.1 Time of devices allocation as well as model parameters of ORR_n.

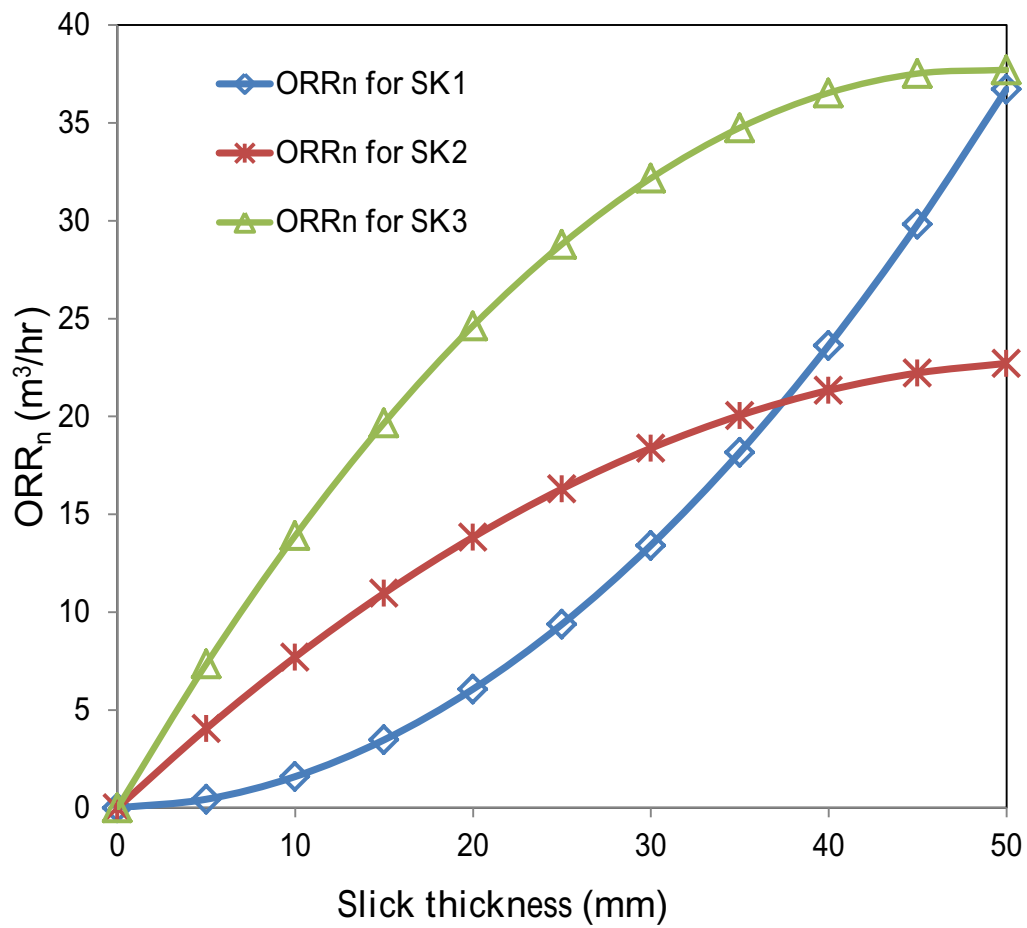| Types of skimmers	Time of devices allocation and deployment (hour)	Model parameter for ORR_n	
		a	b
SK_1	3	0.01437	0.01602
SK_2	6	-0.00791	0.84975
SK_3	12	-0.01591	1.54975

Figure 4.4 Net oil recovery rates for the skimmers

4.3.2 Oil recovery efficiency

According the above information, a general optimization model can be generated as follows:

$$Max\,V = \sum_{j=1}^{3} \int_{0}^{48} SK_j \times ORR_{nj}\;dt \qquad (4.36a)$$

s.t.

$$\sum_{s=1}^{3} SK_j \le 20 \qquad (4.36b)$$

$$0 \le SK_j \le 10 \quad \forall j = 1, 2, 3 \qquad (4.36d)$$

$$SK_j \in integer \quad \forall\; j = 1, 2, 3 \qquad (4.36e)$$

where j is the index of skimmers, t is the point of time during the operational period, SK_j are the numbers of applied skimmers, and ORR_{nj} are the corresponding net oil recovery rates for skimmers.

Because the spill was boomed, it can be assumed that the area of the spilled oil is unchanged at this stage, which was A = 100,000 m^2. Because the initial volume of spilled oil was V_0 = 5,000 m^3, the initial thickness can be calculated as follows:

$$SOT_0 = V_0 / A = 5{,}000 / 100{,}000 = 0.05 \, \text{m} = 50 \, \text{mm} \tag{4.37}$$

and at time t, the thickness can be interpreted as follows:

$$SOT_t = RV_t / A = RV_t / 100{,}000 \tag{4.38}$$

where SOT_t is the spilled oil thickness at time t, and RV_t is the remaining volume of spilled oil at time t.

According to the regression model of ORR_n (Figure 4.4) and the Equation 4.26, the specific regression model for SK_1 efficiency is generated as follows:

$$\begin{aligned} ORR_{n1t} &= 0.01437\left(SOT_t \times 1{,}000\right)^2 + 0.01602\left(SOT_t \times 1{,}000\right) \\ &= 0.01437\left(1{,}000\,\frac{RV_t}{A}\right)^2 + 0.01602\left(1{,}000\,\frac{RV_t}{A}\right) \end{aligned} \tag{4.39}$$

where ORR_{n1t} is the oil recovery rate of SK_1 at time t. In addition, the specific regression model for SK_2 efficiency is generated as follows:

$$ORR_{n2t} = -0.00791(SOT_t \times 1,000)^2 + 0.84975(SOT_t \times 1,000)$$
$$= -0.00791\left(1,000\frac{RV_t}{A}\right)^2 + 0.84975\left(1,000\frac{RV_t}{A}\right) \tag{4.40}$$

where ORR_{n2t} is the net oil recovery rate of SK_2 at time t. Finally, the specific regression

model for SK_3 efficiency is generated as follows:

$$ORR_{n3t} = -0.01591(SOT_t \times 1,000)^2 + 1.54975(SOT_t \times 1,000)$$
$$= -0.01591\left(1,000\frac{RV_t}{A}\right)^2 + 1.54975\left(1,000\frac{RV_t}{A}\right) \tag{4.41}$$

where ORR_{n3t} is the net oil recovery rate of SK_3 at time t.

Accordingly, the Equation 4.36 can be converted as follows:

$$Max\, V = \int_0^{48} V_t\, dt \tag{4.42a}$$

s.t.

$$V_t = \sum_{j=1}^{3} SK_j \times ORR_{njt} \qquad\qquad \forall t$$

$$= SK_1 \times \left(0.01437\left(1{,}000\,\frac{RV_t}{A}\right)^2 + 0.01602\left(1{,}000\,\frac{RV_t}{A}\right)\right)$$

$$+ SK_2 \times \left(-0.00791\left(1{,}000\,\frac{RV_t}{A}\right)^2 + 0.84975\left(1{,}000\,\frac{RV_t}{A}\right)\right) \qquad (4.42b)$$

$$+ SK_3 \times \left(-0.01591\left(1{,}000\,\frac{RV_t}{A}\right)^2 + 1.54975\left(1{,}000\,\frac{RV_t}{A}\right)\right)$$

$$\sum_{j=1}^{3} SK_j \le 20 \qquad\qquad (4.42c)$$

$$0 \le SK_j \le 10 \quad \forall j = 1, 2, 3 \qquad\qquad (4.42d)$$

$$SK_j \in integer \quad \forall\, j = 1, 2, 3 \qquad\qquad (4.42e)$$

where V_t is the collected volume of spilled oil at time t, and the relation between V_t and RV_t is as follows:

$$RV_t = V_0 - \int_0^t V_t\, dt \qquad\qquad (4.43)$$

Accordingly, Equation 4.42 can be converted as follows:

$$Max\, V = \int_0^{48} V_t\, dt \qquad\qquad (4.44a)$$

s.t.

$$V_t = \sum_{j=1}^{3} SK_j \times ORR_{njt} \qquad \forall t$$

$$= SK_1 \times \left(0.01437 \left(\frac{1000\left(V_0 - \int_0^t V_t\, dt\right)}{A} \right)^2 + 0.01602 \left(\frac{1000\left(V_0 - \int_0^t V_t\, dt\right)}{A} \right) \right)$$

$$+ SK_2 \times \left(-0.00791 \left(\frac{1000\left(V_0 - \int_0^t V_t\, dt\right)}{A} \right)^2 + 0.84975 \left(\frac{1000\left(V_0 - \int_0^t V_t\, dt\right)}{A} \right) \right)$$

$$+ SK_3 \times \left(-0.01591 \left(\frac{1000\left(V_0 - \int_0^t V_t\, dt\right)}{A} \right)^2 + 1.54975 \left(\frac{1000\left(V_0 - \int_0^t V_t\, dt\right)}{A} \right) \right)$$

(4.44b)

$$\sum_{j=1}^{3} SK_j \leq 20 \tag{4.44c}$$

$$0 \leq SK_j \leq 10 \quad \forall j = 1, 2, 3 \tag{4.44d}$$

$$SK_j \in integer \quad \forall\, j = 1, 2, 3 \tag{4.44e}$$

This model is recursive and usually cannot be directly solved. According to Equation 4.35, Equation 4.44 can be divided into a multiple-stage dynamic programming. Assume that the controllable time interval for this case was 1 hour, and then the 48-hour time span can be divided into 48 stages. According to a basic

assumption that all parameters remained unchanged within a single stage, the Equation 4.44 can be converted as follows:

$$\text{Max V} = \sum_{m=1}^{48} V_m \tag{4.45a}$$

s.t.

$$V_1 = \sum_{j=1}^{3} SK_j \times ORR_{njm} \qquad \forall m = 1$$

$$= SK_1 \times \left(0.01437 \left(1,000 \frac{V_0}{A} \right)^2 + 0.01602 \left(1,000 \frac{V_0}{A} \right) \right)$$

$$+ SK_2 \times \left(-0.00791 \left(1,000 \frac{V_0}{A} \right)^2 + 0.84975 \left(1,000 \frac{V_0}{A} \right) \right) \tag{4.45b}$$

$$+ SK_3 \times \left(-0.01591 \left(1,000 \frac{V_0}{A} \right)^2 + 1.54975 \left(1,000 \frac{V_0}{A} \right) \right)$$

$$V_m = \sum_{j=1}^{3} SK_j \times ORR_{njm} \qquad \forall m = 2,\cdots,48$$

$$= SK_1 \times \left(0.01437 \left(\frac{1,000 \left(V_0 - \sum_{h=1}^{m-1} V_h \right)}{A} \right)^2 + 0.01602 \left(\frac{1,000 \left(V_0 - \sum_{h=1}^{m-1} V_h \right)}{A} \right) \right)$$

$$+ SK_2 \times \left(-0.00791 \left(\frac{1,000 \left(V_0 - \sum_{h=1}^{m-1} V_h \right)}{A} \right)^2 + 0.84975 \left(\frac{1,000 \left(V_0 - \sum_{h=1}^{m-1} V_h \right)}{A} \right) \right)$$

$$+ SK_3 \times \left(-0.01591 \left(\frac{1,000 \left(V_0 - \sum_{h=1}^{m-1} V_h \right)}{A} \right)^2 + 1.54975 \left(\frac{1,000 \left(V_0 - \sum_{h=1}^{m-1} V_h \right)}{A} \right) \right)$$

$$\tag{4.45c}$$

$$\sum_{j=1}^{3} SK_j \leq 20 \tag{4.45d}$$

$$0 \leq SK_j \leq 10 \quad \forall j = 1, 2, 3 \tag{4.45e}$$

$$SK_j \in integer \quad \forall j = 1, 2, 3 \tag{4.45f}$$

where m is the index of current stage from the divided 48-hour time series, V_m is the amount of collected spilled oil in stage m, h is the index of the stages before stage m and V_h is collected oil in the stage h.

When considering the time of devices allocation and employment of skimmers from warehouse to the spill site, the specific type of skimmer cannot apply for the oil recovery before the accomplishment of its allocation and employment. Accordingly, the Equation 4.45 can be reformulated as follows:

$$Max\, V = \sum_{m=1}^{48} V_m \tag{4.46a}$$

s.t.

$$V_1 = \sum_{j=1}^{3} SK_j \times ORR_{njm} \qquad\qquad \forall m = 1$$

$$= bsk_{1m} \times SK_1 \times \left(0.01437\left(1{,}000\frac{V_0}{A}\right)^2 + 0.01602\left(1{,}000\frac{V_0}{A}\right) \right)$$

$$+ bsk_{2m} \times SK_2 \times \left(-0.00791\left(1{,}000\frac{V_0}{A}\right)^2 + 0.84975\left(1{,}000\frac{V_0}{A}\right) \right) \qquad (4.46b)$$

$$+ bsk_{3m} \times SK_3 \times \left(-0.01591\left(1{,}000\frac{V_0}{A}\right)^2 + 1.54975\left(1{,}000\frac{V_0}{A}\right) \right)$$

$$V_m = \sum_{j=1}^{3} SK_j \times ORR_{njm} \qquad\qquad \forall m = 2, \cdots, 48$$

$$= bsk_{1m} \times SK_1 \times \left(0.01437\left(\frac{1{,}000\left(V_0 - \sum_{h=1}^{m-1} V_h\right)}{A} \right)^2 + 0.01602\left(\frac{1{,}000\left(V_0 - \sum_{h=1}^{m-1} V_h\right)}{A} \right) \right)$$

$$+ bsk_{2m} \times SK_2 \times \left(-0.00791\left(\frac{1{,}000\left(V_0 - \sum_{h=1}^{m-1} V_h\right)}{A} \right)^2 + 0.84975\left(\frac{1{,}000\left(V_0 - \sum_{h=1}^{m-1} V_h\right)}{A} \right) \right)$$

$$+ bsk_{3m} \times SK_3 \times \left(-0.01591\left(\frac{1{,}000\left(V_0 - \sum_{h=1}^{m-1} V_h\right)}{A} \right)^2 + 1.54975\left(\frac{1{,}000\left(V_0 - \sum_{h=1}^{m-1} V_h\right)}{A} \right) \right)$$

$$(4.46c)$$

$$\sum_{j=1}^{2} SK_j \leq 20 \qquad\qquad\qquad\qquad\qquad\qquad (4.46d)$$

$$0 \leq SK_j \leq 10 \quad \forall j = 1, 2, 3 \qquad\qquad\qquad\qquad (4.46e)$$

$$bsk_{jm} = 0 \qquad \forall j = 1, 2, 3; \forall tt_j \geq m \qquad\qquad (4.46f)$$

$$bsk_{jm} = 1 \qquad \forall j = 1, 2, 3; \forall tt_j \leq m \tag{4.46g}$$

$$SK_j \in integer \qquad \forall\, j = 1, 2, 3 \tag{4.46h}$$

where bsk_{jm} is the binary indicator for SK_s in stage m to determine if the SK_j is applied in the oil recovery in this stage and tt_j is the time of devices allocation and deployment for SK_j listed in Table 4.1.

4.3.3 Oil weathering simulation and simulation-optimization coupling

The inputs for the oil weathering processes are shown in Table 4.2.

According to Fingas (2011) and Equation 4.30, the empirical equation of evaporation for the Statfjord oil is as follows:

$$FE = \frac{2.67 + 0.06 \times (T - 273.15) \times Ln(t)}{100} \tag{4.47}$$

According to Equations 4.31, 4.33, 4.34, and 4.47, the Equation 4.46 can be converted as follows:

$$Max\, V = \sum_{m=1}^{48} V_m \tag{4.48a}$$

173

s.t.

$$V_1 = \sum_{j=1}^{3} SK_j \times ORR_{njm} \qquad \forall m = 1$$

$$= bsk_{1m} \times SK_1 \times \left(0.01437 \left(1{,}000 \frac{V_0}{A} \right)^2 + 0.01602 \left(1{,}000 \frac{V_0}{A} \right) \right)$$

$$+ bsk_{2m} \times SK_2 \times \left(-0.00791 \left(1{,}000 \frac{V_0}{A} \right)^2 + 0.84975 \left(1{,}000 \frac{V_0}{A} \right) \right) \qquad (4.48b)$$

$$+ bsk_{3m} \times SK_3 \times \left(-0.01591 \left(1{,}000 \frac{V_0}{A} \right)^2 + 1.54975 \left(1{,}000 \frac{V_0}{A} \right) \right)$$

$$FE_1 = \frac{2.67 + 0.06 \times (T - 273.15) \times Ln(60)}{100} \qquad \forall m = 1$$

$$(4.48c)$$

$$DE_1 = \frac{0.11(U + 1)^2}{1 + 50 \mu_0^{o\,0.5} \left(\dfrac{V_0}{A} \right) s_t} \qquad \forall m = 1$$

$$(4.48d)$$

$$VF_1 = V_0 \times FE_1 \qquad \forall m = 1 \tag{4.48e}$$

$$VD_1 = V_0 \times DE_1 \times 3{,}600 \qquad \forall m = 1 \tag{4.48f}$$

$$V_m = \sum_{j=1}^{3} SK_j \times ORR_{njm} \qquad \forall m = 2, \cdots, 48$$

$$= bsk_{1m} \times SK_1 \times \left(0.01437 \left(\frac{1{,}000\left(V_0 - \sum_{h=1}^{m-1} V_h \right)}{A} \right)^2 + 0.01602 \left(\frac{1{,}000\left(V_0 - \sum_{h=1}^{m-1} V_h \right)}{A} \right) \right)$$

$$+ bsk_{2m} \times SK_2 \times \left(-0.00791 \left(\frac{1{,}000\left(V_0 - \sum_{h=1}^{m-1} V_h \right)}{A} \right)^2 + 0.84975 \left(\frac{1{,}000\left(V_0 - \sum_{h=1}^{m-1} V_h \right)}{A} \right) \right)$$

$$+ bsk_{3m} \times SK_3 \times \left(-0.01591 \left(\frac{1{,}000\left(V_0 - \sum_{h=1}^{m-1} V_h \right)}{A} \right)^2 + 1.54975 \left(\frac{1{,}000\left(V_0 - \sum_{h=1}^{m-1} V_h \right)}{A} \right) \right)$$

(4.48g)

$$FE_m = \frac{2.67 + 0.06 \times (T - 273.15) \times Ln(60)}{100} \qquad \forall m = 2, \cdots, 48$$

(4.48h)

$$DE_m = \frac{0.11(U + 1)^2}{1 + 50\mu_m^{o\,0.5} \left(\dfrac{V_0 - \sum_{h=1}^{m-1} (V_h + VF_h + VD_h)}{A} \right) s_t} \qquad \forall m = 2, \cdots, 48$$

(4.48i)

$$FW_m = K_b \left(1 - \exp\left(\frac{-K_a}{K_b} \right)(U + 1)^2 \times 3{,}600 \right) \qquad \forall m = 2, \cdots, 48 \qquad \text{(4.48j)}$$

$$\rho_m^o = FW_{m-1}\rho_w + (1 - FW_{m-1})\left(\rho_{m-1}^o + K_b FE_{m-1} \right) \qquad \forall m = 2, \cdots, 48$$

(4.48k)

$$\mu_m^o = \mu_{m-1}^o \exp\left(K_c FE_{m-1} \right) \exp\left(\frac{2.5 FW_{m-1}}{1 - K_b FW_{m-1}} \right) \qquad \forall m = 2, \cdots, 48 \qquad \text{(4.48I)}$$

175

$$VF_m = V_0 \times FE_m \qquad \forall m = 2, \cdots, 48 \tag{4.48m}$$

$$VD_m = V_0 \times DE_m \times 3,600 \qquad \forall m = 2, \cdots, 48 \tag{4.48n}$$

$$\sum_{j=1}^{2} SK_j \leq 20 \tag{4.48o}$$

$$0 \leq SK_j \leq 10 \quad \forall j = 1, 2, 3 \tag{4.48p}$$

$$bsk_{jm} = 0 \qquad \forall j = 1, 2, 3; \forall tt_s \geq m \tag{4.48q}$$

$$bsk_{jm} = 1 \qquad \forall j = 1, 2, 3; \forall tt_s \leq m \tag{4.48r}$$

$$SK_j \in integer \quad \forall \ j = 1, 2, 3 \tag{4.48s}$$

where ρ_0^0 is the initial density of the spilled oil, μ_0^0 is the initial viscosity of the spilled oil.

Based on the assumptions that only the provided weathering processes will occur during an oil spill and no sedimentation will happen during the weathering, a dynamic mixed integer nonlinear problem can be finally formed and solved by programming software (i.e., MATLAB® with LINDO API®).

Table 4.2 Statjord crude oil characteristics for the weathering processes of evaporation and dispersion

(Nazir et al., 2008)

Parameter	Value	Parameter	Value
Temperature (T)	298 K	Wind speed (U)	5 m/s
Vapor pressure (P^{sat})	10.4 Pa	Molecular weight (M)	128.2 g/mol
Density of oil (ρ^o)	832 kg/m^3	Gas constant (R)	8.314 m^3·Pa/mol·K
Viscosity of the oil (μ^o)	3.03 cP	Interface tension of oil and water (S_t)	2000 dyne/m

4.3.4 Monte Carlo simulation

In order to test the feasibility of the developed approach in handling uncertainty, slick area, wind speed, and temperature, which have been commonly used to represent uncertain features in offshore oil spill environments, were used as uncertain inputs. The approximate distribution of these three parameters can be generated as follows: slick area was normally distributed with a mean value of 100,000 m^2 and a standard deviation of 8,000 m^2; wind speed was normally distributed with a mean value of 5 m/s and a standard deviation of 0.5 m/s; temperature was normally distributed with a mean value of 298 K and a standard deviation of 10 K. The total trials for the Monte Carlo simulation was set as N = 200. Based on the solution steps shown in Figure 4.3, the random values for these three parameters were assigned in each loop (set as trial I) based on their distribution settings. By solving Equation 4.48 with the assigned random values, the optimal alterative for trial I can be obtained. After finishing 200 trials, all the feasible solutions can be obtained for further trade-off analysis.

4.3.5 Results and discussion

Modeling without consideration of uncertainty

The modeling results indicated that the optimal combination of skimmers is $SK_1 = 9$ entering the oil recovery system at the 3rd hour, $SK_2 = 9$ entering the system at the 6th hour, and $SK_3 = 2$ entering the system at the 12th hour. This yields 3,966 m^3 collected oil

in the 48-hour period which means that the recovery efficiency was 79.3%. At the same time, 926 m^3 (18.5%) of the spilled oil was evaporated and 107 m^3 (2.1%) is dispersed. The details about the dynamic changes of ORR_n, the collected, evaporated, dispersed, and remaining oil, and the changes of oil viscosity and density as well as slick thickness are shown in Figures 4.5 to 4.10.

From Figures 4.5 and 4.6 it can be seen that at the initial stage the net oil recovery rates of SK_1 (ORR_{n1}) and SK_3 (ORR_{n3}) were much higher than that of SK_2 (ORR_{n2}). However, ORR_{n1} significantly decreased with time and became lower than ORR_{n2} after about 6 hours. On the other hand, ORR_{n2} slightly decreased in most time periods. Although SK_3 had higher net oil recovery rate at the initial stage and ORR_{n3} decreased with a low rate in the remaining stages, the device allocation and deployment time of this type of skimmer (12 hours) is much longer than SK_1 (3 hours) and SK_2 (6 hours). Therefore, SK_1 contributed more to the recovery in the first few hours but less in the remaining, while SK_2 had stable and relatively high contribution after being applied. Although the number of applied SK_3 was much lower than those of SK_1 and SK_2, the high ORR_n of SK_3 at low thickness led to a significant contribution during the late stages of the operational period (Figure 4.6).
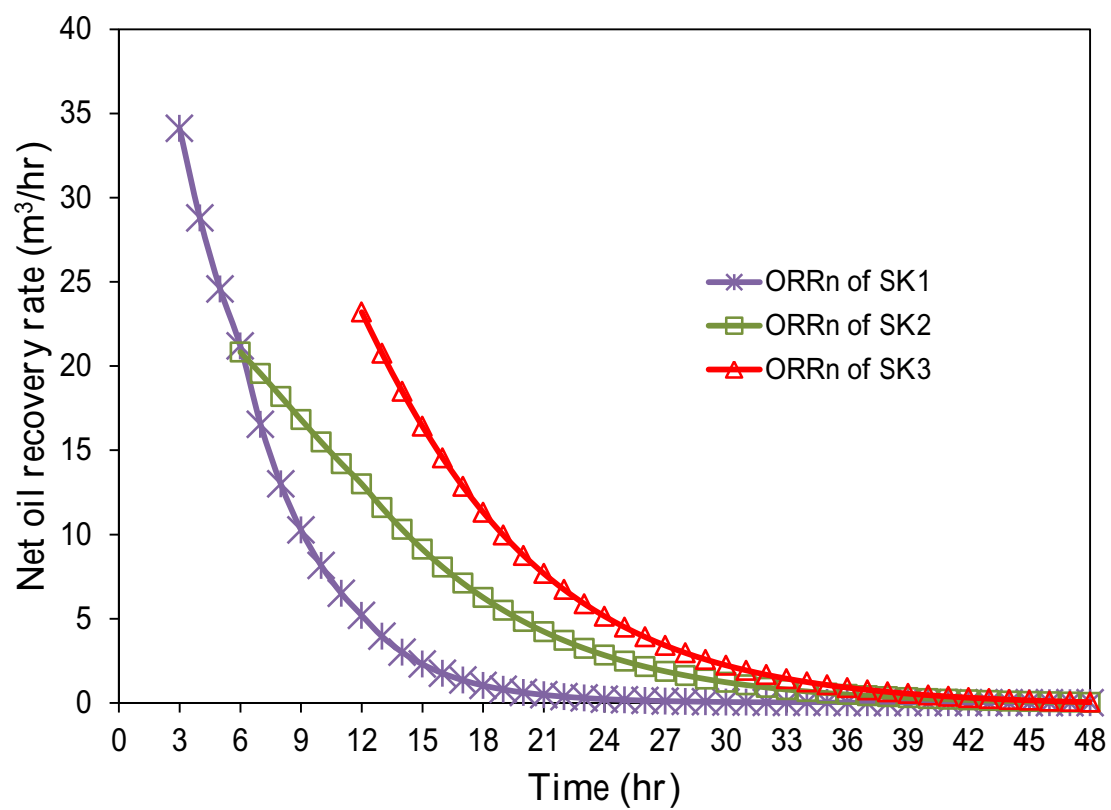
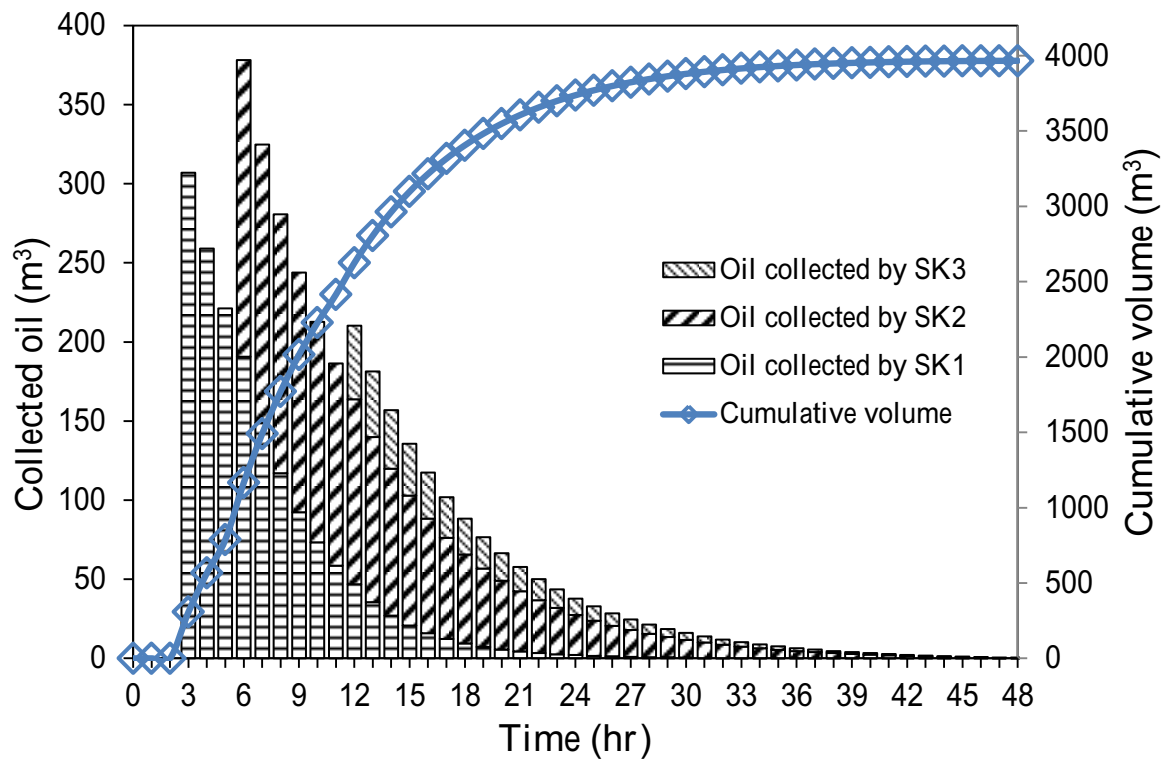Figure 4.5 Changes of ORR_n of skimmers during the operational period

Figure 4.6 Collected and cumulative amounts of spilled oil by skimmers in each stage
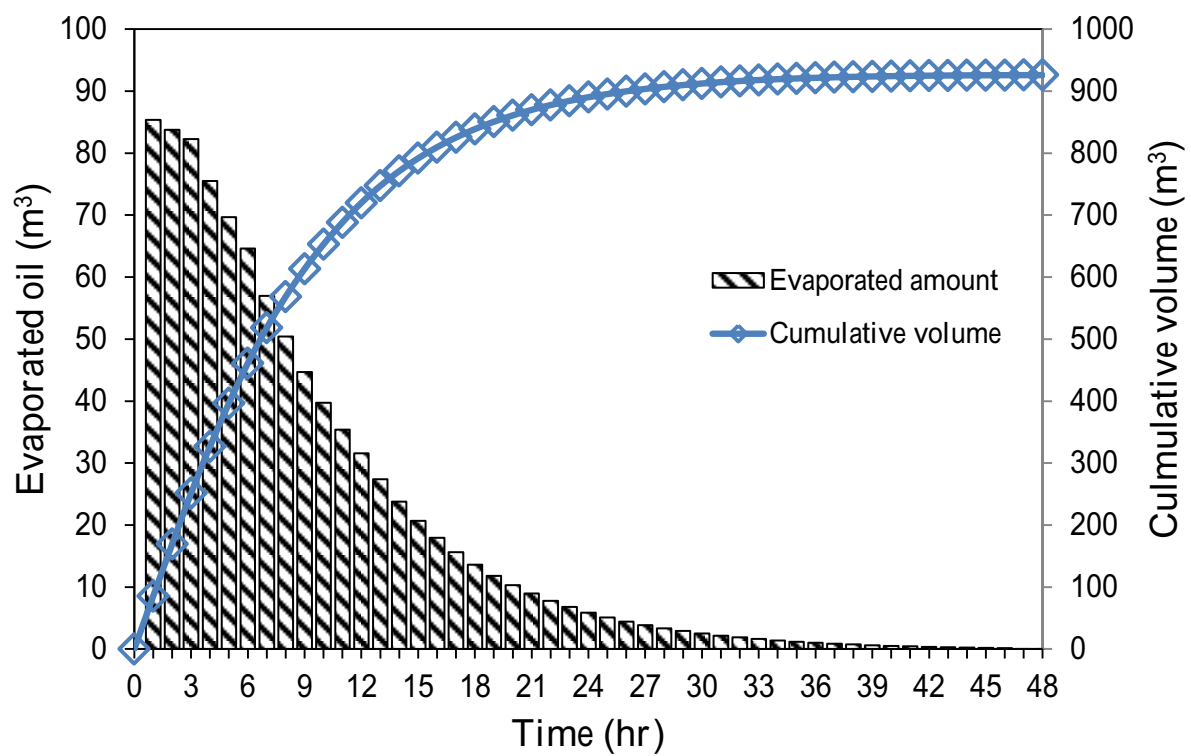
Figure 4.7 Evaporated and cumulative amounts of spilled oil in each stage
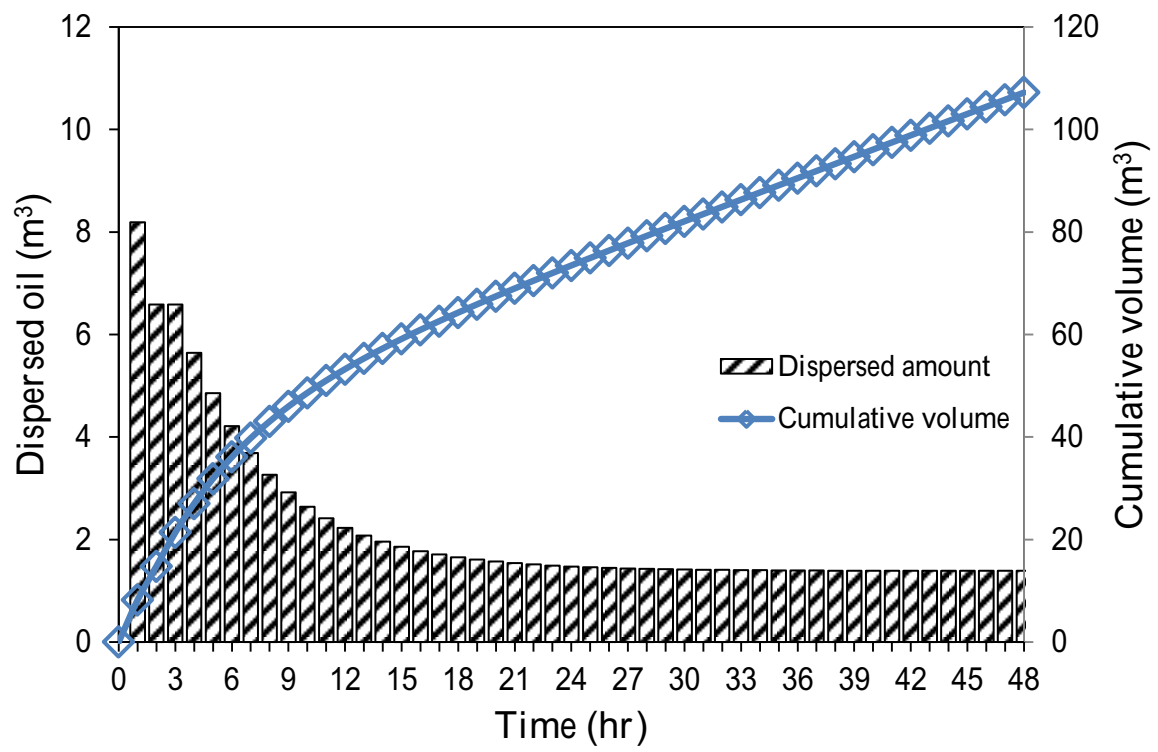
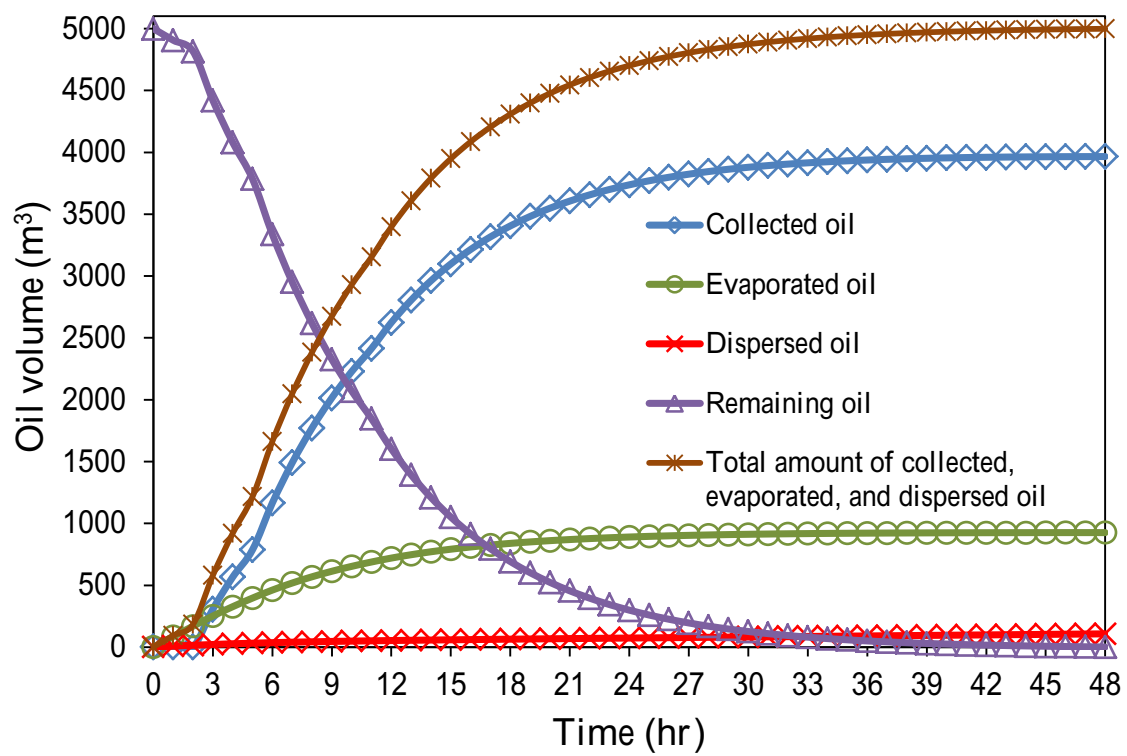Figure 4.8 Dispersed and cumulative amounts of spilled oil in each stage

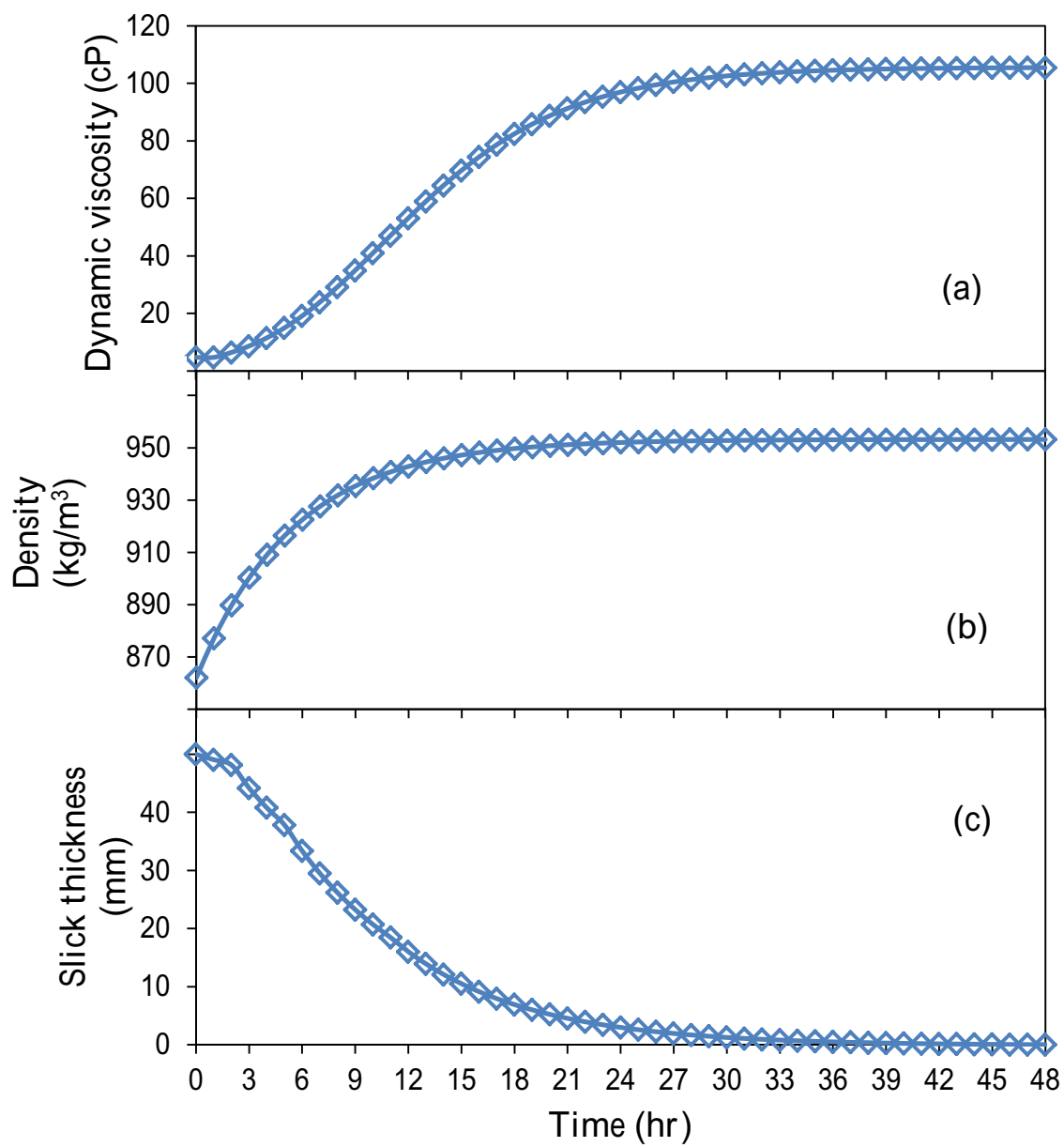Figure 4.9 The transport and fate of spilled oil during the operational period

Figure 4.10 The change of (a) dynamic viscosity, (b) density, and (c) slick thickness during the operational period

The amount of oil lost from the weathering processes (e.g., evaporation and dispersion) played an importation role in the oil transport and fate and therefore significantly affected the change of the net oil recovery rates of skimmers (Figures 4.7 and 4.8). The total amount of collected, evaporated, and dispersed oil in the first 10 hours increased significantly but became stable after 20 hours (Figure 4.9). This was mainly due to the large amount of volatile and semi-volatile components in the oil rapidly lose via evaporation and dispersion. Simultaneously, the properties (e.g., viscosity and density) of spilled oil were also altered by the weathering processes (e.g., evaporation and emulsification) (Figures 4.10a and 4.10b), and vice versa (Figures 4.7 and 4.8). Although the rates of evaporation and dispersion still had certain percentages and kept decreasing, these rates present the percentages of the remaining oil from the previous stage /hour and therefore the lost amount after the 20th hour became stable in a significantly low level (Figure 4.9). Therefore, in the last few stages of the operational period, evaporation and dispersion tended to have negligible contribution to the change of slick thickness and recovery efficiency.

In the first 3 hours of the operational period, because all skimmers were still unready, only evaporation and dispersion affected the transport and fate of the spilled oil. Thus, the amount and thickness of the remaining oil slightly decreased in the first 3 hours (Figures 4.9 and 4.10c). At the fourth hour, 9 sets of SK_1 started to collect oil. Because the collection rates of skimmers were higher than the evaporation rate (more than 3 times),

the remaining amount and slick thickness sharply dropped after the 3rd hour. At the 6th hour, 9 sets of SK_2 started to collect oil. However, because ORR_n of SK_1 had already significantly dropped in this stage, the addition of SK_2 can only make a small difference in the 3rd hour. Therefore, the decrease of remaining oil and slick thickness was accelerated in the 6th hour, but not as significantly as that in the 3rd hour. Similar situation can be observed in the 12th hour when SK_3 were applied for collection (Figures 4.9 and 4.10c).

Modeling under uncertainty

With the uncertain inputs of slick area, temperature, and wind speed, as well as the pre-set trials for modeling, a series of results were obtained, including the skimmer combinations, the amounts of collected, evaporated, and dispersed oil, as well as the changes of net oil recovery rates, slick thickness, viscosity, and density. Accordingly, further statistical analyses were applied to assess 1) the distributions of the numbers of different types of skimmer (Figure 4.11); 2) the mean values and 95% confidence intervals for net oil recovery rates for skimmers (Figure 4.12), cumulatively collected, evaporated and dispersed oil, as well as the remaining oil (Figure 4.13), changes of density, dynamic viscosity, and slick thickness (Figure 4.14) ; 3) the changes of finally collected, evaporated, and dispersed oil with the changes of slick area, temperature, and wind speed, respectively (Figure 4.15); and 4) the changes of the numbers of different skimmers with the changes of slick area, temperature, and wind speed (Figure 4.16).
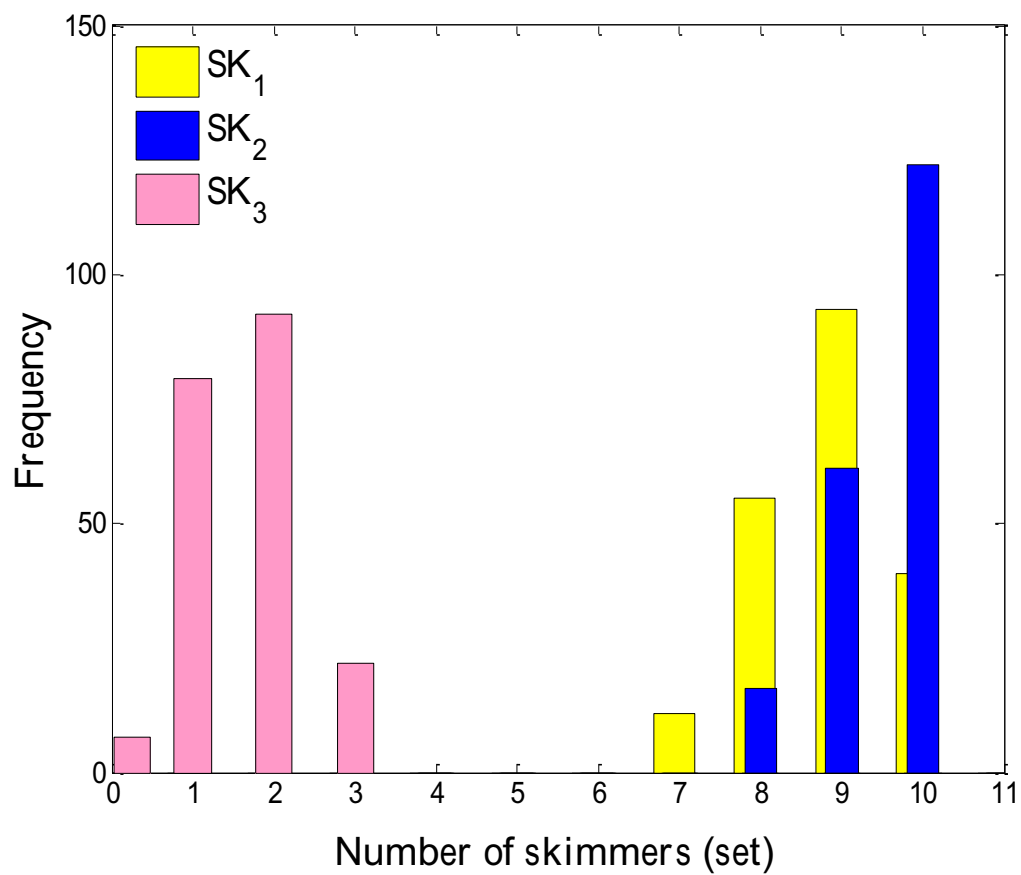
Figure 4.11 Distributions of skimmer numbers
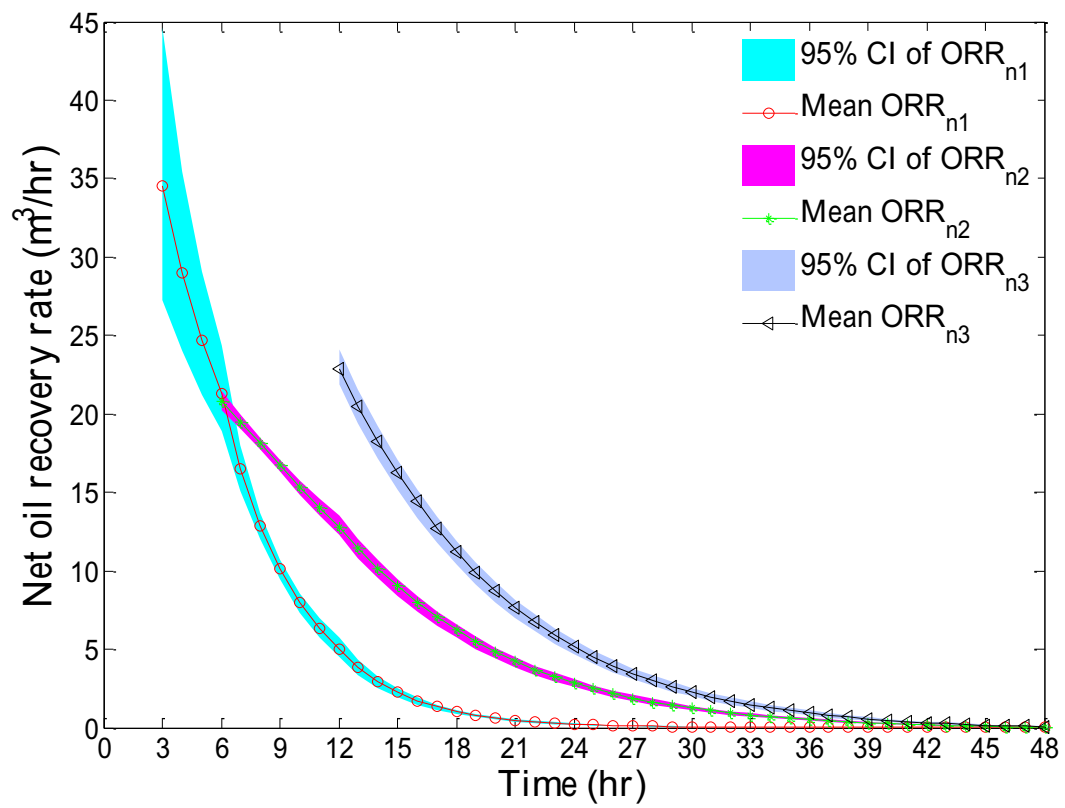
Figure 4.12 Mean values and 95% confidence intervals of net oil recovery rate for skimmers
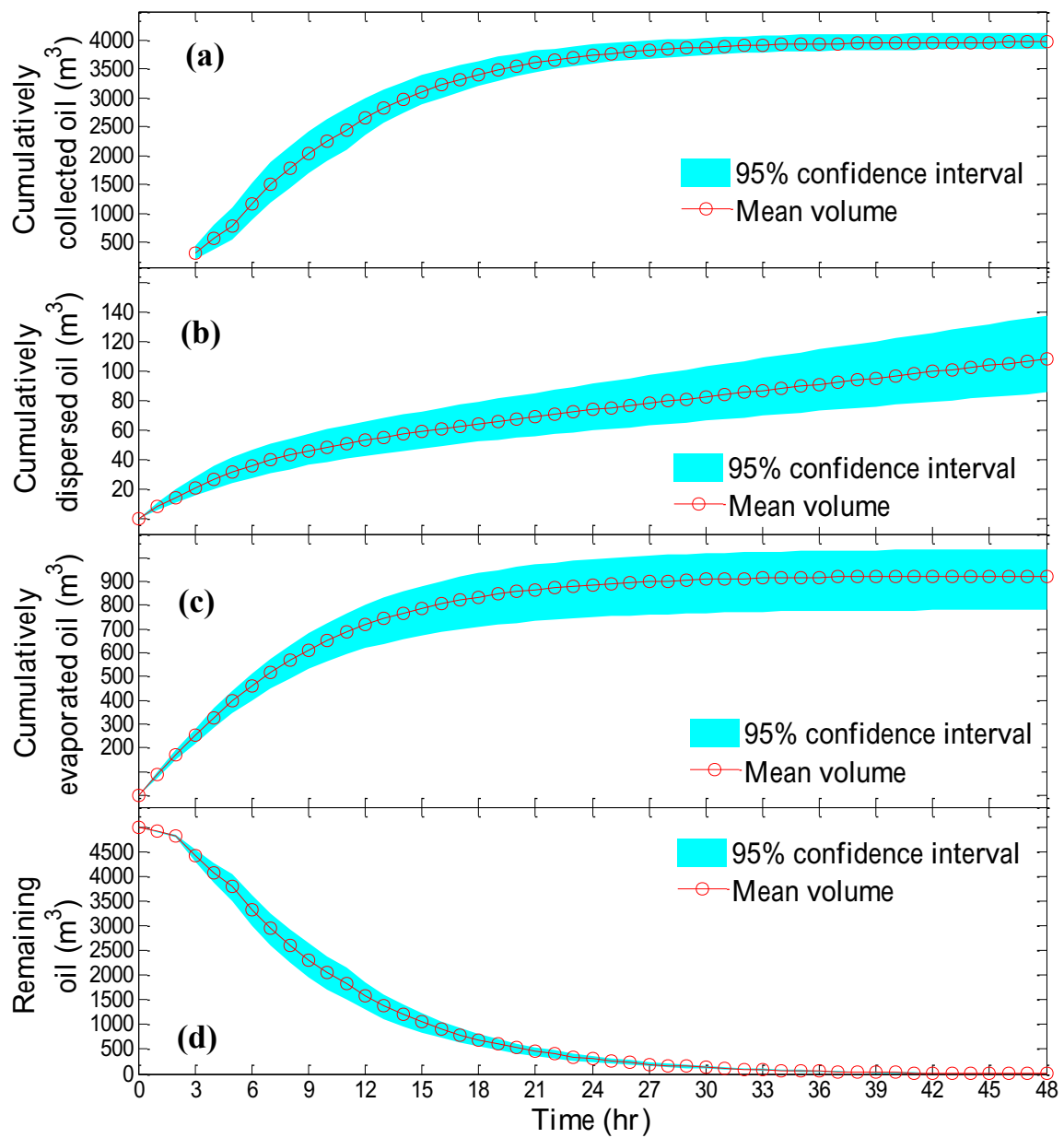
Figure 4.13 Mean values and 95% confidence intervals of cumulatively (a) collected oil, (b) evaporated oil, and (c) dispersed oil as well as (d) remaining oil
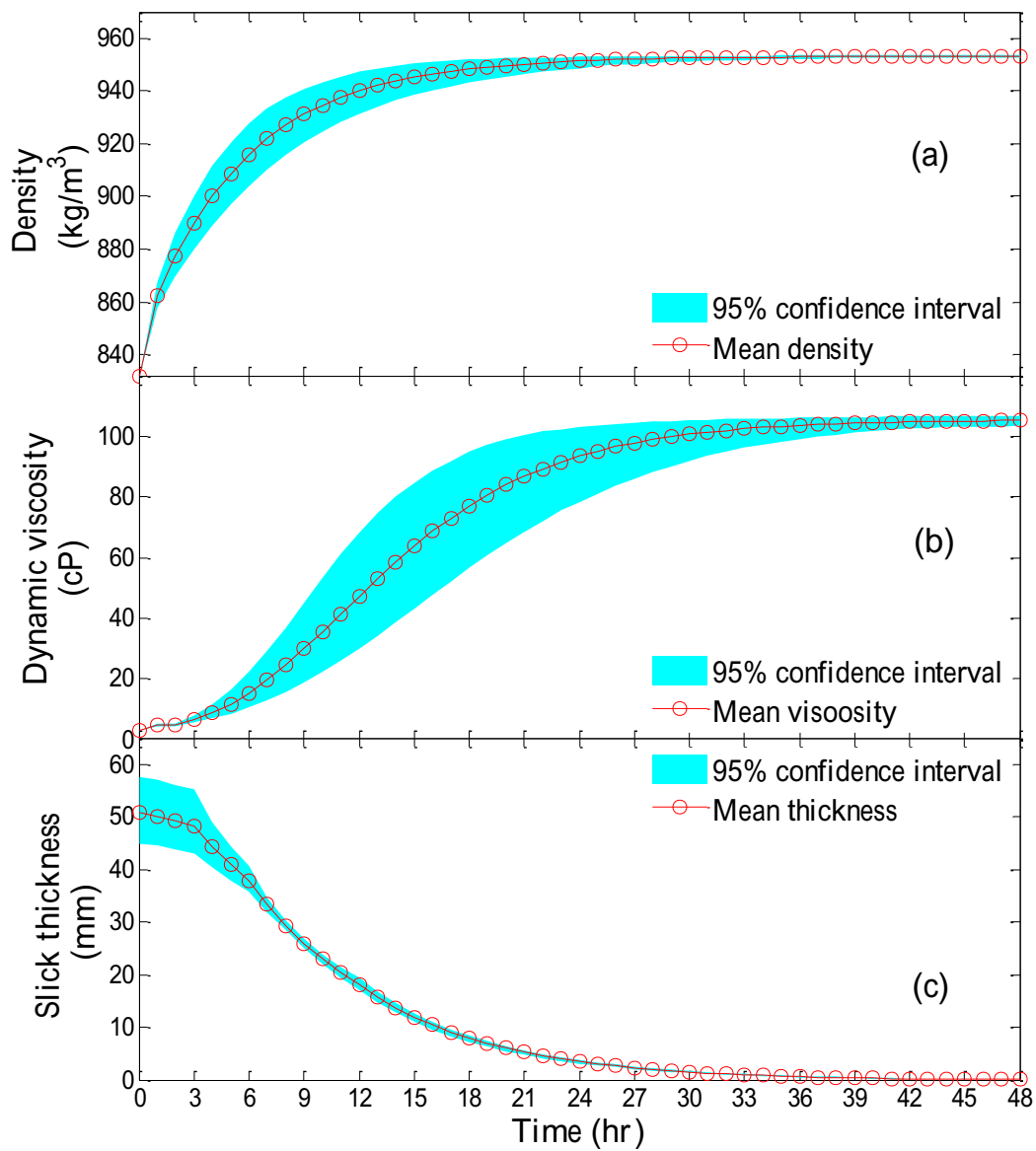
Figure 4.14 Mean values and 95% confidence intervals of (a) density, (b) viscosity, and (c) slick thickness
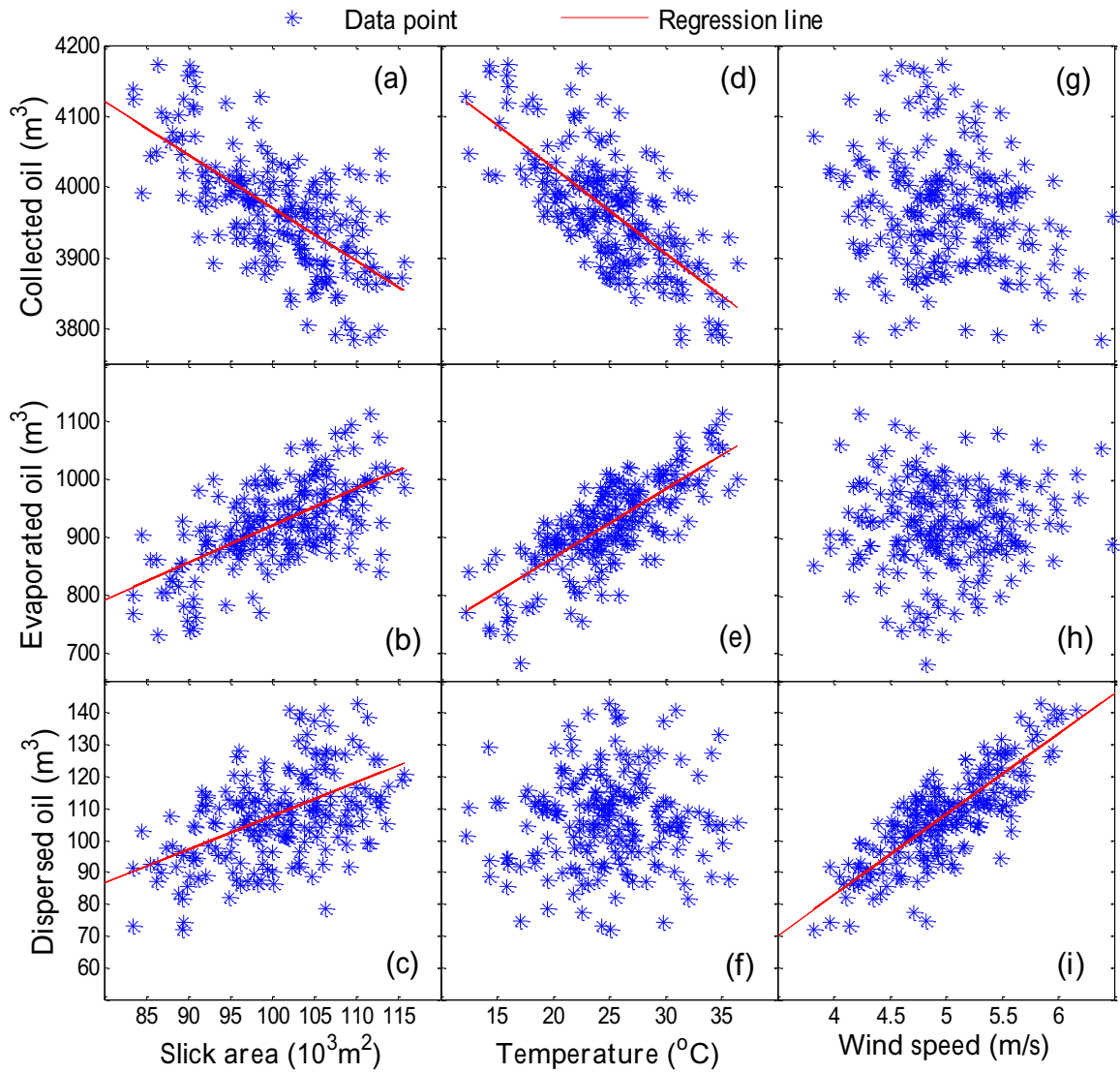
Figure 4.15 The change of finally collected, evaporated, and dispersed oil with the change of slick area, temperature, and wind speed, respectively

Figure 4.16 The change of skimmer numbers with the change of (a) slick area, (b) temperature, and (c) wind speed

As shown in Figure 4.11, the number of SK_1 varied from 7 to 10 sets and the most possible number would be 9 sets under the multi-interactions of uncertain slick area, temperature, and wind speed. The number of SK_2 varied from 8 to 10 sets and the most possible number would be 10 sets. While the number of SK_3 varied from 0 to 3 sets and the m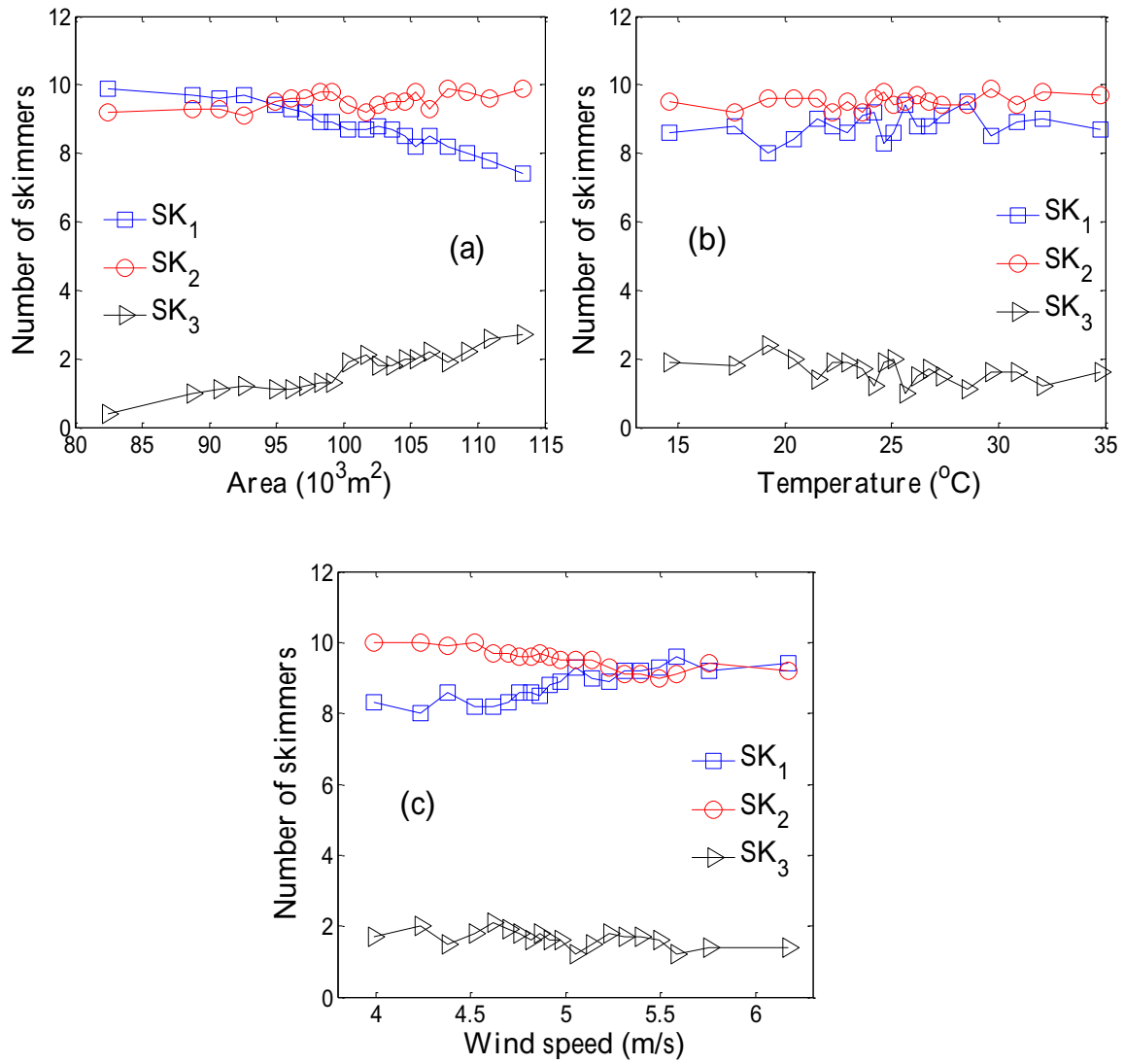ost possible number would be 2 sets, however the possibility of 1 set was significantly close to 2 sets. Such varieties of skimmer combinations were possibly due to the uncertainty of slick thickness. The number of SK_1 may increase when the slick area decreased which caused an increase of slick thickness, and vice versa. In contrast, the numbers of SK_2 and SK_3 may decrease when the slick area decreased and vice versa (Figure 4.16a). This may be attributed to the fact that SK_1 had higher net oil recovery rate with increasing slick thickness (i.e., lower slick area with unchanged spill amount), while SK_2 had lower decrease rate compared with SK_1, and SK_3 had the lowest decrease rate among all three types of skimmers (Figure 4.4). The numbers of SK_1 and SK_2 were significantly higher than the number of SK_3 despite the change of slick area, which was due to the allocation and deployment time of SK_3 (12 hours) was much longer than that of the other two types (3 and 6 hours, respectively). In addition, the increase of wind speed increased the number of SK_1 and decreased the number of SK_2 and SK_3 (Figure 4.16c). This was because the strong wind could strengthen the dispersion especially in the late stages (i.e., the dispersed oil was more and more skewed to its upper bound since 24th hour as shown in Figure 4.13c), leading to low efficiencies to the Skimmers.

Comparatively, the uncertainties in temperature had insignificant effect to the combinations of skimmers (Figure 4.16b). In addition, the net oil recovery rates for all types of skimmers were relatively significant in the early stages and became insignificant with time, and the most effect occurred in the first 6 hours (Figure 4.12). In general, it would be recommended to use a combination of ($SK_1 = 9$, $SK_2 = 10$, and $SK_3 = 1$) if the slick area tended to be smaller, and a combination of ($SK_1 = 8$, $SK_2 = 10$, and $SK_3 = 2$) if the slick area tended to be larger.

During the 48 hour operation period, the variation of the cumulative collected oil were most conspicuous in the mid-stages (i.e., from 9th to 20th hours) and less significant in other stages (Figure 4.13a). The reason was possibly due to the small quantity of applied skimmers in the early stages and low oil recovery rate in the late stages. Despite of this, the variation of the cumulative collected oil was significantly less than those of the evaporated and dispersed oil (Figures 4.13b and 4.13c). This was attributable to the uncertainties in slick area and temperature that had notable but negative effects on the collection of oil (Figures 4.15a and 4.15d). Furthermore, the effects of wind speed were negligible as shown in Figure 4.15g. In contrast, although the effects of uncertain wind speed on evaporation were hardly noticeable (Figure 4.15h), positive effects were from uncertainty of slick thickness and temperature (Figures 4.15b and 4.15e). Furthermore, although dispersion was insignificantly affected by uncertain slick area and temperature (Figures 4.15c and 4.15f), it was highly and positively affected by the wind speed

195

(Figures 4.15i). However, because the collection of oil still contributed the most (about 75% to 80%) in the oil transport and fate, it still held the most effects on the changes of remaining oil, slick thickness, oil viscosity, and density. The uncertainty of remaining oil, density, and dynamic viscosity significantly increased after the application of skimmers and decreased when the efficiency of skimming became low (Figures 4.13d, 4.14a, and 4.14b). Meanwhile, the uncertainty of slick thickness significantly decreased after the application of skimmers (Figure 4.14c).

The MC-DMINP approach is very helpful to the recovery of offshore oil spill in cold and harsh environments such as wide range of wind speed and direction, visibility, and temperature, as well as rough seas, ice coverage, appearance of icebergs, etc. These harsh conditions are always highly uncertain and dynamically changing, posing unique challenges for oil spill response. The MC-DMINP approach can help timely determine the combination of response technology with the considerations of oil recovery efficiency as well as device allocation and deployment to achieve the best oil recovery. Besides the integration of oil recovery and weathering simulation, the proposed approach can be also integrated with other simulation modules such as weather forecasting and ocean dynamics simulation to better support the clean-up of offshore oil spills. Furthermore, this approach is also capable of providing the most reasonable combination of skimmers under various uncertainties. In addition, the proposed approach has high potential in timely adjusting the settings of operation due to its multiple-stage optimization, which is

of importance in offshore oil spill recovery.

4.4 Summary

In this chapter, a fuzzy-stochastic-interval linear programming (FSILP) approach has been firstly developed to support decision making under multiple uncertainties. The developed approach is adapted from Nguyen's method to handle possibilistic and probabilistic uncertainties, and integrated with interval linear programming. It can effectively tackle uncertainties that are presented in terms of probability density functions, fuzzy membership functions, and discrete intervals and incorporate a variety of uncertain information into a general framework. Based on the developed FSILP, a Monte Carlo simulation based fuzzy programming (MCFP) approach has been developed to reflect and quantify dual uncertainties of possibility and continuous probability in environmental management. Such an approach is highly capable in converting fuzzy problems to deterministic ones and achieving the optimal solutions with fewer additional constraints, leading to significant reduction of computation time. Consequently, the MCFP approach can effectively tackle the coexistence of possibilistic and continuously probabilistic uncertainties. In addition, it can provide three levels of the optimal results to help the decision maker effectively manage the offshore oil spill response. The first level is the entire distributions of objective functions and decision variables, which can provide decision support to general policy makers (e.g., regulating and consulting organizations) for long term policy making and trade-off, risk and reliability analyses of the system. The

second level is the range of most frequent occurrences, which can help project or plant managers in designing and planning the production in a medium arrangement. The third level is the expected value of the optimal results, which can directly provide decision alternatives to the plant operators for short term operating and adjusting the facility to minimize system cost.

Based on the previous methods, a Monte Carlo simulation-based dynamic mixed integer nonlinear programming (MC-DMINP) has finally been developed based on the integration of Monte Carlo simulation and dynamic programming. The MC-DMINP approach converts the simulation model into constraints which dynamically link to the decision variables, and break a time series into certain stages according to controllable time intervals in practical manner, leading to a multiple stages dynamic programming. Such a programming approach is further integrated with the Monte Carlo simulation to handle the uncertain conditions. The MC-DMINP can be further integrated with various simulation processes (e.g., hydrodynamic, oil weathering, risk assessment, etc.), forming the simulation-based MC-DMINP approach. For example, the MC-DMINP was integrated with the simulation of oil weathering (i.e., evaporation, dispersion, and emulsification) and oil recovery.

In the case study, regression models were developed to simulate the efficiencies for three types of skimmers based on the past performance evaluation tests. These skimmers required different times for devices allocation and deployment. The models were further

integrated with the optimization and the simulation of oil weathering processes considering evaporation, dispersion and emulsification. Both the number of skimmers and timing of deployment were optimized. The optimization results indicated a 79.3% of oil recovery efficiency; Meanwhile, 18.5% of the spilled oil was evaporated and 2.1% was dispersed. In addition, uncertainty handling ability of the developed model was also tested with the uncertainty inputs of slick area, temperature, and wind speed. Despite the introduction of uncertainties, the oil collection still had the major contribution to the oil transport and fate, holding the most effects to the changes of remaining oil, slick thickness, oil viscosity, and density.

The MC-DMINP approach can represent the dynamic changes of environmental, spilled oil, as well as the resources conditions. In addition, the approach can also provide the most reasonable combination of skimmers with the consideration of uncertainties. Therefore, the developed approach should be helpful to the offshore oil spill recovery in harsh environment where unpredictable weather and oceanic environments prevail.

CHAPTER 5

AN INTEGRATED DECISION SUPPORT SYSTEM FOR OFFSHORE OIL SPILL RESPONSES IN HARSH ENVIRONMENTS (DSS-OSRH)

5.1 Framework of the DSS-OSRH

As shown in Figure 5.1, the proposed integrated decision support system for offshore oil spill response in harsh environments (DSS-OSRH) includes: 1) an updating database of natural and social conditions, spill prevention technologies, control and clean-up technologies, and expert experience; 2) a site characterization module for offshore oil spill vulnerability index (OSVI) classification via a Monte Carlo simulation based two-stage adaptive resonance theory mapping (MC-TSAM) approach for supporting sampling and monitoring, site characterization, risk assessment, and corresponding strategies of spill prevention, with an alert system to indicate the oil spill; 3) a Monte Carlo simulation based integrated rule-based fuzzy adaptive resonance theory mapping (MC-IRFAM) approach for screening/ranking available technologies for offshore oil spill responses based on specific conditions of a spill site; and 4) a Monte Carlo simulation-based dynamic mixed integer nonlinear programming (MC-DMINP) approach based on the simulation of oil weathering and recovery as well as the multi-stage dynamic programming for dynamically optimizing the combination of response technologies and the allocation of response resources.
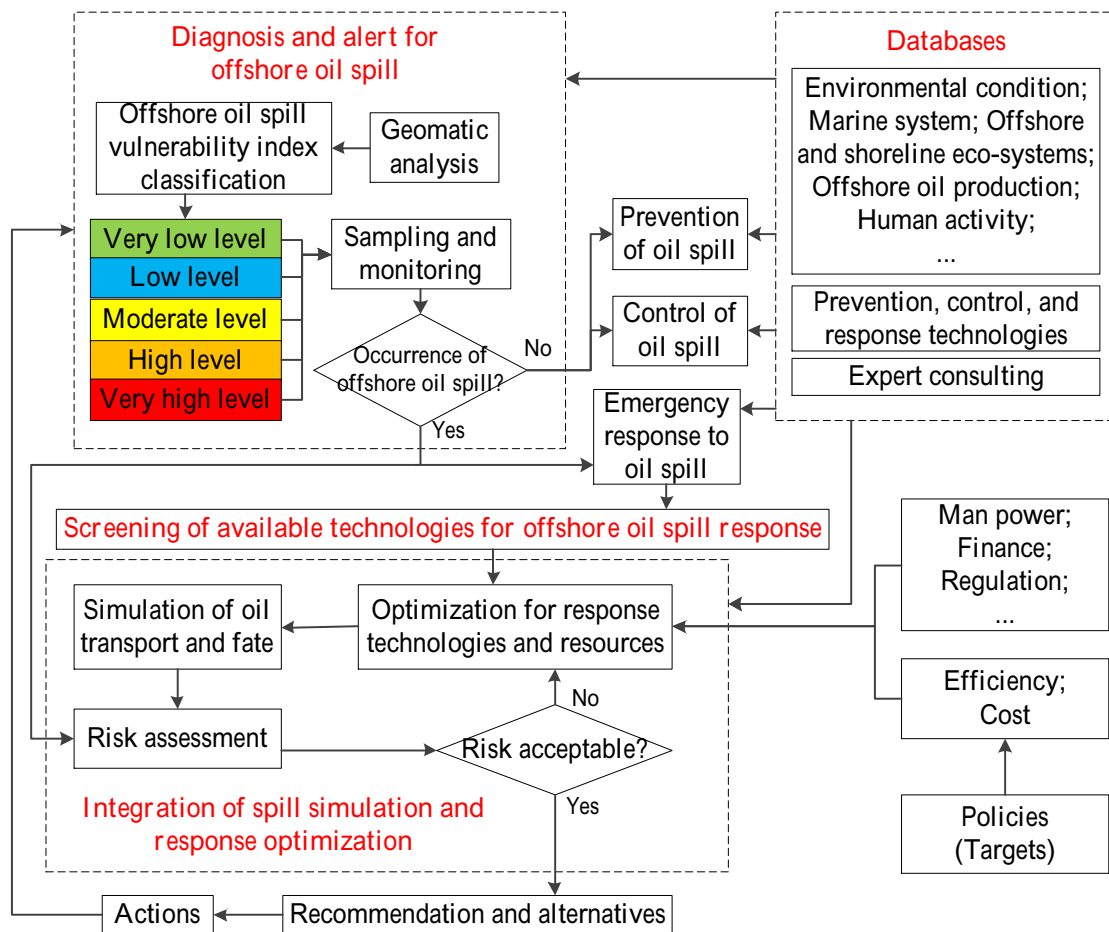
Figure 5.1 Framework of the DSS-OSRH

5.1.1 Databases for background information and available technologies

Different spill sites have different characteristics depending on pollutants' properties, environmental conditions, and a variety of physical, chemical, and biological processes. Thus, the methods selected for different sites vary significantly. The decision on a suitable method at a given site often requires expertise on both response technologies and site conditions. Management of emergencies, resulting from natural or man-made disasters, requires sufficient information as well as experienced responders both in technical and co-ordination matters. In this way, a great amount of information should be used to improve the management of the emergency, which generally means making the best decision at the right moment. In this regard, databases including all oil pollution records with accurate geo-referenced locations and all available response technologies should be developed. The databases include the attributes of each record such as spill volume, oil type, location, sector, source, cleanup percentage in each case, and environmental impacts. Thus, any new case can use the previous experience.

5.1.2 Diagnosis and alert

One major functionality of the diagnosis for rapid responding to an oil spill event is provision of real-time, medium-term and long-term alert information. The approach is based on capitalization of GIS data, remotely sensed data and other monitoring technologies like deployed sensors and observant systems. The management system will

receive information from the diagnosis as follows:

- Offshore OSVI mapping via the MC-TSAM classification.

- Alternatives of offshore oil spill monitoring according to the classified offshore OSVI levels (zones).

- The detection and then location and spread of oil spills over both large and small areas.

- The thickness distribution of an oil spill to estimate the quantity of spilled oil.

- Risk assessment to estimate impacts of the spill site and to take appropriate response action.

- Timely and valuable information to assist in response and clean-up operations.

- Stored and time-stamped, real-time evidentiary data on any spills and response efforts.

Medium- and long-term analysis including risk identification, assessment and monitoring which can be supported by the classification of offshore OSVI in an affected or potentially affected spill site. Subsequently the OSVI map functioning as long-term alert for oil spill risk and trajectory simulation results over this map yields medium-term risk alert. The real time detection and monitoring sensors provide short-term alert for oil spill. There will be several levels indicated by the alert system, such as the green, blue, yellow, orange, and red indicated in Figure 5.1. The green and blue levels indicate a

minor offshore oil leak and correspondingly pollution prevention strategies are then applied. The yellow and orange levels indicate a moderate offshore oil spill and correspondingly control strategies are then applied. The red level indicates serious oil spill and correspondingly response strategies are then applied, supporting by the technology screening and simulation based optimization.

The risk assessment process provides a formal method for assessing the economic risk benefit of offshore oil spill response. By undertaking a formal risk assessment it is possible to identify areas where intervention to reduce the likelihood or consequences of a particular event will be most effective (IMO, 2010). In simple terms the process involves (Queensland Transport, 2000):

- Hazard identification: what can go wrong and why,

- Frequency analysis: how often can things go wrong,

- Consequence analysis: how much harm can be caused by the event,

- Risk calculation: frequency or likelihood combined with consequence.

These risks can be quantified by US EPA methods (GEAE and ERDEM) based on monitoring data and the results of pollution and clean-up process simulation. The corresponding risks are quantified based on habitats, geomorphology characteristics, sensitivity to the oil-spills, natural persistence of oil and conditions of cleanness/removal. The overall risk index (ORI) is very important for the determination of the degree of impact and permanence of the spilled oil, as well as for the types of the employed clean-up procedures. The geomorphology is determinative for the type and density of

biological communities present in the area (Castro et al., 2006). Risk assessment techniques are fundamentally the same whether applied to individual offshore installations, ports and harbours, or even at the national or regional level. However, the execution and detail will vary considerably depending on the scale to which the technique is applied. At a national or regional level, the task is large and, if done to a sufficient level of detail, complex (IMO, 2010). It is thus much better to classify the large scale regions into certain zones with different vulnerability to the spill.

The MC-TSAM will carry out the unsupervised learning for these uncertain conditions and classify a site in to certain distinctive groups representing the characteristics and ORI of the whole site. The classification results from the MC-TSAM can provide different reasonable scenarios in risk zone (vulnerability zone) classification and spill risk mapping. According to different scenarios of categories, decision makers can flexibly place the monitoring spots in some available locations or apply different combination of response technologies in different zones during pollution control and emergency response management. The classification result provides the least or desired number of zones which can sufficiently represent the environmental vulnerability as well as the situation of spill/leak in the whole site, saving time and budget in risk assessment, pollution control and emergency response.

The diagnosis and alert module that support by the offshore OSVI classification module is dynamically linked with the technology screening and simulation based optimization modules to provide real-time interaction of in diagnosis, alert, and response

to offshore oil spill. As the other important component in the diagnosis and alert module, the risk assessment will be conducted by existing methods (e.g., GEAE and ERDEM) in the future study.

5.1.3 Response technology screening

Once an oil spill is determined by the diagnosis, the screening process is then applied to determine the available technologies according to the situation of oil spill and polluted marine system based on the developed database and the MC-IRFAM model. This system is developed by integrating Monte Carlo simulation, fuzzy set theory, and rule-based operation with a conventional Adaptive Resonance Theory (ART) Mapping model. Five ART modules are included to carry out the unsupervised learning for cluster centroid calculation, supervised learning for criteria combination, and fuzzified original input classification in each trial of the Monte Carlo simulation. This system can efficiently handle the screening under uncertainty and complexity. By setting the criteria corresponding to the situation of the pollution and the condition (e.g. spill amount and temperature) available technologies are screened from the database for optimization.

5.1.4 Integration of spill simulation and response optimization

In the initial stage of the emergency management system, the simulation of pollutant transport and fate is firstly processed based on the hydro-dynamic process, mechanical

spreading, evaporation, dissolution, and shoreline deposition. The simulation results show the situation of pollution in the affected area in spatio-temporal base, followed by risk and impact assessment.

Based on the results from simulation and risk assessment, screened technologies, resources and constraints (e.g., budgeting, manpower, policy and regulation), the optimization is applied to provide the best combination from these screened technologies with allocation of existing resources. The MC-DMINP is developed to process this optimization and provide decision support for the oil spill site clean-up strategies. The MC-DMINP consists of a Monte Carlo simulation model to handle the coexistence of uncertainties and an agent based model to handle dynamics in the system. This method can effectively tackle uncertainties that are presented in terms of probability density functions and discrete intervals and incorporate a variety of uncertain information into a general framework. Through the developed model, interactive relationships between different system objectives/constraints will be effectively reflected, potential conflicts and compromises between different system components will be highlighted, and complex features of the study system will be reflected.

The optimal solution for each oil spill clean-up strategy is obtained via the completion of each routine of simulation - risk assessment - optimization. If the risk from the assessment is acceptable, the simulation based optimization is stopped and provides the optimal solutions for all strategies of the offshore oil spill clean-up, otherwise, the

simulation based optimization will repeat until the risk meets the requirement. When the clean-up actions are applied, the diagnosis is kept running to evaluate the efficiency of the actions. If the efficiency underperforms, corresponding changes and rerunning may be needed for the system.

5.2 Integration of Classification, Simulation and Optimization for Offshore Oil Spill Response

The integration of the risk/vulnerability classification, technologies screening, oil weathering simulation, and response optimization approaches is an essential of the DSS-OSRH. The details regarding such integration are shown in Figure 5.2.

The MC-TSAM is firstly applied to assess risk/vulnerability of the target area based on meteorological, oceanic, environmental, and ecological conditions, oil relative activities in a target offshore area under various types of uncertainties. Once an oil spill happens, the classified zones from the MC-TSAM can provide the specific site conditions for the technology screening module (i.e., MC-IRFAM) and the constraints in the simulation-based optimization (i.e., MC-DMINP).

Parameters including temperature, wave height, wind speed, spill viscosity, slick thickness, etc. are used to represent site conditions, feasibilities of available technologies, and the proposed membership functions. The MC-IRFAM is applied to screen the available technologies corresponding to the site conditions and the series alternatives can

be consequently determined.

The operational parameters of the selected technologies such as manpower requirements, operational costs, and efficiencies are determined with probabilistic uncertainties and randomized with stochastic simulation. Meanwhile, according to the uncertain site conditions, the simulations of oil weathering and recovery are conducted in each trial of Monte Carlo simulation. The simulation results, the randomized operational parameters, and the resources/limitations (e.g., manpower, finance, and regulation) form the constraints of the simulation-based optimization model. Then according to the MC-DMINP, a simulation-based optimization approach is generated and solved for one trial (e.g., trial I_3) until the number of trials achieves the preset number (e.g., N_3). Finally a series of decision alternatives are generated according to the optimization results. A decision alternative may include the combination of technologies (e.g., types and number of devices) in each operational stage, allocation of man power and finance, corresponding cost and environmental effects, etc.
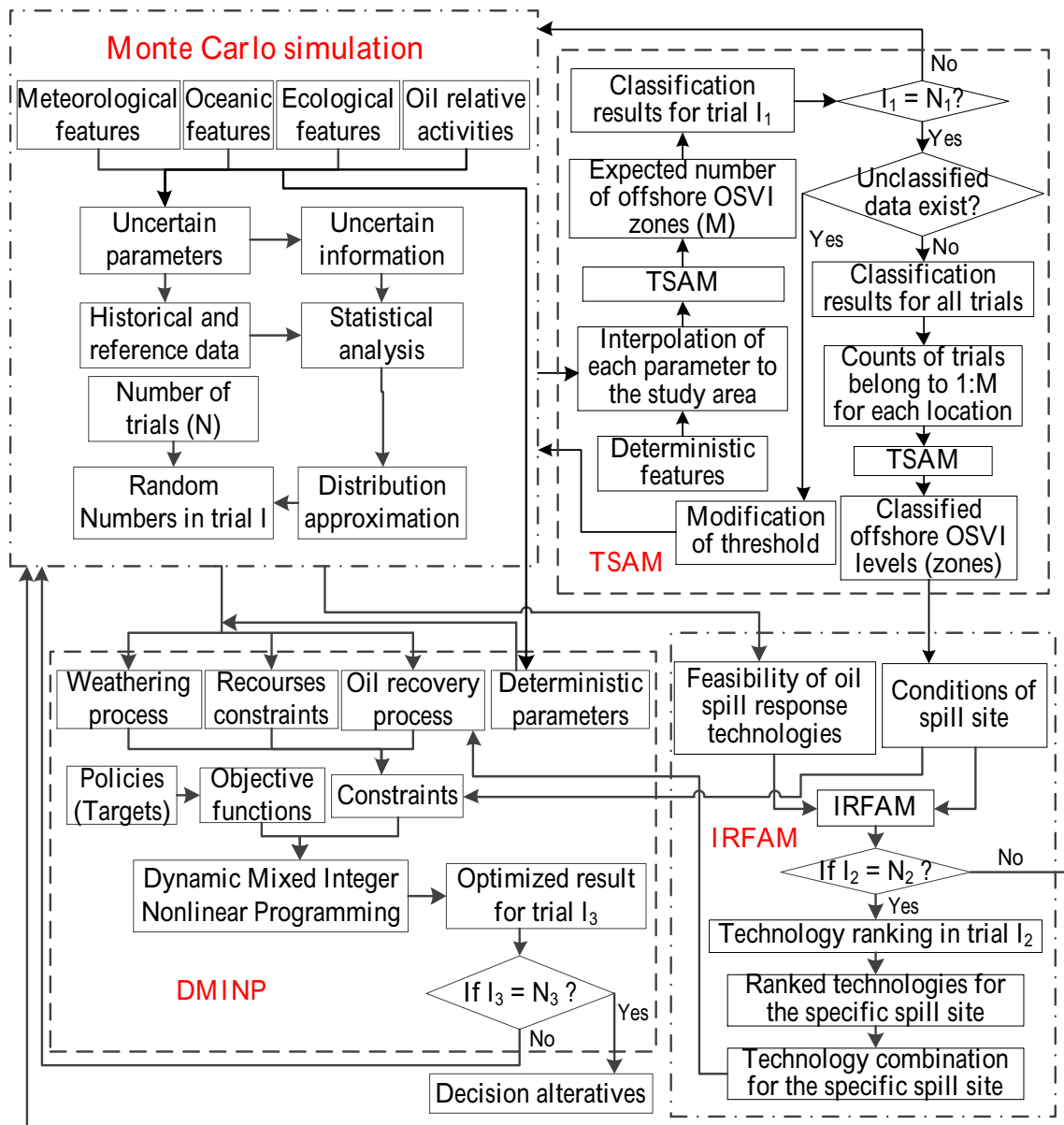
Monte Carlo simulation

| Meteorological features | Oceanic features | Ecological features | Oil relative activities |

Uncertain parameters → Uncertain information

Historical and reference data → Statistical analysis

Number of trials (N)

Random Numbers in trial I ← Distribution approximation

Classification results for trial I_1 → $I_1 = N_1$? — No

Expected number of offshore OSVI zones (M)

TSAM

Interpolation of each parameter to the study area

Deterministic features

Modification of threshold

Unclassified data exist? — Yes / No

Classification results for all trials

Counts of trials belong to 1:M for each location

TSAM

Classified offshore OSVI levels (zones)

TSAM

| Weathering process | Recourses constraints | Oil recovery process | Deterministic parameters |

Policies (Targets) → Objective functions → Constraints

Dynamic Mixed Integer Nonlinear Programming → Optimized result for trial I_3

DMINP

If $I_3 = N_3$? — Yes / No

Decision alteratives

| Feasibility of oil spill response technologies | Conditions of spill site |

IRFAM

IRFAM

If $I_2 = N_2$? — No / Yes

Technology ranking in trial I_2

Ranked technologies for the specific spill site

Technology combination for the specific spill site

Figure 5.2 Integration of the offshore OSVI classification, technologies screening, simulations of oil weathering and recovery, and optimization

211

5.3 A Case Study

5.3.1 Background

In order to test the feasibility and efficiency of the developed DSS-OSRH, a case study was conducted for decision support to an offshore oil spill response in the south coast of Newfoundland. The setting of the target area was the same as which was used in Section 3.2.3 (Figure 3.3), which was from 53^0 W to 60^0 W, 45.5^0 N to 47.5^0 N with pre-gridded 0.1^0 by 0.1^0 cells. The features for the classification were the same as which were used in Section 3.2.3. Therefore, the risk/vulnerability classification result would be the same as which in Section 3.2.3.

5.3.2 Offshore OSVI classification

According to the analysis of the classification result, the distribution of uncertain features in each zone which held similar offshore OSVI could be generated, including wave height, wind speed, wind direction, pressure, sea surface temperature, current speed, current direction, annual movement of tankers and other vessels, and the historically annual oil spill frequency (Figures A5.1 to A5.10 in Appendix B). The analyses and summaries of the site condition of classified zones would be applied as the inputs to the technology screening module (MC-IRFAM) and the simulation module as constraints in the simulation-optimization (MC-MSINP).

Considered an offshore spill of Statfjord oil occurs in the south coast of Newfoundland in the location of 55.7^0 W and 46.3^0 N with a total amount of 5,000 m^3, leading to an initial oil slick thickness of 50 mm. The properties of the spilled oil were listed in Table 4.2 in Section 4.3.3. After booms were applied, the spill area was confined to 100,000 m^2.

5.3.3 Simulation of oil slick movement

A model was developed to simulate the advection of the oil slick. According to the advection models listed in Section 2.3.4, the following model was selected to simulate the oil slick movement (Shen and Yapa, 1987; Wang et al., 2005):

$$\vec{V} = \vec{V}_c + \vec{V}^{'}$$

(5.1)

where $\vec{V}$ is the advection or drift velocity (m/s) during each time step; $\vec{V}_c$ is the mean drift velocity (m/s), representing the surface drift due to the combined effect of wind or ice cover and current; and $\vec{V}^{'}$ is the turbulent fluctuation of the drift velocity (m/s), simulating the horizontal diffusion of the oil slick. In order to simplify the model, an assumption was made that there was no affect from turbulent fluctuation and wind drift. Therefore, the drift velocity of the surface oil advection was expressed as follows (Al-Rabeh et al., 1989, 1992; Chao et al., 2001, 2003):

$$\vec{V} = \vec{V}_c \tag{5.2}$$

The initial location of the spill was 55.7^0 W and 46.3^0 N, which was $x_0 = -55.7$ and $y_0 = 46.3$, respectively. The time step set for the simulation was set to 1 min. Therefore, the location of oil slick can be described as follows:

$$x_t = x_{t-1} - \frac{\cos(cd_{t-1}) \times cs_{t-1} \times 60}{LX} \tag{5.3}$$

$$y_t = y_{t-1} + \frac{\sin(cd_{t-1}) \times cs_{t-1} \times 60}{LY} \tag{5.4}$$

where x_t indicates the location of oil slick in latitudinal direction at time t (degree); y_i indicates the location of oil slick in longitudinal direction at time t (degree); x_{t-1} is the location of oil slick in latitudinal direction at the previous time step (degree); y_{i-1} is the location of oil slick in longitudinal direction at the previous time step (degree); cd_{t-1} is the current direction at time step t-1 (degree); cs_{t-1} is the current direction at time step t-1 (m/s); LX is the length of 1° longitude in the study area which is about 7,724 m; and LY is the length of 1° latitude in the study area which is about 11,120 m (OGP, 2013). Based on the prevailing current speed (Figure A3.6 in Appendix A) and direction (Figure 3.5a in Section 3.2.3), the movement of oil slick was simulated. The simulation result

indicated that the oil slick would reach the shoreline of Newfoundland at the Seal Cove

after 60 hours if no response application was applied. Figure 5.3 illustrates the

movement of oil slick in 1-min time steps and Table 5.1 indicates the location of oil slick
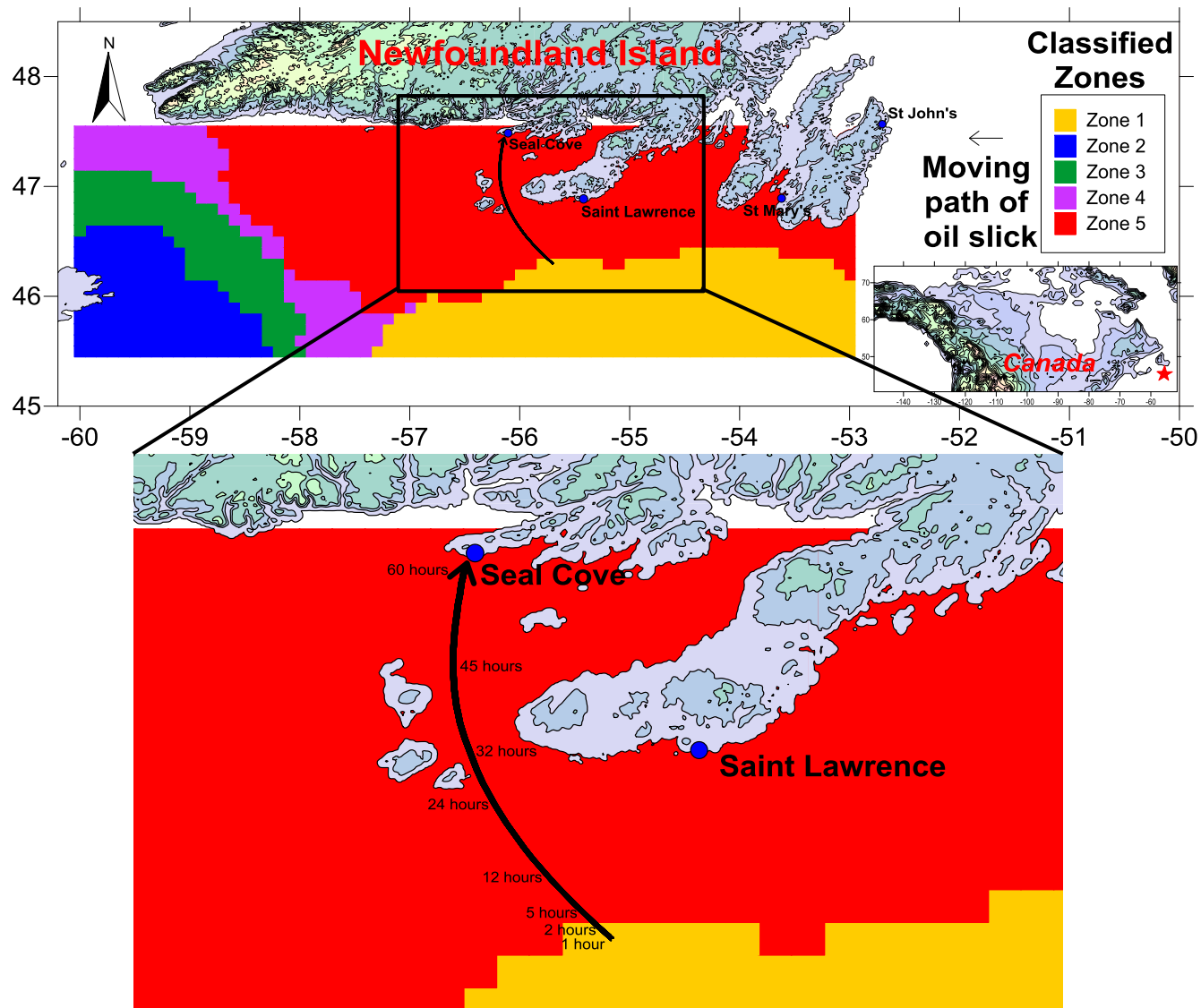
in 1-hour time steps.

Figure 5.3 The movement of spilled oil in 60 hours

Table 5.1 Locations of oil slick in 60 hours

Time (hour)	Oil slick location	
	Longitude (degree)	Latitude (degree)
0	-55.700	46.300
1	-55.718	46.316
2	-55.735	46.331
3	-55.753	46.347
4	-55.770	46.363
5	-55.787	46.379
6	-55.804	46.395
7	-55.820	46.412
8	-55.837	46.428
9	-55.853	46.445
10	-55.869	46.462
11	-55.885	46.478
12	-55.900	46.496
13	-55.915	46.513
14	-55.930	46.530
15	-55.945	46.547
16	-55.959	46.565
17	-55.973	46.583
18	-55.987	46.600
19	-56.000	46.618
20	-56.013	46.637
21	-56.026	46.655
22	-56.039	46.673
23	-56.050	46.691
24	-56.062	46.710
25	-56.074	46.729
26	-56.085	46.747
27	-56.095	46.766
28	-56.106	46.785
29	-56.115	46.805
30	-56.123	46.824
31	-56.132	46.844
32	-56.141	46.863
33	-56.149	46.883

34	-56.156	46.902
35	-56.164	46.922
36	-56.169	46.942
37	-56.175	46.962
38	-56.179	46.983
39	-56.183	47.003
40	-56.187	47.023
41	-56.190	47.044
42	-56.192	47.064
43	-56.195	47.084
44	-56.196	47.105
45	-56.198	47.125
46	-56.199	47.146
47	-56.199	47.166
48	-56.199	47.187
49	-56.198	47.207
50	-56.197	47.228
51	-56.195	47.248
52	-56.194	47.269
53	-56.191	47.289
54	-56.189	47.309
55	-56.186	47.330
56	-56.182	47.350
57	-56.178	47.370
58	-56.174	47.391
59	-56.169	47.411
60	-56.164	47.431

5.3.4 Technology screening

Figure 5.3 indicates that the offshore oil spill initially occurred in the area classified as offshore OSVI Zone 1. Along with the movement of oil slick, the spill oil would move to the area covered by Zone 5 after about 2 hours and toward to the shoreline of Newfoundland after about 60 hours. Therefore, the oil recovery might most probably be applied in these two zones. Assume that the technological feasibilities of oil skimming mainly relied on temperature, wave, wind, oil viscosity, and slick thickness. The fuzzy criteria for these features are shown in Figure 3.9 in Section 3.3.3. Assume there were 7 types of skimmers available in the database that could applied for the oil recovery in the target area including the three types of skimmer that used in Section 4.3.1. According to the analyses (e.g., mean and 95% confidence interval) of distributions of the corresponding features in Zone 1 and Zone 5 (Figures A5.1, A 5.2, and A5.5 in Appendix B) and the oil properties of the spilled oil, the site conditions for these two zones could be summarized. The site conditions and the parameters for the feasibilities of technologies are shown in Table 5.2. Based on the fuzzy criteria of the corresponding features, the fuzzy numbers of site conditions and technology feasibilities could be generated as the inputs to the MC-IRFAM classification approach. The overall score of feasibility ranged from 0 to 1, where 0 indicated completely unfeasible, 1 indicated perfectly feasible, and 0.5 reasonably feasible. The total trials for the Monte Carlo simulation was set as $N_2 = 10,000$.

Table 5.2 Parameters for site conditions and feasibilities of skimmers

	Temperature °C	Wave height m	Wind speed m/s	Spill viscosity cP	Slick thickness mm
Zone 1	0 - 15	0.5 - 5	3 - 13	> 3.03	< 50
Zone 5	-5 - 20	0.2 - 4	0.5 - 15	> 3.03	< 50
Skimmer 1	> -10	0 - 3	0 - 20	> 10	5 - 50
Skimmer 2	-10 - 20	0 - 2.5	0 - 15	> 5	1 - 50
Skimmer 3	-5 - 15	0 - 2	0 - 12	> 2	0 - 50
Skimmer 4	5 - 20	0 - 0.5	> 20	10 - 200	0.01 - 1
Skimmer 5	20 - 30	0.5 - 2	0 - 5	50 - 1000	1 - 5
Skimmer 6	>30	0 - 0.2	> 10	> 1000	>4
Skimmer 7	10 - 15	0 - 0.3	0 - 10	> 50	0.1 - 0.5

The screening results are shown in Tables 5.3 and 5.4, including the means, medians, minimum and maximum values, and 95% conference intervals (CI) of the overall scores for the 7 potential types of skimmers to the areas covered by Zone 1 and Zone 5 of the study area. The detailed distributions of the overall scores are shown in Figures A5.11 to A5.24 in Appendix C.

Skimmers 1, 2 and 3 held similar distributions of overall scores in terms of the feasibility to the area covered by Zone 1. Furthermore, the statistics (mean, median, and 95% CI) of them were also very close. Most of the scores were higher than 0.5, indicating high feasibility. Comparatively, the scores of Skimmer 3 more tended to higher values, while the scores of Skimmer 1 more tended to lower, and the tendencies of scores for Skimmer 2 was not as significant as the other two. The feasibility of Skimmer 5 was lower than Skimmers 1 to 3, but still higher than 0.5. The feasibility of Skimmers 4 and 7 held similar distributions of the overall scores; however, the scores of Skimmer 7 tended to be higher than those of Skimmer 4, indicating that Skimmer 7 was more feasibility. In general, Skimmer 6 was not feasible in this case, although it had some scores higher than 0.5 during the Monte Carlo simulation. Therefore, the ranks for the feasibilities of Skimmers to Zone 1 was Skimmer 3 > Skimmer 2 > Skimmer 1 > Skimmer 5 > Skimmer 7 > Skimmer 4 > Skimmer 6.

The ranking of the feasibilities for the skimmers in Zone 5 was similar to which in Zone 1. One of the differences was that the Skimmer 2 appeared the highest feasibility,

and then the Skimmer 1, then Skimmer 3. The other difference was that the feasibility of

Skimmer 5 to 7 had increased. The ranks for the feasibilities of Skimmers to Zone 5 was

Skimmer 2 > Skimmer 1 > Skimmer 3 > Skimmer 5 > Skimmer 7 > Skimmer 4 >

Skimmer 6.

Table 5.3 Statistics of the overall scores for skimmers to the spill site in Zone 1

	Mean	Median	Minimum value	Maximum value	Lower bound of 95% CI	Upper bound of 95% CI
Skimmer 1	0.674	0.660	0.414	0.881	0.533	0.867
Skimmer 2	0.699	0.667	0.413	0.933	0.546	0.867
Skimmer 3	0.669	0.653	0.356	1.000	0.535	0.853
Skimmer 4	0.544	0.544	0.399	0.666	0.467	0.624
Skimmer 5	0.616	0.624	0.528	0.667	0.540	0.667
Skimmer 6	0.515	0.533	0.400	0.600	0.470	0.600
Skimmer 7	0.588	0.593	0.428	0.824	0.486	0.680

Table 5.4 Statistics of the overall scores for skimmers to the spill site in Zone 5

	Mean	Median	Minimum value	Maximum value	Lower bound of 95% CI	Upper bound of 95% CI
Skimmer 1	0.716	0.730	0.467	0.921	0.548	0.867
Skimmer 2	0.698	0.667	0.467	0.933	0.569	0.867
Skimmer 3	0.659	0.653	0.364	0.933	0.543	0.800
Skimmer 4	0.542	0.543	0.414	0.661	0.475	0.607
Skimmer 5	0.750	0.800	0.528	0.800	0.609	0.800
Skimmer 6	0.549	0.567	0.433	0.667	0.500	0.637
Skimmer 7	0.592	0.602	0.458	0.809	0.504	0.649

5.3.5 Device allocation and oil recovery

According to the ranking results from the technology screening, the top three feasible types of skimmers were selected for the oil recovery in this case. The oil recovery efficiencies of these three types of skimmers and parameters for corresponding simulation were shown in Figure 4.4 and Table 4.1 in Section 4.3.1. There were 8 sets of each type of skimmer in the warehouse and the capacity of vessels used for operation was 20 sets of skimmers. However, because different types of skimmers were located in different locations, different time periods were required for devices allocation and deployment. Assume that the Skimmer 1 (or SK_1) was located in the responder's warehouse in Saint Lawrence, Newfoundland, which required 3 hours for devices allocation and deployment; Skimmer 2 (or SK_2) was located in St Mary's, Newfoundland, which required 6 hours for devices allocation and deployment; the Skimmer 3 (or SK_3) was located in St John's, Newfoundland, which required 12 hours for devices allocation and deployment. According to the advection simulation in Section 5.3.3, without any application of offshore oil spill response, the oil slick would reach the shoreline of Newfoundland (near Seal Cove) after 60 hours (Figure 5.3). Therefore, the objective of the offshore oil spill response was to maximize the spilled oil collection in this 60-hour period. Due to the challenge of transportation, no more skimmers and vessels would be further applied in the coming 60 hours.

The model settings for the MC-DMINP were similar to the one used in Session 4.5.

The uncertain parameters including wind speed and temperature in Zones 1 and 5 were different and characterized by the MC-TSAM. Due to the distribution of wind speed and temperature of these two zones (Figures A5.2 and A5.5 in Appendix B), the distributions for these parameters could be generated for the Monte Carlo simulation. The parameters for the corresponding distributions are list in Table 5.5. Furthermore, uncertainty was also assigned to the slick area as normally distributed with a mean value of 100,000 m^2 and a standard deviation of 8,000 m^2. The total trials for the Monte Carlo simulation was set as N_3 = 200. In each trial, the simulation-based optimization model for device combination and allocation is as follows:

$$\text{Max } V = \sum_{m=1}^{60} V_m \qquad (5.5a)$$

s.t.

$$V_1 = \sum_{j=1}^{3} SK_j \times ORR_{njm} \qquad \forall m = 1$$

$$= bsk_{1m} \times SK_1 \times \left(0.01437 \left(1,000 \frac{V_0}{A} \right)^2 + 0.01602 \left(1,000 \frac{V_0}{A} \right) \right)$$

$$+ bsk_{2m} \times SK_2 \times \left(-0.00791 \left(1,000 \frac{V_0}{A} \right)^2 + 0.84975 \left(1,000 \frac{V_0}{A} \right) \right) \qquad (5.5b)$$

$$+ bsk_{3m} \times SK_3 \times \left(-0.01591 \left(1,000 \frac{V_0}{A} \right)^2 + 1.54975 \left(1,000 \frac{V_0}{A} \right) \right)$$

$$FE_1 = \frac{2.67 + 0.06 \times (T - 273.15) \times Ln(60)}{100} \qquad \forall m = 1$$

$$(5.5c)$$

$$DE_1 = \frac{0.11(U + 1)^2}{1 + 50\mu_0^{o^{0.5}}\left(\dfrac{V_0}{A}\right)s_t} \qquad \forall m = 1 \tag{5.5d}$$

$$VF_1 = V_0 \times FE_1 \quad \forall m = 1 \tag{5.5e}$$

$$VD_1 = V_0 \times DE_1 \times 3{,}600 \quad \forall m = 1 \tag{5.5f}$$

$$V_m = \sum_{j=1}^{3} SK_j \times ORR_{njm} \qquad \forall m = 2, \cdots, 60$$

$$= bsk_{1m} \times SK_1 \times \left(0.01437 \left(\frac{1{,}000\left(V_0 - \sum_{h=1}^{m-1} V_h\right)}{A} \right)^2 + 0.01602 \left(\frac{1{,}000\left(V_0 - \sum_{h=1}^{m-1} V_h\right)}{A} \right) \right)$$

$$+ bsk_{2m} \times SK_2 \times \left(-0.00791 \left(\frac{1{,}000\left(V_0 - \sum_{h=1}^{m-1} V_h\right)}{A} \right)^2 + 0.84975 \left(\frac{1{,}000\left(V_0 - \sum_{h=1}^{m-1} V_h\right)}{A} \right) \right)$$

$$+ bsk_{3m} \times SK_3 \times \left(-0.01591 \left(\frac{1{,}000\left(V_0 - \sum_{h=1}^{m-1} V_h\right)}{A} \right)^2 + 1.54975 \left(\frac{1{,}000\left(V_0 - \sum_{h=1}^{m-1} V_h\right)}{A} \right) \right)$$

$$\tag{5.5g}$$

$$FE_m = \frac{2.67 + 0.06 \times (T - 273.15) \times Ln(60)}{100} \quad \forall m = 2, \cdots, 60 \tag{5.5h}$$

$$DE_m = \frac{0.11(U + 1)^2}{1 + 50\mu_m^{o^{0.5}}\left(\dfrac{V_0 - \sum\limits_{h=1}^{m-1}(V_h + VF_h + VD_h)}{A}\right)s_t} \quad \forall m = 2, \cdots, 60 \tag{5.5i}$$

$$FW_m = K_b\left(1 - \exp\left(\frac{-K_a}{K_b}\right)(U + 1)^2 \times 3{,}600\right) \quad \forall m = 2, \cdots, 60 \tag{5.5j}$$

$$\rho_m^o = FW_{m-1}\rho_w + \left(1 - FW_{m-1}\right)\left(\rho_{m-1}^o + K_b FE_{m-1}\right) \quad \forall m = 2, \cdots, 60 \tag{5.5k}$$

$$\mu_m^o = \mu_{m-1}^o \exp\left(K_c FE_{m-1}\right)\exp\left(\frac{2.5 FW_{m-1}}{1 - K_b FW_{m-1}}\right) \quad \forall m = 2, \cdots, 60 \tag{5.5l}$$

$$VF_m = V_0 \times FE_m \quad \forall m = 2, \cdots, 60 \tag{5.5m}$$

$$VD_m = V_0 \times DE_m \times 3{,}600 \quad \forall m = 2, \cdots, 60 \tag{5.5n}$$

$$\sum_{j=1}^{2} SK_j \leq 20 \tag{5.5o}$$

$$0 \leq SK_j \leq 8 \quad \forall j = 1, 2, 3 \tag{5.5p}$$

$$bsk_{jm} = 0 \quad \forall j = 1, 2, 3; \forall tt_j > m \tag{5.5q}$$

$$bsk_{jm} = 1 \quad \forall j = 1, 2, 3; \forall tt_j \leq m \tag{5.5r}$$

$$SK_j \in integer \quad \forall j = 1, 2, 3 \tag{5.5s}$$

where V is total collected oil in the 60-hour operational period (m^3); V_m and V_h is collected oil in each 1-hour time period (m^3); m indicates time steps; SK_j is number of skimmer (set); j indicates type of skimmer; ORR_n is net oil recovery rate defined in Sections 4.2.3 and 4.3.1 (m^3/hour); bsk_{jm} is binary indicator for SK_j in stage m to determine if the SK_j is applied in the oil recovery in this stage; V_0 is initial volume of spilled oil (m^3); h indicates time steps before m; A is area of the spilled oil (m^2); FE is evaporation rate (m^3/hour·m^3 of oil); T is temperature (K); DE is dispersion rate (m^3/(s·m^3 of oil)); μ_o is dynamic viscosity of the oil (cP); and S_t is interface tension between

228

oil and water (dyne/m); U is wind speed (m/s); VF is evaporated oil in each stage (m^3/hour); VD is dispersed oil in each stage (m^3/hour); FW is fractional water content; K_a is cure fitting constant that varies with wind speed (2×10^{-6}); K_b is mousse viscosity constant (0.7 for crude oils and heavy fuel oil) (Zadeh and Hejazi, 2012); ρ_w is density of water (kg/m^3); ρ^o is oil density (kg/m^3); μ^o is oil viscosity (cP); and K_c is oil-dependent constant between 1 and 10 (1 is for gasoline or light diesel, and 10 for crude oils); and tt_j is the time of devices allocation and deployment for SK_j.

The modeling results indicated that the numbers of SK_1 and SK_2 were most probably 8 sets; and the number of SK_3 significantly relied on the numbers of SK_1 and SK_2 (Figure 5.4). Because the maximum number of each type of skimmer was 8 sets, the optimal combination for skimmers would be 8 sets of SK_1, 8 sets of SK_2, and 4 sets of SK_3. Based on the advection simulation and the simulation-based optimization, it was estimated that all of the spilled oil was gone after about 45 hours before the oil slick reached the shoreline of the Newfoundland (60 hours) (Figure 5.5). The mean value of the collected oil was 4,096 m^3 (82%), evaporated oil was 724 m^3 (14.4%), and dispersed oil was 180 m^3 (3.6%), respectively. The details about the dynamic changes of ORR_n, the collected, evaporated, dispersed, and remaining oil, and the changes of oil viscosity and density as well as slick thickness are shown in Figures 5.6 to 5.12.

Table 5.5 Parameters of fitted distributions for wind speed and temperature

	Wind speed (GEV)			Temperature (GEV)		
	k	sigma	mu	k	sigma	mu
Group 1	-0.112157	2.70999	6.09027	-0.14613	3.99207	4.96715
Group 5	-0.0872002	3.10937	5.6712	-0.107261	5.3761	3.84801
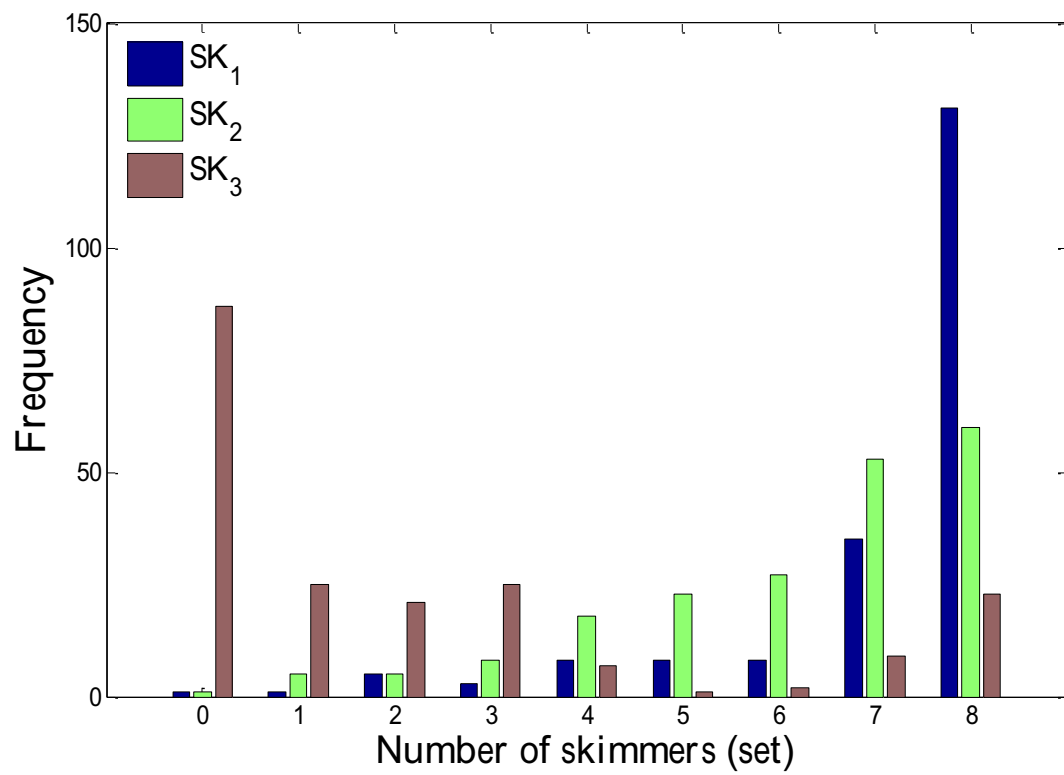
Figure 5.4 Distribution of potential skimmer numbers
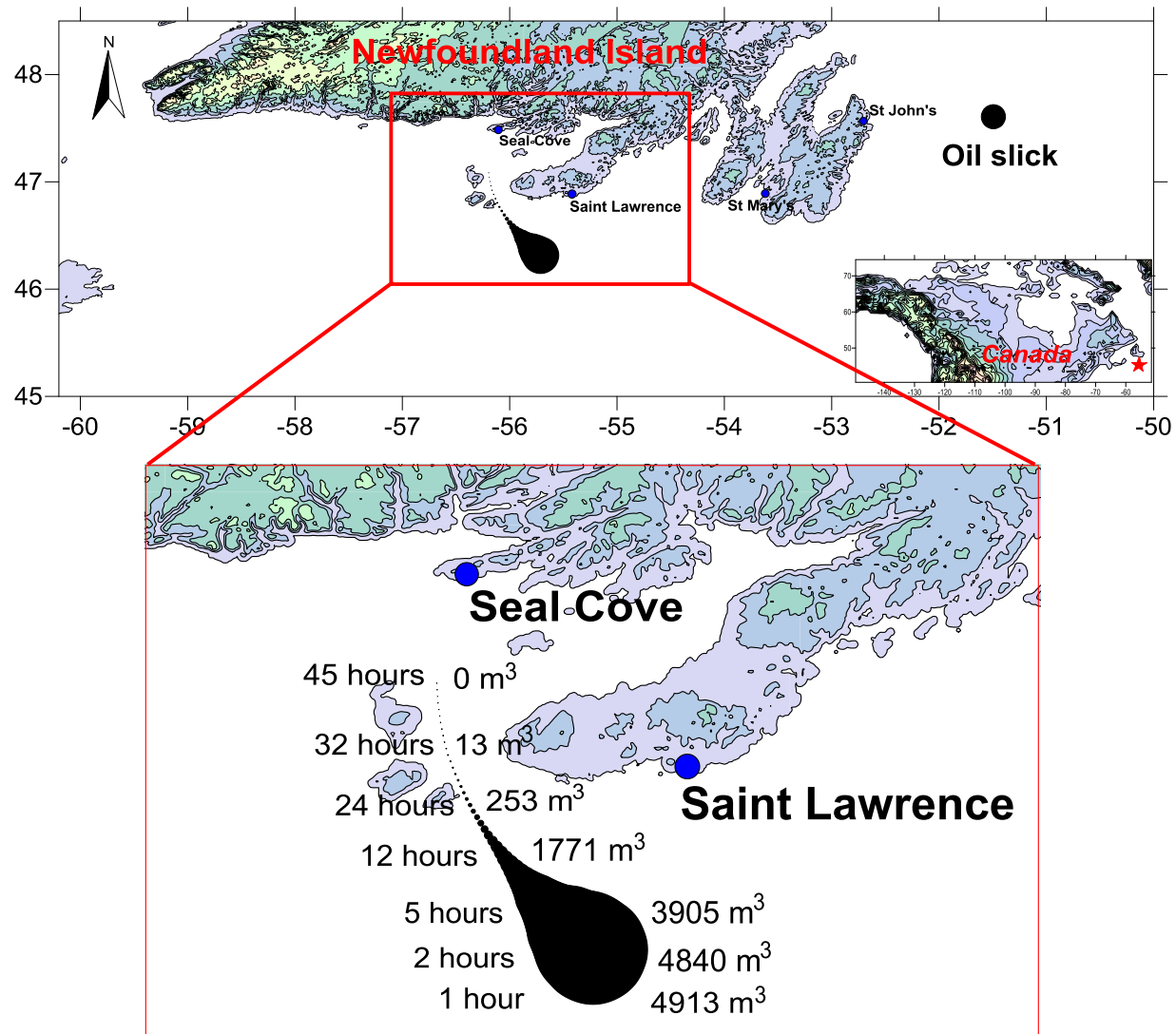
Figure 5.5 The movement and volume change of the spilled oil with the optimal skimmer combination
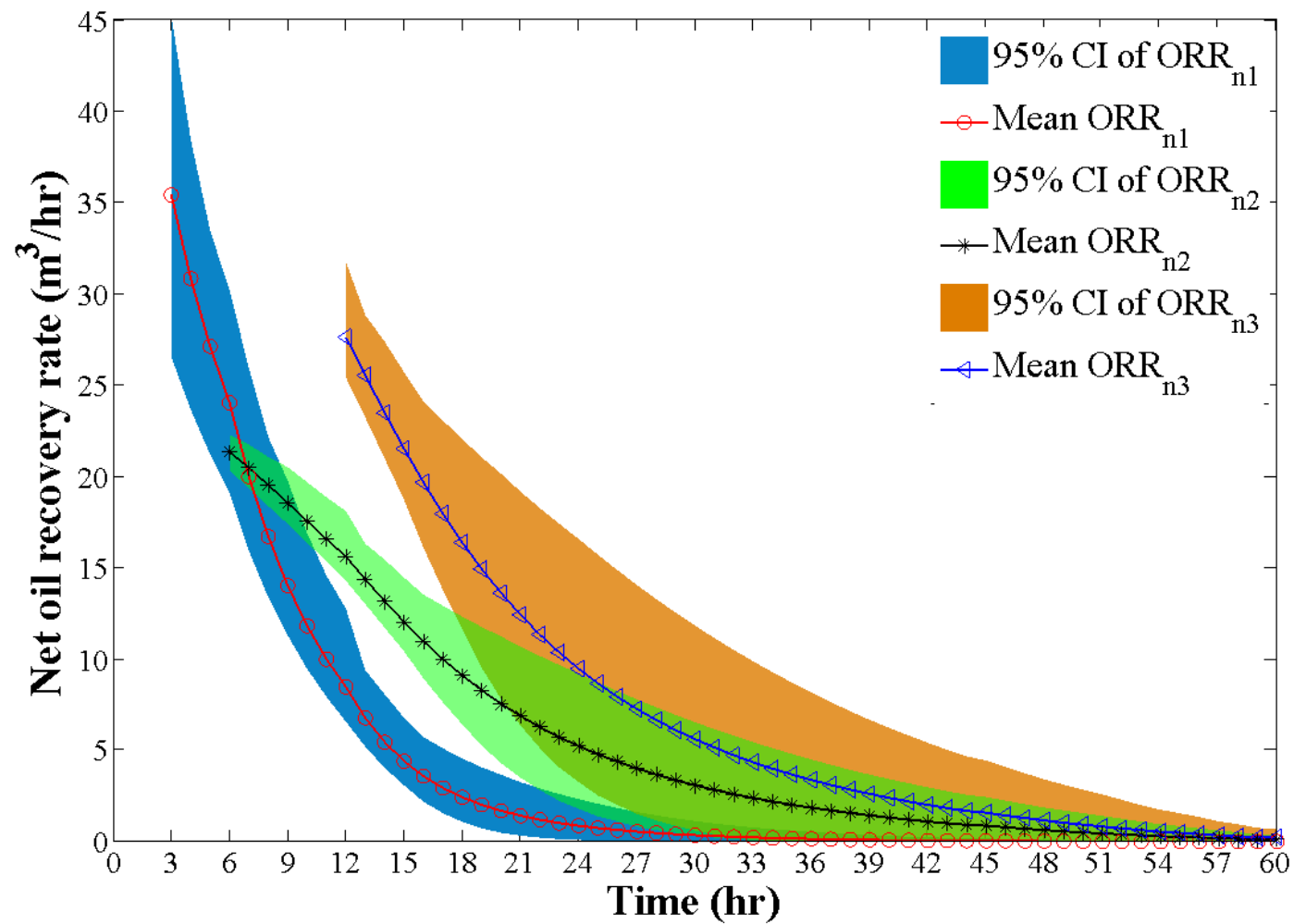
Figure 5.6 Mean values and 95% confidence intervals of net oil recovery rates of skimmers
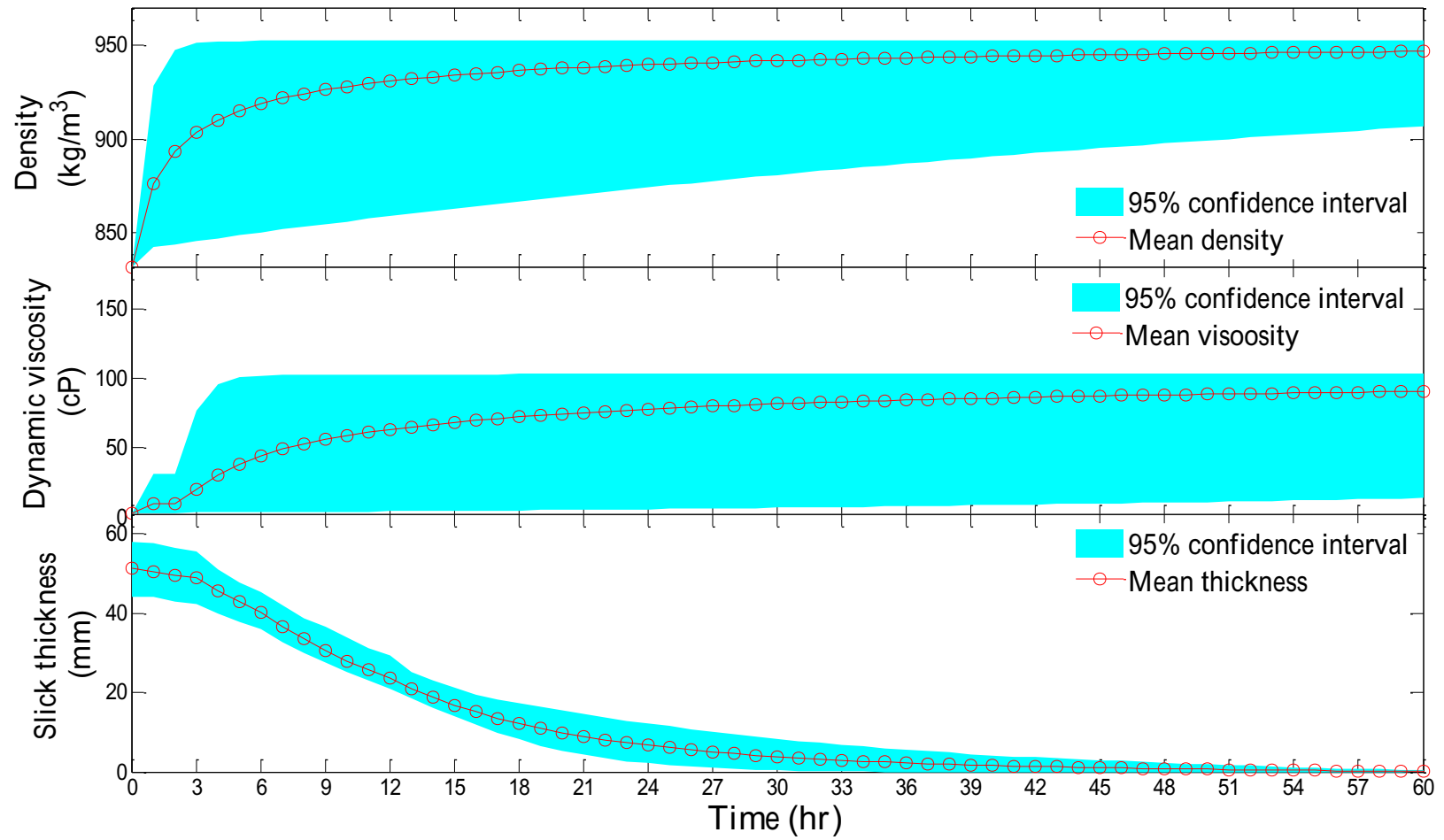
Figure 5.7 Mean values and 95% confidence intervals of oil density, viscosity, and slick thickness
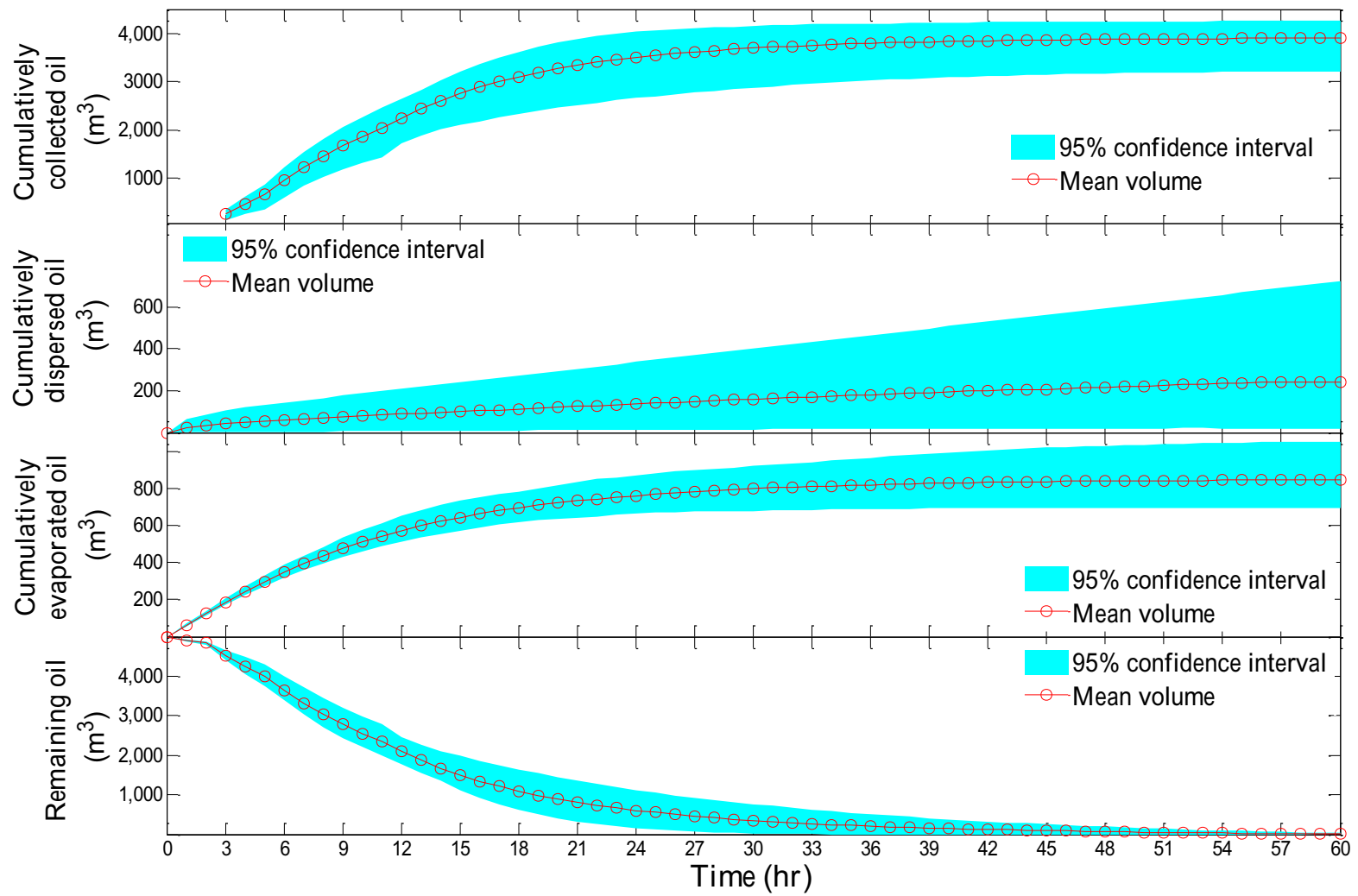
Figure 5.8 Mean values and 95% confidence intervals of cumulatively collected oil, evaporated oil, and dispersed oil as well as remaining oil

235
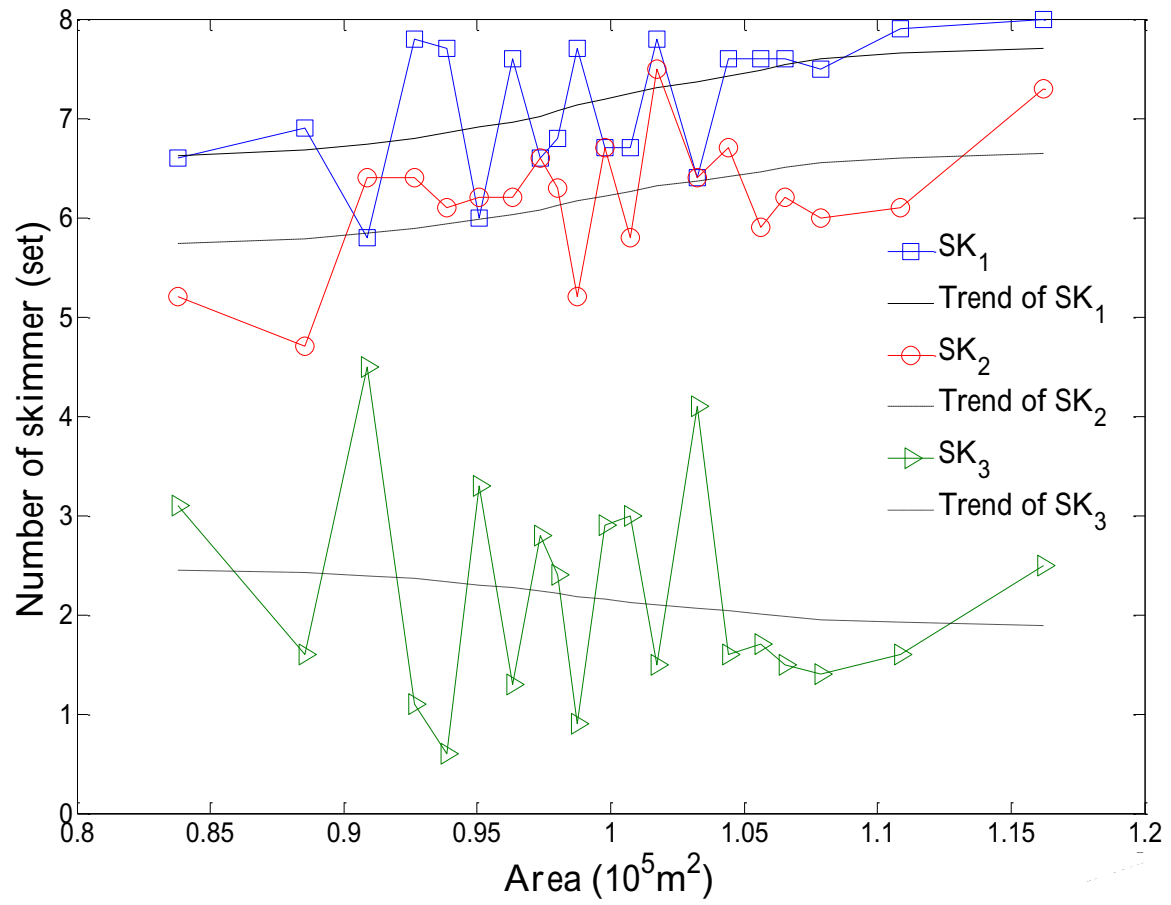
Figure 5.9 The change of skimmer numbers with the variations of slick coverage
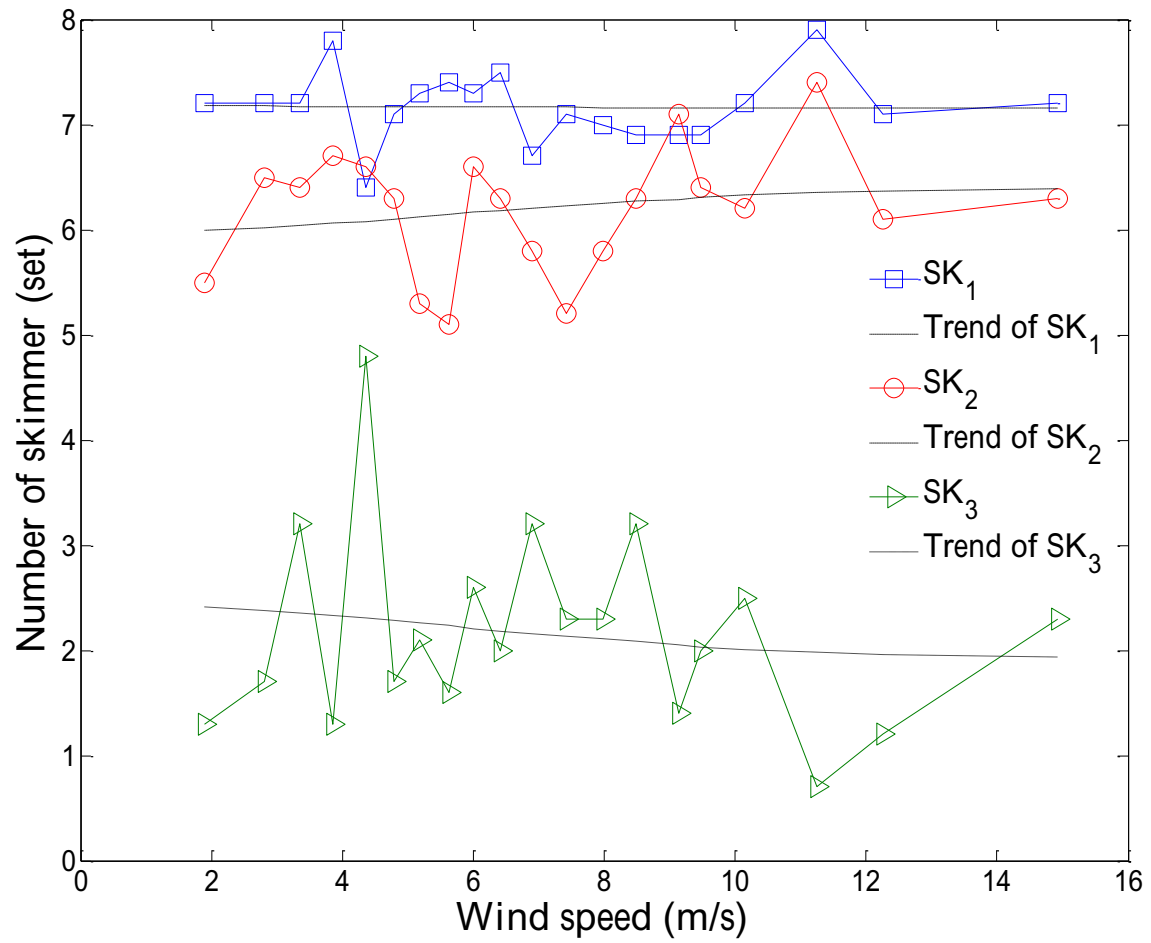
Figure 5.10 The change of skimmer numbers with the variations of wind speed
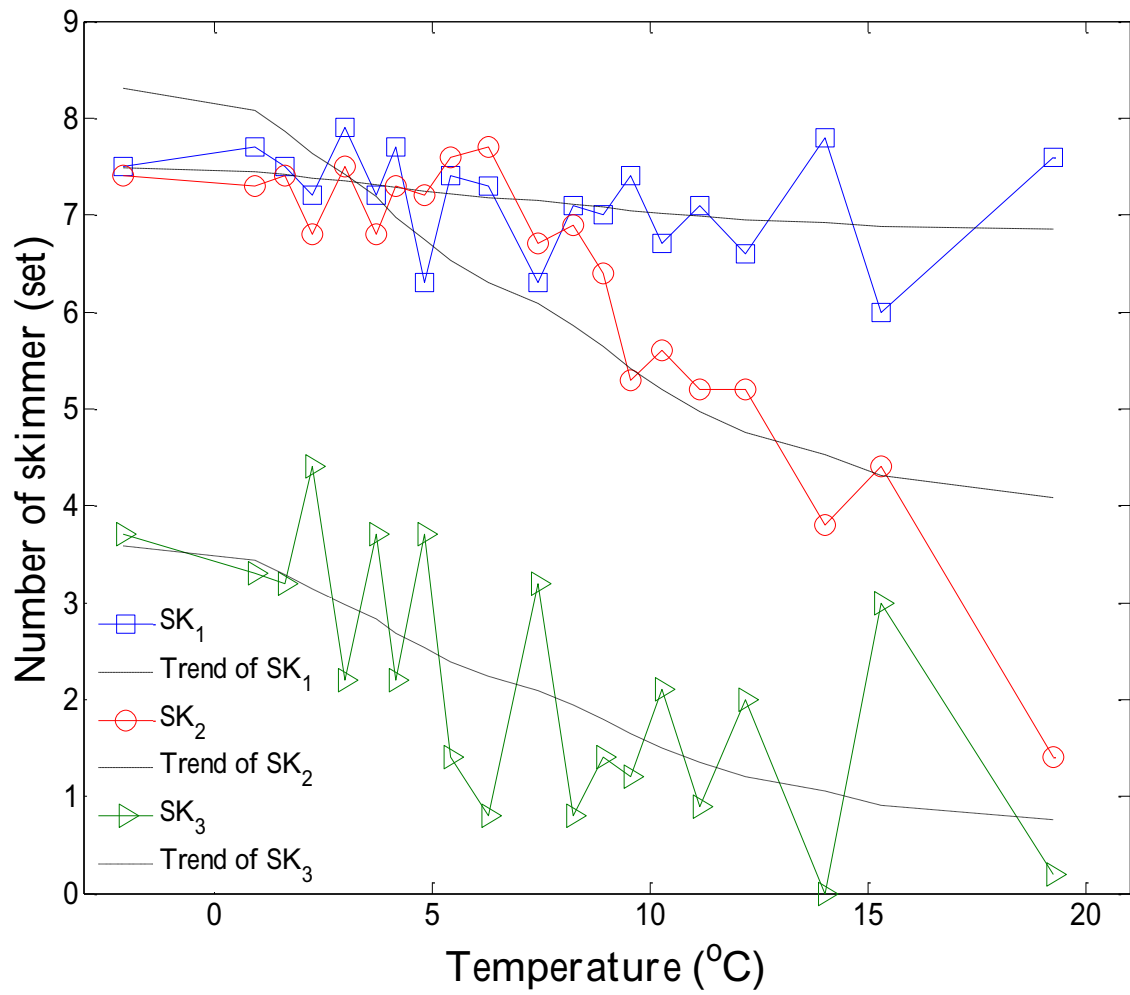
Figure 5.11 The change of skimmer numbers with the variations of temperature
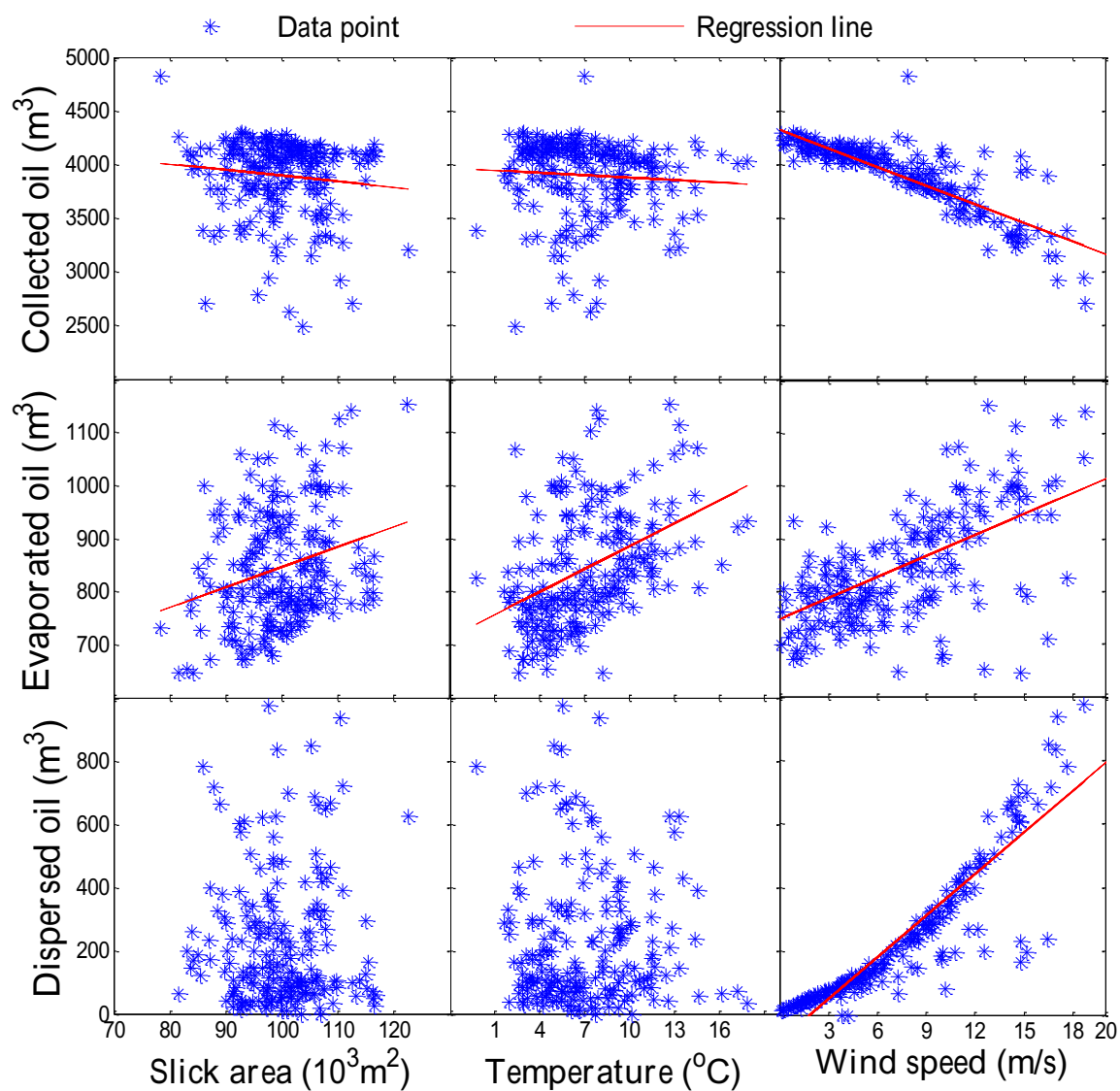
Figure 5.12 The change of finally collected, evaporated, and dispersed oil with the change of slick coverage, temperature, and wind speed, respectively

The uncertainties in features were significantly higher than those in the case in Section 4.3. This was because the site condition in this case was from the risk/vulnerability zone characterization by the MC-TSAM. Such characterization was based on the real-world data with high uncertainty and complexity.

The number of SK_1 and SK_2 might increase when the initial slick coverage increase which caused an increase of initial slick thickness, and vice versa. In contrast, the numbers of SK_3 might slightly decrease when the initial slick coverage decreased and vice versa (Figure 5.9). In addition, the increase of wind speed increased the number of SK_2 and decreased the number SK_3; and the change of SK_1 was insignificant (Figure 5.10). This was because the strong wind could strengthen the dispersion especially in the late stages (Figure 5.8), leading to low efficiencies to the Skimmers. Therefore, the skimmers which required relatively short time for allocation and deployment (e.g., SK_1 and SK_2) would be preferred. The uncertainty in temperature had significantly negative effects on SK_3 and SK_2, and insignificantly negative effects on SK_1. This was probably because the increase of temperature would significantly promote evaporation and thus affected the oil collection. Because the oil recovery rates of SK_2 and SK_3 were more sensitive to the uncertainty (Figure 5.6) than those of SK_1, the effects on the two skimmers were more significant.

In addition, the changes of net oil recovery rates for all types of skimmers were relatively significant in the early stages and became insignificant with time, and the

intensest change occurred in the first 24 hours (Figure 5.6). In general, the uncertainty of oil recovery rates for all the skimmers increased with rising uncertainty in slick coverage, wind speed, and temperature. The wind and temperature in Zones 1 and 5 followed the Generalized Extreme Value (GEV) distributions, leading to significant effects on the weathering processes and consequently the oil recovery rates. As shown in Figure 5.12, the increasing values of all the uncertain parameters (slick area, temperature, and wind speed) would lead to significant increase of evaporation. The uncertainty in wind speed caused the most negative effect on oil recovery, and positive effects on evaporation and dispersion. While the direct effect from temperature on oil recovery were not significant, but the negative effect on dispersion and positive effect on evaporation were significant, eventually influencing the oil recovery. The uncertainty in slick coverage had positive effects on evaporation and dispersion but negative effect on oil recovery.

The optimal combination ($SK_1 = 8$, $SK_2 = 8$, and $SK_3 = 4$) was also compared with the other two combinations, which were Combination 1 ($SK_1 = 4$, $SK_2 = 8$, and $SK_3 = 8$) and Combination 2 ($SK_1 = 8$, $SK_2 = 4$, and $SK_3 = 8$). The comparisons in collected and remaining oil based on these three combinations are shown in Figures 5.13 and 5.14. The comparison indicated that the final collected oil based on the optimal combination (4,096 m^3) was slightly higher than which based on the other two combinations (4,086 and 4,087 m^3). However, the collected oil from the optimal combination was significantly higher than the other two in the first 15 hours (Figure 5.13). Although all the three combination

could lead to the elimination of the spilled oil from the sea surface in about 40 to 45 hours, the decrease of remaining oil was more significant in the first 15 hours due to the optimal combination compared with those were due to the other two combinations (Figures 5.14). Furthermore, based on the advection simulation, the oil slick became close to some islands (e.g., Saint-Pierre, France) and peninsulas (e.g., the Burin Peninsula, Newfoundland, Canada) around 15 hours after spill, which critically required effective oil recovery before the approaching. Therefore, the optimal combination would be most preferred for this case.
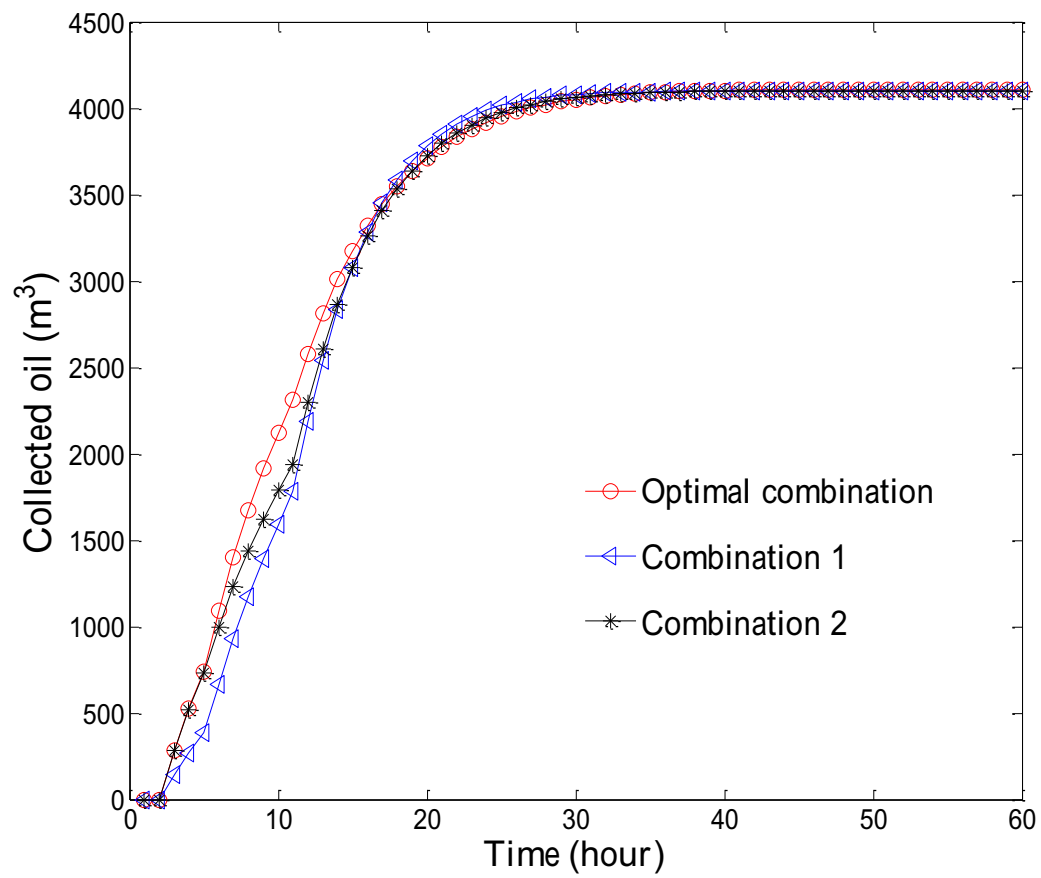
Figure 5.13 Comparison of collected oil based on the optimal combination and other two combinations
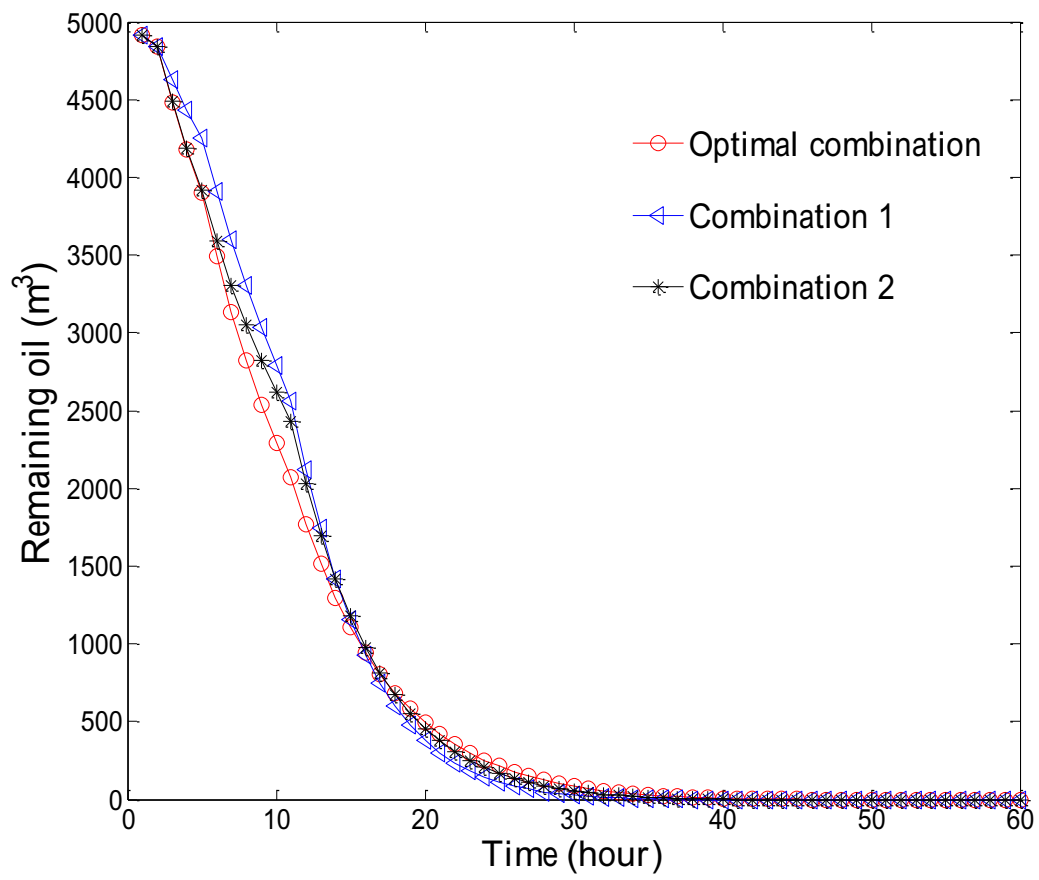
Figure 5.14 Comparison of remaining oil based on the optimal combination and other two combinations

5.4 Summary

This chapter has firstly developed a framework of an integrated decision support system for offshore oil spill response in harsh environment (DSS-OSRH). The proposed decision support system includes an updating database for various information; a diagnosis module consisting of offshore OSVI classification through a Monte Carlo simulation based two-stage adaptive resonance theory mapping (MC-TSAM) approach and offshore monitoring; a technology screening module (MC-IRFAM) to determine the most feasible technologies for offshore oil spill response based on integration of Monte Carlo simulation and rule-based fuzzy adaptive resonance theory mapping; and a simulation-based optimization module (MC-DMINP) to support device allocation and oil recovery by integration of Monte Carlo simulation, dynamic mixed integer nonlinear programming, and spill weathering simulation.

As three key modules in the DSS-OSRH, the MC-TSAM, MC-IRFAM, and MC-DMINP and their integration are of importance. The MC-TSAM is firstly applied to assess the offshore OSVI based on various conditions with uncertainties of a targeted offshore area, providing the specific site conditions for technology screening by MC-IRFAM. The most feasible technologies determined by the MC-IRFAM to form the initial settings for the simulation-based optimization by MC-DMINP. Furthermore, the site conditions characterized by the MC-TSAM are applied as inputs to the simulations in the MC-DMINP. Finally, the MC-DMINP generates a series of decision alternatives

245

considering combinations of technologies (e.g., types and number of devices) in each operational stage, allocations of man power and finance, corresponding cost and environmental effects, etc.

In order to demonstrate the feasibility and efficiency of the developed DSS-OSRH, a case study was conducted for supporting an offshore oil spill response process in the south coast of Newfoundland. A set of modeling results were provided, including the offshore OSVI classification with specific site conditions, a list of feasible technologies with ranking scores, and the best combination of technologies as well as optimized operational option to achieve the maximum oil recovery. The results indicated that more than 50% of the spilled oil could be collected within 12 hours, and over 90% would be removed with 24 hours, demonstrating high feasibility and efficiency of the proposed decision support system.

The DSS-OSRH could provide support to on-site decision making and implementation during offshore oil spill emergency response in an timely and cost-efficient manner. Therefore, the system should be particularly suitable for offshore oil spill response in harsh environments such as the offshore areas in North Atlantic and Arctic oceans. This system could not only advance the knowledge and fill the technical gaps but deliver expeditious and powerful tools for industry and regulators respond to offshore oil spill events under harsh environmental conditions. It would help operators and managers in health, safety and environmental departments (HSE) managers timely

assess risk and impacts, choose suitable technology and make sound and quick decisions

to mitigate the negative effects and save time and costs. The proposed DSS-OSRH would

bring significant short-/long-term benefits to offshore industry, governmental authorities

and coastal communities by improving their knowledge and capacities in responding to

oil spills and reducing the associated impacts on the marine environment and society.

CHAPTER 6

CONCLUSIONS AND RECOMMENDATIONS

6.1 Summary

This thesis research has developed a decision support system (DSS) for supporting offshore oil spill response in harsh environments. Such a system consists of a set of novel concepts and modeling approaches including: 1) a framework of offshore management system by dynamically integrating of oil spill database, diagnosis and alert, technologies screening, simulation-based optimization modules; 2) two Monte Carlo simulation based fuzzy-neuro approaches for offshore oil spill vulnerability index (OSVI) classification and technologies screening under uncertainty and complexity; 3) a simulation optimization coupling approach under dynamics and uncertainties based on the integration of simulations of oil weathering and recovery processes, dynamic programming, and uncertainty analysis approach; 4) the integration of offshore OSVI classification, technologies screening, and the simulation-optimization coupling approaches.

A comprehensive review has firstly been made in offshore oil spills including background, impacts, as well as preparedness and contingency planning. Reviews have also given in classification/ranking especially in classification and ranking under complexity and uncertainty as well as their coexistence which widely exists in offshore oil spills. Accordingly, classification and ranking in supporting offshore oil spill response have been reviewed. Further discussions have been given on optimization approaches in environmental engineering under uncertainty and dynamics, and especially in the field of

offshore oil spill responses. Correspondingly, the utilizations of decision support approaches including classification, simulation, and optimization for supporting offshore oil spill response are examined. Finally, the challenges in offshore oil spill response in cold and harsh environments have been discussed.

Targeting the disclosed knowledge gaps and technological needs, a Monte Carlo simulation-based two-stage adaptive resonance theory mapping (MC-TSAM) approach has been developed based on the integration of Monte Carlo simulation and the previously developed two-stage adaptive resonance theory mapping (TSAM) approach. The approach can carry out unsupervised learning under uncertain and complex conditions, classifying a concerned offshore area that is threatened or affected by offshore oil spills into a desired number of distinctive zones, representing the offshore oil spill vulnerability levels. In order to demonstrate its feasibility, the MC-TSAM has been applied to classify the south coast of the Newfoundland into five offshore zones with different offshore OSVI due to potential offshore oil spills. Ten uncertain features in oceanic conditions, meteorological conditions, and spill information as well as two features reflecting ecological concerns have been considered and used as inputs. The results provided vulnerability zones with corresponding characteristics under different scenarios to support offshore oil spill monitoring.

Furthermore, a previously developed integrated rule-based adaptive resonance theory mapping (IRFAM) approach has been advanced by incorporating Monte Carlo (MC)

simulation to form a MC simulation based IRFAM (MC-IRFAM) approach for technology screening in offshore oil spill responses. The developed approach was tested with a hypothetical case of technologies screening in an offshore oil spill event. The results demonstrated that the provided approach was capable in classifying/ranking the technologies based on uncertain inputs (feasibilities) and criteria (site conditions).

In order to reflect uncertainties into optimization process, a new fuzzy-stochastic-interval linear programming (FSILP) approach has been developed. Meanwhile, a Monte Carlo simulation based fuzzy programming (MCFP) approach has been introduced to handling the coexistence of possibility and continuous probability. Based on these two approaches, a simulation based dynamic mixed integer nonlinear programming (MC-DMINP) approach has been developed to reflect both dynamics and uncertainties in offshore oil spill responses. A case study was conducted to support device allocation and oil recovery in an offshore oil spill event. The optimization of response processes and the simulations of oil weathering (evaporation, dispersion and emulsification) and recovery have been further integrated. The modeling results represented the dynamic and uncertain features with the spilled oil, response resources, and environmental impacts. The results also provided the optimal option of device allocation and response operation.

A framework of the integrated decision support system for offshore oil spill response in harsh environments (DSS-OSRH) has been proposed based on the integration of the

developed approaches, including offshore OSVI classification (MC-TSAM), the technology screening (MC-IRFAM), and the simulation-optimization coupling (MC-DMINP). In the system, the MC-TSAM is firstly applied to assess the offshore OSVI based on various uncertain conditions in a targeted offshore area, providing the specific site conditions for technology screening by MC-IRFAM. Correspondingly, the most feasible technologies determined by the MC-IRFAM form the initial settings for the MC-DMINP. In addition, the classified zones from the MC-TSAM provide site conditions as inputs to the simulations in the MC-DMINP. Finally, the MC-DMINP generates a set of optimal options considering combinations of technologies in each operational stage, allocations of man power and resources, corresponding cost and environmental effects, etc. In order to demonstrate the feasibility of the developed DSS-OSRH, a case study was conducted for supporting an offshore oil spill response process in the south coast of Newfoundland. A set of modeling results were provided, including the offshore OSVI classification with specific site conditions, a list of feasible technologies with ranking scores, and the best combination of technologies as well as the optimized option for response operation to achieve the maximum oil recovery.

6.2 Research Contributions

This research has led to the following major contributions:

1.   A novel Monte Carlo simulation-based two-stage adaptive resonance theory

mapping (MC-TSAM) approach has been developed for the offshore OSVI classification in any concerned area with potential or existing oil leaks/spills. The developed approach can automatically process the classification according to the inputs with uncertain and complex features. The results only depend on the inputs and can avoid the uncertainty from criteria definition. The approach has been applied to the offshore OSVI classification in the south coast of Newfoundland. It demonstrated the practical significance by giving decision support in delineating sensitive zones to oil spills. According to different scenarios of categories, decision makers can flexibly determine plans for the following monitoring and response actions.

2. A new Monte Carlo simulation based integrated rule-based adaptive resonance theory mapping (MC-IRFAM) approach has been developed for classifying and ranking response technologies in offshore oil spill events. The proposed approach can effectively handle the inputs with imprecise information and uncertainty ranges which widely exist in offshore oil spill responses. Furthermore, this approach can not only rank the technology according to feasibility, but also provide the degree of the feasibility.

3. Three new optimization approaches including fuzzy-stochastic-interval linear programming (FSILP), Monte Carlo simulation based fuzzy programming (MCFP), and dynamic mixed integer nonlinear programming (DMINP) have

been developed, and further led to a novel simulation-optimization coupling approach, the Monte Carlo simulation-based dynamic mixed integer nonlinear programming (MC-DMINP) approach. The MC-DMINP can convert simulation model into constraints which dynamically link to the decision variables, and break a time series into stages according to controllable time intervals in a practical manner, leading to a multiple stages dynamic programming. Such programming is further integrated with the Monte Carlo simulation to handle the uncertain conditions. The MC-DMINP approach has been further integrated with the weathering simulation, providing an innovative simulation-optimization coupling means for offshore oil spill response. A case study demonstrated the feasibility and capability in representing the dynamics of environmental conditions, spilled oil properties, and changes of resources. It indicated significantly practical values to the offshore oil spill recovery in harsh environments where unpredictable weather and oceanic conditions exist.

4. An integrated decision support system for offshore oil spill response in harsh environments (DSS-OSRH) has been developed. The key components of the proposed DSS-OSRH include the newly developed MC-TSAM, MC-IRFAM, and MC-DMINP approaches and their integration. The proposed system is the first of its kind to date. It can provide a series of decisions in risk/vulnerability zone classification and characterization, technology screening, and device

allocation and response operation in offshore oil spill management under uncertainty and complexity. A case study of an offshore oil spill response in the south coast of Newfoundland proved the feasibility and efficiency of the proposed DSS-OSRH. This system will not only advance the knowledge and fill the technical gaps but also deliver expeditious and powerful tools for industry and regulators to control and response to offshore oil spill events under harsh environmental conditions. It can help operators and spill responders timely and effectively assess risk and impacts, choose suitable technologies, and make sound and quick decisions to mitigate the negative effects and save costs. The proposed DSS-OSRH will bring significant short-/long-term benefits to industry, government and communities and help reduce the risks posed by oil spills to the marine and coastal ecosystems.

5. The developed approaches and DSS are the first of their kinds to date targeting offshore oil spill responses. These methods are particularly suitable for offshore oil spill responses in harsh environments such as the offshore areas of Newfoundland and Labrador (NL) where cold water/weather, strong wind, rough wave, and sea ice exist. The research will also promote the understanding of the processes of oil transport and fate and the short-/long-term impacts to the affected offshore and shoreline area. The developed methodologies will be capable of providing modeling tools for other related areas that require timely

and effective decisions under complexity and uncertainty.

6.3 Publications

Papers under Preparation

1. Li P., Chen B., Jing L., Li Z.L., and Zheng X. (2013). A Monte Carlo simulation-based two-stage adaptive resonance theory mapping model for site classification in offshore oil spill monitoring. Marine Pollution Bulletin, MPB-D-14-00171. (Under review)

2. Chen B., Li P., Wu H.J. Husain T., and Khan F. (2013). MCFP: a Monte Carlo simulation based fuzzy programming approach for municipal solid waste management under dual uncertainties of possibility and continuous probability. Journal of Environmental Informatics, JEI (13JM073001). (Under review)

3. Li P., Li Z.L., Chen B., and Jing L. (2014). An agent based simulation-optimization approach for device allocation and operation control in response to offshore oil spills. In: proceeding of 37th AMOP Technical Seminar on Environmental Contamination and Response, June 3 - 5, 2014, Canmore, Canada. (Under review)

4. Li P., Cai Q.H., Lin W. Y., Chen B., and Zhang B.Y. (2013). From challenges to opportunities: towards future strategies and a decision support framework for oil

spill preparedness and response in harsh environment. Environmental Science & Technology. (Submitted).

Refereed Journal Publication

1. Li P., Chen B., Zhang B.Y., Jing L., and Zheng J.S. (2014). Monte Carlo simulation-based dynamic mixed integer nonlinear programming for supporting oil recovery and devices allocation during offshore oil spill responses. Ocean & Coastal Management, 89C(2014): 58-70.

2. Li P., Wu H.J., and Chen B. (2013). RSW-MCFP: a resource-oriented solid waste management system for a mixed rural-urban area through Monte Carlo simulation-based fuzzy programming. Mathematical Problems in Engineering, 2013(2013): 15pp.

3. Jing L., Chen B., Zhang B.Y., Li P., and Zheng J.S. (2013). Monte Carlo simulation-aided analytic hierarchy process approach: case study of assessing preferred non-point-source pollution control best management practices. Journal of Environmental Engineering - ASCE, 139(5): 618-626.

4. Jing L., Chen B., Zhang B.Y., and Li P. (2013). A hybrid stochastic-interval analytic hierarchy process approach for prioritizing the strategies of reusing treated wastewater. Mathematical Problems in Engineering, 2013(2013): Article

ID 874805, 10pp.

5. Li P., Chen B., Zhang B.Y., Jing L., and Zheng J.S. (2012). A multiple-stage simulation–based mixed integer nonlinear programming approach for supporting offshore oil spill recovery with weathering process. Journal of Ocean Technology, 7(4): 87-105.

6. Jing L., Chen B., Zhang B.Y., and Li P. (2012). A Stochastic Simulation-Based Hybrid Interval Fuzzy Programming Approach for Optimizing the Treatment of Recovered Oily Water. Journal of Ocean Technology, 7(4): 60-72.

7. Li T., Li P., Chen B., Hu M., and Zhang X. (2012). A simulation-based inexact two-stage chance constraint quadratic programming for sustainable water quality management under dual uncertainties. Journal of Water Resource Planning and Management - ASCE, 140(3), 298 - 312.

8. Chen B., Li P., and Husain T. (2012). Development of an integrated adaptive resonance theory mapping classification system for supporting watershed hydrological modeling. Journal of Hydrologic Engineering - ASCE, 17(6): 679–693.

9. Li P., Chen B., and Husain T. (2011). IRFAM: an integrated rule-based fuzzy adaptive resonance theory mapping system for watershed modeling. Journal of Hydrologic Engineering - ASCE, 16(1): 21-32.

10. Li P. and Chen B. (2011). FSILP: fuzzy-stochastic-interval linear programming for supporting municipal solid waste management. Journal of Environmental Management, 92(4): 1198-1209.

Other Refereed Publication

1. Li P., Chen B., Jing L., Li Z.L., and Zheng X. (2014). An integrated simulation-based optimization approach for devices allocation and operation in offshore oil spill response. Abstract for oral presentation in the 5th Annual Arctic Oil & Gas North America Conference, St John's Newfoundland and Labrador, March 25 - 27.

2. Li P., Chen B., Zhang B.Y. (2013). An integrated rule-based adaptive resonance theory mapping approach for technologies screening in offshore oil spill response. In: Proceedings of CSCE 2013 Annual General Conference, Montréal, Québec, May 29 to June 1, 2013, GEN-236.

3. Wu H.J., Chen B., and Li P. (2013). Comparison of sequential uncertainty fitting algorithm (SUFI-2) and parameter solution (ParaSol) method for analyzing uncertainties in distributed hydrological modeling – A case study. In: Proceedings of CSCE 2013 Annual General Conference, Montréal, Québec, May 29 to June 1, 2013, GEN-309.

4. Li P., Chen B., Jing L., Li Z.L., and Zheng X. (2013), "A Monte Carlo simulation-based two-stage adaptive resonance theory mapping model for site classification in offshore oil spill monitoring", Posters of 4th Annual Arctic Oil & Gas North America Conference, St John's Newfoundland and Labrador, April 10 - 11.

5. Li P., Chen B., Zhang B. Y., Jing L., and Zheng J. S. (2012). Development of a multiple-stage simulation based mixed integer nonlinear programming approach for supporting offshore oil spill recovery. In: Proceeding of the 35th AMOP Technical Seminar on Environmental Contamination and Response, June 5-7, 2012, Vancouver, Canada, 434-447.

6. Li P., Chen B., Zhang B.Y., and Jing L. (2012). A new agro-industrial waste management model for supporting rural co-operative stewardship and sustainable development. In: Proceedings of CRETE2012 - the 3rd International Conference on Industrial and Hazardous Waste Management, Chania, Greece, S13.3: 1-8.

7. Jing L., Chen B., Zhang B.Y., Zheng J.S., and Li P. (2012). A stochastic analytical hierarchy process for supporting nonpoint source pollution control. In: Proceedings of CSCE 2012 Annual General Conference, 2, 1167-1176.

8. Ping J., Zhang B.Y., Chen B. Liu B., Li P., and Liu S. (2012). Integrated health risk assessment of Fe/mn contamination in groundwater - a case study. In: Proceedings of CSCE 2012 Annual General Conference, 2, 1254-1263.

9. Li P. and Chen B. (2011). Management of municipal solid waste under uncertainty through a hybrid optimization approach. In: Proceedings of CSCE 2011 Annual General Conference, June 14-17, 2011, Ottawa, GC-205.

6.4 Recommendations for Future Research

1. The proposed MC-TSAM provides the classification and characterization of vulnerability zones in an area that is affected or potentially affected by offshore oil leaks/spills. It can only provide a roughly qualification of risk in the area, which may not be enough for responses to offshore oil spills occurring in environmentally or ecologically sensitive areas. The integration of MC-TSAM with risk quantification models, such as the exposure related dose estimating model (ERDEM) (U.S. EPA, 2004; Blancato et al., 2006; Zhang et al., 2007) and the generic ecological assessment endpoints (GEAEs) model (U.S. EPA, 2004; Landis and Kaminski, 2007) provided by the U.S. Environmental Protection Agency (U.S. EPA), would help improve the applicability and efficiency of the MC-TSAM.

2. The simulation module in the MC-DSINP has considered some important processes in oil weathering processes including evaporation, dispersion, and emulsification. However, other weathering processes such as dissolution, spreading, biodegradation, photolysis, sedimentation, advection, and oil-shoreline

interaction, may also cause influence to the weathering simulation. Further consideration of these processes will help improve the simulation function of the approach.

3. A simple model was used for the oil slick movement with the assumption that the only driven factor is ocean current. This simplification can help demonstrate the developed DSS-OSRH but compromises its real-world applicability. The integration of hydrodynamic simulation models such as MEDSLIK-II (De Dominicis et al, 2013) will help improve the real-world applicability of the DSS.

4. Offshore oil spills and the corresponding response actions are affected by many complex factors and their interactions, including meteorological, oceanic, and ecological conditions, oil properties, transport and fate, human activities, ecological and social issues, etc. Not all of these factors were considered in this research. The considerations of more features would help improve the applicability and commonality of the proposed DSS.

5. During the development of all the new approaches in this research, continuous communications and consultations have been kept with the relevant government, industry, and communities such as Fisheries and Oceans Canada (DFO), Environment Canada (EC), Eastern Canada Response Corporation (ECRC), Canadian Coast Guard (CCG), Suncor Energy, and American Bureau of Shipping (ABS). Their advice and inputs have been well considered and reflected in the

models. However, the developed approaches need to be further tested and demonstrated by more real-world case studies. This can be achieved by the existing collaborations with local oil spill responders such as the ECRC and the CCG to test the proposed DSS in their oil spill response training and exercises.

APPENDICES

Appendix A: Figures of Interpolated Parameters in the South Coast of

Newfoundland for Offshore OSVI Classification
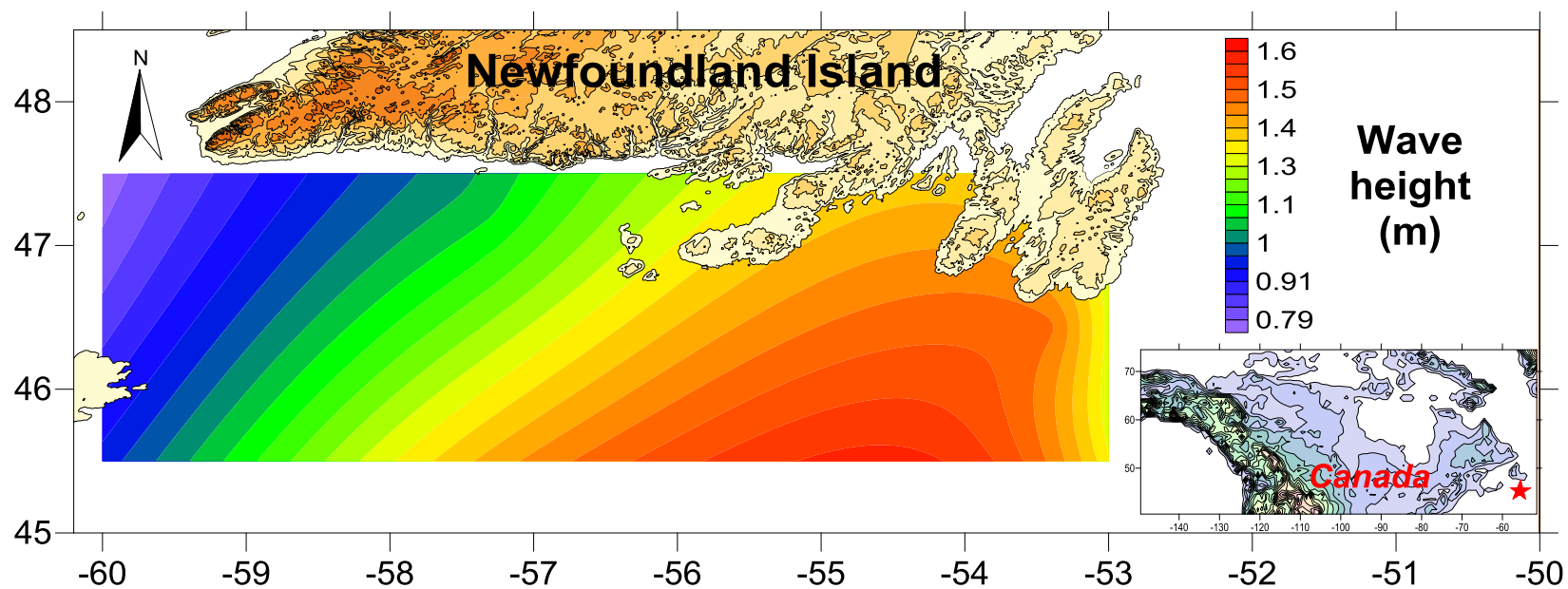
Figure A3.1 Interpolated prevailing wave height in the south coast of Newfoundland
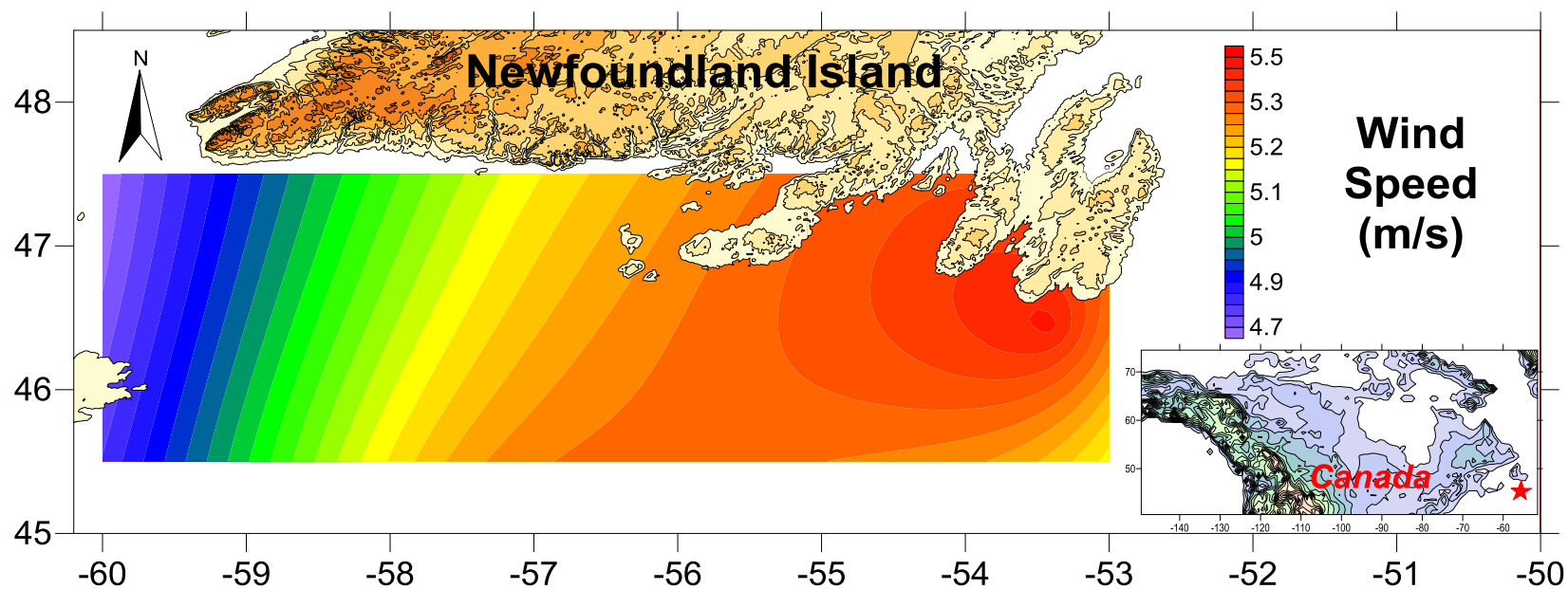
Figure A3.2 Interpolated prevailing wind speed in the south coast of Newfoundland
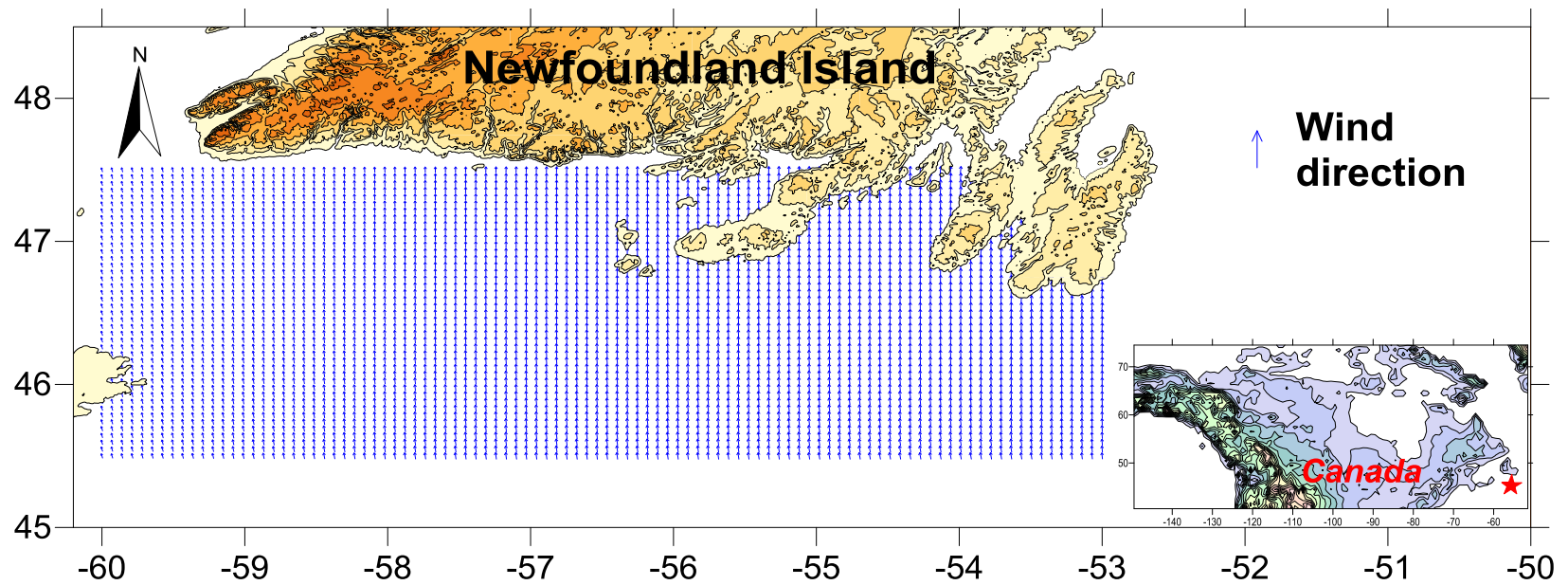
Figure A3.3 Interpolated prevailing wind direction in the south coast of Newfoundland
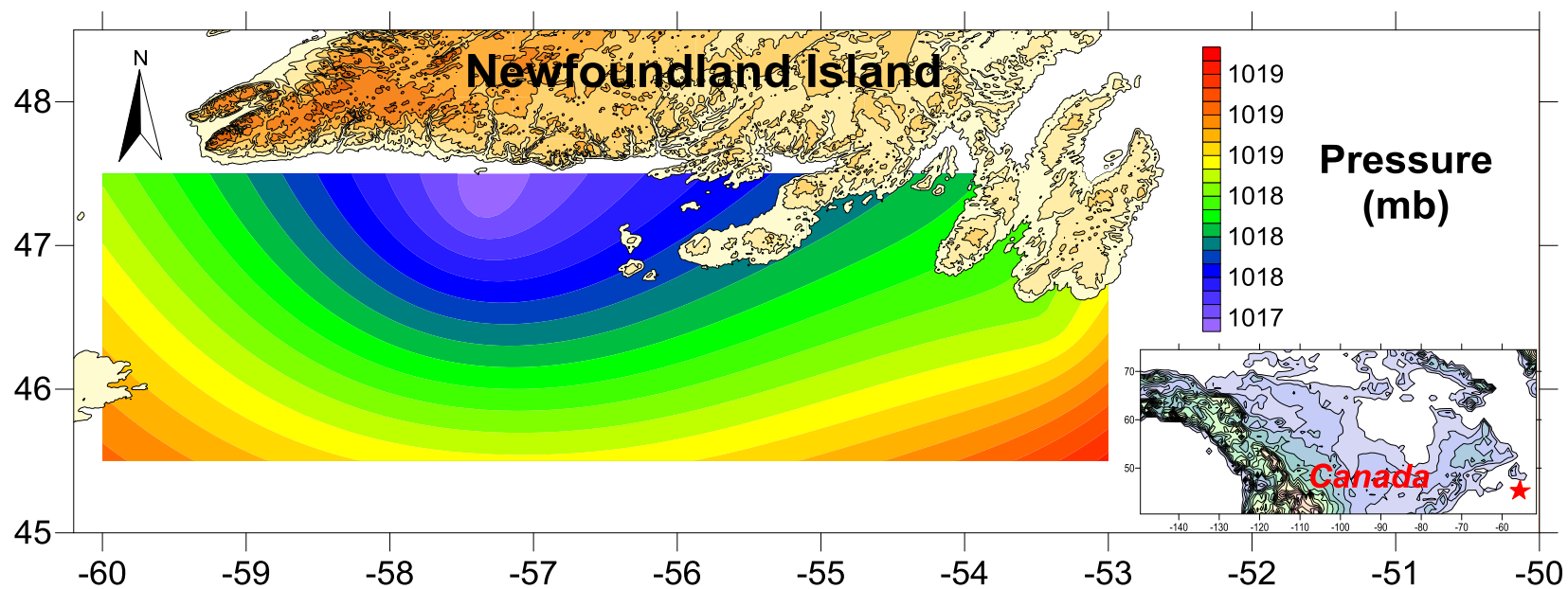
Figure A3.4 Interpolated prevailing pressure in the south coast of Newfoundland
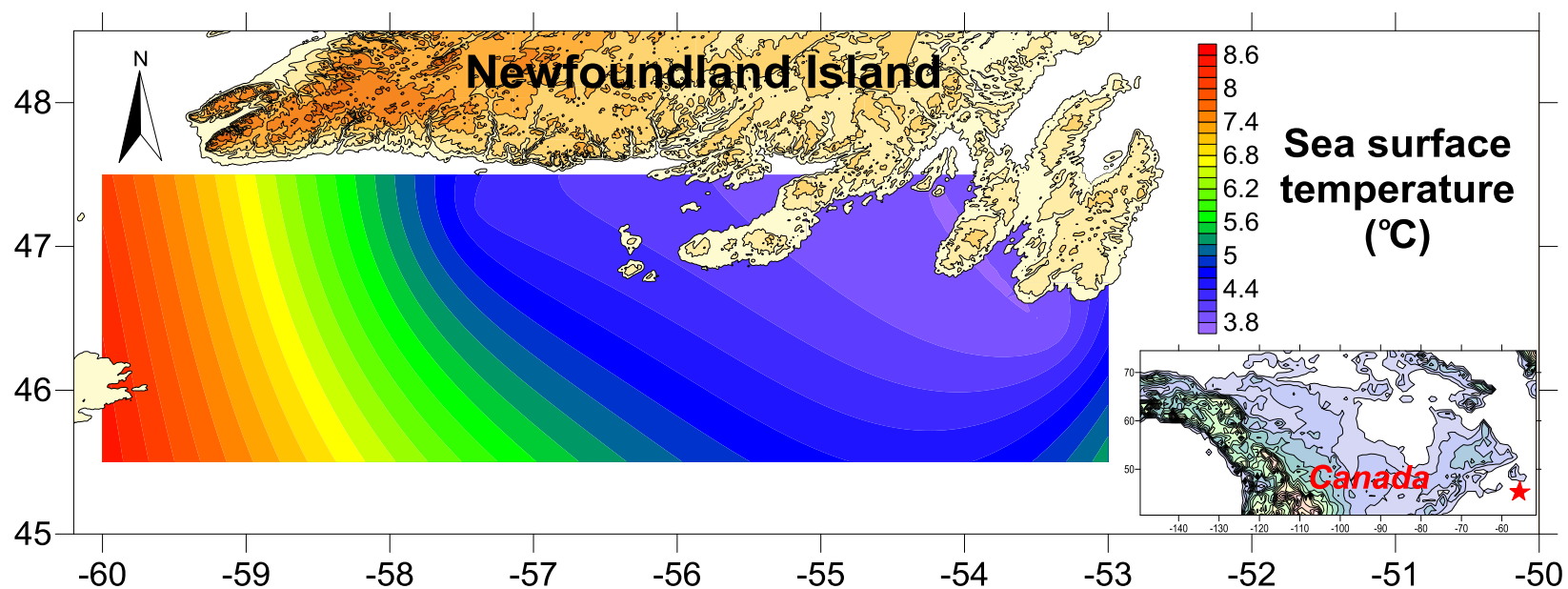
Figure A3.5 Interpolated prevailing sea surface temperature in the south coast of Newfoundland
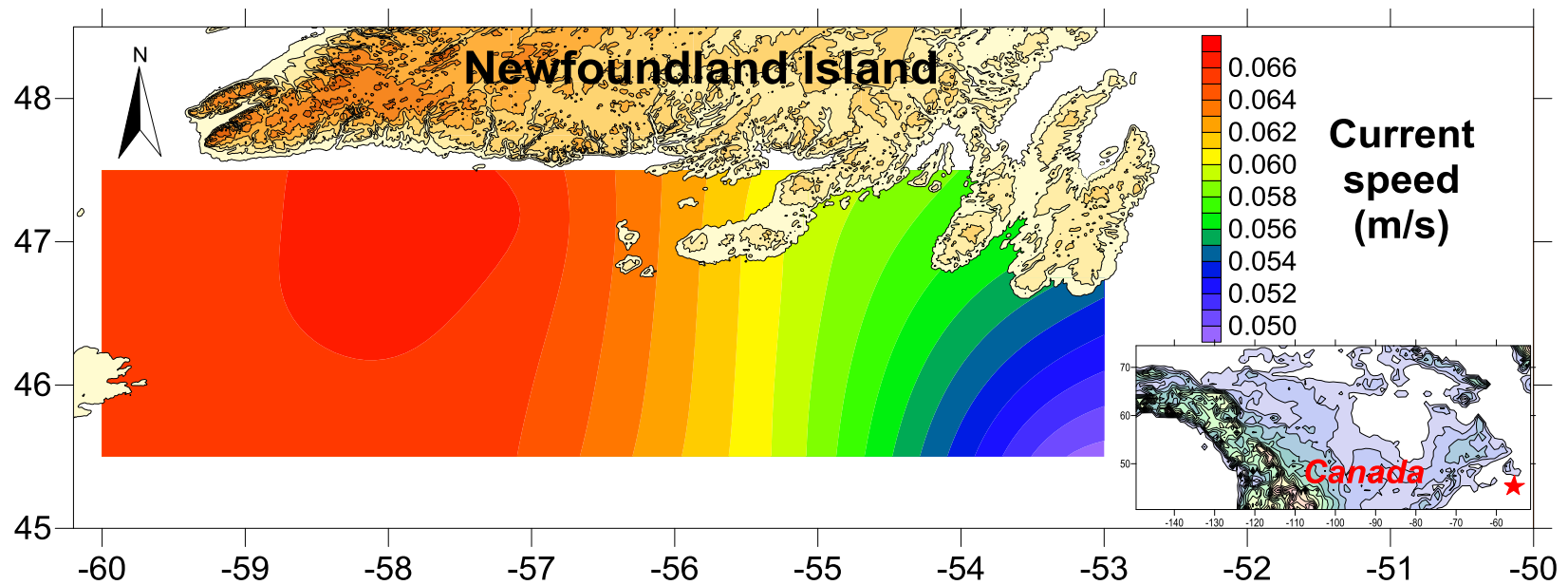
Figure A3.6 Interpolated prevailing current speed in the south coast of Newfoundland
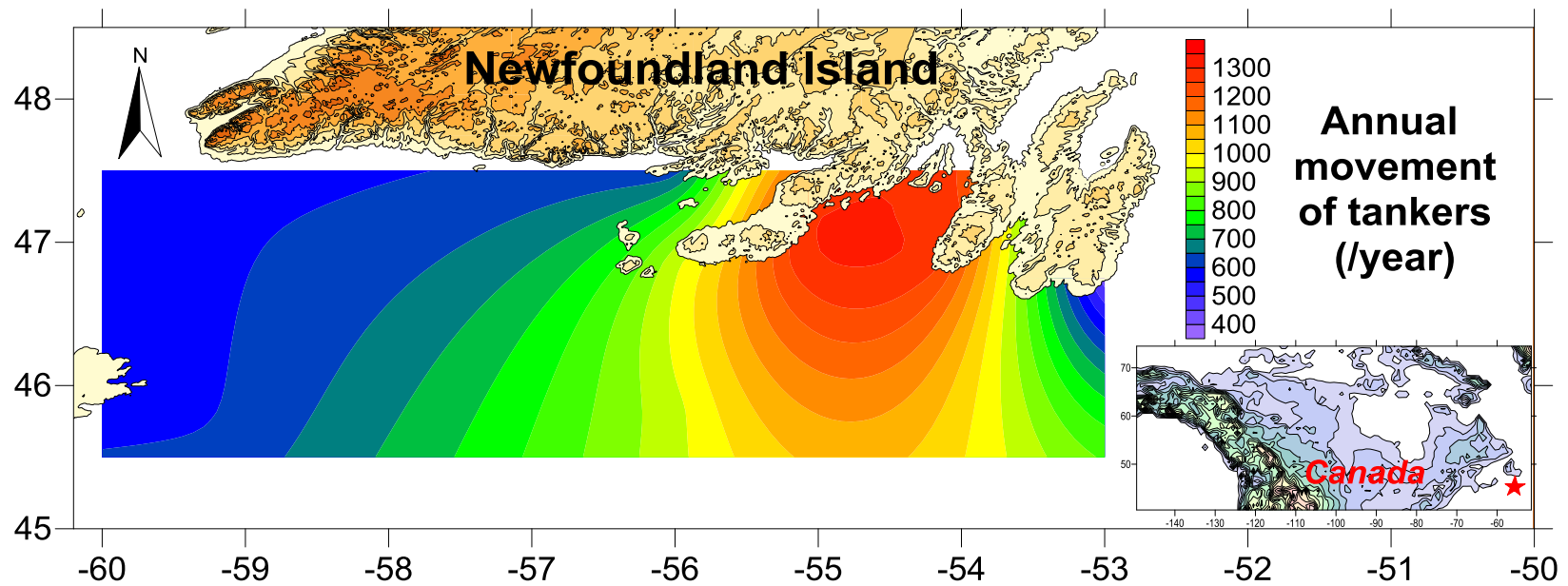
Figure A3.7 Interpolated prevailing tanker movement in the south coast of Newfoundland
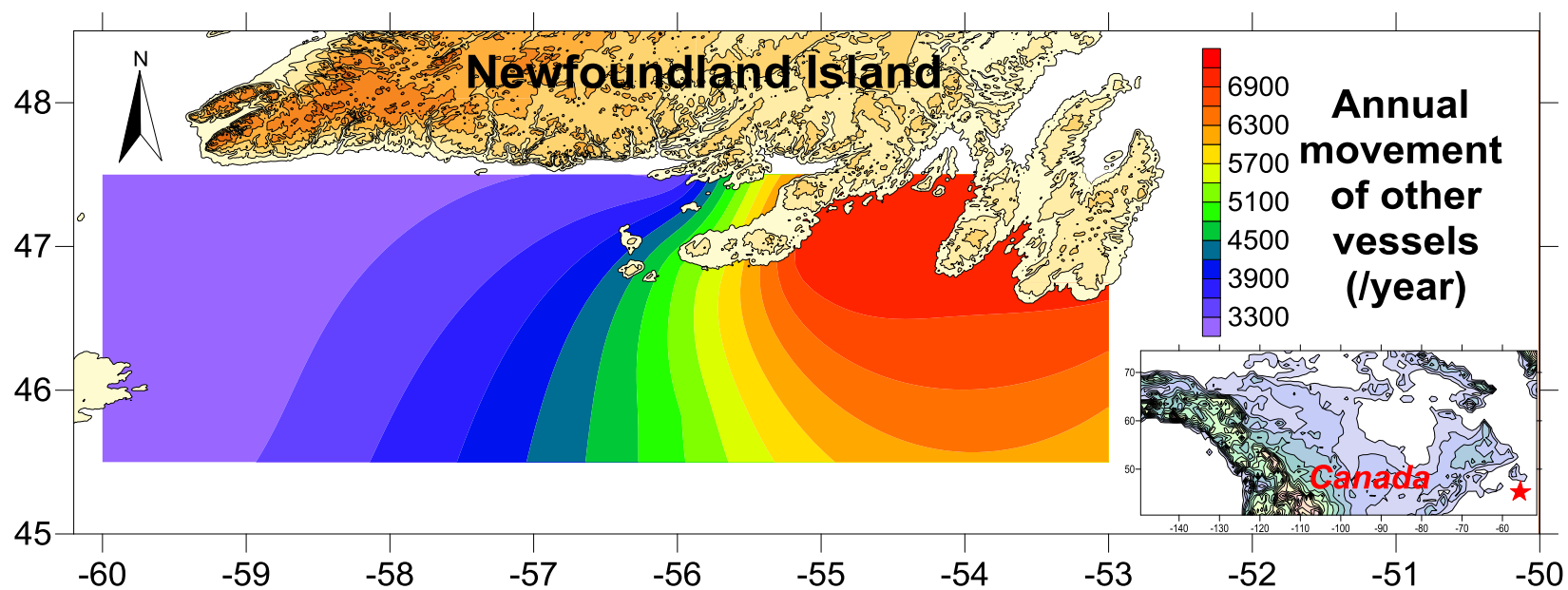
Figure A3.8 Interpolated prevailing other vessels movement in the south coast of Newfoundland

Appendix B: Figures of Parameter Distributions in Zones Classified by MC-TSAM
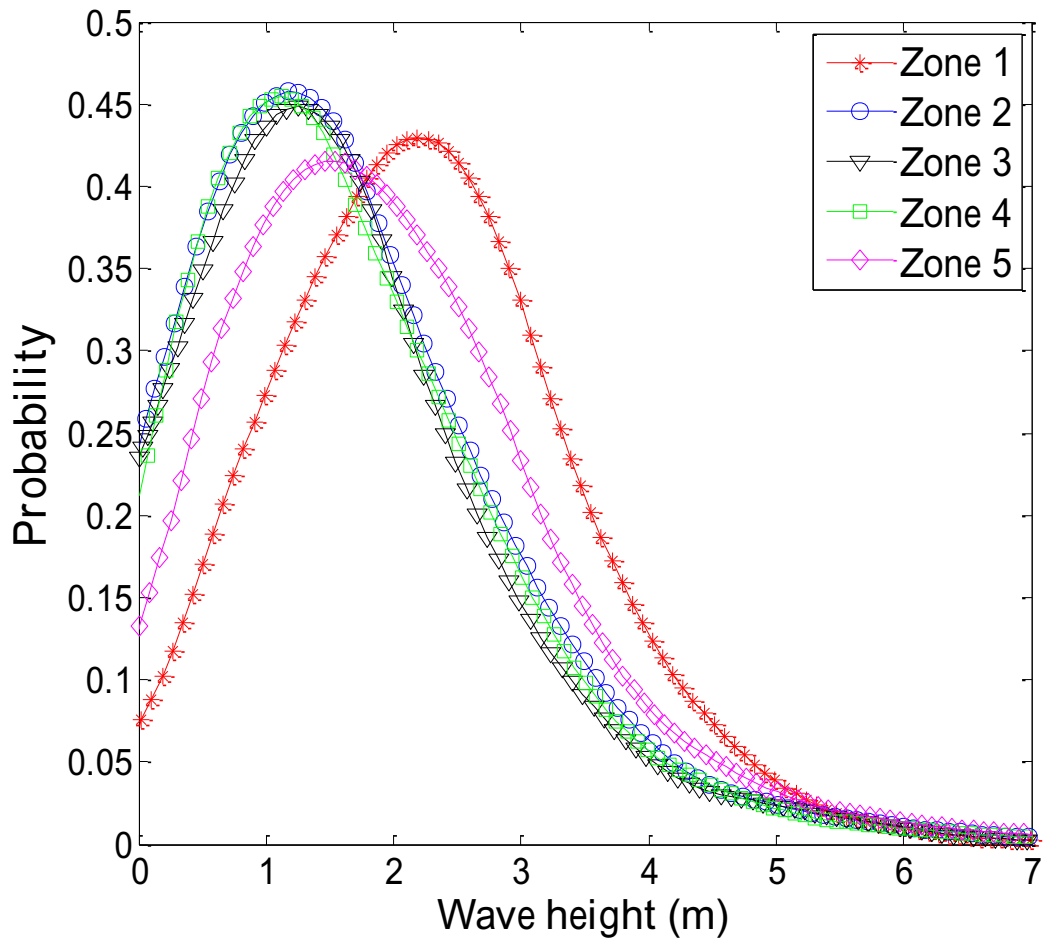
Figure A5.1 Distributions of wave height in zones classified by MC-TSAM
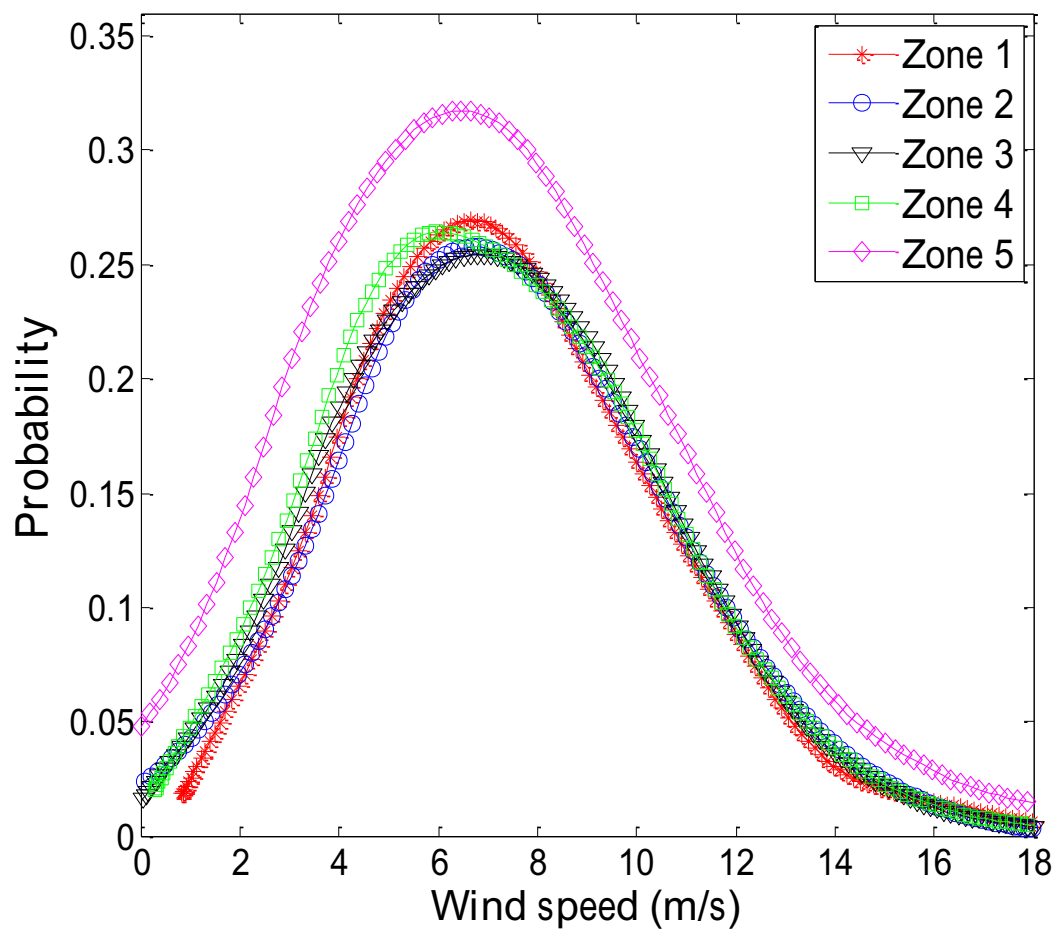
Figure A5.2 Distributions of wind speed in zones classified by MC-TSAM
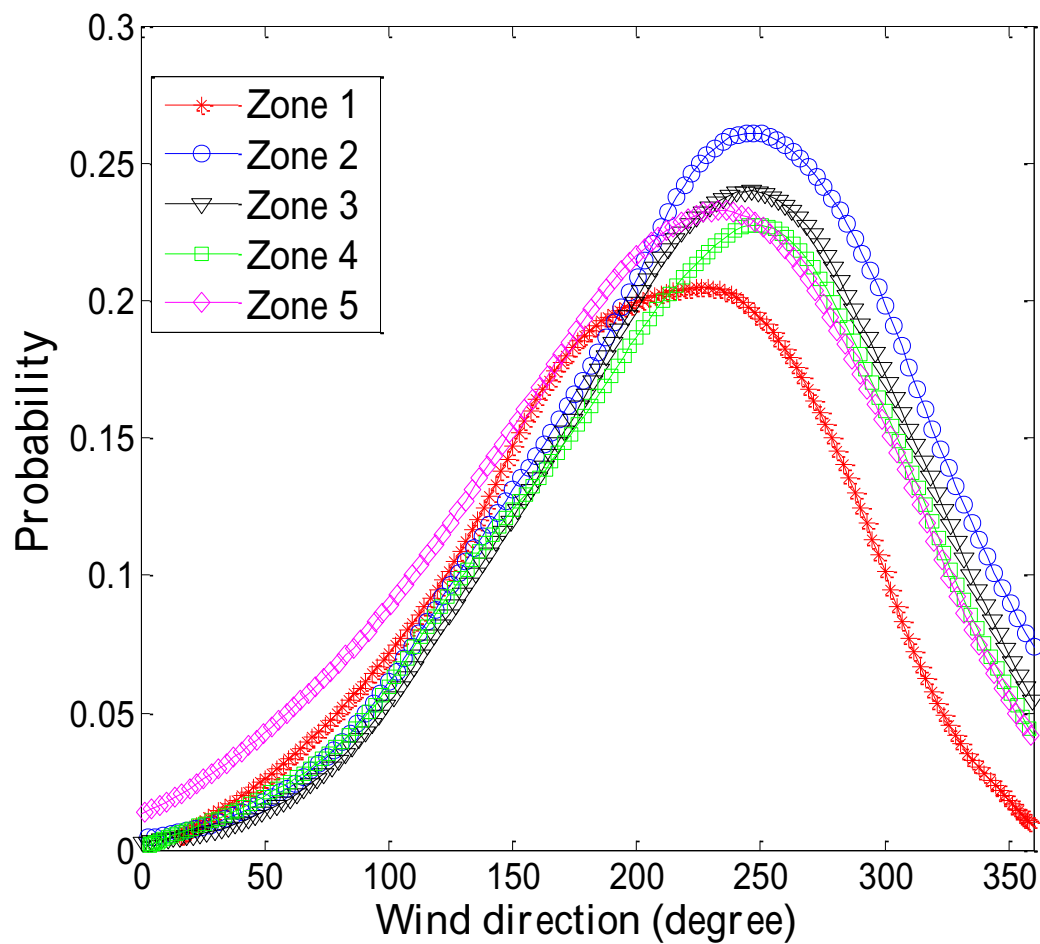
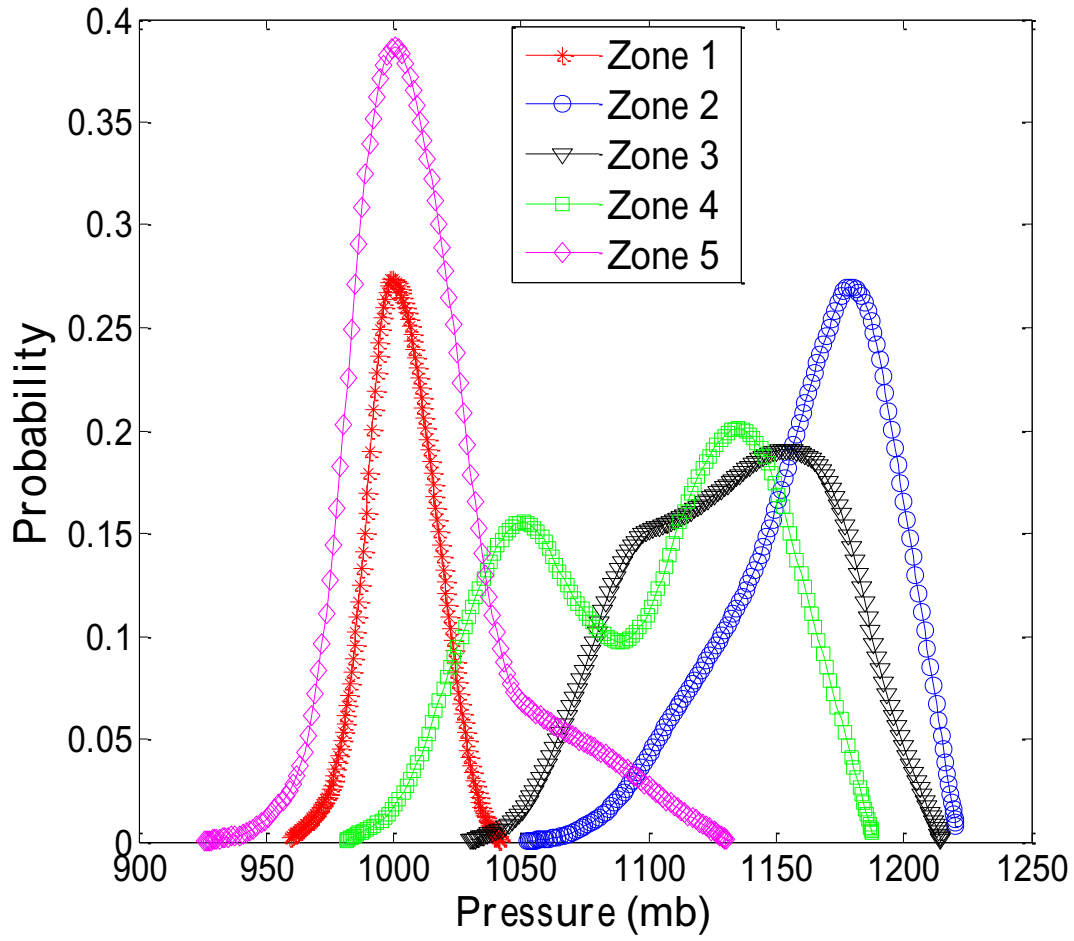Figure A5.3 Distributions of wind direction in zones classified by MC-TSAM

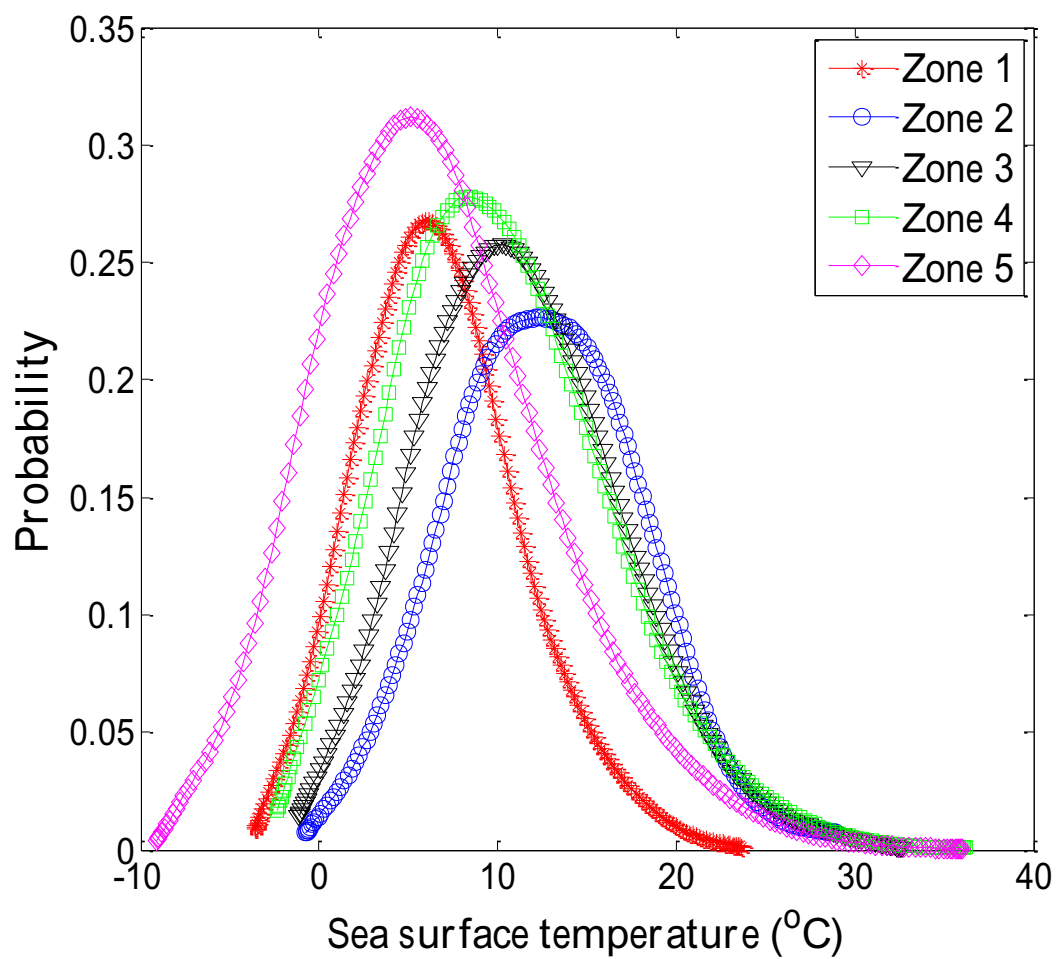Figure A5.4 Distributions of pressure in zones classified by MC-TSAM

Figure A5.5 Distributions of sea surface temperature in zones classified by MC-TSAM
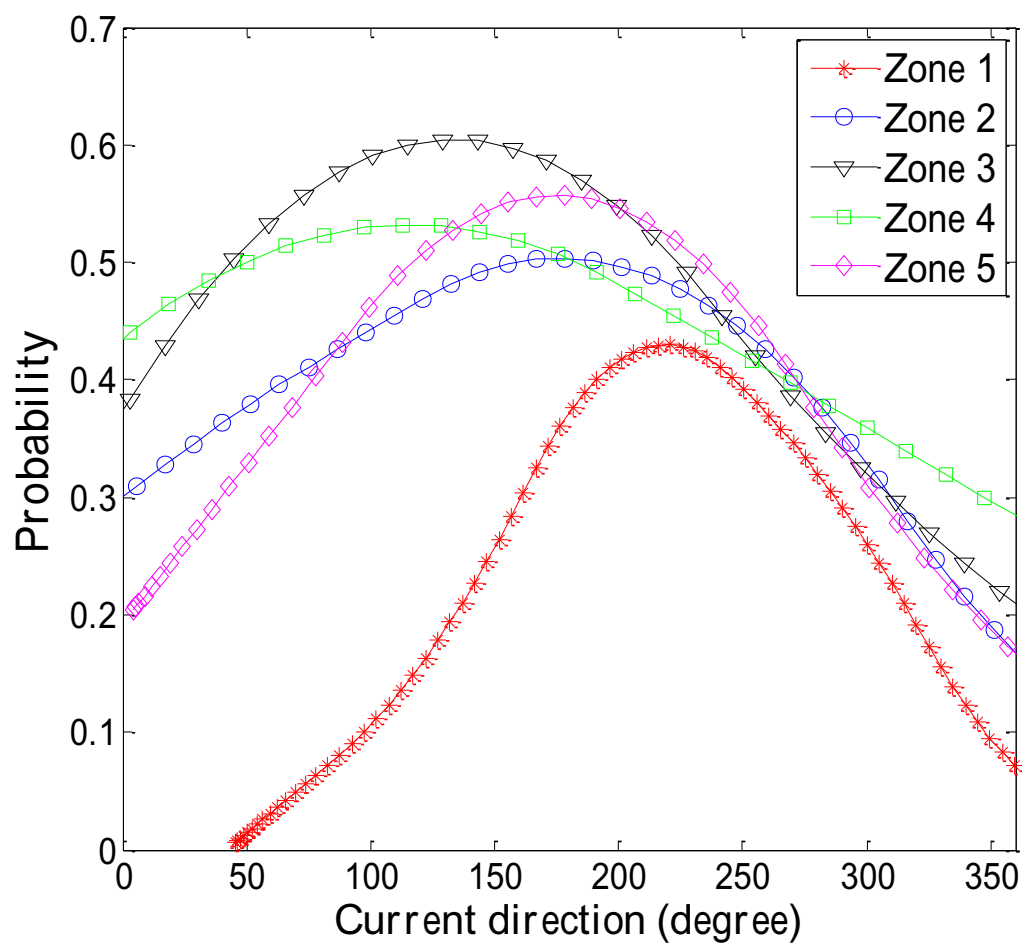
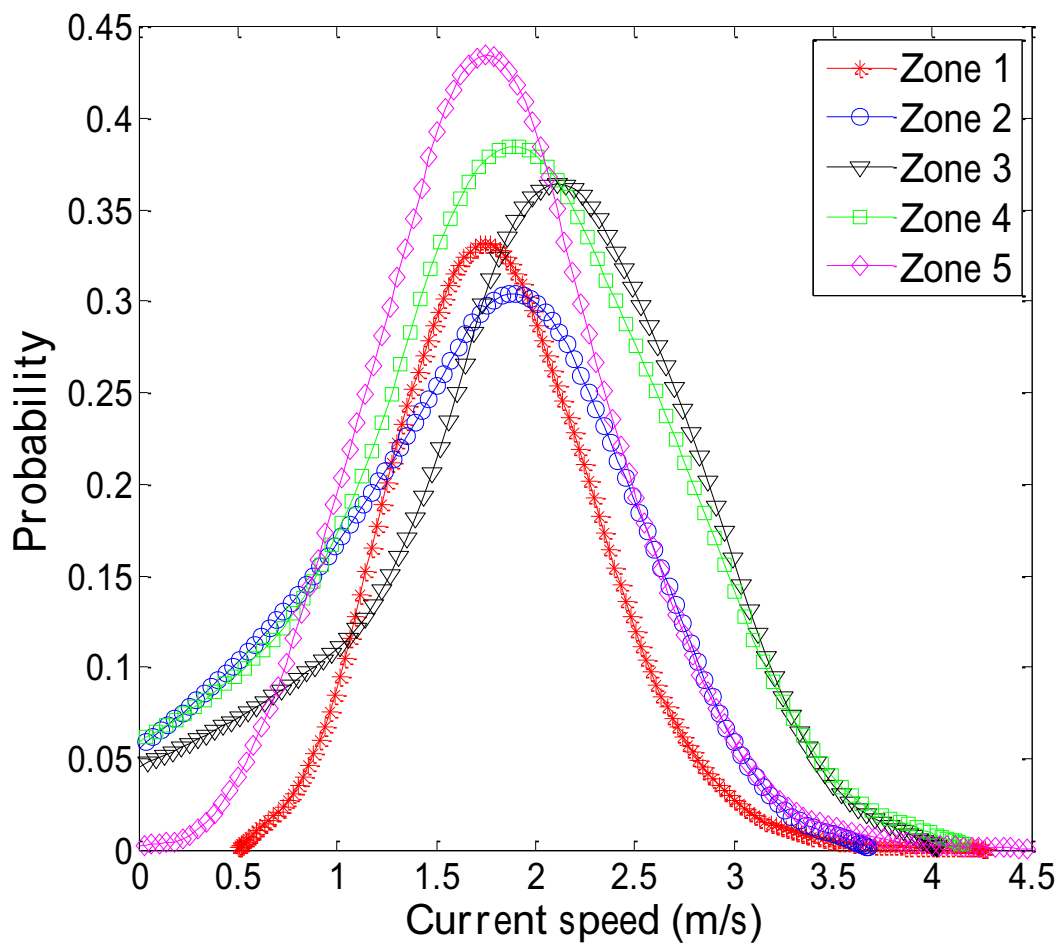Figure A5.6 Distributions of current direction in zones classified by MC-TSAM

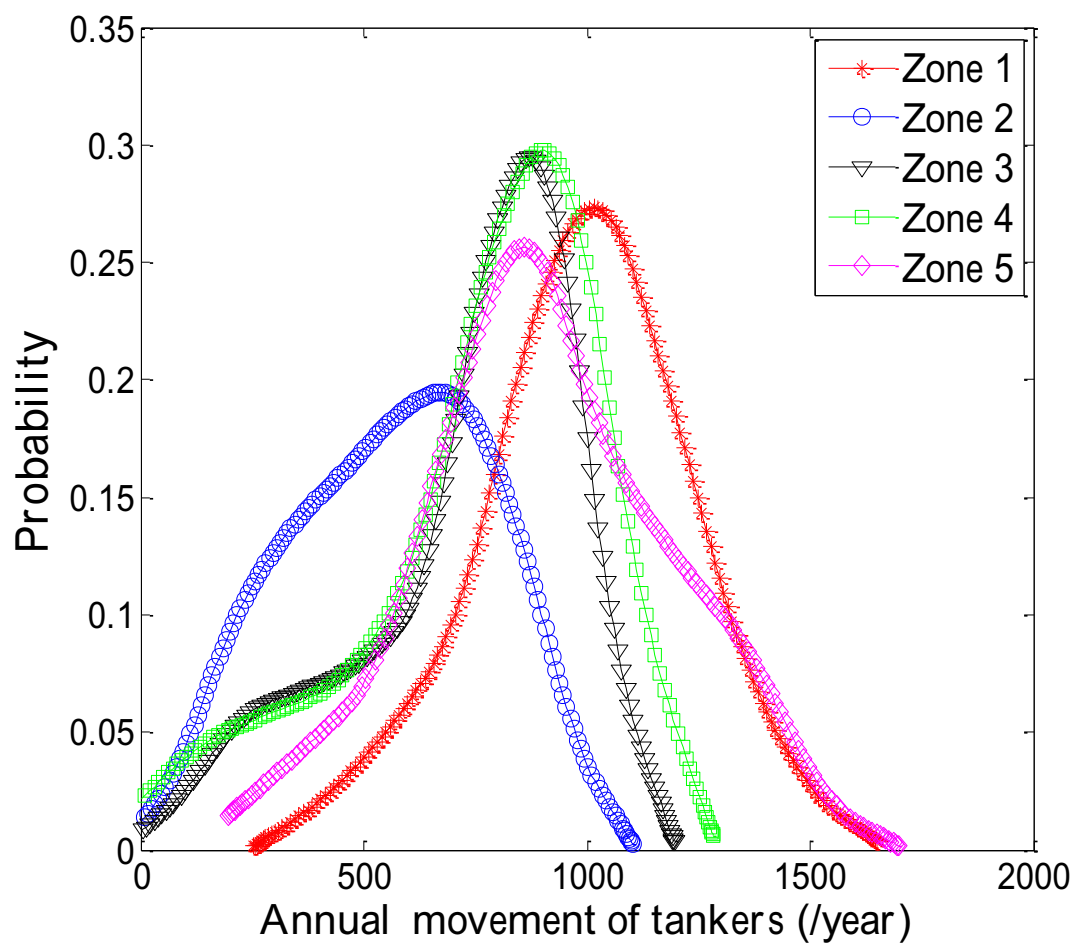Figure A5.7 Distributions of current speed in zones classified by MC-TSAM

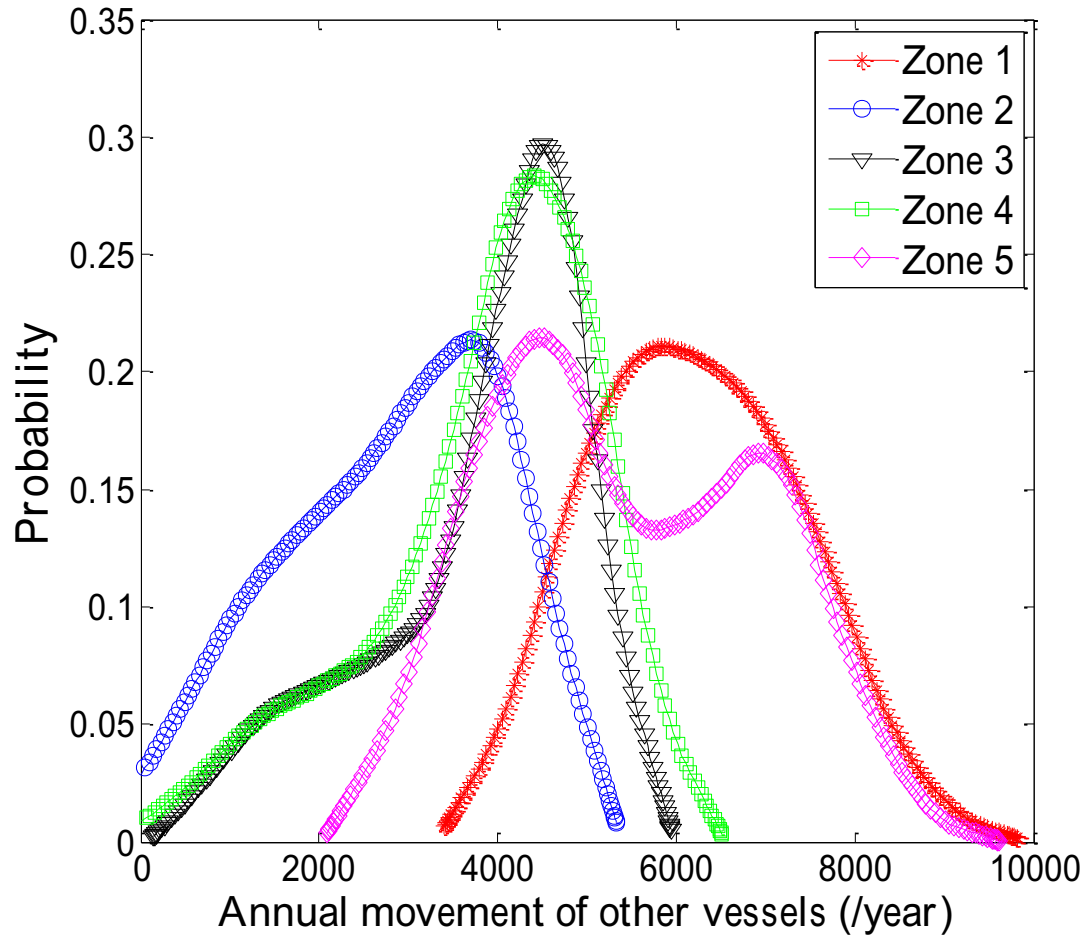Figure A5.8 Distributions of annual movement of tankers in zones classified by
MC-TSAM

Figure A5.9 Distributions of annual movement of other vessels in zones classified by MC-TSAM

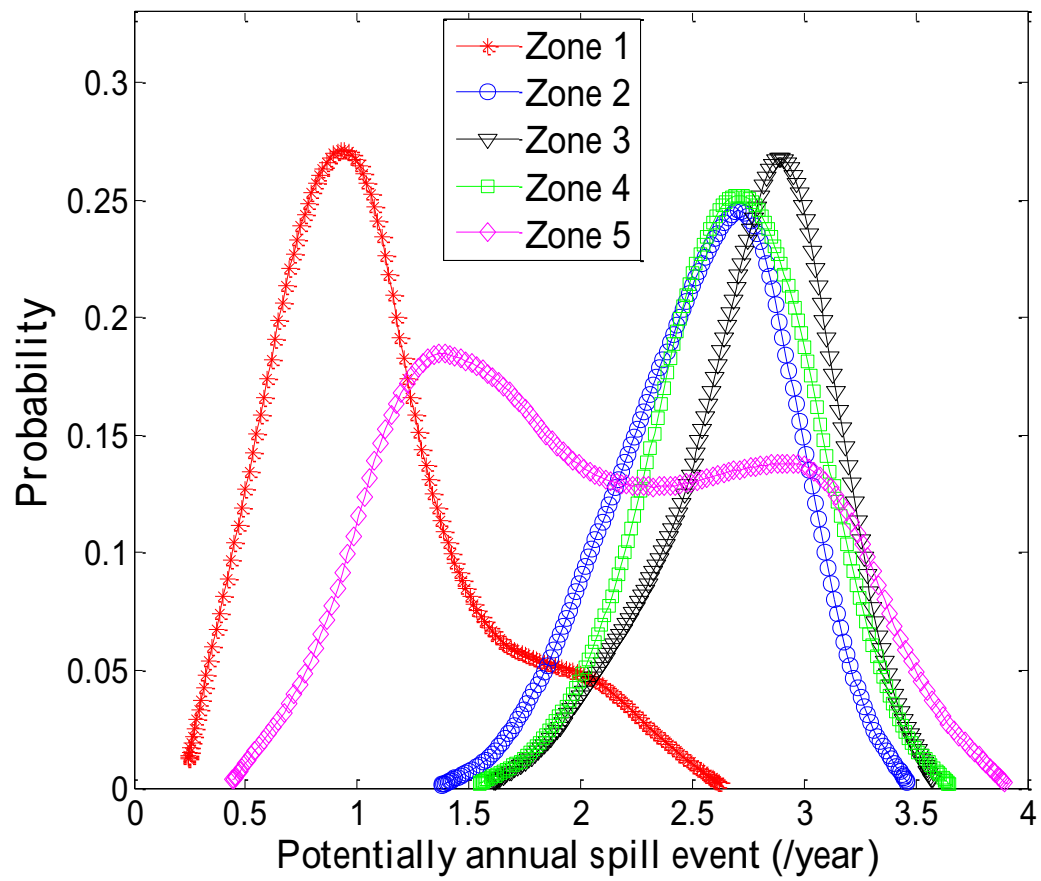Figure A5.10 Distributions of historically annual spill frequency in zones classified by MC-TSAM

Appendix C: Figures of Overall Score Distributions of Skimmers

Figure A5.11 Distributions of overall scores of Skimmer 1 to Zone 1 ranked by MC-IRFAM

Figure A5.12 Distributions of overall scores of Skimmer 2 to Zone 1 ranked by MC-IRFAM

Figure A5.13 Distributions of overall scores of Skimmer 3 to Zone 1 ranked by MC-IRFAM

Figure A5.14 Distributions of overall scores of Skimmer 4 to Zone 1 ranked by MC-IRFAM

Figure A5.15 Distributions of overall scores of Skimmer 5 to Zone 1 ranked by MC-IRFAM

Figure A5.16 Distributions of overall scores of Skimmer 6 to Zone 1 ranked by MC-IRFAM

Figure A5.17 Distributions of overall scores of Skimmer 7 to Zone 1 ranked by MC-IRFAM
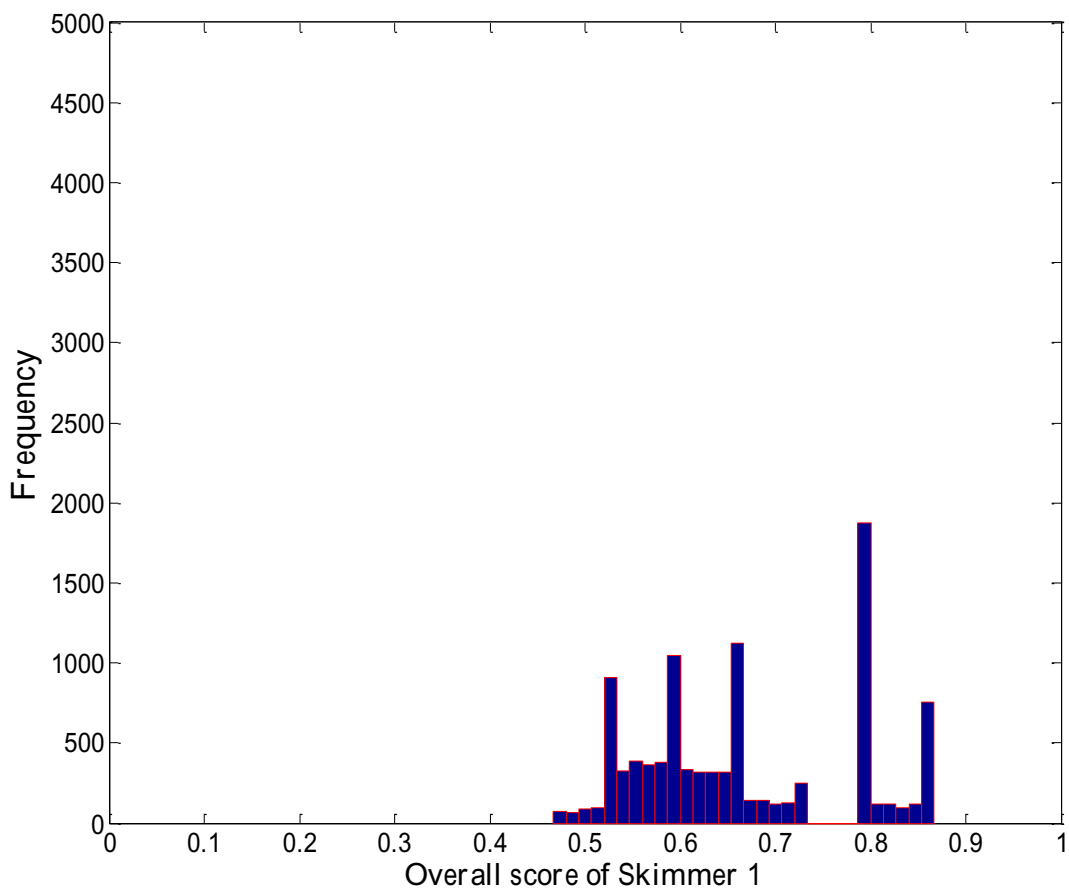
Figure A5.18 Distributions of overall scores of Skimmer 1 to Zone 5 ranked by MC-IRFAM
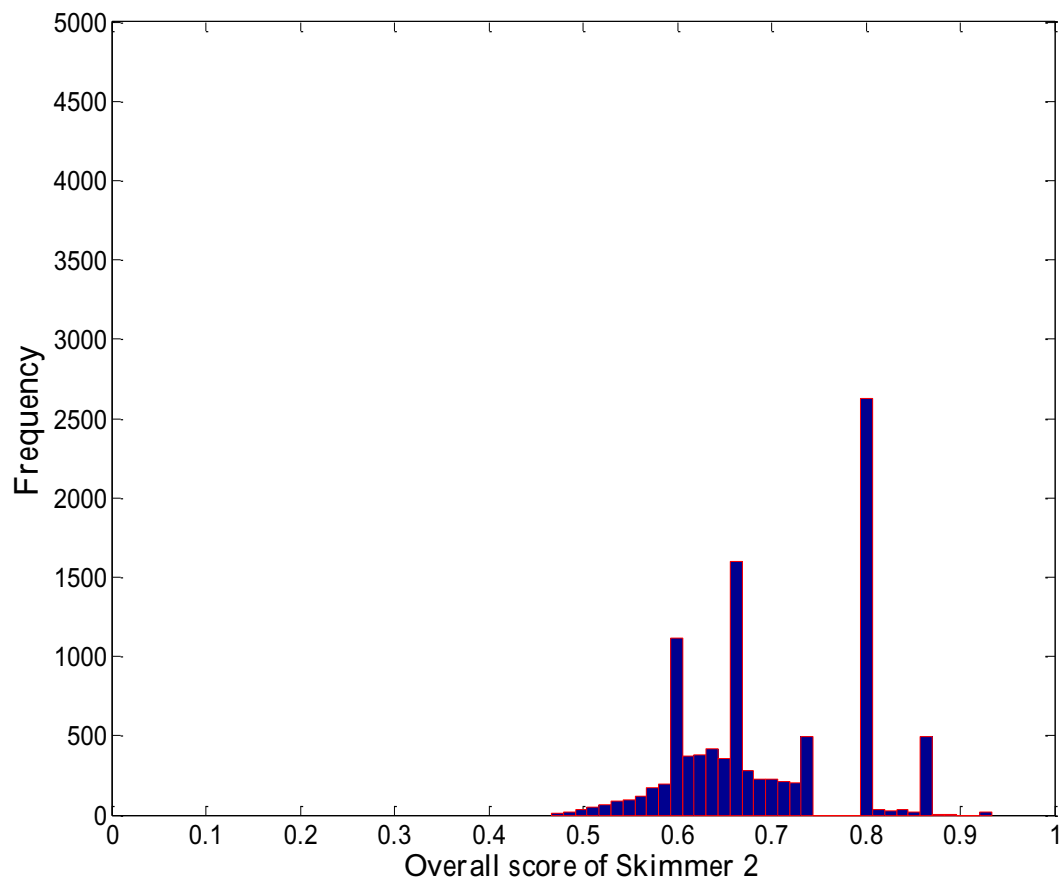
Figure A5.19 Distributions of overall scores of Skimmer 2 to Zone 5 ranked by MC-IRFAM
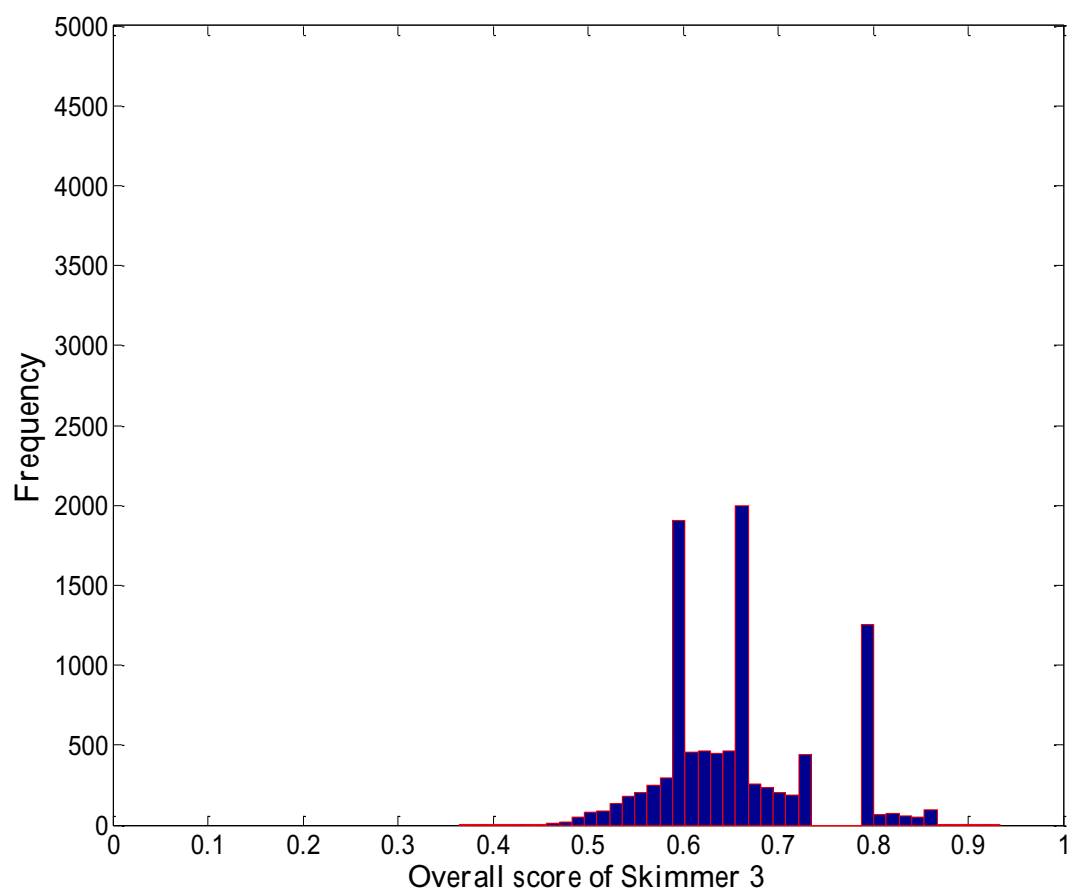
Figure A5.20 Distributions of overall scores of Skimmer 3 to Zone 5 ranked by MC-IRFAM
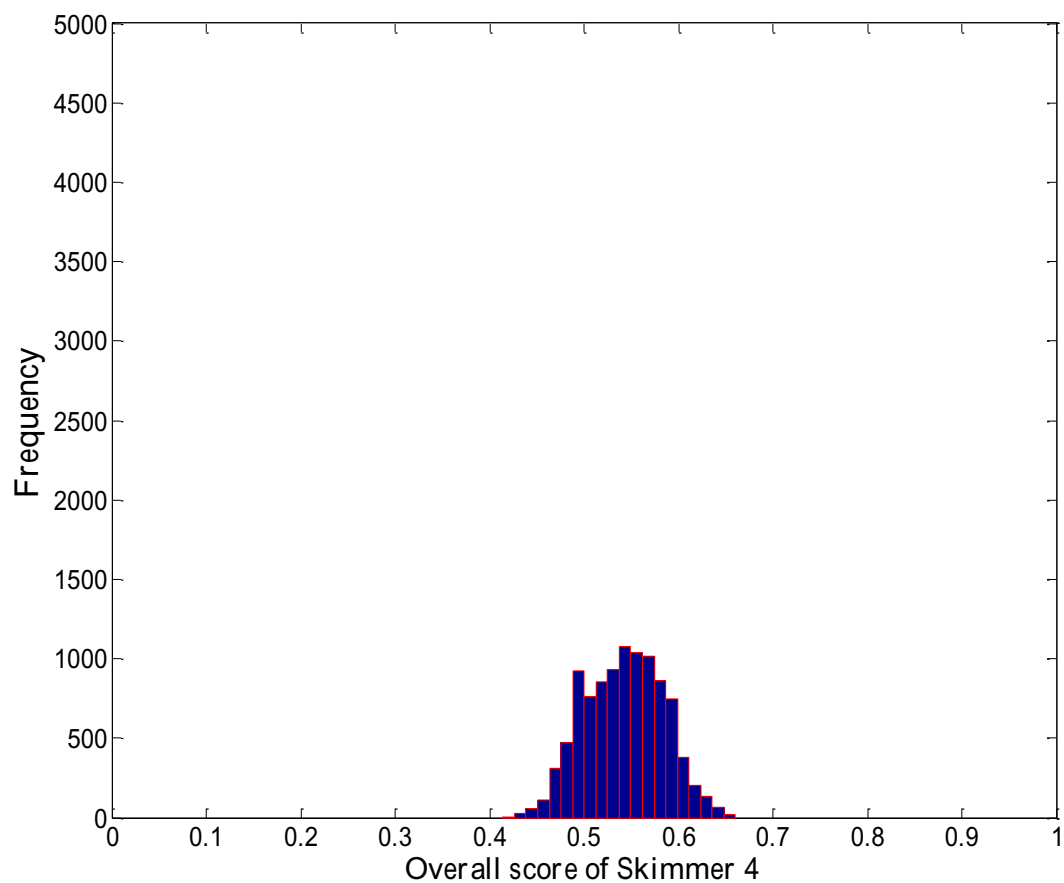
Figure A5.21 Distributions of overall scores of Skimmer 4 to Zone 5 ranked by MC-IRFAM
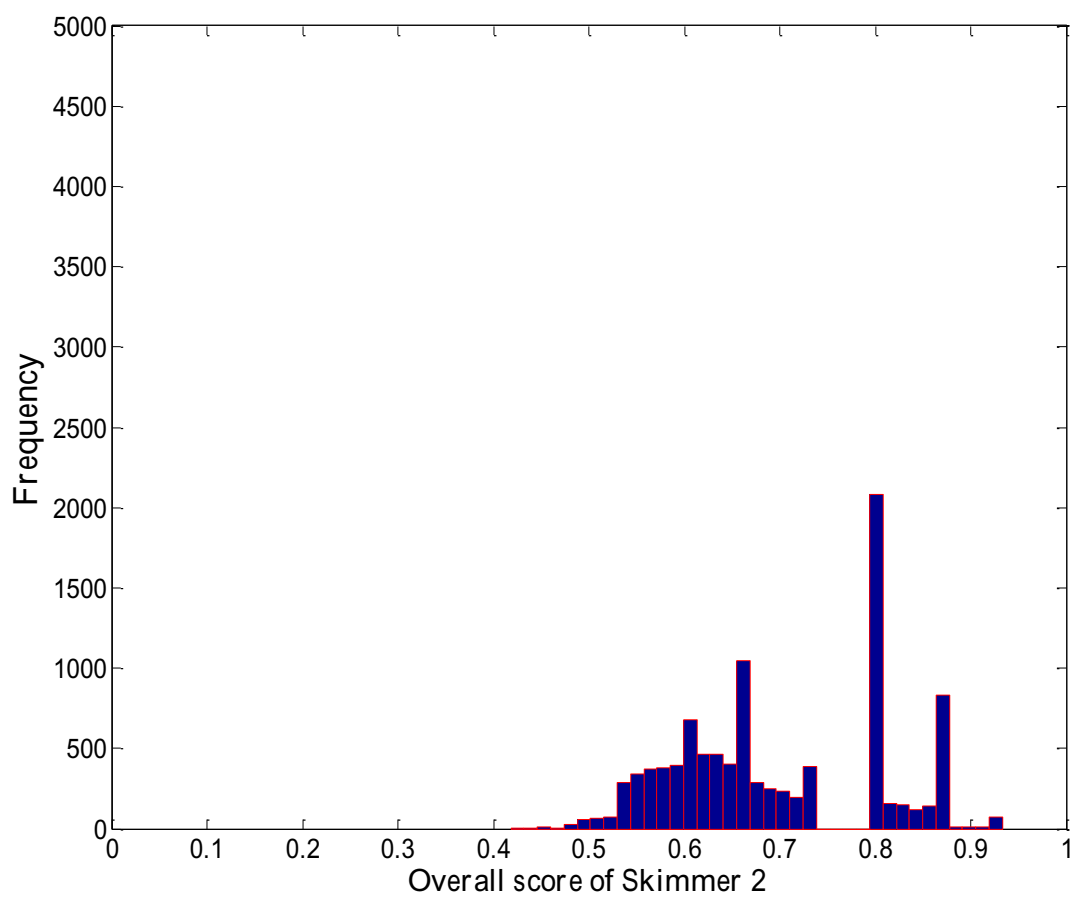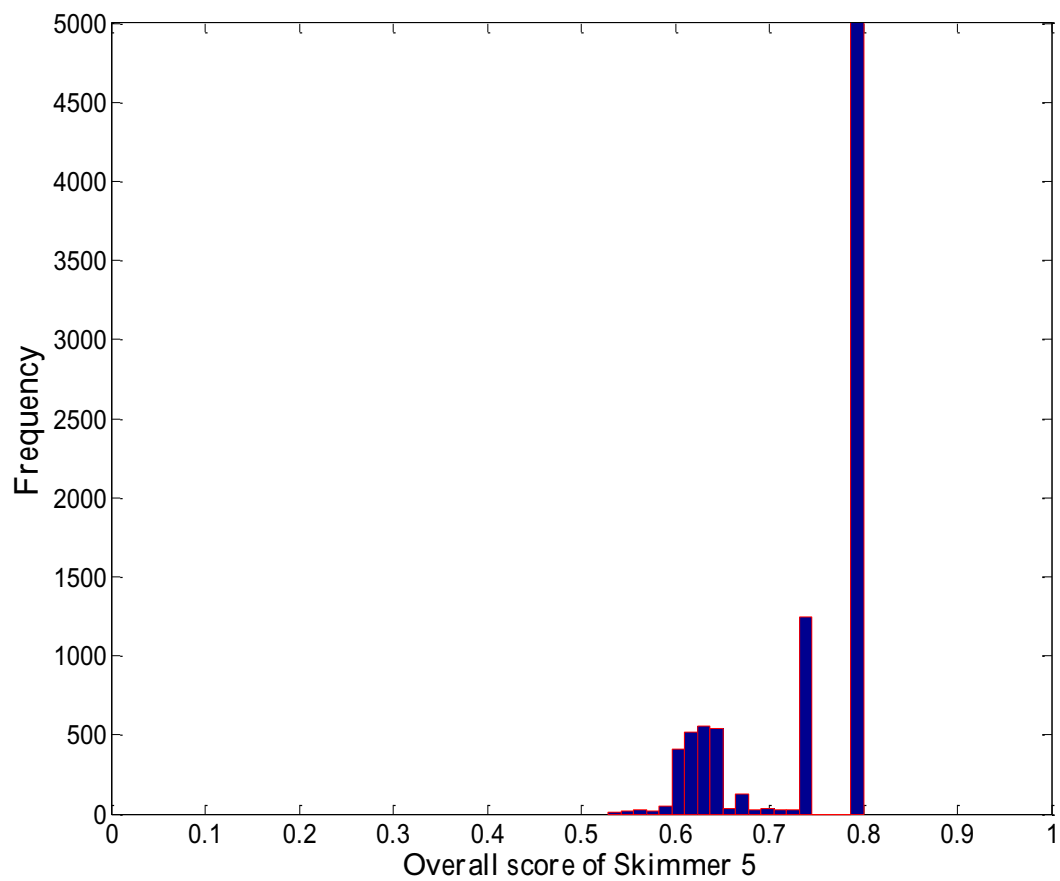
Figure A5.22 Distributions of overall scores of Skimmer 5 to Zone 5 ranked by MC-IRFAM
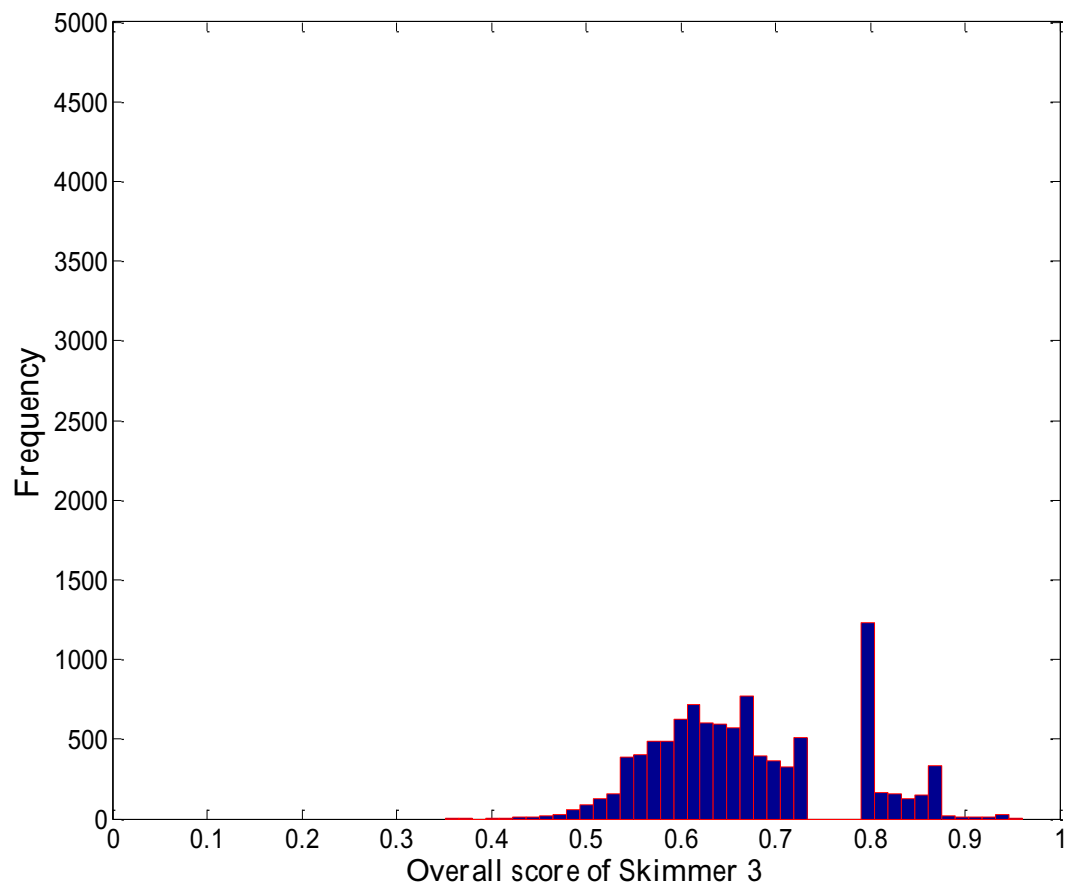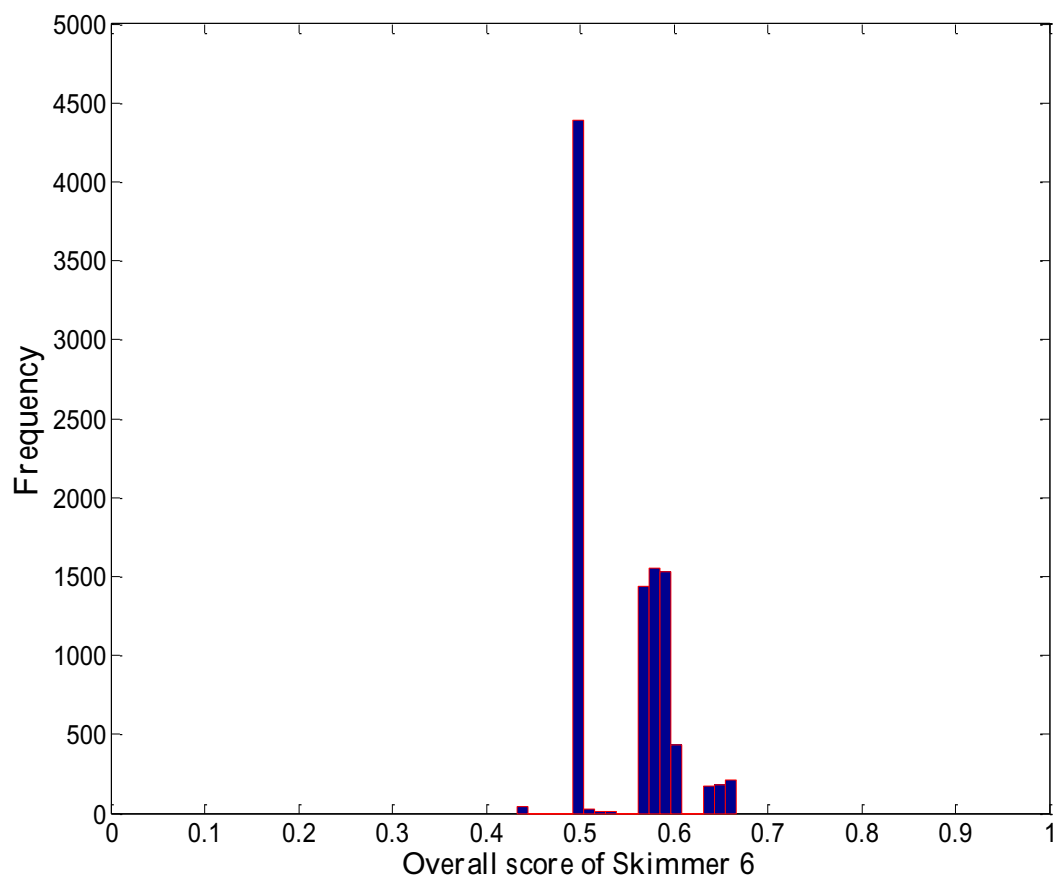
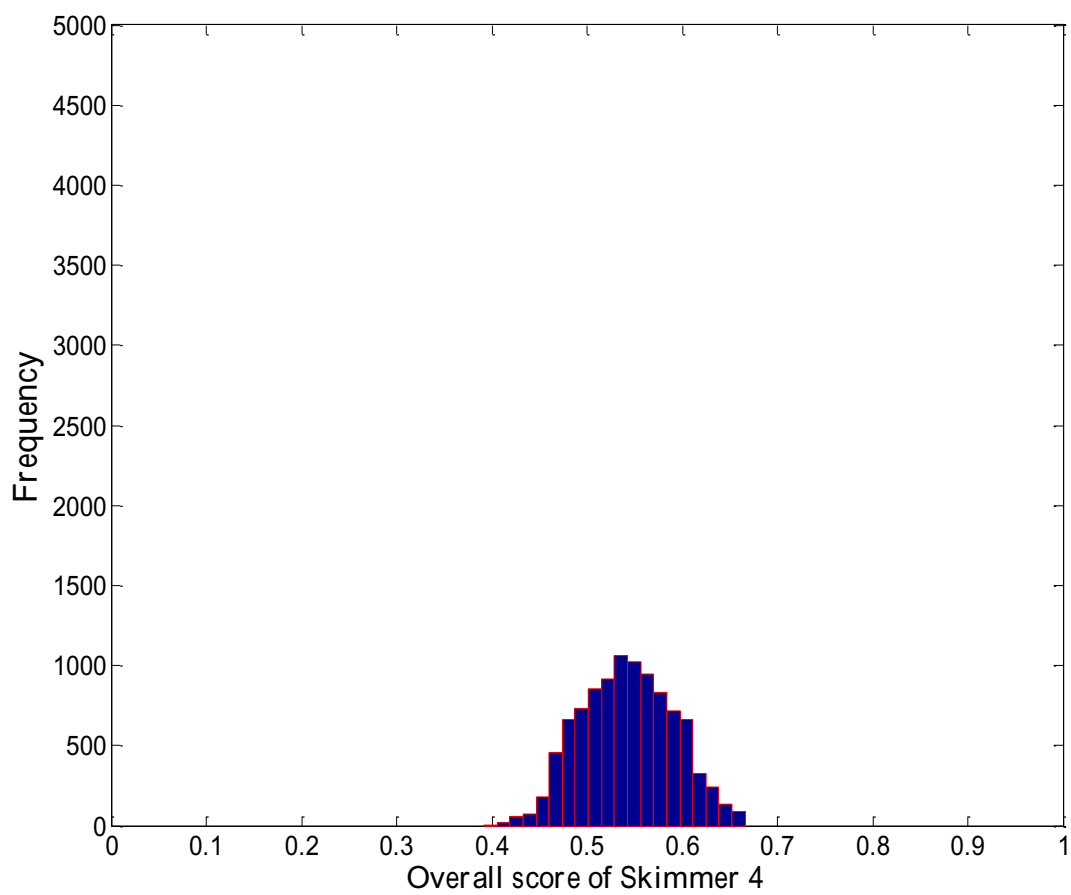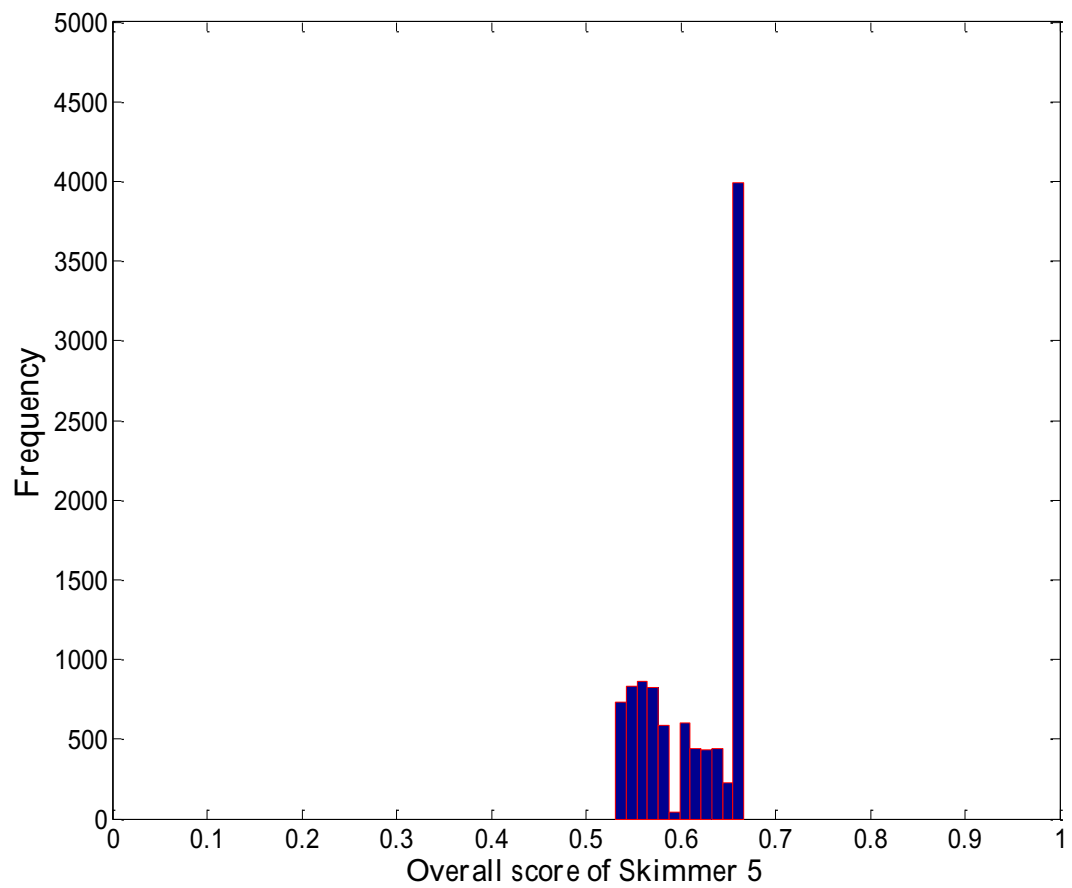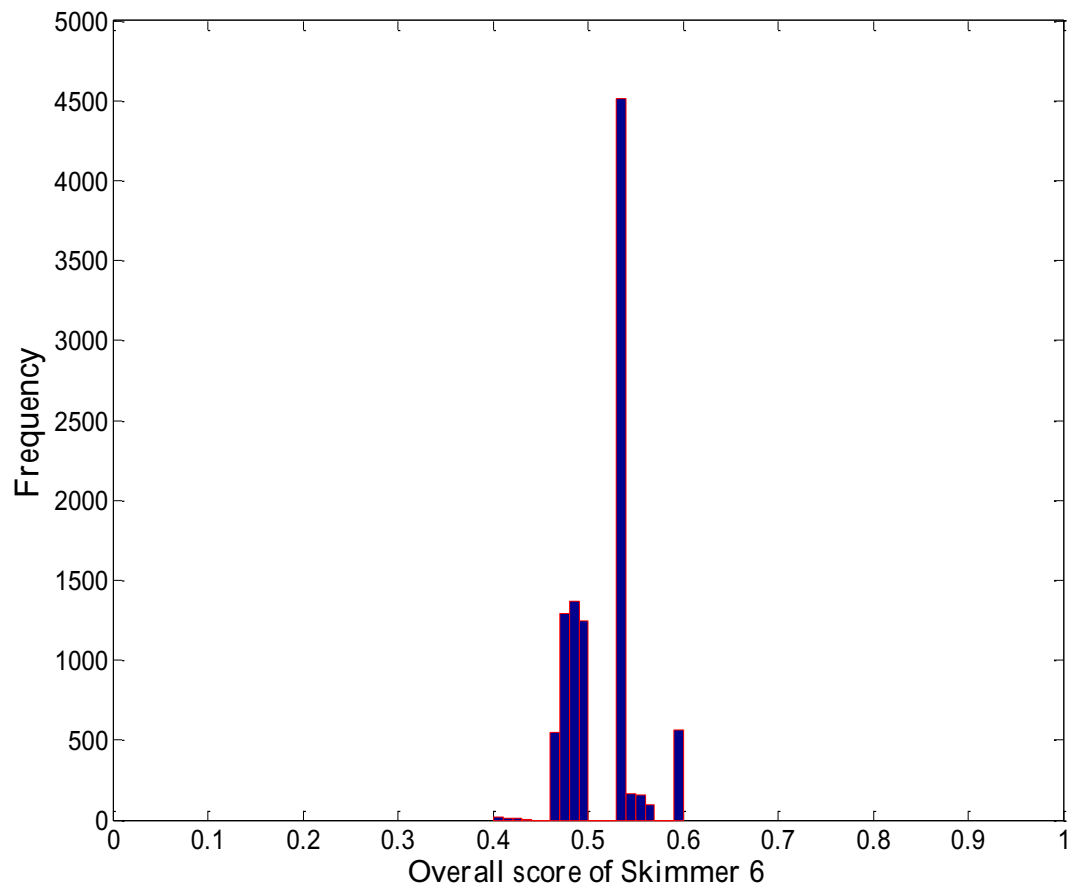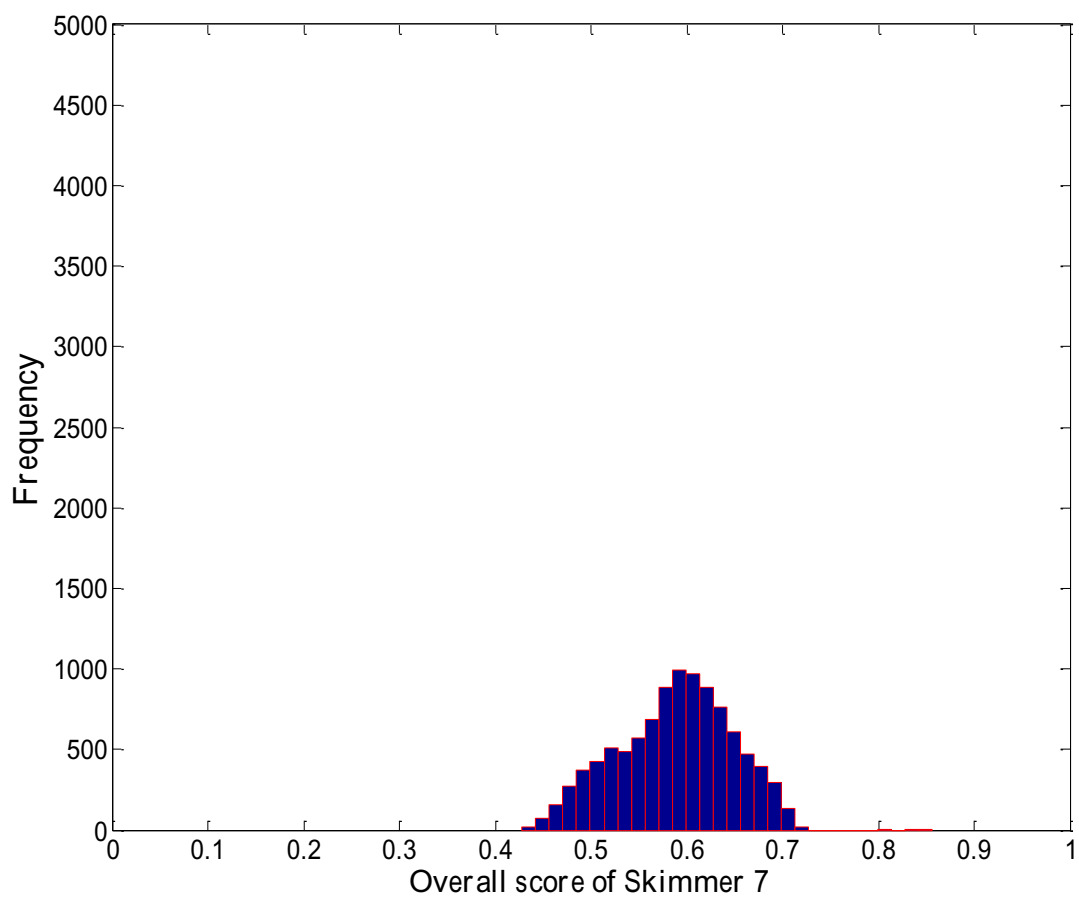Figure A5.23 Distributions of overall scores of Skimmer 6 to Zone 5 ranked by MC-IRFAM

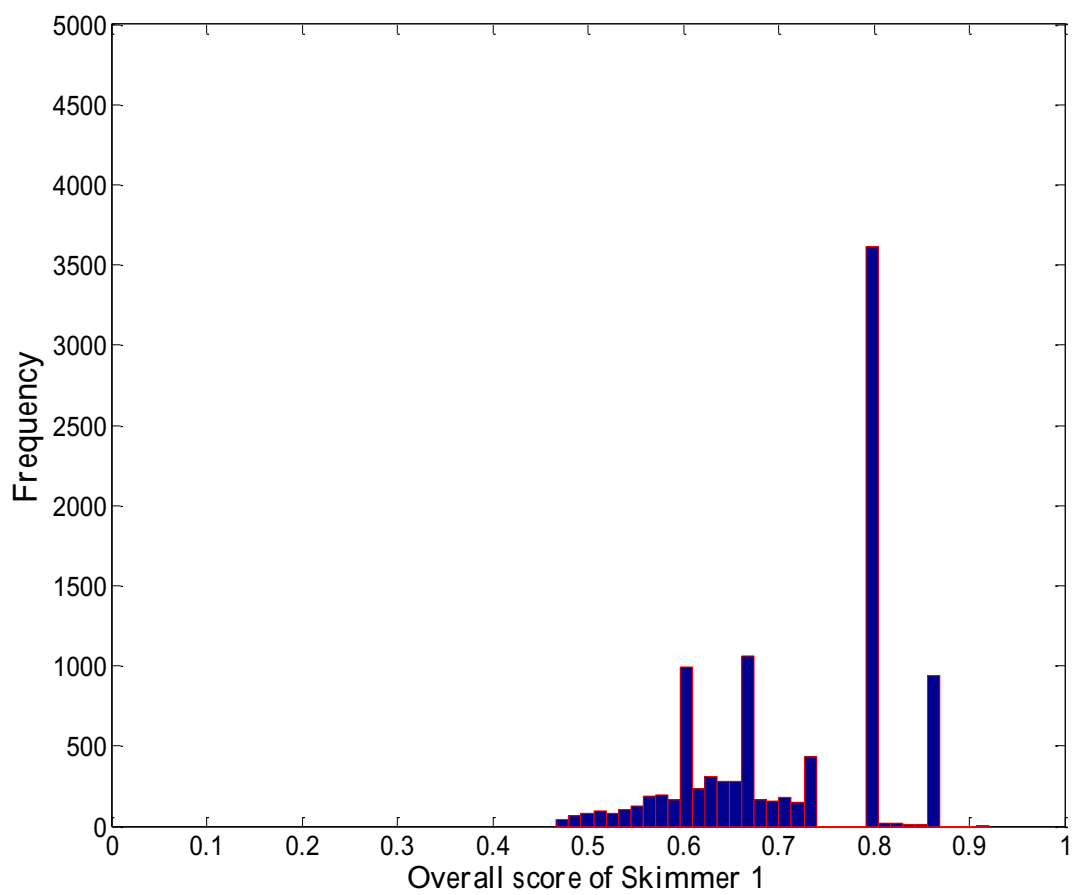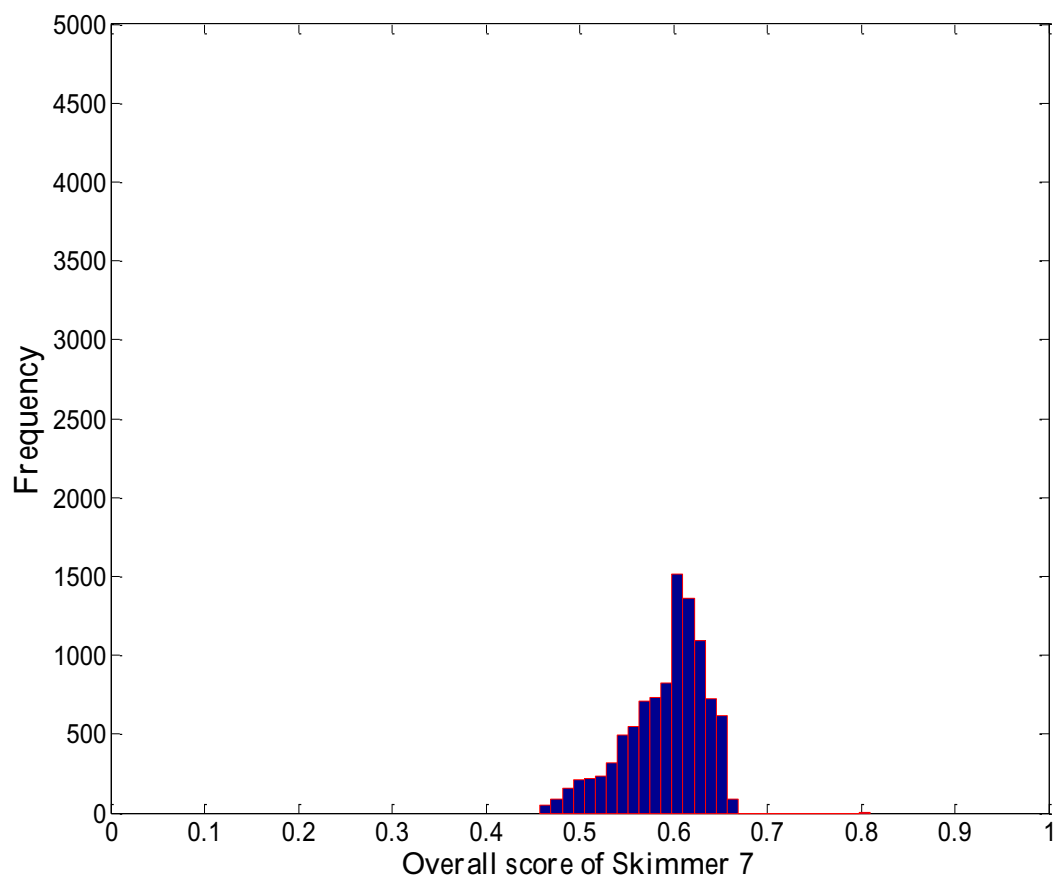Figure A5.24 Distributions of overall scores of Skimmer 7 to Zone 5 ranked by MC-IRFAM

REFERENCES

Abe S. (1997). Neural Networks and Fuzzy Systems: Theory and Applications. Kluwer Academic Publishers, 216pp.

Abe S. (2001). Pattern classification: Neuro-fuzzy methods and their comparison. Springer Verlag, 327pp.

Al-Rabeh A.H., Cekirge H.M., and Gunay N. (1989). A stochastic simulation model of oil spill fate and transport. Applied Mathematical Modelling, 13 (6): 322-329.

Al-Rabeh A.H., Cekirge, H.M., and Gunay N. (1992). Modeling the Fate and Transport of Al-Ahmadi Oil Spill. Water Air Soil Pollution, 65: 257-279.

Anderson H.L. (1986). Metropolis, Monte Carlo and the MANIAC. Los Alamos Science, 14: 96-108.

Andradottir S. (1998). Simulation optimization. Ed. J. Banks, Handbooks of Simulation: Principles, Methodology, Advances, Applications, and Practice, chapter 9. John Wiley & Sons, New York.

Angus W.D. and Mitchell H.G. (2010). *Facts do not justify banning Canada's current offshore drilling operations: A senate review in the wake of BP's Deepwater Horizon* incident. Eighth report of the Standing Senate Committee on Energy, the Environment and Natural Resources, Canada.

Assilzadeh H. and Mansor S.B. (2003). Oil spill contingency planning using geomatic system. In: Proceedings of the 13th Biennial Coastal Zone Conference, July 13-17,

2003, Baltimore, MD, USA.

Assilzadeh H., Mansor S.B., and Ibrahim H.M. (2001). Petroleum hazards management by geomatic systems. In: Proceedings of Asian Conference of Remote Sensing, ACRS2001, 5-9 November, 2001, Singapore, 358-363.

Asunción M.D.L., Castillo L., Fdez-Olivares J., García-Pérez O., González A., and Palao F. (2005). SIADEX: An interactive knowledge-based planner for decision support in forest fire fighting. AI Communications, 18(4): 257-268.

Atlas R.M. (1995). Petroleum Biodegradation and Oil Spill Bioremediation. Marine Pollution Bulletin, 31(4-12): 178-182.

Baeurle S.A. (2009). Multiscale modeling of polymer materials using field-theoretic methodologies: a survey about recent developments. Journal of Mathematical Chemistry, 46 (2): 363-426.

Bahri P. and Meybodi M.R. (1999). A method for adaptation of vigilance factor and choice parameters in fuzzy ART system. In: Proceedings of the 7th Iranian Conference on Electrical Engineering, May 12-14, 1999, Tehran, Iran, 17-27.

Bai Y.L., Wagener T., and Reed P. (2009). A top-down framework for watershed model evaluation and selection under uncertainty. Environmental Modelling & Software, 24(8): 901-916.

Baraldi A., Binaghi E., Blonda P., Brivio, P.A., and Rampini A. (2001). Comparison of

the multilayer perceptron with neuro-fuzzy techniques in the estimation of cover class mixture in remotely sensed data. IEEE Transaction on Geoscience and Remote Sensing, 39(5): 994-1005.

Baudrit C., Guyonnet D., and Dubois D. (2007). Joint propagation of variability and imprecision in assessing the risk of groundwater contamination. Journal of Contaminant Hydrology, 93: 72-84.

Beegle-Krause C.J. and O'Connor C. (2005). GNOME Data Formats and Associated *Example Data Files. NOAA Office of Respon*se and Restoration. Emergency Response Division, Seattle, WA, USA, 49 pp.

Bernardini A., Ferraro G., Meyer-Roux S., Sieber A., Tarchi D. (2005). Atlante *dell'inquinamento da idrocarburi nel Mare Adriatico*. European Commission Report EUR 21767 IT.

Berry A., Dabrowski T., and Lyons K. (2012). The oil spill model OILTRANS and its application to the Celtic Sea. Marine Pollution Bulletin, 64 (2012): 2489–2501.

Bertsekas D.P. (2005). Dynamic Programming and Optimal Control. Athena Scientific, 558pp.

Blair A.N., Ayyub B.M., and Bender W.J. (2001). Fuzzy stochastic risk-based decision analysis with the mobile offshore base as a case study. Marine Structures, 14(1): 69-88.

Blancato J.N., Power F.W., Brown R.N., Dary C.C. (2006). Exposure Related Dose Estimating Model (ERDEM) a Physiologically-Based Pharmacokinetic and Pharmacodynamic (PBPK/PD) Model for Assessing Human Exposure and Risk. EPA/600/R-06/061 (NTIS PB2006-114712), U.S. Environmental Protection Agency Washington, DC, USA.

Bly M. (2011). Deepwater Horizon Accident Investigation Report. DIANE Publishing, Darby, PA, USA.

Bock H.H. (1993), Classification and clustering: problems for the Future. In: New Approaches in Classification and Data Analysis, Eds.: Diday E., et al., Berlin: Springer, 3-24.

Bogdanovsky A, Wardrop J, Kochergin I, Pokrashenko S, Arshinov I, and Rybalko S. (2005). Progress in oil spill risk assessment for sakhalin shelf conditions. In: Proceedings of the 14th North Pacific Marine Science Organization (PICES) Annual Meeting, September 29-October 9, 2005, Vladivostok, Russia, 87-87.

Bonazountas M., Kallidromitou D., Kassomenos P., and Passas N. (2007). A decision support system for managing forest fire casualties. Journal of Environmental Management, 84(4): 412-418.

Boser B.E., Guyon I.M., and Vapnik V.N. (1992). A training algorithm for optimal margin classifiers. In: Proceedings of the 5th Annual ACM Workshop on Computational

Learning Theory, ACM Press, 144-152.

Boskovitz V., and Guterman H. (2002). An adaptive neuro-fuzzy system for automatic image segmentation and edge detection. IEEE Transaction on Fuzzy Systems, 10(2): 247-262.

Bragg J.R., Prince R.C., Harner E.J., and Atlas R.M. (1994). Effectiveness of bioremediation for the Exon Valdez oil spill. Nature, 368: 413-418.

Brandvik P.J., Sørheim K.R., Singsaas I., and Reed M. (2006). Short State-of-the-Art Report on Oil Spills in Ice-Infested Waters: Oil Behaviour and Response Options. SINTEF, Norway.

Brebbia C.A. (2001). Oil Spill Modeling and Processes. WIT Press: UK, 172pp.

Brekke C., and Solberg A. (2005). Oil spill detection by satellite remote sensing. Remote Sensing of Environment, 95: 1-13.

Brimicombe A. (2003). GIS, Environmental Modeling and Engineering. Taylor & Francis, London, 378pp.

Britain G. (2010). UK deepwater Drilling - Implications of the Gulf of Mexico Oil Spill. House of Commons energy and Climate Change Committee, United Kingdom.

Broje V.A. (2006). Optimization of mechanical oil spill recovery equipment under variable environmental conditions. Ph.D. Thesis, University of California, Santa Barbara, USA, 179pp.

Brown K. (2005). Safety first in marine spill response. In: Proceedings of 2005 International Oil Spill Conference, May 15-19, 2005, Miami Beach, Florida, USA, 983-987.

Buckley J.J., Hayashi Y., and Czogala E. (1992). On the equivalence of neural networks and fuzzy expert systems. In: Proceedings of the 1992 International Joint Conference on Neural Networks, June 7-11, 1992, Baltimore, Maryland, USA, 691-695.

Buist I., Potter S., and Nedwed T. (2011). Herding agents to thicken oil spills in drift ice for in situ burning: new developments. In: Proceedings of International Oil Spill Conference, May 23-26, 2011, Portland, Oregon, USA.

Bureau of Ocean Energy Management, Regulation and Enforcement (BOEMRE)/U.S. Coast Guard Joint Investigation Team (2011). Deepwater Horizon Joint Investigation Team Releases Final Report. U.S. Government, USA.

Bureau of Ocean Energy Management, Regulation and Enforcement (BOEMRE) (2010). The Drilling Safety Rule. Bureau of Ocean Energy Management, Regulation, and Enforcement, US.

Camilli R., Reddy C.M., Yoerger D.R., Van Mooy B.A.S., Jakuba M.V., Kinsey J.C., McIntyre C.P., Sylva S.P., and Maloney J.V. (2010). Tracking Hydrocarbon Plume Transport and Biodegradation at Deepwater Horizon. Science, 330 (6001): 201-204.

Canada-Newfoundland and Labrador Offshore Petroleum Board (C-NLOPB) (2011).

Canada-Newfoundland and Labrador Offshore Petroleum Board Annual Report
2010/07. St John's, NL, Canada.

Canada-Newfoundland and Labrador Offshore Petroleum Board (C-NLOPB) (2007).
Canada-Newfoundland and Labrador Offshore Petroleum Board Annual Report
2006/07. St John's, NL, Canada.

Canada-Newfoundland and Labrador Offshore Petroleum Board (C-NLOPB) (2008).
Canada-Newfoundland and Labrador Offshore Petroleum Board Annual Report
2007/08. St John's, NL, Canada.

Carpenter G. A. and Grossberg S. (2003). Adaptive resonance theory. The Handbook of
Brain Theory and Neural Networks, 2nd ed., edited by A. M. Arbib, 87-90,
Cambridge, MA: MIT Press.

Carpenter G., Gjaja M., Gopal S., and Woodcock C. (1997). ART networks in remote
sensing. Journal of IEEE Transactions on Geoscience and Remote Sensing, 35(2):
308-325.

Carpenter G.A and Grossberg S. (1987). Associative learning, adaptive pattern
recognition, and cooperative‑competitive decision making. Optical and Hybrid
Computing, 634: 218-247.

Carpenter G.A., Grossberg S., and Rosen D.B. (1991). Fuzzy ART: Fast stable learning
and categorization of analog patterns by an adaptive resonance system. Neural

Networks, 4: 759-771.

Carpenter G.A., Grossberg S., Markuzon N., Reynolds J.H., and Rosen D.B. (1992). Fuzzy ARTMAP: A neural network architecture for incremental supervised learning of analog multidimensional maps. IEEE Transactions on Neural Networks, 3: 698-713.

Castellet E.B.I., Valentín M.G., and Ripollés J.D. (2006). Decision support system for flood risk assessment and management. In: Proceedings of the 7th International Conference on Hydroinformatics, September 4-8, 2006, Nice, France.

Castro C.B., Segal B., Pires D.O., Medeiros M.S. (2006). Distribution and diversity of coral communities of the Abrolhos Reef Complex, Brazil. In: Eds.: Dutra G.F., Allen G.R., Werner T., and McKenna S.A., A rapid marine biodiversity assessment of the Abrolhos Reef Complex, Brazil. Washington: Conservation International, 19-39.

Chang N.B. and Lu H.Y. (1997). A new approach for long-term planning of solid waste management system using fuzzy global criterion. Journal of Environmental Science and Health, Part A. Toxic/Hazardous Substances and Environmental Engineering, 32: 1025-1047.

Chao X., Shanka J., and Cheong H.F. (2001). Two-and three-dimensional oil spill model for coastal waters. Ocean Engineering, 28(12): 1557-1573.

Chao X., Shankar J., Wang S.S.Y. (2003). Development and application of oil spill model

for singapore coastal waters. Journal of Hydraulic Engineering-ASCE, 129 (7): 495-503.

Chao X.; Shankar J.; and Cheong H.F. (2001). Two-and three-dimensional oil spill model for coastal waters. Ocean Engineering, 28(12): 1557-1573.

Chao X.; Shankar J.; and Wang S.S.Y. (2003). Development and application of oil spill model for singapore coastal waters. Journal of Hydraulic Engineering-ASCE, 129 (7): 495-503.

Chen B. and Li P. (2012). A Preliminary study on decision making for supporting oil spill diagnosis, warning and emergency response. Technical Report, Prepared for the Water Governance Program of United Nations Development Program (UNDP), 235pp.

Chen B., Li P., and Husain T. (2012a). Development of an integrated adaptive resonance theory mapping classification system for supporting watershed hydrological modeling. Journal of Hydrologic Engineering-ASCE, 17(6): 679-693.

Chen B., Li P., and Wu H.J. (2013). MCFP: a Monte Carlo Simulation based Fuzzy Programming Approach for Municipal Solid Waste Management under Dual Uncertainties of Possibility and Continuous Probability. Journal of Environmental Informatics. (Accepted)

Chen B., Zhang B.Y., Li P., Cai Q.H., Lin W.Y., and Liu B. (2012b). From challenges to

opportunities: towards future strategies and a decision support framework for oil spill preparedness and response in offshore Newfoundland and Labrador. Technical Report, Prepared for The Harris Centre, Memorial University of Newfoundland, Canada, 264 pages.

Chen H.Z., Li D.M., and Li X. (2007). Mathematical modeling of oil spill on the sea and application of the modeling in Daya Bay. Journal of Hydrodynamics, 19(3):282-291.

Chen Z., Huang G.H., and Chakma A. (2003). Hybrid fuzzystochastic modeling approach for assessing environmental risks at contaminated groundwater system. Journal of Environmental Engineering, 129(1): 79-88.

Cheng G.H., Huang G.H., Cao M.F., and Fan Y.R. (2009). Planning of municipal solid waste management systems under dual uncertainties: a hybrid interval stochastic programming approach. Stochastic Environmental Research and Risk Assessment, 236: 702-720.

Cleveland C. (2010). The challenges of oil spill response in the Arctic. National Commission on the BP Deepwater Horizon Oil Spill and Offshore Drilling, US.

Cohen Y., Mackay D., and Shiu W.Y. (1980). Mass transfer rates between oil slicks and water. The Canadian Journal of Chemical Engineering, 58: 569–574.

Costa L.R.T.A., Coppe V.J.M.F., Andrade F.N.P., and Hidroclean A.R.A. (2005). Strategic optimization and contingency planning model for oil-spill response. In: Proceedings

of SPE Latin American and Caribbean Petroleum Engineering Conference, 20-23
June, 2005, Rio de Janeiro, Brazil.

Craven M. and Shavlik J.W. (1993). Learning symbolic rules using artificial neural
networks. In: Proceedings of the 10th International Conference on Machine Learning,
June 27-29, 1993, Amherst, MA, USA.

Cybenko G. (1989). Approximation by superpositions of a sigmoidal function.
Mathematics of Control, Signals and Systems, 2: 303-314.

De Dominicis M., Pinardi N., Zodiatis G., and Archetti R. (2013a). MEDSLIK-II, a
Lagrangian marine surface oil spill model for short-term forecasting - Part 2:
Numerical simulations and validations. Geoscientific Model Development, 6:
1871-1888.

De Dominicis M., Pinardi N., Zodiatis G., and Lardner R. (2013b). MEDSLIK-II, a
Lagrangian marine surface oil spill model for short-term forecasting - Part 1: Theory.
Geoscientific Model Development, 6: 1851-1869.

De Souza D., Neto A., and Da Mata W. (2006). Intelligent system for feature extraction
of oil slicks in SAR images: speckle filter analysis. Neural Information Processing,
4233: 729-736.

DeCola E., Robertson T., Fletcher S., and Harvey S. (2006). Offshore Oil Spill Response
in Dynamic Ice Conditions. A Report to WWF on Considerations for the Sakhalin II

Project, Alaska, Nuka Research, 74pp.

Del Frate F., Petrocchi A., Lichtenegger J., and Calabresi G. (2000). Neural networks for oil spill detection using ERS-SAR data. IEEE Transactions on Geoscience and Remote Sensing, 5: 2282-2287.

Delvigne G.A.L. and Sweeney C.E. (1988). Natural dispersion of oil. Oil and Chemical Pollution, 4: 281–310.

Deng Z.G., Yu T., Jiang X.Y., Shi S.X., Jin J.Y., Kang L.C., and Zhang F. (2013). Bohai Sea oil spill model: a numerical case study. Marine Geophysical Research, 34(2): 115-125.

Department of Energy and Climate Change (DECC) (2010). UK Deepwater Drilling—Implications of the Gulf of Mexico Oil Spill. House of Commons, UK.

Depellegrin D. and Blazauskas N. (2013). Integrating ecosystem service values into oil spill impact assessment. Journal of Coastal Research, 29(4): 836-846.

Diday E. and Simon J.J. (1976). Clustering analysis. In: Digital Pattern Recognition, ed.: Fu K.S., Berlin: Springer, 47-94.

Diday E., and Govaert G. (1977). Classification automatique avec distances adaptatives. R.A.I.R.O. informatique Computer Science, 11: 329-349.

Dimakis N., Filippoupolitis A., and Gelenbe E. (2010). Distributed building evacuation simulator for smart emergency management. The Computer Journal, 53: 1384-1400.

Ding C. and He X.F. (2004). K-means Clustering via Principal Component Analysis. In: Proceedings of international Conference Machine Learning (ICML 2004), July 4-8, 2004, Banff, Alberta, Canada, 225-232.

Djennas M., Benbouziane M., and Djennas M. (2012). A neural network and genetic algorithm hybrid model for modeling exchange rate: the Dollar – Kuwaiti Dinar case. International Research Journal of Finance and Economics, 92(2012): 141-162.

Dubois D. and Prade H. (1988). Fuzzy Sets and Systems: Theory and Applications. Academic Press, 393pp..

Dunne A.R. (2007). A Statistical Approach to Neural Networks for Pattern Recognition. John Wiley & Sons, 30pp.

Edmonds B. (1995). What is Complexity? The philosophy of complexity per se with application to some examples in evolution. In: The Evolution of Complexity, Eds.: Heylighen F. and Aerts D., Kluwer, Dordrecht.

Edwards R. (1999). The sea empress oil spill: environmental impact and recovery. In: Proceeding of The International Oil Spill Conference 1999, March 7-12, 1999, Seattle, USA.

El-Zahaby A.M., Kabeel A.E., Bakry A.I., and Khaira A.M. (2011). Effect of disk offset angle on the hydrodynamic performance of rotating disk skimmers during oil spill recovery. Environmental Engineering Science, 28(2): 113-119.

Erminio D. and Guerrisi F. (2002). A fuzzy clustering algorithm based on the analogy with mechanical physics: MeccFuz. Quality and Quantity, 36(3): 239-257.

Ertekin S. and Rudin C. (2011). On equivalence relationships between classification and ranking algorithms. Journal of Machine Learning Research, 12(2011): 2905-2929.

Espedal H.A. and Wahl T. (1999). Satellite SAR oil spill detection using wind history information. International Journal of Remote Sensing, 20: 49-65.

Espedal H.A., and Johannessen J.A. (2000). Detection of oil spills near offshore installations using synthetic aperture radar (SAR). International Journal of Remote Sensing, 11: 2141-2144.

Essaid H.I., Bekins B.A., Godsy E.M., and Warren E. (1995). Simulation of aerobic and anaerobic biodegradation processes at a crude oil spill site. Water Resources Research, 31(12): 3309-3327.

Etkin D.S., and Welch J. (1997). Oil spill intelligence report international oil spill database: trends in oil spill volumes and frequency, In: Proceedings International Oil Spill Conference, April 8-10, 1997, Florida, USA, 949-952.

Everitt B. Landau A. and Leese M. (2009). Cluster Analysis. 4ed, Wiley, 256pp.

Fay J.A. (1971). Physical Processes in the Spread of Oil on a Water Surface. In: Proceedings of the Joint Conference on Prevention and Control of Oil Spills, June 15-17, 1971, Washington, D.C., USA, 463-467.

Fernando P.M., Arturo M.Q.M., Enrico C.P., Carlos H.B., Pamela W., and Luis M.M. (2004). Analysis of RADARSAT-1 data for offshore monitoring activities in the Cantarell Complex, Gulf of Mexico, using the unsupervised semivariogram textural classifier (USTC). Canadian Journal of Remote Sensing, 30(3): 424-436.

Fernando W.G.D., Ramarathnam R., Krishnamoorthy A.S., and Savchuk S. (2005). Identification and use of bacterial organic volatiles in biological control of Sclerotinia sclerotiorum. Soil Biology & Biochemistry, 37(2005): 955-964.

Ferraro G., Bernardini A., David M., Meyer-Roux S., Muellenhoff O., Perkovic M., Tarchi D., and Topouzelis K. (2007). Towards an operational use of space imagery for oil pollution monitoring in the Mediterranean basin: a demonstration in the Adriatic Sea. Marine Pollution Bulletin, 54: 403-422.

Ferraro G., Bernardini A., Meyer-Roux S., Tarchi D. (2006). Satellite Monitoring of Illicit Discharges from Vessels in the French Environmental Protection Zone (ZPE) 1999-2004. European Commission Report EUR 22158 EN.

Fingas M.F. (1995). A literature review of the physics and predictive modelling of oil spill evaporation. Journal of Hazardous Materials, 42 (1995): 157-175.

Fingas M.F. (2001). The Basics of Oil Spill Cleanup. Lewis, New York, USA, 233pp.

Fingas M.F. (2010). Oil Spill Science and Technology. Wiley-Blackwell, Mississauga, Ontario, Canada, 704pp.

Fingas M.F. (2011). Oil spill science and technology: prevention, response, and cleanup. Elsevier/Gulf Professional Publishing, 1156pp.

Fiscella B., Giancaspro A., Nirchio F., and Trivero P. (2000). Oil spill detection using marine SAR images. International Journal of Remote Sensing, 21: 3561-3566.

Fischer H.B., List E.J., Yikoh R.C., Imberger J., and Brooks N.H. (1979). Mixing in Inland and Coastal Waters. Aacdemic Press, New York, NY, 483pp.

Fisheries and Oceans Canada (2010). Audit of the Canadian Coast Guard - Environmental Response Services (6B091). Fisheries and Oceans Canada, Canada.

Flinders Ports (2012). Oil Spill Contingency Plan. Flinders Ports, Australia.

Franco-Lopez H., Ek A.R., and Bauer M.E. (2001). Estimation and mapping of forest stand density, volume, and cover type using the k-nearest neighbors method. Remote Sensing of Environment, 77(3): 251-274.

Freeze A., Massmann J., Smith L., Sperling T., and James B. (1991). Hydrogeological decision analysis: 1. A framework. Ground Water, 28 (5): 738-766.

French-McCay D.P. (2004). Oil Spill Impact Modeling: Development and Validation. Environmental Toxicology and Chemistry, 23(10): 2441–2456.

Friedman M. and Kandel A. (1999). Introduction to pattern recognition: statistical, structural, neural, and fuzzy logic approaches. World Scientific Publishing, 329pp.

Fu M. (1994). Optimization via simulation: a review. Annals of Operations Research, 53:

199-248.

Fu M. (2002). Optimization for simulation: theory vs. practice. INFORMS Journal on Computing, 14(3): 192-215.

Fu M. and Hu J. (1995). Sensitivity analysis for Monte Carlo simulation of option pricing. Probability in the Engineering and Information Sciences, 9(3): 417-446.

Funahashi K. (1989). On the approximate realization of continuous mappings by neural networks. Neural Networks, 2(3): 183-192.

Furnkranz J., Hullermeier E., Mencia E.L., and Brinker K. (2008). Multilabel Classification via Calibrated Label Ranking. Machine Learning, 73(2): 133-153.

Gade M. and Alpers W. (1999). Using ERS-2 SAR images for routine observation of marine pollution in European coastal waters. Science of the Total Environment, 237-238: 441-448.

Galeev A.D. and Ponikorov S.I. (2011). Numerical Analysis of the Process of Heated Oil Evaporation from the Emergency Spill Surface. Journal of Engineering Physics and Thermophysics, 84(6): 1398-1407.

Galt J.A., Watabayashi G.Y., Payton D.L. and Petersen J.C. (1991). Trajectory analysis for the Exxon Valdez: Hindcast study. In: Proceedings of International Oil Spill Conference, March 4-7, 1991, San Diego, California, 629-634.

Gamba P. and Dellacqua F. (2003). Increased accuracy multiband urban classification

using a neuro-fuzzy classifier. International Journal of Remote Sensing, 24(4): 827-834.

Garthwaite P., Kadane J., and O'Hagan A. (2005). Statistical methods for eliciting probability distributions. Journal of the American Statistical Association, 100: 680–701.

Geng L., Chen Z., Chan C.W., and Huang G.H. (2001). An intelligent decision support system for management of petroleum contaminated sites. Expert System with Applications, 20: 251-260.

Ghosh A., Pal N.R., and Pal S.K. (1993). Self-organization for object extraction using a multilayer neural network and fuzziness measures. IEEE Transaction on Fuzzy Systems, 1(1): 54-69.

Giles M.F. (1995). Land cover classification by an artificial neural network with ancillary information. International Journal of Geographical Information Systems, 9(5): 527-542.

Gkonis K.G., Kakalis N.M.P., Ventikos N.P., Ventikos Y., and Psaraftis H.N. (2007). A model-based approach for tactical decision making in oil spill response. In: International Symposium on Maritime Safety, Security & Environmental Protection, September 20-21, 2007, Athens, Greece.

Goncharov V.K. (2009). Simulation of oil drops dynamics in seawater environment.

Journal of Marine Engineering and Technology, 2009(15): 21-28.

Gopal S., Woodcock C. and Strahler A. (1999). Fuzzy ARTMAP classification of global land cover from the 1 degree AVHRR data set. Remote Sensing of Environment, 67: 23-43.

Gordon A.D (1999). Bisimilarity as a Theory of Functional Programming. Theoretical Computer Science, 228(1-2): 5-47.

Gosavi A. (2003). Simulation-Based Optimization: Parametric Optimization Techniques and Reinforcement Learning, Springer, 554pp.

Government of Australia (2005). National Marine Oil Spill Contingency Plan. AMS.9001.0001.0028. Australia.

Government of Norway (1981). Pollution Control Act. Government of Norway, Norway.

Government of United Kingdom (1998). The Merchant Shipping (Oil Pollution Preparedness, Response and Co-operation Convention) Regulations 1998 (SI 1998/1056). Government of United Kingdom, UK.

Government of United Kingdom (2002). The Offshore Installations (Emergency Pollution Control) Regulations 2002 (SI 2002/1861). Government of United Kingdom, UK.

Griggs J.W. (2011). BP Gulf of Mexico Oil Spill. Energy Law Journal, 31(1): 57-79.

Grimm V., Ashauer R., Forbes V., Hommen U., Preuss T.G., Schmidt A., Brink P.J., Wogram J., Thorbek P. (2009). CREAM: a European project on mechanistic effect

models for ecological risk assessment of chemicals. Environmental Science and Pollution Research, 16(6): 614-617.

Grossberg S. (1976). Adaptive pattern classification and universal recoding, 1: Parallel development and coding of neural feature detectors. Biological Cybernetics, 23: 187-202.

Grossberg S. (1980). Intracellular mechanisms of adaptation and self-regulation in self-organizing networks: The role of chemical transducers. Bulletin of Mathematical Biology, 42: 365-396.

Gundlach E.R. and Hayes M.O. (1978). Vulnerability of coastal environments to oil spill impacts. Marine Technology Society Journal, 12: 18-27.

Guo P. and Huang G.H. (2009). Inexact fuzzy-stochastic mixed-integer programming approach for long-term planning of waste management - Part A: Methodology. Journal of Environmental Management, 91(2): 461-470.

Guo P., Huang G.H., Zhu H., and Wang X. L. (2010). A two-stage programming approach for water resources management under randomness and fuzziness. Environmental Modelling and Software, 25: 1573-1581.

Guo W.J. and Wang Y.X. (2009). A numerical oil spill model based on a hybrid method. Marine Pollution Bulletin, 58 (2009): 726–734.

Guyonnet D., Bourgigne B., Dubois D., Fargier H., Come B., and Chiles J. (2003).

Hybrid approach for addressing uncertainty in risk assessments. Journal of Environmental Engineering, 129(1): 68-78.

Hajovsky R., Filipova B., Pies M., and Ozana, S. (2012). Using Matlab for thermal processes modeling and prediction at mining dumps. In: Proceedings of the 12th International Conference on Control, Automation and Systems (ICCAS), October 17-21, 2012, Jeju Island, Korea, 584 - 587.

Han J., Lee S., Chi K., and Ryu K. (2002). Comparison of neuro-fuzzy, neural network, and maximum likelihood classifiers for land cover classification using IKONOS multispectral data. Geoscience and Remote Sensing Symposium, 6: 24-28.

Hänninen S. and J. Sassi (2010). Acute Oil Spills in Arctic Waters–Oil Combating in Ice, VTT Technical Research Centre of Finland report prepared for the Research Council of Norway, 64pp.

Hashemi S.S, Baghernejad M., Pakparvar M., and Emadi M. (2007). GIS classification assessment for mapping soils by satellite images. In: Proceedings of Middle East Spatial Technology, 4th Conference & Exhibition, December 10-12, 2007, Manama, Bahrain.

Helsel D.R. and Hirsch R.M. (2002). Statistical Methods in Water Resources. Techniques of Water Resources Investigations, Book 4, chapter A3., U.S. Geological Survey, 522pp.

Hernandez J.Z. and Serrano J.M. (2001). Knowledge-based models for emergency management systems. Expert Systems with Applications, 20(2): 173-186.

Hollnagel E. and Woods D.D. (2006). Epilogue: Resilience Engineering Precepts. In: Resilience engineering: concepts and precepts, Eds.: Leveson N., Hollnagel E., and Woods D.D., Aldershot: Ashgate , 347 - 358.

Hornik K., Stinchcombe M., and White H. (1989). Multilayer feedforward networks are universal approximators. Neural Networks, 2(5): 359-366.

Howlett E., Jayko K., and Spaulding M.L. (1993). Interfacing real-time information with OILMAP. In: Proceedings of the 16th Arctic and Marine Oil Spill Program Technical Seminar, June 7-9, 1993, Edmonton, Alberta, Canada, 517-527.

Hu J. (1995): Methods of Generating Surfaces in Environmental GIS Applications. In: Proceeding of 1995 Esri User Conference, May 22-26, 1995, Palm Springs, CA, USA.

Huang G.H., Baetz B. W. and Patry G.G. (1992). An interval linear programming approach for municipal solid waste management planning under uncertainty. Civil Engineering and Environmental Systems, 9: 319-335.

Huang G.H., Baetz B.W. and Patry G.G. (1993). A grey fuzzy linear programming approach for municipal solid waste management planning under uncertainty. Civil Engineering and Environmental Systems 10: 123-146.

Huang G.H., Sae-Lim N., Liu L., and Chen Z. (2001). An interval-parameter fuzzy-stochastic programming approach for municipal solid waste management and planning. Environmental Modeling and Assessment, 6: 271-283.

Huang J.C. (1983). A review of the state-of-the-art of oil spill fate/behavior models. In: Proceedings of the International Oil Spill Conference, February 28-March 3, 1983, San Antonio, Texas, USA, 313-322.

Huang J.C. and Monastero F.C. (1982). Review of the State-of-the Art of Oil Spill Simulation Models. Technical report submitted to the American Petroleum Institute, by Raytheon Ocean Systems Co., East Providence, R.I., USA.

Humphrey B., Owens E., and Sergy G. (1993). Development of a stranded oil in coarse sediment model. In: Proceedings of the International Oil Spill Conference, March 13-15, 1973, Washington, DC, 1993(1): 573-582.

Huntington H.P. (2008). Arctic Oil and Gas 2007 Overview Report. Arctic Monitoring and Assessment Program (AMAP), Norway.

Iakovou E., Douligeris C., and Korde A. (1994). A synthesis of decision models for analysis, assessment, and contingency planning for oil spill incidents. Omega, 22(5): 457-470.

IMO (International Maritime Organization) (2010). Manual on Oil Spill Risk Evaluation and Assessment of Response Preparedness. International Maritime Organization.

IMO Publishing: London, UK.

Inan A., and Balas L. (2010). Numerical Modelling of Oil Spill. In: Proceedings of the 5th IASME / WSEAS, February 23-25, 2010, Cambridge, UK.

International Association of Oil and Gas Producers (OGP) (2013).Coordinate Conversions and Transformations including Formulas. International Association of Oil and Gas Producers, OGP Publication 373-7-2, 142pp.

Iskander M.G. (2005). A suggested approach for possibility and necessity dominance indices in stochastic fuzzy linear programming. Applied Mathematics Letters, 18: 395-399.

Ivanov A.Y. and Zatyagalova V.V. (2008). A GIS approach to mapping oil spills in a marine environment. International Journal of Remote Sensing, 29(21): 6297-6313.

Jaber A., Guarnieri F., and Wybo J.L. (2001). Intelligent software agents for forest fire prevention and fighting. Safety Science, 39(2001): 3-17.

Jain A.K., Murty M.N., and Flynn P.J. (1999). Data Clustering: A Review. ACM Computing Surveys, 31: 264-323.

Jeffrey J.D., Kristen L.U., and Donna M.R. (2004). A watershed classification system using hierarchical artificial neural networks for diagnosing watershed impairment at multiple scales. In: Proceedings of The 2004 World Water and Environmental Resources Congress, June 27-July 1, 2004, Salt Lake City, UT, USA.

Jing L., Chen B., Zhang B.Y., and Li P. (2012a). A stochastic simulation-based hybrid interval fuzzy programming approach for optimizing the treatment of recovered oily water. Journal of Ocean Technology, 7(4): 59-72.

Jing L., Chen B., Zhang B.Y., and Li P. (2013). A hybrid stochastic-interval analytic hierarchy process (SIAHP) approach for prioritizing the strategies of reusing treated wastewater. Mathematical Problems in Engineering, 2013 (2013): 1-10.

Jing L., Chen B., Zhang B.Y., and Peng H.X. (2012b). A review of ballast water management practices and challenges in harsh and arctic environments. Environmental Reviews, 20: 83-108.

Jing L., Chen B., Zhang B.Y., Li P., and Zheng J.S., (2012c). A Monte Carlo simulation aided analytic hierarchy process (MC-AHP) approach for best management practices assessment in nonpoint source pollution control. Journal of Environmental Engineering-ASCE, 139(5): 618-626.

Jonckheere A.R. (1954). A distribution-free k-sample test against ordered alternatives. Biometrika, 41: 133-145.

Kappa N.M, Sabourina R., and Maupinb P. (2012). A dynamic model selection strategy for support vector machine classifiers. Applied Soft Computing, 12(2012): 2550-2565.

Karathanassi V., Topouzelis K., Pavlakis P., and Rokos D. (2006). An object-oriented methodology to detect oil spills. International Journal of Remote Sensing, 27:

5235-5251.

Keller A.A. and Clark K. (2008). Oil recovery with novel skimmer surfaces under cold climate conditions. In: Proceedings of International Oil Spill Conference, May 4-8, 2008 Savannah, Georgia, USA, 667-671.

Keller J.K., and Hunt D.J. (1985). Incorporating fuzzy membership functions in to the perceptron algorithm. IEEE Transaction on Pattern Analysis Machine Intelligence, 7(6): 693-699.

Keramitsoglou I., Cartalis C., and Kiranoudis C. (2006). Automatic identification of oil spills on satellite images. Environmental Modelling & Software, 21: 640-652.

Khan I.F., Sadiq R., and Husain T. (2002). Risk-based process safety assessment and control measures design for offshore process facilities. Journal of Hazardous Materials, 94(1): 1-36.

Kim P. and Ding Y. (2005). Optimal engineering system design guided by data-mining methods. Technometrics, 47(3): 336-348.

Kolluru V.S., Spaulding M.L., and Anderson E.L. (1994). A three-dimensional oil dispersion model using a particle based approach. In Proceedings of the 17th Arctic and Marine Oil Spill Program Technical Seminar, June 8-10, 1994, Vancouver, British Columbia, Canada, 867-894.

Korotenko K.A., Mamedov R.M., and Mooers C.N.K. (2001). Prediction of the Dispersal

of Oil Transport in the Caspian Sea Resulting from a Continuous Release. Spill Science & Technology Bolletin, 6(5): 323-339.

Koutseris E., Filintas Ag., and Dioudis P. (2010). Antiflooding prevention, protection, strategic environmental planning of aquatic resources and water purification: the case of Thessalian basin, in Greece. Desalination, 250 (2010): 318-322.

Kraskov A., Stögbauer H., Andrzejak G.R., and Grassberger P. (2003). Hierarchical Clustering Based on Mutual Information. ArXiv q-bio, 11pp.

Kumar T.S., Kumar C.P., and Nayak S. (2010). Performance of the Indian tsunami early warning system. The International Archives of the Photogrammetry, Remote Sensing and Spatial Information Science, 38(8): 271-274.

Kuncheva L.I. (2000). Fuzzy classifier design. Springer-Verlag, 315pp.

Landis W.G. and Kaminski L.A. (2007). Population-Scale assessment endpoints in ecological risk assessment Part II: selection of assessment endpoint attributes. Integrated Environmental Assessment and Management, 3(3): 450-457.

Law A. and Kelton W. (2000). Simulation Modeling and Analysis. McGraw-Hill, 760pp.

Law R.J., Kirby M.F., Moore J., Barry J., Sapp M. and Balaam J. (2011). PREMIAM – Pollution Response in Emergencies Marine Impact Assessment and Monitoring: Post-incident monitoring guidelines. Science Series Technical Report, Cefas, Lowestoft,146: 164pp.

Lee H.K. (2000). Consistency of Posterior Distributions for Neural Networks. Neural Networks, 13(6): 629-642.

Lee S.G., Jong G.H. Kwang H.C., Jae Y.S., Hee H.L., Michio M. and Kageo A. (1999). A neuro-fuzzy classifier for land cover classification. In: Proceedings of Fuzzy Systems Conference, August 11-25, 1999, Seoul, Korea.

Leech M., Walker M., Wiltshire M., Tyler A. (1993). OSIS: A Windows 3 Oil Spill Information System. In: Proceedings of 16th Arctic Marine Oil Spill Program Technical Seminar, Ottawa, ON, Canada, 549-572.

Lehr W.J., Fraga R.J., Belen M.S. and Cekirge H.M. (1984). A new technique to estimate initial spill size using a modified Fay-type spreading formula. Marine Pollution Bulletin, 15: 326-329.

LGL (2010), Southern Newfoundland Strategic Environmental Assessment. LGL Rep. SA1037, Canada-Newfoundland and Labrador Offshore Petroleum Board, St. John's, Newfoundland and Labrador, Canada, 333pp.

Li J. (2001). A GIS planning model for urban oil spill management. Water Science and Technology, 43(5): 239-244.

Li J.B., Huang G.H., Zeng G., Maqsood I., Huang Y.F. (2007). An integrated fuzzy-stochastic modeling approach for risk assessment of groundwater contamination. Journal of Environmental Management, 82: 173-188.

Li P. and Chen B. (2011). FSILP: fuzzy-stochastic-interval linear programming for supporting municipal solid waste management. Journal of Environmental Management, 92(4): 1198-1209.

Li P., Chen B., and Husain T. (2009a). Development of two-stage ART-ARTMap classification system for supporting watershed management. In: Proceedings of CSCE 2009 Annual General Conference, GC-094, May 27-30, 2009, St John's, Canada.

Li P., Chen B., and Husain T. (2011). IRFAM: an integrated rule-based fuzzy adaptive resonance theory mapping system for watershed modeling. Journal of Hydrologic Engineering-ASCE, 16(1): 21-32.

Li P., Chen B., and Zhang B.Y. (2013a). An integrated rule-based adaptive resonance theory mapping approach for technologies screening in offshore oil spill response. In: Proceedings of CSCE 2013 General Conference, May 29 to June 1, 2013, Montréal, Québec, Canada.

Li P., Chen B., Li Z.L., Wu H.J., and Zheng X. and Jing L. (2013b). A Monte Carlo simulation based two-stage adaptive resonance theory mapping model for site classification in offshore oil spill monitoring. Marine Pollution Bulletin. (Sbumitted)

Li P., Chen B., Zhang B.Y., Jing L., and Zheng J.S. (2012a). Development of a multiple-stage simulation based mixed integer nonlinear programming approach for supporting offshore oil spill recovery. In: Proceedings of the 35th AMOP Technical

Seminar on Environmental Contamination and Response, June 5-7, 2012, Vancouver, British Columbia, Canada, 434-447.

Li P., Chen B., Zhang B.Y., Jing L., and Zheng J.S. (2013c). Monte Carlo simulation-based dynamic mixed integer nonlinear programming for supporting oil recovery and devices allocation during offshore oil spill responses, Ocean & Coastal Management, Paper ID: OCMA-D-13-00290. (Accepted)

Li P., Chen B., Zhang, B.Y., Jing, L., and Zheng, J.S., (2012b). A multiple-stage simulation –based mixed integer nonlinear programming approach for supporting offshore oil spill recovery with weathering process. Journal of Ocean Technology, 7(4): 88-105.

Li P., Wu H.J., and Chen B. (2013d). RSW-MCFP: a resource-oriented solid waste management system for a mixed rural-urban area through Monte Carlo simulation-based fuzzy programming. Mathematical Problems in Engineering, 2013(2013): 1-12.

Li Y., Brimicombe A.J., and Rlphs M.P. (2000). Spatial data quality and sensitivity analysis in GIS and environmental modeling: the case of coastal oil spills. Computers, Environment and Urban Systems, 24(2): 95-108.

Li Y.P., Huang G.H., and Nie S.L. (2007). Mixed interval-fuzzy two-stage integer programming and its application to flood-diversion planning. Engineering

Optimization, 39(2): 163-183.

Li Y.P., Huang G.H., Huang Y.F., and Zhou H.D. (2009b). A multistage fuzzy-stochastic programming model for supporting sustainable water-resources allocation and management. Environmental Modelling & Software, 24: 786-797.

Li Y.P., Huang G.H., Nie S.L., Nie X.H., and Maqsood I. (2006). An interval-parameter two-stage stochastic integer programming model for environmental systems planning under uncertainty. Engineering Optimization, 38(4): 461-483.

Li Y.P., Huang G.H., Yang Z.F., and Nie S.L. (2008). An integrated two-stage optimization model for the development of long-term waste-management strategies. Science of the Total Environment, 3392: 175-186.

Lin C.T. and Lee C.S.G. (1991). Neural-network-based fuzzy logic control and decision system. IEEE Transactions on Computers, 40(12): 1320-1336.

Lin G.H., Chen X.J., and Fukushima M. (2009). Solving stochastic mathematical programs with equilibrium constraints via approximation and smoothing implicit programming with penalization. Mathematical Programming, 116: 343-368.

Liu B. (2001). Fuzzy random chance-constrained programming. IEEE Transactions on Fuzzy Systems, 9: 713-726.

Liu B. and Liu Y.K. (2002). Expected value of fuzzy variable and fuzzy expected value models. IEEE Transactions on Fuzzy Systems, 10: 445-450.

Liu L., Cheng S.Y., and Guo H.C. (2004). A simulation-assessment modeling approach for analyzing environmental risks of groundwater contamination at waste landfill sites. Human and Ecological Risk Assessment, 10(2): 373-388

Liu Y.K. and Liu B. (2005). Fuzzy random programming with equilibrium chance constraints. Information Sciences, 170: 363-395.

Liu Z.F., Huang G.H., Nie X.H., and He L. (2009). Dual-interval linear programming model and its application to solid waste management planning. Environmental Engineering Science, 26(6): 1033-1045.

Lloyd S. (2006). Programming the Universe: A Quantum Computer Scientist Takes On the Cosmos. Knopf, 240pp.

Long M.D. (2012). Remote Sensing for Offshore Marine Oil Spill Emergency Management, Security and Pollution Control. Business Development for The Americas, Optimare Senso systeme, AG., Bremerhaven, Germany.

Lonin S.A. (1999). Lagrangian model for oil spill diffusion at Sea. Spill Science and Technology Bulletin, 5(5-6): 331-336.

Lu H.J., Setiono R., and Liu H. (1996). Effect data mining using neural networks. IEEE Transaction on knowledge and data engineering, 8: 957-961.

Lucas L.A., Centeno T.M., and Delgado M.R., (2008). General type-2 fuzzy classifiers to land cover classification. In: Proceedings of the 2008 ACM symposium on Applied

computing, March 16-20, 2008, Fortaleza, Ceara, Brazil.

Luhandjula M.K. (1996). Fuzziness and randomness in an optimization framework. Fuzzy Sets and Systems, 77: 291-297.

Luhandjula M.K. (2004). Optimization under hybrid uncertainty. Fuzzy Sets and Systems, 146: 187-203.

Lv Y., Huang G.H., Li Y.P., Yang Z.F., and Li C.H. (2009). Interval-based air quality index optimization model for regional environmental management under uncertainty. Environmental Engineering Science, 26(11): 1585-1597.

Mackay D. and McAuliffe C.D. (1988). Fate of hydrocarbons discharged at sea. Oil & Chemical Pollution, 5: 1-20.

Mackay D., Paterson S., and Nadeau S. (1980). Calculation of the evaporation rate of volatile liquids. In: Proceedings of National Conference on Control of Hazardous Material Spills, May 13-15, 1980, Louisville, Kentucky, USA, 364-368.

Mandic D. and Chambers J. (2001). Recurrent Neural Networks for Prediction: Architectures, Learning algorithms and Stability. Wiley, 308pp.

Mann H.B. and Whitney D.R. (1947). On a test of whether one of two random variables is stochastically larger than the other. Annals of Mathematical Statistics, 18 (1): 50-60.

Maqsood I. and Huang G.H. (2003). A two-stage interval-stochastic programming model

for waste management under uncertainty. Journal of the Air & Waste Management Association, 53(5): 540-552.

Marine Mammal Commission (MMC) (2011). Assessing the Long-term Effects of the BP Deepwater Horizon Oil Spill on Marine Mammals in the Gulf of Mexico: A Statement of Research Needs. Marine Mammal Commission, Maryland, USA.

Marine Management Organisation (MMO) (2012). Marine Pollution Contingency Plan. Marine Management Organisation, UK.

Maritime and Coastguard Agency (2009). SOSREP Role and Responsibilities. Maritime and Coastguard Agency, UK.

Maritime New Zealand (1992). Marine Oil Spill Risk Assessment. Maritime New Zealand, New Zealand.

Maritime New Zealand (2006). New Zealand Marine Oil Spill Response Strategy. Maritime New Zealand, New Zealand.

Maritime Safety Queensland (2011). Queensland Coastal Contingency Action Plan. Maritime Safety Queensland, Australia.

Massaguer D., Balasubramanian V., Mehrotra S., and Venkatasubramanian N. (2006). Multi-agent simulation of disaster response. In: Proceedings of the First International Workshop on Agent Technology for Disaster Management, May 8, 2006, Hakodate, Japan, 124-130.

Mayer A. and Muñoz-Hernandez A. (2009). Integrated water resources optimization models: an assessment of a multidisciplinary tool for sustainable water resources management strategies, Geography Compass, 3(2009): 1176-1195.

McCulloch W.S. and Pitts W. (1943). A logical calculus of the ideas immanent in nervous activity. Bulletin of Mathematical Biophysics, 5: 115-133.

Mercier G., Girard-Ardhuin F. (2006). Partially supervised oil-slick detection by SAR imagery using kernel expansion. IEEE Transactions on Geoscience and Remote Sensing, 44: 2839-2846.

Migliaccio M. and Trangaglia M. (2004). Oil spill observation by SAR: a review. In: Proceedings of US-Baltic International Symposium, June 14-17, 2004, Klaiped, Lithuania.

Ministry of the Environment Canada (2012). Emergency Response Plan for Spill and Drinking Water Emergencies and other Emergencies that Require a Ministry Response. Ministry of the Environment, Canada.

Minsky M.L. and Papert S.A. (1969). Perceptrons. MIT Press, Cambridge, Massachusetts.

Mirfenderesk H. (2009). Flood emergency management decision support system on the gold coast, Australia. The Australian Journal of Emergency Management, 24(2): 48-58.

Moghaddamnia A., Gousheh G.M., Piri J., Amin S., and Han D. (2009). Evaporation estimation using artificial neural networks and adaptive neuro-fuzzy inference system techniques. Advances in Water Resources, 32(1): 88-97.

Moharramnejad N., Roayaii E., Lotfi F.H., Javid A.H., and Razavian F. (2010). Developing an expert system and fuzzy-based model for the oil spill environmental risk assessment. Journal of Food Agriculture & Environment, 8(2): 919-923.

Nazir M., Khan F., Amyotte P. Sadiq R. (2008). Multimedia fate of oil spills in a marine environment - An integrated modelling approach. Process Safety and Environmental Protection, 86:141–148.

Ng R.T. and Han J. (1994). Efficient and effective clustering methods for spatial data mining. In: Proceedings of the 20th VLDB Conference, September 12-15, 1994, Santiago, Chile, 144-155.

Nguyen V.P. (2007a). Fuzzy stochastic goal programming problems. European Journal of Operational Research, 176: 77-86.

Nguyen V.P. (2007b). Solving fuzzy (stochastic) linear programming problems using superiority and inferiority measures. Information Sciences, 177: 1977-1991.

Nguyen V.P. (2007c). Solving linear programming problems under fuzziness and randomness environment using attainment values. Information Sciences,177: 2971-2984.

Nirchio F., Sorgente M., Giancaspro A., Biamino W., Parisato E., Ravera R., and Trivero P. (2005). Automatic detection of oil spills from SAR images. International Journal of Remote Sensing, 26(6): 1157-1174.

Nordvik A.B. (1999). Time window-of-opportunity strategies for oil spill planning and response. Pure Applied Chemistry, 71(1): 5-16.

Øien K. (2001a). Risk indicators as a tool for risk control. Reliability Engineering and System Safety, 74: 129-145.

Øien K. (2001b). A framework for the establishment of organizational risk indicators. Reliability Engineering and System Safety, 74: 147-167.

Øien K. (2008). Development of early warning indicators based on accident investigation. In: Proceedings of PSAM 9. International Probabilistic Safety Assessment and Management Conference, May 18-23, 2008, Hong Kong, China.

Øien K., Massaiu S., Tinmannsvik R.K., and Størseth F. (2010). Development of early warning indicators based on resilience engineering. In: Proceedings of International Probabilistic Safety Assessment and Management Conference, June 7-11, 2010, Seattle, USA.

Ollerhead L.M.N., Morgan M.J., Scruton D.A., and Marrie B. (2004). Mapping spawning times and locations for 10 commercially important fish species found on the Grand Banks of Newfoundland. Canadian Technical Report of Fisheries and Aquatic

Sciences, 2522: iv + 45 p.

Olson J., McLaughlin S.D., Osborn R.N., and Jackson D.H. (1984). An initial empirical analysis of nuclear power plant organization and its effect on safety performance, NUREG(CR-3737, PNL-5102, BHARC-400/84/007. US Nuclear Regulatory Commission, Washington, D.C., USA.

Olson J., Osborn R.N., Jackson D.H., and Shikiar R. (1985). Objective indicators of organizational performance at nuclear power plants, NUREG/CR-4378, PNL-5576, BHARC-400/85/013. US Nuclear Regulatory Commission, Washington, D.C., USA.

Ornitz B. and Champ M. (2003). Oil Spills First Principles: Prevention and Best Response. Elsevier: Netherlands, 678pp.

Osborn R.N., Olson J., Sommers P.E., McLaughlin S.D., Jackson J.S., Nadel M.V., Scott W.G., Connor P.E., Kerwin N., and Kennedy J.J.K. (1983a). Organizational analysis and safety for utilities with nuclear power plants. Volume 2, Perspectives for organizational assessment, NUREG/CR-3215. Washington, D.C., US Nuclear Regulatory Commission, USA.

Osborn R.N., Olson J., Sommers P.E., McLaughlin S.D., Jackson J.S., Scott W.G., and Connor P.E. (1983b). Organizational analysis and safety for utilities with nuclear power plants, Volume1, An organizational overview, NUREG/CR-3215, PNL-4655, BHARC-400/83/011. US Nuclear Regulatory Commission, USA.

Owens E.H., Solsberg L.B., West M.R., and McGrath M. (1998). Field Guide for Oil Spill Response in Arctic Waters. Emergency Prevention, Preparedness, and Response (EPRR) Working Group, Arctic Council.

Oyana T.J. (2009). Visualization of high-dimensional clinically acquired geographic data using the self-organizing maps. Journal of Environmental Informatics, 13(1): 33-44.

Pal S.K., and Ghosh A. (1996). Neuro-fuzzy computing for image processing and pattern recognition. International Journal of Systems Science, 27: 1179-1193.

Pal S.K., and Mitra S. (1999). Neuro-fuzzy pattern recognition: methods in soft computing. Wiley-Interscience, 378pp.

Pal S.K., Ghosh A., and Kundu M.K. (2000). Soft computing for image processing. Spinger, 591pp.

Pal S.K., Ghosh A., and Shankar B.U. (2000). Segmentation of remotely sensed images with fuzzy thresholding, and quantitative evaluation. International Journal of Remote Sensing, 21(11): 2269-2300.

Paltrinieri N., Cozzani V., Øien K., and Grøtan T.O. (2012). Prevention of atypical accident scenarios through the use of resilience based early warning indicators. In: Proceedings of the European Safety and Reliability Conference, ESREL 2011, September 2011,Troyes, France.

Patino L. (2005). Fuzzy relations applied to minimize over segmentation in watershed

algorithms. Pattern Recognition Letters, 26(6): 819-828.

Pavlakis P. (1996). Investigation of the Potential of ERS-1/2 SAR images for monitoring Oil Spills on the Sea Surface. Joint Research Centre, European Commission Report EUR 16351 EN.

Pavlakis P., Tarchi D., and Sieber A. (2001). On the Monitoring of Illicit Vessel Discharges, A reconnaissance study in the Mediterranean Sea. European Commission Report EUR 19906 EN.

Payne J.R. and Phillips C.R. (1985). Photochemistry of petroleum in water. Environmental Science & Technology, 19(7): 569-579.

Payne J.R., Clayton J.R., Kirstein B.E. (2003). Oil/Suspended Particulate Material Interactions and Sedimentation. Spill Science & Technology Bulletin, 8(2): 201-221.

Pedrycz W. (1990). Fuzzy sets in pattern recognition: methodology and methods. Pattern Recognition, 23(1): 121-146.

Peleg K. and Pliskin J.S. (2004). A geographical information system simulation model of emergency medical services: reducing ambulance response times. The American Journal of Emergency Medicine, 22(3):164-170.

PEMSEA (Partnerships in Environmental Management for the Seas of East Asia) (2008). Proceedings of the Second East Asian Seas Partnership Council Meeting. July 14-17, 2008, Tokyo, Japan.

Pereira M.V.F. and Pinto L.M.V.G. (1985). Stochastic optimization of a multireservior hydroelectric system: a decomposition approach. Water Resources Research, 6: 779-792.

Perianez R. (2007). Chemical and oil spill rapid response modeling in the Strait of Gibraltar–Alboran Sea. Ecological Modelling, 207(2007): 210-222.

Peterson D. and Fensling S. (2011). Risk-based regulation: good practice and lessons for the victorian context. In: Proceedings of Victorian Competition and Efficiency Commission Regulatory Conference, March 31 - April 1, 2011, Melbourne, Australia.

Ping J., Chen Y., Chen B., and Howboldt K. (2010). A robust statistical analysis approach for pollutant loadings in urban rivers. Journal of Environmental Informatics, 16(1): 35-42.

Pourvakhshouri S.Z., Shattri B.M., Zelina Z.I., and Noordin A. (2006). Decision support system in oil spill management. international archives of photogrammetry. Remote Sensing, and Spatial Information Sciences: 36(2): 93-96.

Power D.J. (2002). Decision Support Systems: Concepts and Resources for Managers. Praeger, 272pp.

Preuss T.G., Hommen U., Alix A., Ashauer R., Brink P. J., Chapman P., Ducrot V., Forbes V., Grimm V., Schäfer D., Streissl F., and Thorbek P. (2009). Mechanistic effect models for ecological risk assessment of chemicals (MEMoRisk) - a new

SETAC-Europe Advisory Group. Environmental Science and Pollution Research, 16(3): 250-252.

Price J.M., Johnson W.R., Marshall C.F., Ji Z.G., and Rainey G.B. (2003). Overview of the oil spill risk analysis (OSRA) model for environmental impact assessment. Spill Science & Technology Bulletin, 8(5): 529-533.

Price M., Reed M., Howard M.K., Johnson W.R., Ji Z.G., Marshall C.F., Guinasso N.L., and Rainey G.B. (2006). Preliminary assessment of an oil-spill trajectory model using satellite-tracked, oil-spill-simulating drifters. Environmental Modelling & Software, 21(2): 258-270.

Prince R.C., Elmendorf D.L., Lute J.R., Hsu C.S., Haith C.E., Senius J.D., Dechert G.J., Douglas G.S. and Butler E.L.(1994). 17. alpha.(H)-21. beta.(H)-hopane as a conserved internal marker for estimating the biodegradation of crude oil. Environmental science & technology, 28(1): 142-145.

Psaraftis H.N. and Ziogas B.O. (1985). A tactical decision algorithm for the optimal dispatching of oil spill cleanup equipment. Management Science, 31(12): 1475-1491.

Pula R., Khan I.F., Veitch B., and Amyotte R.P. (2005). Revised fire consequence models for offshore quantitative risk assessment. Journal of Loss Prevention in the Process Industries, 18(4-6): 443-454.

Qiao B., Chu J.C., Zhao P., Yu Y., and Li Y. (2002). Marine oil spill contingency planning.

Journal of Environmental Sciences-China, 14: 102-107.

Qin X.S., and Huang G.H. (2008). Characterizing uncertainties associated with contaminant transport modeling through a coupled fuzzy-stochastic approach. Water, Air, and Soil Pollution, 197(1-4): 331-348.

Qinlan J.R. (1986). Introduction of decision trees. Machine Learning, 1: 86-106.

Qiu F., and Jensen J.R. (2004). Opening the black box of neural networks for remote sensing image classification. International Journal of Remote Sensing, 25(9): 1749-1768.

Queensland Transport (2000). Oil Spill Risk Assessment for the Coastalwaters of Queensland and the Great Barrier Reef Marine Park. Jointly prepared by Queensland Transport and the Great Barrier Reef Marine Park Authority. Brisbane, Australia.

Rainville L. and Woodgate R.A. (2009). Observations of internal wave generation in the seasonally ice-free Arctic. Geophysical Research Letters, 36: L23604, 5PP.

Ramalho G.L.B. and Medeiros F.N.S. (2006). Using Boosting to Improve Oil Spill Detection in SAR Images. In: Proceedings of the 18th International Conference on Pattern Recognition (ICPR), August 20-24, 2006, Hong Kong, China, 1066-1069.

Ramik J. and Vlach M. (2004). Fuzzy mathematical programming: a unified approach based on fuzzy relations. Fuzzy Optimization and Decision Making, 1(4): 335-346.

Ramseur J.L. (2010). Deepwater Horizon Oil Spill: The Fate of the Oil. Congressional

Research Service, USA, 24pp.

Rasmussen D. (1985). Oil Spill Modeling-a Tool for Cleanup Operations. In: Proceedings of International Oil Spill Conference, February 1985, Los Angeles, California, USA, 243-249.

Reed M. Gundlach E. and Kana T. (1989). A coastal zone oil spill model: development and sensitivity studies. Oil and Chemical Pollution, 5(6): 411-449.

Reed M., Johansen I., Brandvik P.J., Daling P., Lewis A., Fioccoà R., Mackay D., and Prentki R. (1999). Oil Spill Modeling Towards the Close of the 20th Century: Overview of the State of The Art. Spill Science & Technology Bulletin, 5(1): 3-16.

Riazi M.R. and Roomi Y.A. (2008). A Model to Predict Rate of Dissolution of Toxic Compounds into Seawater from an Oil Spill. International Journal of Toxicology, 27:379-386.

Richard F.L. (2003). Photo-oxidation and Photo-toxicity of Crude and Refined Oils. Spill Science & Technology Bulletin, 8(2): 157-162.

Richard O.D., Petter E.H., and David G.S. (2001). Pattern Classification. John Wiley & Sons Inc, 635pp.

Richards J.A. and Jia X. (2006). Remote sensing digital image analysis: an introduction. Springer-Verlag, Heidelberg, 464pp.

Rish I. (2001). An empirical study of the naive Bayes classifier. In: Proceedings of IJCAI

2001 Workshop on Empirical Methods in Artificial Intelligence, August 4-10, 2001, Seattle, Washington, USA.

Rosenblatt F. (1962). Principles of Neurodynamics. Spartan Books, 616pp.

Rotkin-Ellman M., Wong K.K., Solomon G.M. (2012). Seafood contamination after the BP Gulf oil spill and risks to vulnerable populations: a critique of the FDA risk assessment. Environmental Health Perspectives, 120(2): 157-161.

Rubinstein R.Y. and Melamed B. (1998). Modern Simulation and Modeling. Wiley-Interscience, 384pp.

Running S.W., Pierce L.L., Nemani R., Hunt E.R., and Loveland T.R. (1995). A remote sensing based vegetation classification logic for global land cover analysis. Journal of Remote sensing of environment, 51: 39-48.

Sadeghi N., Fayek A.R., and Pedrycz W. (2010). Fuzzy Monte Carlo simulation and risk assessment in construction. Computer-Aided Civil and Infrastructure Engineering, 25: 238-252.

Sanders R. and Tabuchi S. (2000). Decision support system for flood risk analysis for the River Thames, United Kingdom. Photogrammetric Engineering & Remote Sensing, 66(10): 1185-1193.

Santosh P.B. and Yousif A.H. (2004). A comparison of Sub-Pixel and maximum likelihood classification of Landsat ETM+ images to detect illegal logging in the

tropical rain forest of Berau, east Kalimantan, Indonesia. In: Proceedings of Geo-Imagery Bridging Continents XXth ISPRS Congress, July 2004 Istanbul, Turkey, 12-23.

Sauder J., McMahan J.B., and Weber K.T. (2003). Fuzzy classification of heterogeneous vegetation in a complex arid ecosystem. African Journal of Range and Forage Science, 20(2): 126.

Schultz R., Stougie L. and Vlerk M.H. (1996). Two-stage stochastic integer programming: a survey. Statistica Neerlandica, 50(3): 404-416.

Schulze R. (1998). Oil Spill Response Performance of Skimmers. American Society for Testing and Materials, West Conshohocken, USA,141pp.

Schurmann J. (1996). Pattern Classification: a Unified View of Statistical and Neural Approaches. Wiley-Interscience, 392pp.

Sebastiao P. and Sores C.G. (1995). Modeling the fate of oil spills at sea. Spill Science & Technology Bulletin, 2: 121-131.

Semini M. and Fauske H. (2006). Applications of discrete-event simulation to support manufacture logistics decision-making: A survey. In: Proceedings of the 2006 Winter Simulation Conference, December 3-6, 2006, Monterey, California, USA, 1946-1953.

Serra-Sogas N., O'Hara P.D., Canessa R., Keller P., and Pelot R. (2008). Visualization of spatial patterns and temporal trends for aerial surveillance of illegal oil discharges in

western Canadian marine waters. Marine Pollution Bulletin, 56: 825-833.

Seuntjens P. (2002). Field-scale cadmium transport in a heterogeneous layered soil. Water, Air, and Soil Pollution, 140(1-4): 401-423.

Shen H.T. and Yapa P.D. (1988). Oil slick transport in rivers. Journal of Hydraulic Engineering-ASCE, 114: 529-543.

Shen H.T. and Yapa P.D. 1987. A simulation model for oil slick transport in lakes. Water Resource Research, 23:1949–1957.

Shen H.T., Yapa P. and Petroski M.E. (1986). Simulation of oil slick transport in Great Lakes connecting channels. Report Nos. 86-1 to 4, vols. I-IV, Department of Civil and Environmental Engineering, Clarkson University, Potsdam, NY, USA.

Shirazi A.S., Mammen S., and Jacob C. (2013). Abstraction of agent interaction processes: Towards large-scale multi-agent models. Simulation, 89(4): 524-538.

Simpson P.K. (1992). Fuzzy min-max neural networks. I. Classification. IEEE Transactions on Neural Networks, 3: 776-786.

Solberg A. and Brekke C. (2008). Oil spill detection in Northern European Waters: Approaches and Algorithms. In: Remote Sensing of the European Seas, Eds.: Barale V. and Gade, M., Springer, 359-370.

Solberg A., Storvik G., Solberg R., and Volden E. (1999). Automatic detection of oil spills in ERS SAR images. IEEE Transactions on Geoscience and Remote Sensing,

37: 1916-1924.

Song S.K. (2008). Key elements in building up preparedness & response capability against major oil spills at sea in China. WMU Journal of Maritime Affairs, 7(1): 51-62.

Spaeth H. (1980). Cluster Analysis Algorithms for Data Reduction and Classification of Objects. Ellis Horwood, 226pp.

Spaulding M.L. (1995). Oil spill trajectory and fate modeling: state-of-the art review. In: Proceedings of the Second International Oil Spill Research and Development Forum, May 23-26, 1995, London, UK, 45-55.

Stathakis D., Topouzelis K., and Karathanassi V. (2006). Large-scale feature selection using evolved neural networks. In: Proceedings of SPIE, Image and Signal Processing for Remote Sensing XII, September 13-14, 2006, Stockholm, Sweden.

Steinmetz T., Raape U., TeBmann S., Strobl C., Friedemann M., Kukofka T., Riedlinger T., Mikusch E., and Dech S. (2010). Tsunami early warning and decision support. Natural Hazards and Earth System Sciences, 10: 1839-1850.

Stiver W. and Mackay D. (1984). Evaporation rates of spills of hydrocarbons and petroleum mixtures. Environmental Science & Technology, 18(11): 834-840.

Swail V.R., Cardone V.J., Ferguson M., Gummer D.J., Harris E.L., Orelup E.A., and Cox A.T. (2006). The MSC50 wind and wave reanalysis. In: Proceedings of International

Workshop on Wave Hincasting and Forecasting, September 25-29, 2006, Victoria, British Columbia, Canada

Sydnes M. and Sydnes A.K. (2011). Oil spill emergency response in Norway: coordinating interorganizational complexity. Polar Geography, 34(4): 299-329.

Tang Z.Y. and Yan X.A. (2007). Voting algorithm of fuzzy ARTMap and its application to fault diagnosis. Fuzzy Systems and Knowledge Discovery, 4: 535-538.

Tarchi D., Bernardini A., Ferraro G., Meyer-Roux S., Muellenhoff O., and Topouzelis K. (2006). Satellite Monitoring of Illicit Discharges from Vessels in the Seas around Italy 1999-2004. European Commission Report EUR 22190 EN.

Terpstra T.J. (1952). The asymptotic normality and consistency of Kendall's test against trend, when ties are present in one ranking. In: Proceedings of the Section of Sciences, Koninklijke Nederlandse Akademie van Wetenschappen, 55 (Series A): 327-333.

Terry R. (2008). More oil spills than predicted in Newfoundland fields. The Western Star, Canada.

The Emergency Prevention, Preparedness and Response Working Group (EPPR) (2012). The Norwegian Response Organisation in Cases of Oil Pollution, Emergency Prevention Preparedness and Response. the Arctic Council.

The International Association of Oil & Gas producer (OGP) (2011). Process Safety – Recommended Practice on Key Performance Indicators. London, United Kingdom.

The Organisation for Economic Co-operation and Development (OECD) (2008). Guidance on developing safety performance indicators related to chemical accident prevention, preparedness and response. OECD Environment Directorate, Environment, Health and Safety Division, Paris, France.

Tkalich P., and Chan E.S. (2002). Vertical mixing of oil droplets by breaking waves. Marine Pollution Bulletin, 44: 1219-1229.

Topouzelis K., Bernardini A., Ferraro G., Meyer-Roux S., and Tarchi D. (2006). Satellite mapping of oil spills in the Mediterranean Sea. Fresenius Environmental Bulletin,15: 1009-1014.

Topouzelis K., Karathanassi V., Pavlakis P., and Rokos D. (2007). Detection and discrimination between oil spills and look-alike phenomena through neural networks. ISPRS Journal of Photogrammetry and Remote Sensing, 62: 264-270.

Topouzelis K., Stathakis D., and Karathanassi V. (2009). Investigation of genetic algorithms contribution to feature selection for oil spill detection. International Journal of Remote Sensing, 30(3): 611-625.

Topouzelis N.R. (2008). Oil spill detection by SAR images: dark formation detection, feature extraction and classification algorithms. Sensors, 8: 6642-6659.

Torgrimson G.M. (1980). The On-Scene-*Spill Model: A User's Guide*. Technical Report, Hazardous Master. Response Branch, the National Oceanic and Atmospheric

Administration (NOAA), Seattle, Wash.

Transport Canada (2007). Environmental oil spill risk assessment for the south coast of Newfoundland. Transport Canada, Canada, TP 14740E.

Turner M. (2010). Review of Offshore Oil-Spill Prevention and Remediation Requirements and Practices in Newfoundland and Labrador, Department of Natural Resources. Government of Newfoundland and Labrador, Canada, 257pp.

U.S. Arctic Research Commission (2004). Advancing oil spill response in ice-covered waters. Prince William Sound Oil Spill Recovery Institute (Cordova) and United States Arctic Research Commission, Arlington, Virginia and Anchorage, Alaska, USA.

U.S. Department of the Interior Minerals Management Service (U.S. IMMS) (2008). Service Arctic Oil Spill Response Research and Development Program: A Decade of Achievement. U.S. Department of the Interior Minerals Management Service, USA.

U.S. Environmental Protection Agency (U.S. EPA) (1998). Human Health Risk Assessment Protocol (HHRAP) for Hazardous Waste Combustion Facilities. EPA520-R-05-006, U.S. Environmental Protection Agency, USA.

U.S. Environmental Protection Agency (U.S. EPA) (1999). Screening Level Ecological Risk Assessment Protocol (SLERAP) for Hazardous Waste Combustion Facilities. EPA 530-D-99-001A, U.S. Environmental Protection Agency , USA.

U.S. Environmental Protection Agency (U.S. EPA) (2004). Generic Ecological Assessment Endpoints (GEAE) for Ecological Risk Assessment. EPA/630/P-02/004F, U.S. Environmental Protection Agency, Risk Assessment Forum, Washington, DC, USA.

Vapnik V.N. (1995). The Nature of Statistical Learning Theory. Springer Verlag, 187pp.

Varshney P.K., and Arora M. (2004). Advanced image processing techniques for remote sensed hyperspectral data. Germany: Springer-Verlag, 323pp.

Vaughan S. (2010). 2010 Fall Report of the Commissioner of the Environment and Sustainable Development. Environment and Sustainable Development, Canada.

Venosa A.D., Suidan M.T., Wrenn B.A., Strohmeier K.L., Haines J.R., Eberhart B.L., King D. and Holder E. (1996). Bioremediation of an experimental oil spill on the shoreline of Delaware Bay. Environmental Science & Technology, 30(5): 1764-1775.

Vik R. (2005). Emergency preparedness and rescue arrangements. Safety At Sea LTD, UK.

Vock M., and Balakrishnan N. (2011). A Jonckheere–Terpstra-type test for perfect ranking in balanced ranked set sampling. Journal of Statistical Planning and Inference, 141(2): 624-630.

Vose D. (1996). Quantitative Risk Analysis: A Guide to Monte Carlo Simulation Modelling. Wiley, 340pp.

Wang J.H. and Shen Y.M. (2010). Modeling oil spills transportation in seas based on unstructured grid, finite-volume, wave-ocean model. Ocean Modelling, 35(2010): 332-344.

Wang L.X. and Mendel J.M. (1992). Generating fuzzy rules by learning from examples. IEEE Transactions on systems, Man, and Cybernetics, 26(12): 1182-1191.

Wang S., Huang G.H., and Yang B.T. (2011). An interval-valued fuzzy-stochastic programming approach and its application to municipal solid waste management. Environmental Modelling & Software, 29: 34-36.

Wang S.D., Shen Y.M. and Zheng Y.H. (2005). Two-dimensional numerical simulation for transport and fate of oil spills in seas. Ocean Engineering, 32(2005): 1556–1571.

Wang S.D., Shen Y.M., Guo Y.K., and Tang J. (2008). Three-dimensional numerical simulation for transport of oil spills in seas. Ocean Engineering, 35(2008): 503-510.

Wang Y., Cai G.D., and Duan Q. (2006). An Adaptive Dynamic Load Balancing Algorithm. Computer Engineering and Applications, 42(21): 121-123.

Wenger L.M. and Isaksen G.H. (2002). Control of hydrocarbon seepage intensity on level of biodegradation in sea bottom sediments. Organic Geochemistry, 33(2002): 1277-1292.

Wilhelm W.E. and Srinivasa A.V. (1997). Prescribing tactical response for oil spill clean up operations. Management Science, 43(3): 386-402.

Wing C.K. (2005). Oil spill response management and transboundary issues in Malaysia. In: Proceedings of SPE Asia Pacific Health, Safety and Environment Conference and Exhibition, September 19-21, 2005, Kuala Lumpur, Malaysia.

Woods D.D. (2006). Essential characteristics of resilience. In: Resilience engineering: concepts and precepts, Eds.: Leveson N., Hollnagel E., and Woods D.D., Aldershot: Ashgate, 21 - 34.

Wu Z.C. (2010). Simulation of the Oil Slick Movement in Tidal Water-Ways. Journal of Hydrodynamics, 22(1): 96-102.

Xie H., Yapa P.D., and Nakata K. (2007). Modeling emulsification after an oil spill in the sea. Journal of Marine Systems, 68(2007): 489-506.

Xiong D.Q., Zhang X.B., and Lamine S. (2010). Numerical simulation of the trajectory and fate of spilled oil at sea. In: Proceedings of Bioinformatics and Biomedical Engineering (iCBBE), 2010 4th International Conference, June 18-20, 2010, Chengdu, China.

Xu R., du Plessis L., Damelin S.B., Sears M., and Wunsch D. (2009). Analysis of hyperspectral data using diffusion maps and fuzzy art. In: Proceedings of the 2009 International Joint Conference on Neural Networks, June 14-19, 2009 , Atlanta, Georgia, USA, 2302-2309.

Xu Y., Huang G.H., Qin X.S., and Huang Y. (2009). SRFILP: a stochastic robust fuzzy

interval linear programming model for municipal solid waste management under uncertainty. Journal of Environmental Informatics, 14: 72-82.

Yang A.L., Huang G.H., and Qin X.S. (2010). An integrated simulation-assessment approach for evaluating health risks of groundwater contamination under multiple uncertainties. Water Resources Management, 24(13): 3349-3369.

Yang C.G, Yu J.B., Hao Z.C., Lin Z.H., and Wang H.M. (2013). Effects of vegetation cover on hydrological processes in a large region: the Huaihe River Basin, China. Journal of Hydrologic Engineering-ASCE, 18(11): 1477-1483.

Yapa P.D., Shen H.T. and Angammana K.S. (1994). Modeling oil spills in a river-lake system. Journal of Marine Systems, 4(6): 453-471.

Yoo J.H. (1993). Symbolic Rule Extraction from Artificial Neural Networks. PhD thesis, Wayne State University, USA.

You F.Q., Leyffer S. (2011). Mixed-integer dynamic optimization for oil-spill response planning with integration of a dynamic oil weathering model. AIChE Journal, 57(12): 3555-3564.

Yuan Y.F. and Shaw J.M. (1995). Induction of fuzzy decision trees. Fuzzy Sets and Systems, 69: 125-139.

Zadeh E.S, Hejazi K. (2012). Eulerian oil spills model using finite-volume method with moving boundary and wet-dry fronts. Modelling and Simulation in Engineering, 2012

(2012):7pp.

Zadeh L.A. (1965). Fuzzy sets. Information and Control, 8: 338-352.

Zadeh L.A. (1968). Fuzzy algorithms. Information and Control, 12(2): 94-102.

Zaindin A.S. (1995). Saudi Aramco Oil Spill Contingency Plan. In: Proceedings of the Oil Spill Symposium '95, Match 23-24, 1995, Tokyo, Japan.

Zaindin A.S. (1995). Saudi Aramco oil spill contingency plan. In: Proceedings of the Oil Spill Symposium '95, Match 23-24, 1995, Tokyo, Japan.

Zepp R.G., Cline D.M. (1977). Rates of direct photolysis in aquatic environments. Environmental Science & Technology, 11 (1977): 359-366.

Zhang X.F., Tsang, A.M. Okino M.S., Power F.W., Knaak J.B, Harrison L.S., and Dary C.C. (2007). A physiologically based pharmacokinetic/pharmacodynamic model for carbofuran in Sprague-Dawley rats using the Exposure-Related Dose Estimating Model. Toxicological Sciences, 100 (2): 345-359.

Zhong Z. and You F. (2011). Oil spill response planning with consideration of physicochemical evolution of the oil slick: a multiobjective optimization approach. Computers & Chemical Engineering, 35(8): 1614-1630.

Zhu X., Venosa A.D., Suidan M.T. and Lee K. (2001). Guidelines for the bioremediation of marine shorelines and freshwater wetlands. US Environmental Protection Agency, USA.